Multiomics identification of effectors candidates from oomycete root plant pathogen Aphanomyces euteiches

Andrei Kiselev

Université Fédérale
Toulouse Midi-Pyrénées

THÈSE

En vue de l'obtention du

DOCTORAT DE L'UNIVERSITÉ DE TOULOUSE

Délivré par :

Université Toulouse 3 Paul Sabatier (UT3 Paul Sabatier)

Présentée et soutenue par :
Andrei KISELEV

le jeudi 15 décembre 2022

Titre :

Identification multiomique d'effecteurs candidats de l'oomycète Aphanomyces euteiches, parasite racinaire des légumineuses

---

École doctorale et discipline ou spécialité :
ED SEVAB : Interactions plantes-microorganismes

Unité de recherche :
LRSV - Laboratoire de Recherche en Sciences Végétales

Directeur/trice(s) de Thèse :

Elodie GAULIN

Jury :
Mme Nathalie POUSSEREAU, Université Claude Bernard Lyon I, Rapporteure
M Pieter van WEST, University of Aberdeen, Rapporteur
Mme Elodie GAULIN, Université Paul Sabatier Toulouse III, Directrice de thèse
M. Christophe ROUX, Université Paul Sabatier Toulouse III, Président
Mme Martina RICKAUER, Ecole Nationale Supérieure Agronomique de Toulouse, Invitée

Abstract

Aphanomyces euteiches is a soil-borne oomycete pathogen of leguminous plants, affecting production of peas and alfalfa all over the world. One of the major pathogenicity factors of filamentous organisms are the proteinaceous secreted effectors, which targets host plant physiology or modify microbiome composition to facilitate invasion. The pathogens have myriads of effectors encoded in their genome, which evolve rapidly during host-pathogen arm race and possess fine transcriptional regulation during the infection process. Genome sequencing of various pathogens demonstrated that each species encodes hundreds putative effectors with a high degree of lineage-specific genes. Whereas prediction of the effectors based on -omics data is rather easy and robust as the amount of the genome data is growing, the elucidation of the effector function is a laborious task and for each species the number of characterized effectors counts from none to dozens. Therefore, the selection of the effector for functional characterization is the important task for studying plant-pathogen interactions.

This PhD work by comparative genomics studies firstly highlighted the large arsenal of secreted Crinklers (CRNs), Small Secreted Proteins (SSPs), cell wall degrading enzymes (CAZymes) and proteases in the genome of *A. euteiches*. Then the main aim of the work was related to the development of proteomics-based assays to support genomic prediction of putative effector that may play a role during infection of leguminous hosts. During the PhD I developed assays for rapid detection of the apoplastic proteases and nuclear targeting proteins present during the infection. The different approaches supported the genomic prediction of main effector categories. I also described modular microbial cysteine/serine proteases and various type of nuclear-localized proteins that participate in *A. euteiches* invasion by acting on plant development, plant genomic stability or plant immune responses.

This PhD work is a part of a four-year European ITN ‘Protecta’ project (2018-2022) dedicated to study oomycete pathogenicity factors 766048 (MSCA-ITN-2017 PROTECTA).

Resumé

Aphanomyces euteiches est un oomycète filamenteux pathogène racinaire de nombreuses légumineuses comme le pois et la luzerne. Ce microorganisme tellurique est responsable d'importants dégâts et restreint la culture de légumineuse. L'un des principaux facteurs de pathogénicité des organismes filamenteux eucaryotes sont les effecteurs protéiques, sécrétés par le parasite pendant l'interaction et affectant la physiologie de la plante ou modifier la composition du microbiome pour faciliter l'infection. Les agents pathogènes possèdent des myriades d'effecteurs, qui sont finement régulés au niveau de leur expression et peuvent évoluer au contact de la plante hôte. Le séquençage des génomes d'agents pathogènes a démontré que chaque espèce code des centaines d'effecteurs putatifs. Alors que la prédiction des effecteurs basée sur des données génomique est plutôt facile et robuste, l'élucidation de la fonction des effecteurs est une tâche longue et spécifique à chaque effecteur. Par conséquent, la sélection d'effecteurs candidats à partir des centaines prédits est une étape clé pour les analyses fonctionnelles.

Ce travail de thèse avait donc pour objectif, tout d'abord, via des études de génomique comparative de prédire le répertoire d'effecteur *d'A. euteiches* et de définir si certains étaient impliqués dans la préférence d'hôte (pois *vs* luzerne). Cette analyse a mis en exergue le large arsenal de Crinklers sécrétés (CRNs), d'enzymes dégradant la paroi cellulaire végétale (CAZymes), de protéases. Enfin des Petites Protéines Sécrétées (SSPs) sans fonction prédite pourrait intervenir dans la préférence d'hôte. Dans un second temps deux techniques expérimentales ont été mises en place afin d'identifier les effecteurs présents chez l'hôte végétal au cours de l'interaction. Un premier focus a été réalisé sur les protéases extracellulaires et leur caractérisation par protéomique à partir d'extrait apoplastique de racines de pois infectées par le parasite. Cette approche a permis de confirmer les prédictions génomiques et révélée l'existence de protéases originales dotées en plus d'un site catalytique d'un domaine de liaison à des carbohydrates et lipides. La seconde approche visait à identifier les protéines extracellulaires *d'A. euteiches* présentes dans le noyau de racines de *M. truncatula* infectées afin d'en identifier les effecteurs *via* une combinaison d'analyse en FACS et de protéomique. Des effecteurs candidats ont pu être également identifiés avec succès.

Cette thèse à contribuer à une meilleure connaissance des facteurs de pathogénicité mis en place par les oomycètes au cours de l'infection de la plante hôte et révélé leur complexité. Cette thèse est soutenue par un projet Marie Skłodowska-Curie Actions - ITN 'PROTECTA' (2018-2022, 766048 (MSCA-ITN-2017 PROTECTA) dédié à l'étude de la pathogénicité des oomycètes.

Acknowledgments

Firstly, I'd like to thank the members of the thesis jury Nathalie Poussereau, Martina Rickauer and Pieter van West for your agreement to evaluate my thesis and participate in the defence. I'm looking forward very much to presenting you my results and have a fruitful discussion with you, and hopefully seeing you in Toulouse. Also a great thanks to Laurence Godiard and Isabelle Fudal for your valuable comments and interesting discussions during my thesis committees.

I would like to express my sincere gratitude to my thesis supervisor Elodie Gaulin for following me during this exciting journey of an international PhD student. It will never be too much to stay how supportive you were during this time. A special thank you for letting me try my crazy ideas and being tolerant when I failed with them. It was a great pleasure to work under your supervision. Un grand merci à toi pour la motivation d'étudier le français et d'avoir parlé avec moi en français et d'avoir compris mon 'funny' accent !

I'm also very grateful to a whole team RHIZO and former IPM at LRSV for your openness and helpfulness. First to the team leaders Bernard Dumas and Christophe Roux for the smooth work of the team and help with all the formalities. Then to the whole team especially to Charlene, Lea, Nathanel, Clement and many others. Thank you, Maryam, for our long conversations over the lunch about the science, but not only.

Laurent, the special paragraph for you. It couldn't be better than having you in the team working on *Aphanomyces* and 'all this stuff'. Without your patience and experience at the bench and your passion to the microscopy, the large part of this thesis couldn't be done so quickly and smoothly. And you know, you can always 'consult bioinformatician' if you have any questions.

A big thanks to Helene and Marielle for guiding me to the world of bioinformatics and statistics, your support at the beginning of my thesis was very useful and helped me develop my skills further.

I'm very grateful to my collaborators for our fruitful work together. Especially to the Plant Chemetics team in Oxford for a warm welcoming and extreme help during my stay, Laura, Marianna, Renier, thank you, it was a great experience. The great students of PROTECTA project: Valentina, Bikal, Christian, Murilo, Magda, Tatiana, Clara, Noellia, Jeniffer, Dania, I wish we could spend more time together.

Last but far not the least a great thank you to my lovely family. My wife Kseniia, your love supported me and gave me power and motivation to work. And thank you to my parents and brother for believing in me and for your support of my chosen way.

Table of Contents

1. Introduction

During their life cycle plants are exposed to abiotic and biotic challenges originated from plant-environment interaction. When the plant faces suboptimal conditions in any environmental parameter, it activates programmed stress response (Gaspar et al., 2002). The abiotic stresses are mostly linked to weather, climate and soil conditions. Due to a rapid climate change recorded over past century, the most prominent abiotic factors affecting plant communities and therefore agriculture, nowadays and in near future are: longer exposure to extreme low or high temperatures, extended drought periods and/or stronger rainfalls, which cause soil floodings, changes in soil composition, remarkably increase in soil salinity and heavy metals pollutions (Gideon Onyekachi et al., 2019). In combination with abiotic stresses plants are exposed to biotic stresses such as pro- and eukaryotic pathogens, herbivorous animals, plant competitors etc. The most dangerous biotic factors for agricultural production are insects that globally consume 5-20% of grain yield (Deutsch et al., 2018) and pathogens which cause 10 – 30% yield loss globally (Ficke et al., 2018; Savary et al., 2019). Pathogens in agriculture are originated from four major groups: bacteria, nematodes, fungi and oomycetes, last two commonly referred as filamentous organisms.

To fight against pathogenic microbe plants evolved comprehensive immune system to counteract the pathogen attack. It's mainly based on the recognition of Microbial Associated Molecules (MAMP) released by the pathogen (Jones and Dangl, 2006) that trigger an immune response that could be sufficient to protect the plant against the invader. To overcome this first layer of defence, adapted pathogens secrete molecules to perturb plant physiology and enhance host colonisation through the production of molecules called effectors. While some species are able to detect specially some effectors to induce stronger immune response and cell death of invading-cells, others plant species will be colonized by the pathogen. Thus infection of the plant appears as an evolutionary arms race between a host and a pathogen (Kamoun, 2006).

This introductive chapter after a description of filamentous eukaryotic microorganisms, will give an overview of the molecular mechanisms related to the dialogue between plant and fungal/oomycetes pathogens during infection and the major objectives of my PhD work.

1.2.1 Fungi

Filamentous organisms threaten the yield of all major crops in the world: wheat, maize, rice, etc. Filamentous pathogens are represented by two phylogenetically unrelated groups

fungi and oomycetes, however, exploiting similar strategy for host invasion, which relates in large extent on a secreted proteins delivered to the particular host compartment (Kamoun, 2006, 2009). The particular success of the filamentous pathogens is thought to be ensured by the genome plasticity of the organisms. Often the genes encoding the pathogenic determinants are located in telomeric or gene-sparse region, subjected to a higher mutation rate. Such plasticity combined with tuned epigenetic and transcriptional regulation offers the rapid evolution of the pathogens to overcome plant resistance mechanisms (Dong et al., 2015, 2016).

Plant pathogenic fungi are mainly represented by the species from two phylum Ascomycota and Basidiomycota. Among ascomycetes, plant pathogens are in various classes such as the Dothideomycetes (e.g., *Cladosporium* spp.), Sordariomycetes (e.g., *Magnaporthe* spp.), or the Leotiomycetes (e.g., *Botrytis* spp.). Basidiomycetes are represented by the two largest plant pathogen groups: the rusts (Pucciniomycetes) and smuts (spread among the subphylum of Ustilaginomycotina). *Fusarium* is among the most devastating plant pathogenic fungi. It's a polyphyletic groups of ascomycetes, which includes up to 300 species and characterized by the presence of fusiform multiseptate macroconidia (O'Donnell et al., 2015). Groups of *Fusarium* species (*F. graminearum, F. culmorum, F. avenaceum,* etc) induce a Fusarium head blight (FHB) disease in wheat cultures. It drastically affected the production of durum wheat and made it impossible to cultivate it in zones endemic for FHB. *Fusarium* produce large amount of mycotoxin, deoxynivalenol as example, seeds contaminated by mycotoxins are dangerous for the human or animal consumption (Fernandez and Knox, 2012). Species from *Botrytis* genera are another important pathogens of crops, vegetables and ornamental plants. (Elad et al., 2007). The most studied pathogen is a broad host range necrotrophic fungus *B. cinerea* able to infect over 200 dicotyledon species. It causes grey mould disease and have a great impact on production of protein-rich crops in Asia. *B. cinerea* is difficult to control because it has a variety of modes of attack, diverse hosts as inoculum sources, and it can survive as mycelia and/or conidia or for extended periods as sclerotia in crop debris (Williamson et al., 2007).

1.2.2 Oomycetes

1.2.2.1 Classification

Oomycete is a phylum within SAR (Stramenopiles, Alveolata, Rhizaria) supergroups, which along with oomycetes includes brown algae, diatoms and apicomplexa (Grattepanche et al., 2018). As other Stramenopiles Oomycetes have an evolution footprint of the photosynthetic ancestors and thought to lose the chloroplast endosymbiont (Kamoun, 2009). Phylogenetically

the intracellular parasites of animals *Plasmodium* and *Toxoplasma* are the closest pathogens to oomycetes.

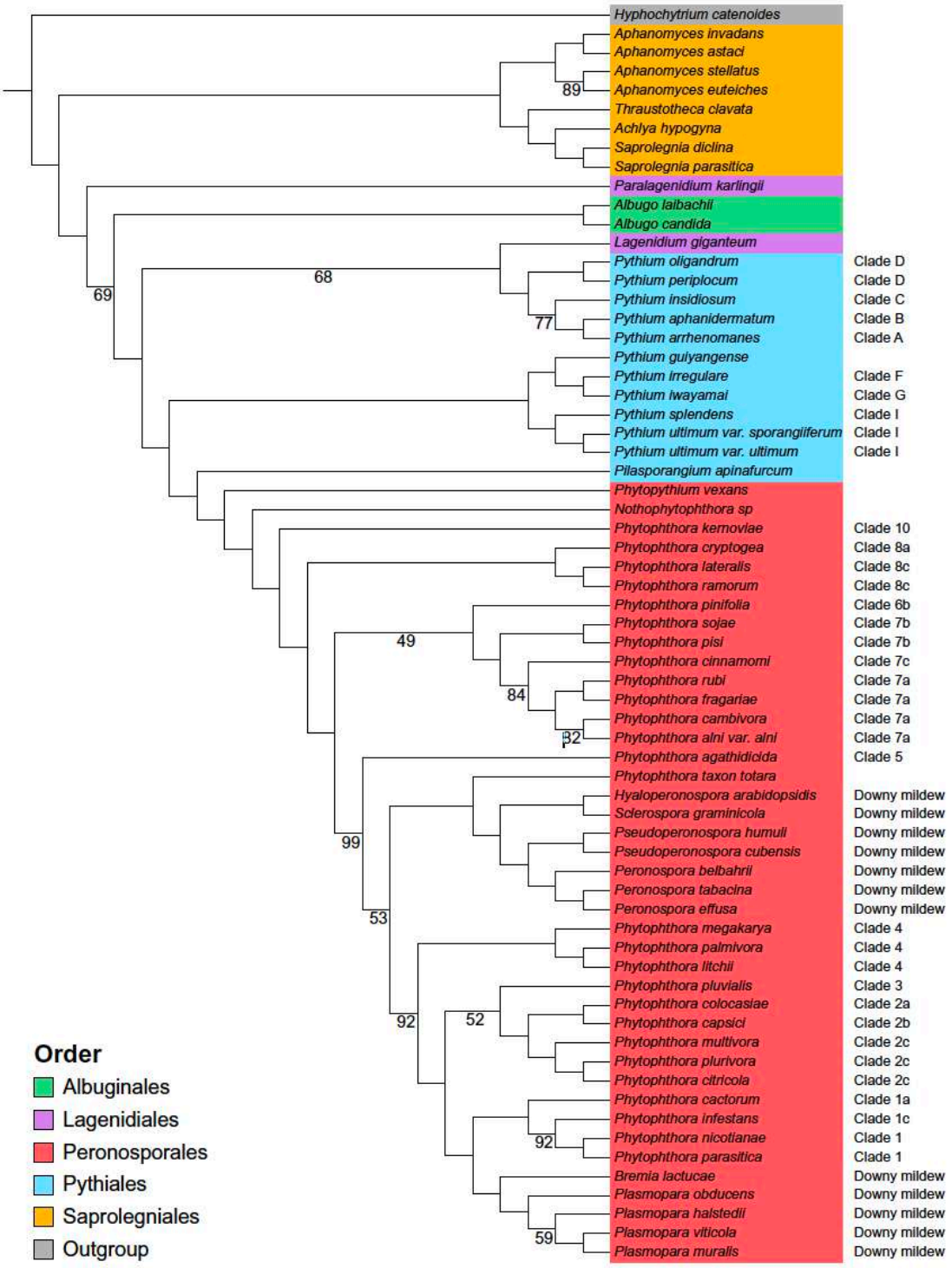

Figure 1. Maximum-likelihood phylogeny of the 65 oomycete species based on the concatenation of 102 conserved BUSCO sequences. The stramenopile *Hyphochytrium catenoides* is included as an outgroup. Adapted from McGowan and Fitzpatrick, 2020.

Oomycetes are relatively small lineage, which species abundance is estimated around 900-1500 species (Lang-Yona et al., 2018). 101 genome of 89 oomycete species is available on the NCBI database (https://www.ncbi.nlm.nih.gov/genome, access date 04.2022), more than 60% of studied species is represented by plant pathogens (Thines and Kamoun, 2010). By using single-copy orthologous genes (McGowan and Fitzpatrick, 2017) the phylogenetic tree of oomycetes was resolved forming 4 major orders: Peronosporales, Albuginales, Pythiales and Saprolegniales **(Fig. 1)**. Peronosporales are the most studied oomycetes and represented by plant pathogens *Phytophthora, Notophythophthora, Peronospora, Plasmopara* genus. Albuginales is a small order represented by *Albugo* genus which causes 'white blisted rust' on angiosperms, including such crops as *Brassica spp,* spinach, sweet potato, sunflower and model plant *A. thaliana* (Furzer et al., 2022). In contrast to other oomycetes, *Albugo* species are obligate biotrophs and cannot be cultivated on synthetic media (Goyal et al., 1995). The two other orders Pythiales and Saprolegniales include both animal and plant pathogens even inside one genus, for example, *Pythium* genus where *P. insidiosum* induces pythiosis in animals, *P. ultimum* is responsible for root rot diseases and *P. oligandrum* is a mycoparasite with a potential for a biocontrol (Faure et al., 2020). In Saprolegniales the genus *Saprolegnia* contains two broad spectrum pathogens of aquatic animals. Saprolegniosis disease caused by *S. parasitica* and *S. diclina* is a dangerous threat for aquaculture in temperate climate all around the world (Sarowar et al., 2013). The genus *Aphanomyces* includes both plant and animal pathogens as well as saprotrophic organisms (Bazyli et al., 2015; Gaulin et al., 2007a).

1.2.2.2 Lifestyle

The recent study by Gomez-Perez and Kemen (2021) linked the genomic and metabolomic difference of oomycetes with their lifestyle **(Fig. 2).** According to their study, another classification based on species' available biochemical pathways was proposed, which confirms the phylogenetic tree and adds additional functional characteristics: i) obligate biotrophs, ii) Saprolegniales and iii) the group where most of the Peronosporales and Pythiales species fall.

Biotrophic organisms get nutrients from live tissue of the host to support the growth and life cycle. As an adaptation to biotrophy obligatory biotrophs lost their biosynthetic genes, relying completely on the host supply (Spanu and Kämper, 2010). The loss of the biosynthetic genes is tightly connected with an expansion of genes, which are used for nutrients acquisition. Within oomycetes biotrophs are represented by the Albuginales order and downy mildew from

Peronosporales (*Bremia lactucae, Plasmopara halstedii, Peronospora effusa, Hyalopernospora arabidopsidis*). The most striking characteristic was an overall reduction in their metabolism, evident by the lack of many functional annotations in comparison with other oomycetes. This lack of core biosynthetic pathways, including vitamin and cofactor biosynthesis, makes them reliant on their host for growth and survival (Gomez-Perez and Kemen, 2021).

The second group corresponds to Saprolegniales which are not auxotrophic on sterol, in comparison to other oomycetes (Madoui et al., 2009), and possess their own biosynthetical pathway (Dahlin et al., 2017; Madoui et al., 2009) as compared to others oomycetes. Saprolegniales order is very diverse in terms of host range, they include invertebrate and vertebrate animals and plants. It was previously described that in this order experienced expansion of a kinases and secreted enzymes, such as CAZymes and proteases (Gaulin et al., 2018; Jiang et al., 2013a). The lifestyle of plant pathogens *A. euteiches* and *A. cochlioides* from this group is not studied in details, but it is thought to be closer to a hemibiotrophy, as they could be cultivated without a host and massive cell death was not observed during the infection (Gaulin et al., 2007; Taguchi et al., 2009).

The third group consists of hemibiotrophs from Pythiales order and non-biotroph *Phytophthora* species. Those organisms usually could be cultivated on the synthetic media without a host, in contrast to obligate biotrophs (Gomez-Perez and Kemen, 2021). Hemibiotrophic infection consists of biotrophic and necrotrophic stages, which are tightly regulated and present different set of the expressed genes from a pathogen. On the example of *P. infestans* the necrotrophic stage begins several days after the infection, while at this stage the effectors inducing plant cell death are activated (Zuluaga et al., 2016)

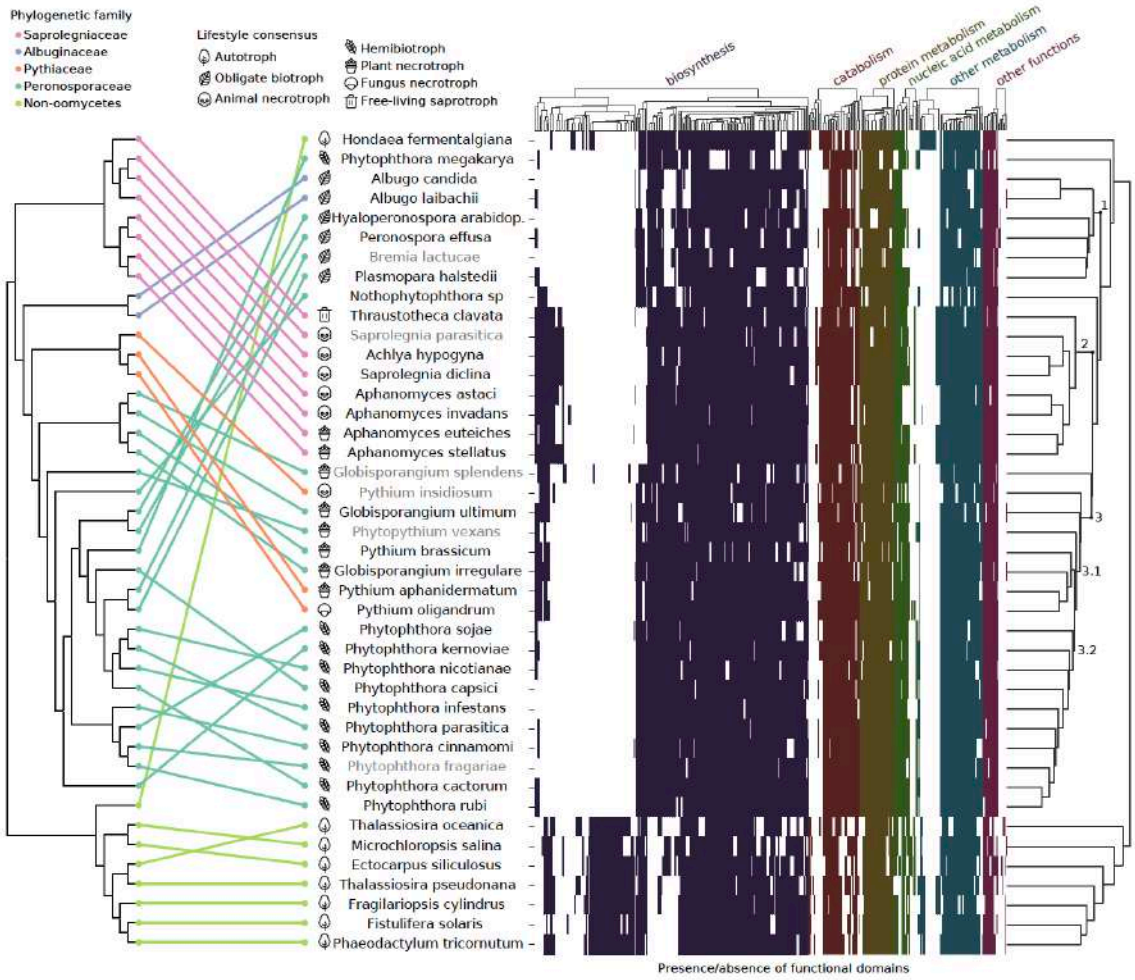

Figure 2. Presence/absence of functional attributes in the genomes of the Stramenopiles dataset correlated with phylogeny. Equal distance cladogram constructed from conserved families inferred by the maximum likelihood on the left and clustering by Unweighted Pair Group Method with Arithmetic Mean (UPGMA) of genome properties of the dataset on the right. In the equal distance phylogenetic tree, colored lines match phylogeny to the clustered taxa with annotated lifestyles. All nodes in the tree have a 100-bootstrap support. In the heatmap, different colors represent the presence or absence of particular functional groups belonging to the specified categories. Names in grey represent long-read sequencing assemblies in the dataset for that species. Adapted from (Gómez-Pérez and Kemen, 2021).

1.2.2.3 Life cycle

Oomycetes are apically growing filamentous microorganisms, with non-septate hyphae (Hardham, 2007). They are known as 'water molds' and usually found in aquatic or wet habitats as saprotrophs or pathogens (Thines, 2018). Throughout the life cycle oomycetes exploit two reproduction system: asexual (zoospores) and sexual (oospores**) (Fig. 3)**. For a rapid dissemination, for example, in the infested field, oomycete produce myriads of motile bi-flagellate zoospores, which can swim in soil water film and recognize the host roots through chemotaxis and electrical fields (van West et al., 2002). During the sexual reproduction oomycetes form the thick-walled oospore, which could preserve their germination ability for years in the environment, hardening the crop rotation of the infested fields (Babadoost and Pavon, 2013). Oomycetes have diploid mycelium, to form the gametes nuclei undergo meiotic division in oogonium and antheridium. The oogonium and antheridium from the same (homothallic) or different (heterothallic) mycelia conjugate and a single gametic nuclei from antheridia is transferred into oogonia to form an oospore. Upon maturation oospore develop a large lipid-containing vacuole and a thick cell wall, altogether that contributes to a long preservation of oospores (Judelson, 2009).

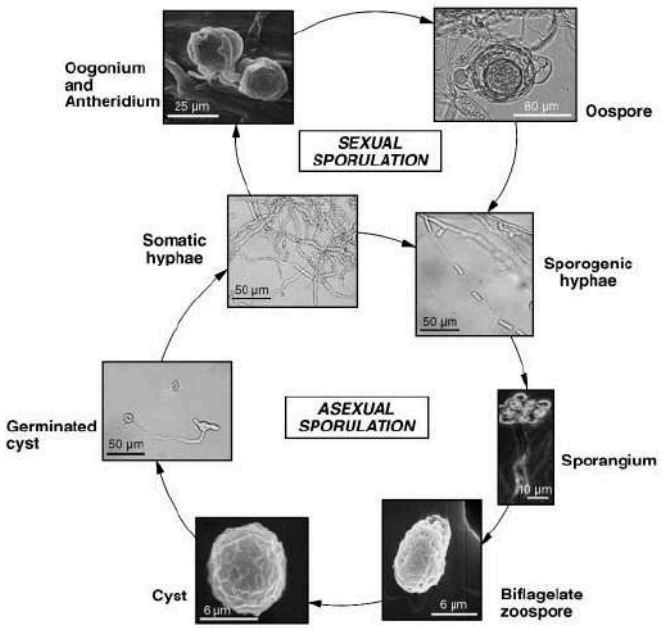

Figure 3. Diagram depicting the life cycle of *Aphanomyces euteiches*. Adapted from Gaulin et al., 2007a.

1.3 Plant defence

In contrast to motile organisms, plants cannot avoid the interaction with pathogens, therefore to counteract biotic stresses plants evolved a defence system based on early recognition of pathogens and induction of defence to minimize development of a pathogen (**Fig. 4**). In analogy to animals this system usually referred as a plant immune system. In 2006 Jones and Dangl presented a 'zigzag' model of functioning of a plant immunity, where they defined the major actors in plant immunity, which enabling recognition extracellular or intracellular pathogen-related molecules and induce defence response.

Apoplastic space of a plant is often an entry point of the infection. Plants evolved the extracellular receptors – Pattern Recognition Receptors (PRR) – to recognize molecules associated with pathogens – Pathogen Associated Molecular Pattern (PAMP or MAMP for Microbial) and elicit immune response. PAMPs/MAMPs are usually evolutionary conserved essential elements of pathogen's cells such as bacterial flagellin or fungal chitin from the cell wall. Plants are also able to recognize Danger Associated Molecular Patterns (DAMP) that correspond to the plant endogenous molecules such as parts of cuticula or cell wall released upon the pathogen invasion. The activation of PRR lead to Pathogen Triggered Immunity (PTI). The rapid transcriptional reprogramming in the cell results in primary defence reaction such as ROS production, stomata closure, callose deposition, production of antimicrobial compounds and programmed cell death to localise the pathogen at the point of infection and induce resistance (Bigeard et al., 2015; Li et al., 2016; Polturak and Osbourn, 2021).

To overcome the PTI plant pathogens evolved pathogenicity factors, mainly secreted and delivered into host cell, called effectors, which help overcome PTI and induce Effector Triggered Susceptibility (ETS) by direct or indirect modification of major components of plant immunity. The pep1 effector from maize pathogen *Ustilago maydis* is indispensable for a successful infection. Host plant triggers rapid H_2O_2 accumulation upon the infection by *U. maydis*, while the Pep1 protein is able to directly bind the POX12 peroxidase and diminish peroxide production (Hemetsberger et al., 2012).

To neutralize effectors delivered into the cell plants evolved intracellular receptor proteins often referred as resistance proteins (R), able to recognise pathogen's effector and reported is this case as 'avirulence protein' and induce effector triggered immunity (ETI). Although, ETI involves different receptors at the detection stage, the physiological output is similar to one induced by PTI (Yuan et al., 2021b). This qualitative interaction is also reported

as ‘gene-for-gene model’ is opposition to the quantitative resistance against a pathogen which is mediated by a combination of different genomic region coding different proteins required for an optimized protection of the host against the invader (Pilet-Nayel et al., 2017).

Whether the initial zigzag model described PTI and ETI as independent and sequential processes, the current understanding of plant immunity suggests that PTI and ETI uses the similar mechanisms to induce defence response and represents different layers of the immune systems with extensive crosstalk between the layers offering the adaptive and fine tuning system (for detailed review see: Dodds and Rathjen, 2010; van der Burgh and Joosten, 2019; Yuan et al., 2021).

1.3.1 The PTI

MAMPs/PAMPs are recognized by surface localized pattern recognition receptors (PRR) to trigger PTI. The most studied MAMPs correspond to lipooligosaccharides of gram-negative bacteria, bacterial flagellin, bacterial Elongation Factor-Tu (EF-Tu), part of glucans and glycoproteins from oomycetes or chitin from fungus cell wall (Zhang and Zhou, 2010). Plants also recognize proteinaceous oomycete MAMPs or PAMPS such as Cellulose binding domain (Gaulin et al., 2006) cell wall transglutaminase, oligopeptide elicitor protein, elicitin family of sterol-binding proteins, endoglucanase XEG1, CBEL glycoproteins (Gaulin et al., 2002; Judelson and Ah-Fong, 2019). Oomycete as other pathogens release PAMPS/MAMPs recognized by plants. These include cell wall composites as beta-glucans, arachidonic acid and chitosaccharides (Judelson and Ah-Fong, 2019).

PRR bound with the PAMP often needs to form a complex with a Receptor-like Kinase to induce the signalling cascade (Fig. 4). PRRs are represented by two distinct classes: Receptor-Like Kinases (RLK) and Receptor-Like Proteins (RLP), both often having extracellular leucine-rich repeats, perceiving PAMPs/MAMPs. The activated receptor activated Receptor-Like Cytoplasmic Kinase (RLCK), which induces the cascade reaction, leading to physiological and transcriptional reprogramming of the cell (Bigeard et al., 2015).

One of the most studied LRRs is FLS2, which is able to recognize a part of bacterial flagellin protein corresponding to 22 amino acid (Flg22) and conserved within bacteria. *In A. thaliana,* FLS2 formed a complex with flg22 recruits the receptor like kinase BAK1 and induces the signalling cascade (Saijo et al., 2018). *A. thaliana* has several extracellular receptors of LYK-family (LysM-containing receptor-like kinases), which bind the chitin released from fungal cell wall. LYK5 receptor changes its conformation upon chitin binding

and form a complex with CERK1 kinase to intracellular signalling cascade resulting in abundant ROS production (Fesel and Zuccaro, 2016). Elicitor protein INF1 from oomycete *P. infestans* is recognized by conserved in Solanaceae family BAK1/SERK3 kinase with five extracellular LRR domains. The activation of BAK1/SERK3 kinase triggers PTI in Solanaceae plant leading to ROS accumulation and a rapid cell death (Chaparro-Garcia et al., 2011).

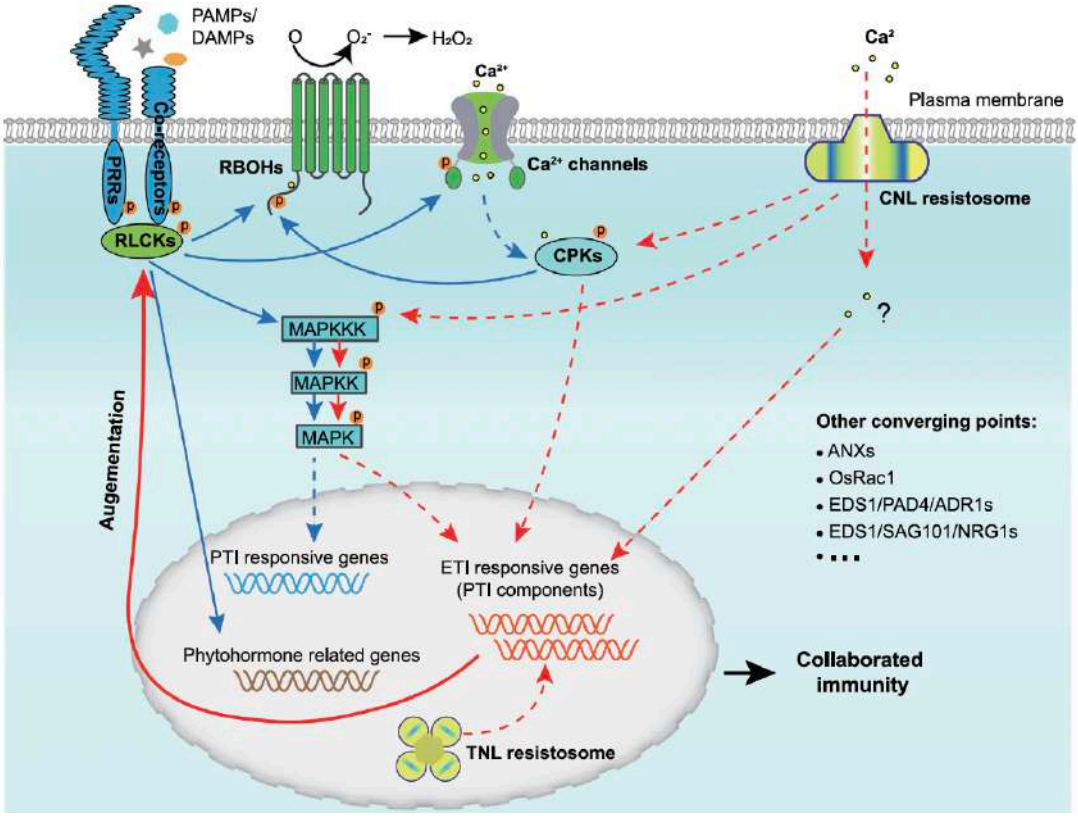

Figure 4. PRR (blue arrows) and NLR (red arrows) signalling co-regulate immune responses and converge at multiple points. Upon recognition of PAMPs/DAMPs, cell surfacelocalized PRRs recruit co-receptors to form receptor complexes and activate downstream RLCKs, which subsequently phosphorylate downstream components (e.g. RBOHD, CNGCs/OSCA1.3, MAPKKKs, WRKYs) to trigger ROS burst, Ca2+ influx, MAPK activation, phytohormone production and transcriptional reprograming. Importantly, ETI resistance and responses are dependent on PTI pathway components and ETI potentiates PTI. Therefore, the two signalling cascades work together in a collaborative manner to ensure effective immunity. Solid arrows indicate direct effects and dashed arrows indicate indirect effects. Question marks indicate unknown mechanisms. Adapted from Yuan et al., 2021b.

1.3.2 The ETI

Another layer of microorganism recognition by the plant host is the direct or indirect recogntion of microbial virulence factors inside the cells by nucleotide-binding leucine-rich receptors (NLRs), often referred as Resistance (R) proteins, and activation of Effector triggered immunity (ETI) resulted in an enhanced resistance and hypersensitive response (HR) (Yuan et al., 2021b).

Intracellular R proteins usually consist of a middle nucleotide binding (NB) domain, a C-erminal leucine rich domain (LRR) and a N-terminal variable domain. NLRs proteins can recognize pathogen effectors by direct protein-protein interaction or by perception of the changes in other effector target. The database of functionally validated plant NLRs RefPlantNLR contains 481 proteins from 31 genera of plants (Kourelis et al., 2021). Upon activation, NLRs form a multimer structure for further signal transduction. Recent advances in structural biology demonstrated that Arabidopsis ZAR1 protein froms a complex with a resistance-related kinase 1 (RSK1) to sense bacterial effector AvrAc from *Xanthomonas campestris,* which uridylates the PBS1-like protein 2 (PBL2) kinase. PBL2 is reqruited into RSK1-ZAR1 complex, which oligomerize into pentamer having pore-like structure (Wang et al., 2019). When anchored into membrane induce Ca2+ flux into plant cell to activate cell death (Bi et al., 2021). While ZAR1 is acting itself in the resistosome serving both functions as sensor and executor, some other NLRs recruit helpers to transduce the signal for ETI activation. NRG1 protein serves as a helper for numerous sensing NLRs, which activate NRG1 to induce calcium flux and cell death by the mechanism similar to ZAR1 (J. Chen et al., 2021).

Rice genome encodes paired NLRs Pik-1/Pik-2 and RGA5/RGA4, which are responsible for recognition of MAX effectors of a fungal pathogen *Magnaporthe oryzae.* Both of these NLR pairs are harbouring a heavy metal-associated domain (HMA) and for both NLR pairs the physical interactions of an effector and a HMA domain is needed. Pik-1/2 NLR pair is able to recognize AVR-Pik effector of *M. orizae,* Pik-1 receptor is able to recognize the effector and requires Pik-2 to induce downstream signalling. In RGA5/4 mechanism, RGA4 is able to induce downstream reaction upon recognition of AVR-Pia and AVR-CO39, while RGA5 serves as inhibitor of RGA4 signalling in the absence of a pathogen (Białas et al., 2018; Césari et al., 2014).

1.3.3 ETI-PTI crosstalk

The succesfull activation of PTI and/or ETI prevents the infection and leads to incompatible to interaction between a plant host and the pathogen. The most common output of the recognition is a hypersensitice response (HR), characterized by a rapid and a local cell death at the point of a pathogen contact (Balint-Kurti, 2019). Activated R protein initiate signal transduction, which leads to transcriptional reprogramming of the cells. The signal transduced through mitogen-activated kinase cascade, which at the end induces the biochemical changes in the cells (Meng and Zhang, 2013). Activation of immune response leads to transient accumulation of intracellular calcium. Several cyclic-nucleotide gated calcium channels (CNGC) were shown to be involved in the Ca2+ spikes in Arabidopsis induced by PTI or ETI. The calcium signal is important for further reaction such as ROS accumulation and stomata response (Yuan et al., 2021b). In the immune response the major role is also played by the hormonal regulation: mainly jasmonate (JA), ethylene (ET) and salycilate (SA) pathways. SA pathway is preferentially implicated into the response to biotrophic or hemobiotrophic pathogens, while JA and ET pathways are induced against necrotrophic pathway. SA and JA/ET pathway act antagonistically and their interaction tunes the immune response leading to adaptive reaction to various symbionts: pathogens and symbionts (Bari and Jones, 2009).

ETI and PTI are activated by the perception of different ligands by different receptors, the outcome of both immune cascades converge into similar output, leading to incompatible interaction between pathogen and host (**Fig. 4**). The recent studies conducted on *Arabidopsis* plant lacking receptors of either ETI or PTI demonstrated that two layers of plant defence are indispensible parts of plant immunity and are implicated in cross-regulation and cross-potentiation for adequate response (Ngou et al., 2021; Yuan et al., 2021a) .

1.3.4 Qualitative and quantitative resistance

ETI is playing a dominant role in the protection of plant againts microbial attack in certain plant genotype against specific races of microbes certain and is related to the development of the HR that restrict pathogen growth. Quantitative disease resistance (QDR) in constrast to qualitative resistance leads to a reduction of symptoms rather to an inhibition of symptoms. QDR is generally associated to mulitple quantitative trait loci (QTL) found in various genomic regions of the host plant (Pilet-Nayel et al., 2017). This resistance is more difficult to decipher at the molecular level and to use in breeding programm as compared to the introduction of R genes in susceptible genotype (French et al., 2016).

The introduction of R genes is a popular strategy in breeding for resistance since mid-XX century. During the period from 1960s to 2000s in breeding programs of tomato in Japan, several R genes (called Cf-4, Cf-5, Cf-9) were introduced conferring resistance to biotrophic fungal pathogen *Cladosporium fulvum.* Cf genes encode LRR proteins, which can recognize Avr proteins from *C. fulvum.* However, several years after the introduction of resistant line into the commercial line, the new races of *C. fulvum* able to avoid recognition by Cf-proteins were detected in the environment (Iida et al., 2015). However, there are R genes which confer the resistance against multiple pathogens during many years, such as Lr34 and Lr67 genes in cereals (Spielmeyer et al., 2013).

In this context new source of resistance is required and the use of QDR is a great strategy to overcome this limitation. QDR shows incomplete resistance and is controlled by multiple genes with small effect of each, but more durable in terms of time and development of more aggressive races of pathogen. In contrast to qualitative, where genotypes could be divided into susceptible and resistance, the quantitative resistance is represented by continuum of the genotypes from low to high resistance, often following a normal distribution (Nelson et al., 2018). One stratetgy to identify genomic regions implicated in quantitative resistance, genome wide association studies (GWAS) are performed using the collection of diverse genotype or quantitative trait loci (QTL) mapping in population produced in artificial crosses (Khan et al., 2021).The genome regions contributing into the resistance are identified as QTLs, often the role of particular genes in building a resistant phenotype remain largerly unknown. The GWAS of a collection of genotypes of *Medicago truncatula* – a model legume plant – revealed a quantitaive resistance against root rot disease induced by oomycete *A. euteiches.* The study identified a major QTL, located on the third chromosome and include F-Box protein, which is known to play a role in the plant development and disease response (Bonhomme et al., 2014). To increase durability and resistance power of a genotype, in breeding program a pyramiding of a QTL is used, which is aiming to accumulate several QRLs in one line (Ashikari and Matsuoka, 2006; Pilet-Nayel et al., 2017).

1.4 Fungal and oomycete pathogenicity

1.4.1 Microbial Effectors

During the infection process of the host plant, eukaryotic filamentous pathogens such as fungi and oomycetes release molecules that act as virulence factors also called 'effectors. Those molecules could be proteins (Gaulin, 2017), metabolites (Lievens et al., 2017), toxins (Lamour and Kamoun, 2009) and small RNA (Iki, 2017). Increasing evidence and experimental studies have recently revealed that non-pathogenic organisms such as mycorrhizal (Voß et al., 2018), endophytic (Queiroz and Santana, 2020) and saprotroph (Feldman et al., 2020) also produce such type of molecules. Thus 'effectors' should be described as molecules that are secreted by microorganisms to affect physiology of host cells or environment and facilitate microbial invasion or niche colonization.

Numerous effector proteins harbor a signal peptide at the N-terminus to be secreted in the extracellular space making easier their *in-silico* detection by genome mining (Sperschneider and Dodds, 2021). Around 15% of all predicted proteins of fungi and oomycetes are supposed to be secreted (Choi et al., 2010). Nevertheless, size and composition of 'effectomes' vary greatly between microorganisms including at the intraspecific level, ranging from as little as 80 in entomopathogenic fungi *Nosema ceranae* to over a thousand of effector proteins per isolate in some fungi, and oomycetes as *Phytophthora* spp. with a tendency of higher secretome size in plant pathogenic hemibiotrophs (Kim et al., 2016; McGowan and Fitzpatrick, 2017). Presence of a signal peptide is a good characteristic of the sequence for effectors selection from whole predicted secretome. However, numerous effectors without a signal peptide, but still acting outside a pathogen's cell were described in filamentous pathogens. Thus effectors secreted by unconventional secretion pathway were reported, for example in fungus *Magnaporthe oryzae* and oomycete *P. infestans* (Giraldo et al., 2013; Liu et al 2014).

One key point regarding effectors studies is their functional characterization, thus secreted 'effectors' are usually classify based on different criteria as: i) by the target cell compartment (e.g. apoplastic vs intracellular effectors), ii) by the putative function (predicted or not predicted), by the size and amino acid component (small secreted proteins, cysteine-rich) , iii) by the expression profile (early, later stage of infection), or iv) by structural prediction (sequence-unrelated structurally similar effectors). All of these criteria are useful to support genomic annotation and to predict activity of the secreted protein (Kim et al., 2016; McGowan

and Fitzpatrick, 2020, 2017; Seong and Krasileva, 2021) but functional studies are required to validate the putative function.

1.4.1.1 Effectors with a conserved functional domain

To get first information about the molecular function of the effector, the prediction of a functional domain PFAM/SMART or InterPro could be done. Among the effectors with functional domain fungi and oomycetes secrete proteins, which serve for adhesion, nutrient acquisition and also for triggering necrotic/cell death symptoms Such proteins are often rich in cysteine residues (usually 6 or 8 residues per protein), which stabilize 3D structure of the protein.

Numerous effectors with a functional domain present necrotic activity within the host cell. Among them *Phytophthora* species have two families of cell death inducing proteins: elicitins (PFAM PF00964) and NLP domain (PF05630, necrosis- and ethylene-inducing peptide 1)-like proteins to less extent some pectate lyases or glycoside hydrolases can also act as cell death inducing proteins. (Li et al., 2020). One of the most studied proteins are elicitins, which demonstrate the sterol binding activity (Mikes et al., 1998), which could be important for nutrient function for sterol auxotrophic Peronosporales oomycetes, while its cell death induction is not dependent on sterol binding activity (Derevnina et al., 2016). As sterol and fatty acids stimulate sexual reproduction and oospore formation in *Phytophthora,* elicitins may also contribute to the development of more aggressive strains (Chepsergon 2020). Elicitins actively induce cell death on *N. benthamiana* and different plant species as tomato or potato, however differential responses can occur within a given taxon of plant (Kamoun et al., 1998, 1997). The small ~24k Da NLPs proteins have a dual function in dicotyledonous plants, i.e activating immune responses and inducing necrosis, but the mechanisms are still not well understood. While NLPs genes are identified in fungi and oomycetes with a large expansion in *Phytophthora* species thanks to tandem duplication events, NLPs seems to be absent from Saprolegniales genomes, except for *A. euteiches* (Gaulin et al., 2008). The vast majority of fungal and oomycetes NLPs have a N-terminal signal peptide (Seidl and Van den Ackerveken, 2019). Among cell death inducing effector with a functional domain, Cerato-platanin family proteins (IPR010829) are another secreted protein family found only in filamentous fungi including in *B. cinerea, S. sclerotiorum*, and *Magnaporthe oryzae* (Yang et al., 2009) but seems to be absent in oomycetes (Gao et al., 2020). Another cell-necrotic effector belongs to the CBEL family firstly reported as a cell wall protein from *Phytophthora parasitica.* CBEL-like

protein with cellulose-binding domain (CBM1, PF00734) within the sequence in addition to PAN-Apple domain (PF00024) are largely distributed within oomycetes and contribute to *P. parasitica* pathogenicity (Gaulin et al., 2002).

A large set of effectors predicted with a functional domain, as a PFAM domain, correspond to plant cell wall degrading enzymes (CWDE) acting consequently in the apoplastic space of the infected tissues in contact to the pectocellulosic plant wall. The apoplast is the cell matrix located beyond the plasma membrane and is the first point where microbes contact the plant either in roots or leaves (Sattelmacher, 2001). The root cell wall is built from cellulose-xyloglucan framework with prevalence of xyloglucans in dicots embedded in a network of pectic polysaccharides (Pauly et al., 1999). Thus to get through plant cell wall, plant-associated pathogens release a set of CWDE, which mostly consist or glycosyl hydrolases families (GH) and pectate lyases (PL) also regrouped as CAZymes (Lombard et al., 2014). Interestingly, the secreted CAZymes appeared to be not only apoplastic effectors targeting the cell wall. Indeed, Glycoside Hydrolase family 11 protein from fungal plant pathogen *Verticillium dahliae* promotes the pathogenicity through nuclear localisation (Liu et al., 2021)

Along with CAZYmes, filamentous pathogens possess a large repertoire of proteases. According to a MEROPS database the proteolytic enzymes are classified into clans and then families according to the structure and function of their catalytic pocket (Rawlings et al., 2014). Analyses of fungal and oomycetes genome identified families of secreted proteases whose expression may support a putative role as pathogenicity factors probably to facilitate growth of the pathogen. Global analysis of fungal proteases revealed 22 families of proteases are present in the secretomes of fungi. The major groups of these proteases correspond to serine, cysteine, aspartic, metalloproteases (for review see Franceschetti et al., 2017). A clear enrichment in trypsin (S1) and subtilisin (S8) proteases are observed in pathogenic fungi (Muszewska et al., 2017). The recent analysis of Metalloproteases (MP) of Stramenopila, with focus on Oomycetes, revealed the high variability in MP content and potential involvement in pathogenicity process of *P. infestans* (Schoina et al., 2021). Secreted trypsin-like protease from *Septoria nodorum* SNP1 constitute the unique example of purified and functionally characterized serine protease. SNP1 was demonstrated to directly destruct plant cell wall (Carlile et al., 2000) by targeting Hydroxyprolin-rich (HRGP) structural proteins (Mazau and Esquerré-Tugayé, 1986). Jashni et al 2015 identified collaborating secreted fungal serine- and metalloproteases from *Fusarium oxysporum*, which are responsible for cleavage of Chitin Binding Domain (CBD) of the tomato secreted antifungal chitinases *SlChi1* and *SlChi13*

leading to a less active immune enzyme. Genome mining of the fish pathogen *S. parasitica* linked the abundance of secreted proteases with an adaptation to animal hosts (Jiang et al., 2013). Gene editing of an extracellular serine subtilisin protease from *Aphanomyces invadans* drastically reduced fish ulcerative symptoms (Majeed et al., 2018) and extracellular proteases from *Saprolegnia parasitica* and *A. invadans* secreted in culture medium have been reported as active against fish immune IgM antigen, suggesting their contribution as virulence factors (Jiang et al., 2013; Majeed et al., 2017).

Growing evidences highlight the importance of proteolytic cascades in the plant apoplastic space for activation of plant defense (Misas-Villamil et al., 2016; Paulus et al., 2020). Plants and pathogens evolved various defensive and counter-defensive proteases and inhibitors acting in the apoplastic space, which signalize about the importance of proteolytic cascades in plant-pathogen interaction. Thus fungal/oomycetes effectors harboring a protease inhibitor activity are reported (Avr2 from *Cladosporium fulvum* (Shabab et al., 2008), Pit2 from *Ustilago maydis* (Mueller et al., 2013)). Some are also known to act within the host cytoplasm as suspected for cysteine protease inhibitor UfRTP1p from the obligate rust fungi *Uromyces fabae*. Within oomycetes genomes, the serine protease inhibitor 'Kazal-like domain' (PFAM PF07648) is enriched in 33 of 37 oomycetes species analyzed by Fitzpatrik et al., 2017. Accordingly, *P. infestans* as other oomycetes, genome encodes numerous secreted protease inhibitors, among them two Kazal-like inhibitors EPI1 and EPI10 were characterized as inhibitors of defense-related serine protease P69B, which is known as an immune hub (Tian et al., 2005, 2004). Furthermore, two cystatin-like inhibitors EPIC1 and EPIC4 were also described in *P. infestans,* which target pathogen-related cysteine protease PIP1 (Tian et al., 2007).

1.4.2.2 Effectors with a conserved sequence motif

Numerous of fungal or oomycete secreted proteins have weak or no sequence similarity with functional domain (Feldman et al., 2020). These proteins tend to have low molecular weight, high cysteine content and low serine content (Sperschneider et al., 2018). Comparative analysis of avirulence proteins from *Phytophthora* species led to an identification of modular secreted proteins thanks to a conserved N-terminal RxLR motif, which stands for R(arginine)-X(any amino acid)-L(leucine)-R(arginine) motif (for review see (Anderson et al., 2015; Birch et al., 2008; Fabro, 2022), while the Cterminal part is highly variable. The role of RxLR motif is still under controversy, however it was shown that it is responsible for the protein

translocation, since a protein mutated in RxLR domain fails to translocate into plant cells (Birch et al., 2008). Nevertheless the later studies showed that N-terminal motif is cleaved out within the pathogen's cell, before translocation within the plant cell (Wawra et al., 2017). Hundreds of RxLRs are predicted in *Phytophothra spp, Peronospora spp, Bremia spp, Pythium* spp (Chepsergon et al., 2021). However, the oomycete phytopathogenic species within *Albugo, Saprolegnia* and *Aphanomyces* genus encode for none or very few RxLR effectors (Furzer et al., 2022; Elodie Gaulin et al., 2018; Jiang et al., 2013a). Comparative genomics of fungi revealed that the RxLRs proteins if not absent, at least not so abundant in fungi as compared to oomycetes (Lo Presti et al., 2015).

Description of modular proteins such as RxLRs stimulated the search for the other conserved motifs. It led to a discovery of proteins harbouring conserved N-terminal LFLAK motif responsible for translocation and C-teminal part governing its function (Haas et al., 2009; Schornack et al., 2010). Oomycete genomes contain numerous CRN effectors, while the numbers vary between the species: *P. infestans* > 400, *P. sojae* > 80, *A. euteiches* > 160 (Gaulin et al., 2018; Haas et al., 2009). Being firstly described as oomycete effectors, CRNs are ubiquitously present in filamentous organisms and some of them probably horizontally transferred between evolutionary unrelated organisms, as CRN13, which homologs were identified in the genome plant pathogenic oomycete *A. euteiches* and animal pathogenic animal pathogenic fungus *B. dendrobatidis.* AeCRN13 harbours HNH-like endonuclease module and shown to interact directly with a DNA of a host cell and induce DNA-damage (Ramirez-Garcés et al., 2016). The studies of symbiotic fungus *R. irregularis* demonstrated that it has a large set of 82 CRNs (Voß et al., 2018) demonstrating that CRNs are important effectors for establishing pathogenic or symbiotic interactions between plants and fungi or oomycetes.

The screening of fungal genomes for the putative pathogenicity factors led to the identification of Small Secreted Proteins (SSP), which are induced during pathogenicity process (Kim et al., 2016). SSP's are less than 300 amino acids in length without predictable functional and transmembrane domains, and accounts for a large proportion (40-60%) of a fungal secretome (Kim et al., 2016). SSPs were identified in the genomes of pathogens and saprotrophs, signifying that SSPs has various roles in fungal interactions (Feldman et al., 2020). Among the fungal SSPs, numerous effectors contributing to virulence were identified, a 74 amino acid peptide encoded in the genome of *Colletotrichium gloeosporioides* supresses host cell death of death during the infection of *Stylosanthes guianensis* and shown to be indispensable for a biotrophic stage of a pathogen (Stephenson et al., 2000). *V. dahliae* genome

encodes over hundred cysteine rich SSP, some of them were shown to be involved in plant pathogen interaction and induce BAK1 and SOBIR1 dependent cell death in *N. benthamiana* (Wang et al., 2020). The SSPs were identified not only in pathogenic organisms, but also in symbiotic and saprotrophic fungi, which signifies about the broad functions carried out by SSPs. Poplar ectomycorrhizal fungus *Laccaria bicolor* secretes SSP7 protein, which interacts with jasmonate defense pathway proteins (i,e JAZ) putatively favours the establishment of the symbiosis (Daguerre et al., 2020).

Recently the presence of SSP in oomycetes were supported by studies of our research group. In genome of plant pathogenic *A. euteiches* around 300 genus-specific SSPs were detected, while in crayfish pathogen *A. astaci* 138 SSPs were found. Functional analysis of one cluster of six SSPs revealed an effector candidate AeSSP1256, which enhances plant susceptibility through inhibition of root development and binding to RNA helicase MtRH10 (Camborde et al., 2022; Gaulin et al., 2018). Genome-wide screenings of SSPs in oomycetes were not performed, therefore it could be expected that other oomycete possesses own set of SSPs as well. Since by definition SSPs are a very wide group of proteins the development of its classification is needed for better description of the SSPs repertoire in the organisms.

1.4.2.3 Effectors with a conserved structure

It is well established that protein structure is more conserved that amino acid sequence (Illergård et al., 2009). Almost 50% of oomycete RxLR effectors do not carry W/Y/L motifs, which are responsible for alpha-helix structure, however bioinformatics modelling predicted alpha-helixes at the N-terminus (Ye et al., 2015). The two studies published by Seong and Krasileva (2021 and 2022) demonstrated that phenomenon of sequence-unrelated structurally similar effector is widespread within several plant pathogenic fungi such as *Magnaporthe oryzae, Ustilago maydis, Puccinia graminis* etc. To perform such studies the reliable algorithm for structure prediction is needed, in 2021 the AlphaFold 2 neural network predictor was released, which significantly outperformed the available algorithms such as i-Tasser and trRosetta during 14th CASP (14th Community Wide Experiment on the Critical Assessment of Techniques for Protein Structure Prediction, https://predictioncenter.org/casp14/). The very recent release of predicted structures for 200 million proteins in the AlphaFold database gives a great opportunity to incorporate the structure analysis in the study of effectors (Jumper et al., 2021). In some fungal pathogenic species, the effectors with similar 3D structure were identified using predictive modeling approach, despite their low sequence similarity (less than

25% aa identity). As example one MAX effectors were identified in several fungal pathogens such as *Leptosphaeria maculans, P. tritici-repentis, Z. tritici and Botrytis oryzae*, from 2 to 6 effectors from the family were identified in *Colletotrichium* genus (de Guillen et al., 2015). However, MAX family undergone a huge expansion in the *Magnaporthe* genus with over 150 effectors per species (de Guillen et al., 2015). In addition, within structurally conserved MAX effectors the molecular mechanism of host target protein-binding is conserved rather than the host target proteins themselves (Guo et al., 2018). Another family of structurally-similar effectors correspond to LARS effectors. Firstly identified in biotrophic oilseed rape pathogen *L. maculans* as avirulence proteins (Lazar et al., 2022) , LARS effectors are conserved between *Leptosphaeria* species. (Lazar et al., 2022). The MAX and LARS effectors could be considered as lineage-specific effector as they are detected mostly within a single class of Dothideomycetes fungi.

Up to date, several structurally-similar effectors classes are described in fungi: LARS, RALPH, MAX, FOLD and ToxA-like. Those examples allows to hypothesize that a wide variety of effectors, without any apparent sequence relationship, could in fact constitute a limited set of structurally conserved effector families and that they have expanded in some fungal lineages or even in several fungal classes (Guo et al., 2018; Lazar et al., 2022). The structural prediction facilitates the identification of effectors, which have similar fold, but unrelated on a sequence level, however, it's far from the correct prediction of their activity in the host cell.

Within oomycete the structural similarity was shown for NLP effectors, which can trigger immune responses in plants cells, and cytotoxic mechanisms of NLPs have been recently precise thanks to the crystal structure of NLPs from *Pythium aphanidermatum*, which reveals a fold similar with pore-forming toxin from marine organism (Ottmann et al., 2009) and up to know 3D modeling approaches have not been used but can be probably useful to predict function of the large set of effectors with unknown function (i.e RxLR, CRN (Crinklers families), SSPs).

1.4.2.4 Molecular Function of effector: a special place of nuclear effectors

To promote microbial colonization, effectors could favour microbial growth by manipulation of plant defences, escape of pathogen's recognition and/or enhance invader nutrition (Gaulin, 2017). Thus, functions and targets of effectors are diverse and range from

altering plant cell surface or metabolic pathways, signalling cascades, supressing immune responses, blocking trafficking and/or acting on RNA silencing, transcription, and interfering with DNA machinery.

Plants can sense the presence of chitin as fungal PAMPs by the extracellular chitin receptors. To avoid triggering the plant immune response fungal pathogen *Cladisporium fulvum* encode apoplastic LysM domain containing effector Ecp6, which is able to sequester chitin residues so they are not detected by the plant receptors (de Jonge et al., 2010). LysM-domain effectors orthologs are widely present among plant pathogenic and beneficial fungi with the similar action of preventing chitin oligomer recognition (Kombrink and Thomma, 2013). Such effectors are present not only in pathogenic, but in beneficial fungi: Tal6 from the beneficial root-colonizing endophytic fungus, *Trichoderma atroviride*, and RiLysM from the root-colonizing arbuscular mycorrhizal fungus, *Rhizophagus irregularis* (Rocafort et al., 2020).

To avoid the transduction of immune signal, plant pathogens evolved to subvert the metabolism processes of the host. So *Ustilago maydis* effector Cmu1, which is one of the most strongly induced genes during the infection, encodes a chorismate mutase, which is delivered inside host cell. It interacts with a maize chorismate mutase ZmCm2 and enhance the flow of chorismate from plastids to the cytosol, in turn depleting the substrate for salicylic acid synthesis in plastids. This metabolism priming inhibits quick distribution of immune signals mediated by salicylic acid (Djamei et al., 2011). Another *U. maidys* intracellular effector Jsi1 reprograms the hormone signalling through binding to TOPLESS family protein, which leads to biotrophic susceptibility (Darino et al., 2021).

Host nucleus appears to be an important subcellular localization of pathogen's intracellular effectors. As was discussed above, host defense response is regulated by nuclear gene expression and protein trafficking inside and outside the nucleus (Yuan et al., 2021b). So it is expected for pathogen's effector to act in this compartment to alternate host transcriptional reprogramming through various modes as modification of histone patterns, modify transcription by direct interaction with nucleic acids or targeting host transcription factors (Stam et al., 2021). In addition, direct nucleic acid damage by introducing of double-strand break and aberration of the development of host cell also exploited by the pathogens (Camborde et al., 2019). Therefore, effectors localized in host nucleus take a special place in studying of a plant-pathogen interaction. In addition, numerous intracellular effectors have been shown to target this compartment. As example, a large screening assays of CRNs or RxLR

effectors in oomycetes revealed over 60% as nuclear localized, demonstrating that nuclei are important targets for intracellular effectors (Liu et al., 2018, Caillaud et al., 2012, Stam et al., 2013, Chen et al., 2020). Mining the literature data, identified over a hundred of oomycete nuclear effectors, among them the largest part is dedicated to study of RxLRs effectors and smaller part is for CRNs, outside of these two groups is only SSP from *A. euteiches*. The screening of 61 effector from Brassicaceae pathogen *Colletotrichum higginsianum* revealed the nuclei localization as the most frequent among effectors encountered for 40 nucleo-cytoplasmic and 9 nuclear effectors (Robin et al., 2018).

Inside the nucleus, one of the key functions of nuclear effectors is the manipulation of transcription machinery and transcription regulators to alleviate immune system induction (Fabro, 2022). Two nuclear effectors from rice blast pathogen *M. oryzae* MoHTR1 and MoHTR2 bind to a regulatory sequence of immune-related genes and act as transcription repressors, as a result downregulate the expression of many immune-associated genes in rice (Kim et al., 2020). Another mechanism of inhibition of early is exploited by oomycete pathogen *Phytophthora infestans* through inhibition of signal transduction through MAP kinase pathway. Pi22926 interacts with a potato mitogen-activated protein kinase kinase kinase, StMAP3Kβ2, in the nucleoplasm and supresses activation of MEK2, which in normal condition leads to a cell death induction (Ren et al., 2019). AeCRN13 effector from oomycete *Aphanomyces euteiches* carries HNH endonuclease domain and induce cytotoxicity and aberrant development in host cells through introduction of double-strand breaks (Ramirez-Garcés et al., 2016)
Several fungal and oomycete effectors were shown to modulate the transcription of host cells through alteration of histone acetylation patterns (Chen et al., 2022; Kong et al., 2017). Effector UvSec117 from the rice false smut fungus *Ustilaginoidea virens* is able to enhance histone H3K9 acetylation level through a translocation of host HDA701 histone acetylase into nucleus (Chen et al., 2022). Controversy, suppression of H3K9 acetylation is exploited by oomycete *Phytophthora sojae,* which. PsAvh23 effector binds to ADA2 subunit of histone acetylase complex SAGA and as a result supresses H3K9 histone acetylation. Silencing of ADA2 or overexpression of PsAvh23 leads to increased susceptibility of soybeans (Kong et al., 2017).

The direct interaction with the transcription factor and modulation of its activity is another mechanism used by the pathogens to promote the infection. Oomycete *Hyaloperonospora arabidopsidis* nuclear targeting effector RxLL470 can bind the HY5 transcription factor, which positively regulates pathogen-related genes. RxLL470 attenuates HY5 binding activity to DNA and negatively regulates the expression of many immune-related

genes (Chen et al., 2021). RxLR effector from *P. infestans* Pi22798 promotes the infection through induction of homodimerization of the transcription factor KNOX3, which regulates transcription of susceptibility genes, as its overexpression enhance host susceptibility while the silencing decreases it (Zhou et al., 2022).

In addition to targeting DNA and proteins, the effectors also can target ribosomal subunits as pseudoenzyme effector CSEP0064/BEC1054 from biotroph *B. graminis,* which binds the ribosome to inhibit the action of plant ribosome-inactivating proteins (RIPs) (Pennington et al., 2019). Nuclear effector Pst_A23 from *Puccinia striiformis* directly binds to pre-mRNA of immune related host proteins TaXa21-H and TaWRKY53 and induce incorrect splicing of their mRNA (Tang et al., 2022). Another effector, which perturbs transcription process is AeSSP1256 from *A. euteiches*, which hijacks nuclear RNA Helicase MtRH10 from *Medicago truncatula* and enhance host susceptibility and delays host root development (Camborde et al., 2022).

1.4.2.4 Environmental effectors

In the natural environment, the interaction between a microbe and a plant never happens in one-to-one settings and the infection success doesn't only depend on overcoming plant defense, but also the interaction with plant microbiota (Gaulin, 2017). One can suspect that the effector repertoire used far beyond manipulation of host immunity, but manipulation of environmental condition (pH, redox status) or microbe-microbe communication to shape the microbiome. Indeed recent studies show that the infection by pathogens modulates the host microbiome composition (Panstruga and Kuhn, 2019). Therefore, Snelders et al. (2018) suggested the following grouping for effectors: 1) effectors implicated in manipulation of host immunity; 2) effectors manipulating both pathogen immunity and host microbial community; and 3) effectors directed only to manipulation of host microbial community. Many studies of microbial communities highlighted that virulence of pathogen is dependent of host microbial composition (Carrión et al., 2019; Klein et al., 2012; Mariotte et al., 2018) and those interaction with host microbiome could be mediated through secreted effectors that could be identified as 'environmental/ecological effectors'. To colonize niches and combat with other microbes the fungal pathogens may probably exploit their effector arsenal using two major ways: by direct antimicrobial function or by manipulation of the microbial host metabolism, which shapes plant microbiome (Snelders et al., 2018b). Few example illustrate this concept as the Zt6 effector from the wheat pathogen *Z. tritici* that induce toxicity either on plant, bacteria yeast and filamentous fungi (Kettles et al., 2018). In addition, VdAve1 effector from *Verticillium dahliae*

continuously expressed during infection and during mycelia stage, possesses antimicrobial functions, and is able to modify microbial community organisation during the soil and infection stages (Snelders et al., 2020). Future studies of the pathogen-microbiome interaction at the level of environmental effector will open new perspectives in sustainable pest management (Hashemi et al., 2022, Gaulin et al., 2017).

1.5 Genomics and Effectors Evolution

Fungi and Oomycetes have rather small genomes, in average less than 100 Mb in size, with few exceptions as *Phytophthora infestans* (> 200Mb). Up to date hundreds genomes of fungi and oomycete were sequenced, with a great participation of a fungal 1000 genomes project (Grigoriev et al., 2014). Some fungal pathogens possess dispensable chromosomes, carrying pathogenicity genes, and their loss diminish the infection ability of the strain, up to now 14 fungal species described to carry dispensable chromosomes (Plaumann et al., 2018). For both fungal and oomycete genomes the high duplication rate of the pathogenicity genes was observed (McGowan et al., 2019; Pendleton et al., 2014)

Genome sequence is the starting point and one of the major prerequisites for genome-wide analysis of pathogen's biology and effectors identification. The first oomycete genomes were published in 2006 for *P. ramorum* and *P. sojae* (Tyler, 2006) and in 2009 for *P. infestans* (Haas et al., 2009). Those two studies showed the great variability in genome size even within one genus of oomycete: genomes of *P. ramorum* and *P. sojae* were sized at 65 Mb and 95 Mb respectively, while genome size of *P. infestans* reached 229 Mb. Up to date, the smallest oomycete genome is biotroph *Peronospora effusa* 32 Mb and the largest is another biotroph *Plasmopara obducens* with a genome size of 295 Mb. (Fletcher et al., 2018; McGowan and Fitzpatrick, 2020). The size of predicted proteome is also varies greatly within oomycetes from 10 to 26 thousands of proteins in *P. nicotianae* and *P. parasitica* respectively, while the proportion of the secretome varies between 2% and 8% (McGowan and Fitzpatrick, 2017).

Whole genome sequencing of multiple species allowed discovering that genetic landscape is not equal throughout the genome. Comparative analysis of the whole genome sequences and studying of the landscape of the genome regions, where the effectors are localized led to the development of 'two-speed' genome concept (Croll and McDonald, 2012; Dong et al., 2015; Raffaele and Kamoun, 2012), where it was demonstrated that pathogenicity effectors localized mainly in the gene-sparse region enriched in transposable element, whereas the 'housekeeping' genes are localized in the gene-rich regions. The evolution rate of the gene-

sparse region is shown to be higher than in gene-dense regions. One of the possible ways to speed-up the evolution is the presence of transposable elements in the proximity of the effector genes, which replication and recombination within genome can regulate lifecycle of the genes in the genome (Fouché et al., 2018). Strikingly, the effector genes of *P. infestans* were predominantly found in such gene-sparse TE-rich regions, such compartmentalisation of the genome gives advantages of rapid evolution of the effector repertoire and protect the housekeeping genes from unwanted mutational burden (Dong et al., 2015). Further studies demonstrated, that the clear two-speed divergence of the genome is not the rule for all plant pathogens (Dong et al., 2015), whereas the compartmentalization of the genomes is more correct description of the organization of the effectors-encoding genes (Torres et al., 2020). As example, for oomycete pathogen *A. euteiches* the absence of clear two-speed genome was demonstrated, but the clusters of effectors-encoding genes were described (Gaulin et al., 2018).

Activity of transposable elements are linked to the gene duplication events, where the duplicated genes can acquire new function during the pathogenicity (**Fig. 5a**). Another source of novel pathogenicity genes within filamentous pathogens is Horizontal Gene Transfer (HGT), which enables cross-kingdom exchange of genetic material. The processes, which increase amount of effectors in the genome lead to a redundancy in an effectome of a pathogen (Sánchez-Vallet et al., 2018). The redundant effectome helps to rapidly adapt effectors to recognition of one of the effectors by a host plant. Thus, pathogens need to maintain the rapid evolution to be able to escape from the recognition by the plant NLRs. The most efficient mechanism leading to the loss of an effector gene is related to the activity of TEs. TEs can drive multiple effects on gene sequence, from gene disruption to repeat-induced point (RIP) mutations, Open Reading Frame (ORF) disruption, epigenetic silencing or promotor insertion (**Fig. 5b**). Adaptive loss of function was reported in the fungal pathogen of wheat *Zymoseptoria tritici*, where gene losses affected more than 10% of all genes in the genome, including both effectors and genes with conserved functions such as secondary metabolite gene clusters (Hartmann and Croll, 2017). The point mutations are also the driving factors of the effectors evolutions, which could be divided into two classes. The first, are insertions, deletion, substitutions, which directly affect the protein properties, while the second are mutations, which have a weak effect on the protein properties but are cumulative. Fixation of beneficial mutations leads to optimization of the effector function and can infer the past selective history at the effector locus. (Sánchez-Vallet et al., 2018).

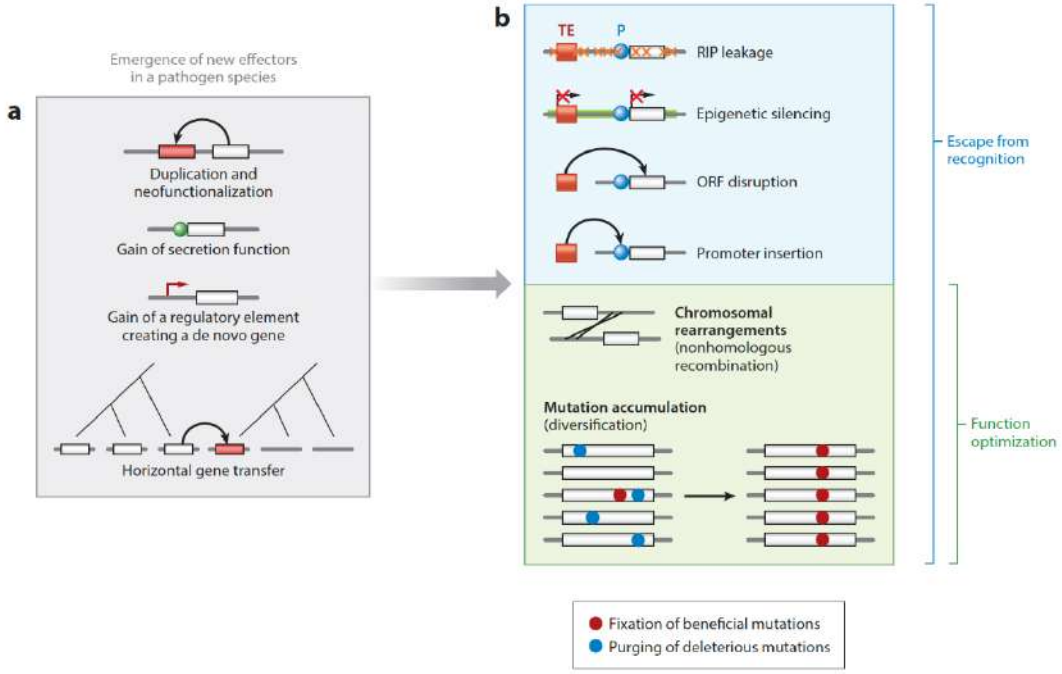

Figure 5. Evolutionary death and birth of the effectors. (A) New effectors can emerge through gene duplication or the gain of a secretion function. Effector genes may also evolve de novo from noncoding sequences through the gain of a regulatory element or be acquired horizontally from a different pathogen species. (B) Effector genes can undergo rapid sequence evolution upon recognition of the encoded effector by the host. The major mechanism leading to the loss of an effector gene is the presence and activity of nearby transposable elements (TEs). The effects of the transposable elements can include repeat-induced point (RIP) mutations, epigenetic silencing or the disruption of the gene sequence. Escape from recognition can also be mediated by chromosomal rearrangements or the fixation of beneficial mutations. Rearrangements and selection for beneficial mutations are also major routes for effectors to optimize their function. Abbreviations: ORF, open reading frame; P, promoter regions. From Sánchez-Vallet et al., 2018.

Comparative genomics studies helped to uncover the adaptation tendencies in the effectome of various oomycetes. In general, biotrophic pathogens have smaller arsenal of the secreted effectors compared to necrotrophs and hemibiotrophs (Gómez-Pérez and Kemen, 2021). Oomycete show large genome plasticity upon the adaptation for the host and lifestyles and demonstrate multiple events of lineage-specific gene acquisition and duplication events (McGowan and Fitzpatrick, 2020). As illustration, the pathogens of organism containing chitin at their outer barriers, fungi and crayfishes, demonstrate the enrichment of chitin-targeting enzymes as in genomes of *P. oligandrum* and *A. astaci.* Remarkably, these species possess specific chitin targeting-enzymes such as GH19, GH46 in *P. oligandum,* which are not present in phytopathogenic species of the same genus (Faure et al., 2020; Gaulin et al., 2018).

1.6 Methods to identify and prioritize effectors for functional characterization

Recent advances in high-throughput sequencing technologies have facilitated the availability of several fungal/oomycetes genomes and of transcriptomes, allowing the prediction of extremely large repertoire of putative effectors. The bottleneck of the studies resides firstly in the selection of candidate effector for functional experiments and secondly in the functional methods to identify the role of such genes for plant-microbe and microbe-microbe interactions.

1.6.1 In-silico methods, efficient approaches to predict effectors

The *in-silico* prediction of microbial effectors is often based on several software, which can predict the biochemical properties based on protein sequence. There is a large diversity of tools available for the identification of signal peptide, conserved motifs, signature sequences and structural features in the proteins. Many pipelines and online servers, which combine several tools, are made available to help for genome-wide identification of effector proteins (for review see Sonah et al., 2016). In general steps presented in **Figure 6** are commonly used.

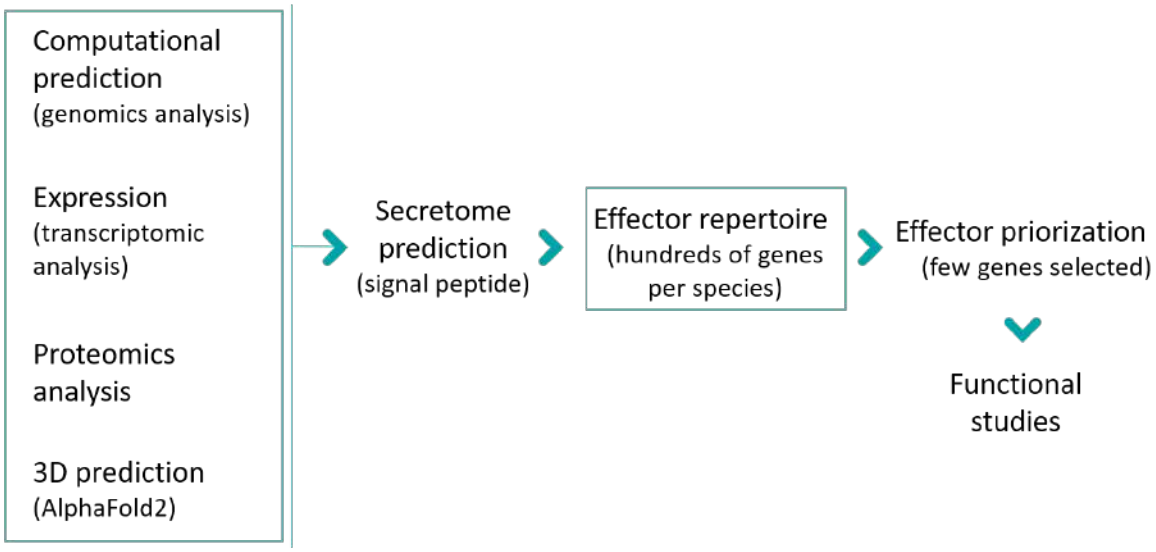

Figure 6. Flowchart of *in-silico* analysis can be used for the prediction of secretome and candidate secretory effector proteins in fungi and oomycetes and their prioritization for functional analysis.

First step of *in-silico* selection is filtering by the presence of signal peptide with SignalP (José Juan Almagro Armenteros et al., 2019) algorithm and absence of transmembrane domains with TMHMM algorithm (Krogh et al., 2001), so the proteins secreted into extracellular space or the 'secretome' of the microorganism can be predicted. This approach cannot cover all the secreted proteins due to the unconventional secretion pathway, which utilized by the pathogens to deliver the effectors. Previously it has been shown that around half of the CRN effectors from oomycetes do not possess a secretion signal at their N-terminus (Gaulin et al., 2018; Stam et al., 2013). *Magnaporthe spp*. intracellular effectors secreted through biotrophic interfacial using exocytosis for delivering proteins and such effectors do not have the secretion signal (Giraldo et al., 2013).

The other features, predicting subcellular localization of the secreted protein could be also predicted using various combination of algortihms, such as TargetP for prediction of mitochondrial, chloroplast and thylakoid transit peptide (Armenteros et al., 2019), or various options for nuclear localization signal (NLS) (Brameier et al., 2007; Horton et al., 2005; Nguyen Ba et al., 2009) Depending on species this filter ends up in from several hundred to over a thousand secreted proteins for each species. To restrict the list proteins with a conserved motif, i.e. at the N-terminus for CRNs and RxLRs, may be searched using regular expression

as realized in EffectR package (Tabima and Grünwald, 2019). Relying on the motif search only could mislead to the false positive effectors due to a random match of the motif. Therefore, the verification of the correct start-stop codons and if possible, expression should be done.

The massive work of genome sequencing and functional characterization of fungal and oomycete proteins creates a valuable dataset for further exploration. Recently machine learning algorithms were developed to predict the effector activity and subcellular localization of the proteins. EffectorP v3.0 is a tool, which using machine learning models trained on 64 apoplastic and 112 intracellular effectors. The software can discriminate the localization of the protein with a precision of 80-90% (Sperschneider and Dodds, 2021). The increase in diversity of characterized effectors should increase the predictive ability of EffectorP software. When the secretome of the species is predicted, the next step of the characterization of the effector candidate is the prediction of the functional domain. For that the sequence similarity search with a blast (Altschul et al., 1990) against lineage-specific or global RefSeq database and domain search using HMM algorithm against InterProScan databases can be performed (Jones et al., 2014). The rapid development of the structural prediction of the proteins thanks to development of precise algorithm, especially AlphaFold2 (Jumper et al., 2021) allows to introduce the structure similarity search for protein annotation. The studies performed by Seong and Krasileva, 2021, 2022 demonstrated the possibility of the secretome-wide search for protein structural similarity. Especially, this approach was useful for the identification of sequence-unrelated structurally similar effectors, such as MAX or LARS as reported previously. To discover novel families of structurally similar proteins, the accumulation and availability for the research community of the predicted structures is necessary to perform such studies.

Identification of the ortholog groups is an important task to study the effectome in the evolutionary and comparative genomics context. Several popular softwares such as OrthoMCL, OrthoFinder, OMA, InParanoid are available for identification of the paralogs based on the genome data. The orthologs analysis, for example, was used to decipher the gene losses linked to biotrophy in oomycetes (Dussert et al., 2019; Gómez-Pérez and Kemen, 2021; McGowan and Fitzpatrick, 2017). Also, OrthoMCL algorithm was used to identify the intragenus adaptation of the effectome to various hosts as could be seen on examples of *Aphanomyces* (Gaulin et al., 2018) or *Pythium* (Faure et al., 2020) genes. Functionally verified effectors are added into manually curated Pathogen-host interaction (PHI) database. In the version 4.8 released in 2019, the top three organisms were represented by plant pathogens

Fusrium graminearum, Magnaporthe oryzae and *Ralstonia Solanaceae* with 1340, 748 and 132 genes listed. A very important tool is PHI-blast, which allows a blast search for homologous sequences present in PHI database (Urban et al., 2019). *In silico* analysis outputs the secretome composition of the species, which consists of hundreds putative effectors. Up to now computational tools can hardly predict the function. Therefore, further shortlisting of gene set is necessary, which is based on the transcription profile of the corresponding gene (e.g. induction on the infection phase), or on a positive signal in screening tests, including transient overexpression of putative effectors (e.g. subcellular localization or enhancing susceptibility)

Expression data of the microorganism at different step of its life cycle and during different stages of the host infection provide important dataset to predict and select effectors for functional studies). For some of the effectors a tight regulation of the expression timing is observed. For example the microarray transcriptomics analysis of *M. orizae* effectors revealed the set of biotrophy-associated effectors, whose expression is highly induced in a biotrophic phase (Mosquera et al., 2009). Waves of expression in *Leptospahearia maculans* effector (Gay et al., 2021). Following the expression profile of effector candidates can give valuable information for the further selection of the candidate for a functional analysis and give hints about their function if they have a stage-specific expression profile.

In addition to genomics studies the exploitation of multi-omics approaches for the modelling of the filamentous organisms' lifestyles and deciphering its biology is now a key point to predict genes related to the microorganism biology. The combination of the proteomics and genomics approaches gives a first validation of the presence of the effectors in the pathosystem. Proteomics studies of *P. sojae* and *P. ramorum* validated the presence of 62 RxLR effectors in the infected tissue (Meijer et al., 2014). The time-resolved proteomics study of fungus *F. graminearum* revealed that the transcription and translation of the majority of the secreted proteins employed in the infection process already happened at the very early stage of the infection, when no symptoms could be observed (Fabre et al., 2019). Such time-resolved studies are useful to validate or correct the expression profiles of the genes, obtained by transcriptomics analysis.

For the pathogens with a high-quality reference genome, the association mapping could be used to identify virulence genes. Selection scams could identify the loci under selection without a priori knowledge. Quantitative trait locus mapping (QTL) and genome-wide association studies (GWAS) are designed to identify loci that mediate heritable phenotypic variation. GWAS and QTL differ primarily in the selection of the mapping populations. QTL

mapping analyses genetic variants segregating among progenies of a cross, whereas GWAS utilizes genetic variation among unrelated individuals from a natural population. For QTL approach only the species, for which two strains could be crossed and their progeny could be followed and tested for pathogenicity are suitable, while for GWAS studies the diversity of the field isolates needed to identify the genetic underlies of heritable traits. When both conditions are satisfied the QTL and GWAS approaches could complement each other (Plissonneau et al., 2017). Large GWAS study included 106 isolates of fungal wheat pathogen *Zymoseptoria tritici* revealed 25 genomic loci linked to the success of the pathogen, while the major loci encoded for a small secreted protein highly expressed during the infection (Hartmann et al., 2017).

Finally, the emerging applications of machine learning algorithms, which predict the organism lifestyle (Gómez-Pérez and Kemen, 2021), protein localization (Sperschneider and Dodds, 2021) and protein structure (Jumper et al., 2021) will help to aggregate and analyze the available data on multi-omics scale for better prediction of candidate effectors and prioritization strategy.

1.6.2 Screening methods to prioritize effectors for functional studies

Large set of predicted effectors are available within oomycetes and fungi, therefore a prioritization of the candidate is required before starting functional validation approaches. Thus prioritization could be done on the predicted subcellular localization of the effectors, the presence of a functional domain or motif, etc. In addition, screening methods to evaluate the activity of the effector toward plant defence responses or physiology have been developed. When available the genetic transformation of the pathogen is performed. These methods could be also used as screening methods since most of them are high throughput.

To screen the effector for their capacity to enhance the infection and/or affect plant immune responses, a set of effectors could be overexpressed in planta. This approach was used to screen the pathogenicity effect of the SSPs from a gene cluster in *A. euteiches*. The different putative effectors from the cluster were transiently expressed in *N. benthamiana* and the leaves were spot inoculated with *P. capsici*. The effector that showed the positive signal in the screening, was selected for functional studies and shown to enhance the pathogenicity of *A. euteiches*, on natural host plant roots (Elodie Gaulin et al., 2018).

A more throughput assay is based on the identification of the ability of the effector to suppress hypersensitive response and thus facilitate growth of bacteria used for its transfer

within the host cell. The bacteria are expressing luciferase construct and the luminescence is read to estimate the effect of the protein. Using this assay 64 RxLR effectors from biotrophic oomycete *Hyaloperonospora arabidopsidis* were tested, identifying over 70% being positive in enhancement of bacterial growth (Fabro et al., 2011).

Another readout corresponds to the absence of cell-death rather than development of a microorganism. In this system, recognition of the candidate protein within the cell by the NLR protein triggers ETI and leads to a programmed cell death. INF1 is known elicitin protein from *P. infestans* which triggers a cell death through recognition by ELR (Elicitin Response Protein) (Du et al., 2015). Co-expression of INF1 and testing effectors from oomycete biotroph *Pl. viticola* revealed that 52 of the tested effectors supress and 11 partially supress INF1-induced cell death, contrary, 10 effectors expressed alone induce cell death, 10 others do not have any effects on *N. benthamiana* cell death (Liu et al., 2018).

1.6.3 Methods to identify function of selected effectors

Effector proteins shortlisted during the selection process described above enter the functional characterization pipeline, which often starts from subcellular localization assay. The method of choice is an *Agrobacterium tumefaciens* mediated transient transformation of tobacco leaves for *in-planta* effector production (Marsian and Lomonossoff, 2016). To identify the localization of an effector, it is fused to a fluorescence tag (GFP, CFP, YFP, etc.) at C-terminus to identify localization (Sparkes et al., 2006). The great advantage of the method is relatively quick and simple procedure, which make possible to know protein localization within one or two weeks. Therefore, a semi-high-throughput studies could be performed to identify localization of a batch of effector candidates. Caillaud et al., 2012 characterized 49 RxLR proteins predicted in *H. arabidopsidis* genome and assigned them into 5 groups with regards to their subcellular localization: nuclear, nucleo-cytoplasmic, cytoplasmic, membrane, vacuolar. as was performed in several studies of effectors. Liu et al., 2018 studied subcellular localisation of 82 *Pl. viticola* effectors, which were localized in nucleus, nucleus + cytosol, chloroplast and membrane.

To check whether the candidate effector is secreted and could be delivered into host cell two widely used assays were developed: Yeast trap invertase assay and expression of the corresponding effector with or without signal peptide in plant cell. Yeast invertase is an essential secreted protein which allows yeast growing on sucrose or raffinose containing media.

The strains lacking invertase gene could not use sucrose or raffinose as a carbohydrates source. In yeast trap assay the plasmid carrying functional invertase gene lacking native C-term signal peptide fused to a signal peptide of an interested protein. The mock transformants are not able to sustain growth on sucrose media, but when a functional signal peptide is inserted, it produces secreted invertase, which complements initial invertase deletion in a strain (Jacobs et al., 1997; Klein et al., 1996; Lee et al., 2020). This assay is widely used in the testing of functionality of the signal peptide and could be used for both fungal, for example *Rizoctonia solani* (Wei et al., 2020), and oomycete, for example *Plasmopara viticola* (Lei et al., 2019) effectors.

As a first step in functionnal characterization, the cell-death activity of the effector is often evaluated by transient expression in Tobacco leaves. The necrosis could be caused by the direct cytotoxic effect of the effector or to its capacity to modify plant cellular process or to interact with a unknown resistance protein. This approach was sucessfully used for the massive screening of oomycete *Bremia lactucae* effectors which identified 11 WY proteins without canonical RxLR motif, which elicit the cell death in *N. benthamiana* (Wood et al., 2020). The detection of the cell death could be done visually or automatically by fluorescent imaging (Xi et al., 2021).

The classical reverse genetics approaches are widely used in studying the effectors' role in the pathogenicity such as effector silencing/overexpression. The RNAi techniques were used to identify the effect of the absence of certain effectors on the infection process. RNAi silencing is used in various filamentous pathogens such as *Phytophthora capsisi* (Cheng et al., 2022), *Fusariumn oxysporum* (Tetorya and Rajam, 2021), *Botrytis cinerea* (García et al., 2017) etc. The CRISPR/Cas systems were also developed for numerous fungi such as *Ustilago maydis* (Schuster et al., 2016), or oomycete like *Aphanomyces invadans* (Majeed et al., 2018), *Phytophthora sojae* (Qiu et al., 2021). The reverse genetics approaches require genetic manipulation of the pathogen, which is available for a limited number of filamentous organisms. However, the transient overexpression of the effector in the 'natural' host plant followed by microbial infection, could give some hints of the role of the effector for the pathogenicity (Camborde et al., 2022).

Identification of a host target is one of the most complicated tasks during effector functional characterization, which needs extensive analysis of the results because all the available methods will generate a lot of false positive hits (Free et al., 2009; Serebriiskii et al., 2000). Up to now, two methods of choice to identify if an effector interacts with a protein target are be co-immunoprecipitation (CoIP-MS) followed by mass spectrometry (Maccarrone et al.,

2017) and Yeast-two-hybrid assay (Y2H) (Brückner et al., 2009). Both of these methods exploit direct interaction between studied proteins. Co-immunoprecipitation assay with a GFP-tagged SSPs of *M. larici-populina* revealed multiple protein targets in the plant cells (Petre et al., 2015). This example reveals that the major limitation of Co-IP assay is the obtention of a large list of potential interactors. However, the application of multiple scoring systems, based on number of identified peptides by mass-spectrometry, for example, could help solving this issue. The application of scoring system and search for a unique target-effector helped to identify the poplar TOPLESS-related protein 4 as the target for an effector MLP124017 (Petre et al., 2015). Yeast-two-hybrid (Y2H) assay could be used for a genome-wide search of interactions between bait and prey protein and required in this case the composition of a library of the host genes encoded as prey proteins (Erffelinck et al., 2018). The recent study of lettuce downy mildew causative agent *Bremia lactucae* using Y2H genome-wide system allowed to identify the network of 61 protein-protein interactions between 21 *B. lactucae* effectors and 46 lettuce proteins (Pelgrom et al., 2020). As for co-IP numerous false positive or interactors could be identified by Y2H.Proximity-dependent biotin identification, also known as BioID, is a relatively recent method that can be used to identify protein interactions *in vivo* (Gingras et al., 2019; Kim & Roux, 2016; Roux et al., 2012). The assay exploits the ability of the bacterial biotin ligase BirA to promiscuously biotinylate proximal protein within a 10 nm range that contain a short peptide (Avitag). Once proteins are biotinylated, they can be extracted under denaturing conditions, isolated using affinity purification, and identified by mass spectrometry. BioID was firstly applied in human cells to identify Lamin A interactors proteins (Roux et al., 2012). It was successfully applied in plant-bacteria interactions to identify novel interactors of *P. syringae* effector HopF2 (Khan et al., 2018). Similarly, by using *Arabidopsis* plants stably expressing biotin ligase, Khan et al., 2018 identified 99 effectors proteins from *Fusarium graminearum,* (Miltenburg, 2019). BioID system is under development to characterize targets of *M. grisea* effectors using rice protoplasts (T. Kroj, personal communication).

Microbials effectors may also interact with nucleic acid rather than proteins. In this context, our research group developed a FRET-FLIM approach to decipher in *Nicotiana benthamiana* leaves nucleic acid / protein interaction (Camborde et al. 2017). FRET (Förster resonant energy transfer), utilizes energy transfer from a fluorescent donor (tagged-GFP effector) to an acceptor (sytox-labelled nucleic acid) that can take place only when the two fluorophores are situated at distances <~10 nm. Decreasing of the GFP fluorescence lifetime indicating a proximity of both interactors. Such approaches have been successfully used to

identify the interaction with nucleic acid for two *A. euteiches effectors:* AeCRN13 and AeSSP1256 (Camborde et al., 2022; Ramirez-Garcés et al., 2016).

1.7 Aphanomyces genus

Aphanomyces genus was firstly described by de Bary in 1860 as new genus of aquatic 'fungi' to include saprothrophic and parasitic fungi. The genus *Aphanomyces* corresponds to a Saprolegniales order, consisting of plant and animal pathogens and saprotroph organisms (Diéguez-Uribeondo et al., 2009). Currently *Aphanomyces* genus includes 19 species (NCBI taxonomy browser). Among them four species have commercial importance: *A. euteiches* (Gaulin et al., 2007b; Wu et al., 2018) and *A. cochlioides* (Kazunori Taguchi et al., 2009) that are plant pathogen on legumes and sugarbeet respectively (**Fig. 7**); and *A. invadans* (Iberahim et al., 2018) and *A. astaci* (Caprioli et al., 2018) that are animal pathogens of fish and crayfish respectively. Such broad host range within a genus makes *Aphanomyces* an interesting object to study the host adaptation within pathogenic oomycetes. Four *Aphanomyces* species are sequenced: *A. euteiches, A. astaci, A. invadans, A stellatus, A. cochloides* (Gaulin et al. 2018; Makkonen, Jussila, and Kokko 2012; Minardi et al. 2018, http://www.polebio.lrsv.ups-tlse.fr/aphanoDB/). The detailed review of biology, distribution, pathogenicity and measures to combat against of four economically important *Aphanomyces* species is presented in **Chapter I** of this manuscript in a form of a published co-authored review article in the journal of Fungal Biology Review (Becking et al., 2021).

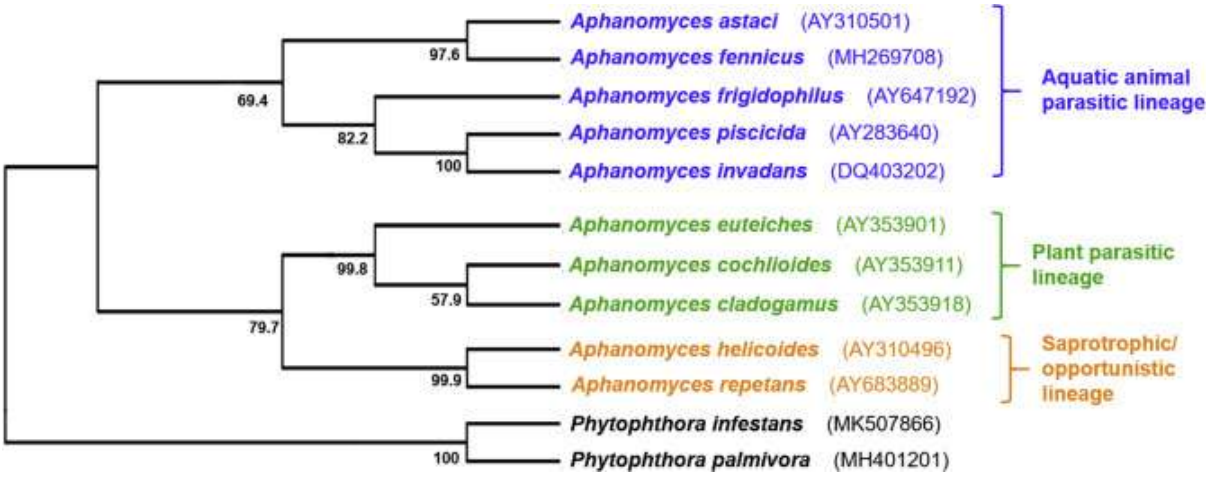

Figure 7. Cladogram of *Aphanomyces* species showing the three major lineages based on the host category. The phylogeny is based on 5.8S ribosomal RNA gene with a 691 nucleotides alignment length. The identifier written between brackets correspond to the NCBI accession number Adapted from Becking et al. 2022.

1.7.1 *Aphanomyces euteiches*, the legume pathogen interacting with *Medicago truncatula*

Aphanomyces euteiches is a causative agent of root rot disease of legumes, firstly described by Drechsler in 1925 after observation of pea fields in USA (Gaulin et al., 2008a) . *A. euteiches* is one of the major limitations to pea production worldwide and extensively studied in main production areas: North America (Gossen et al., 2016; Wu et al., 2018), France (Gaulin et al., 2007b; Quillévéré-Hamard et al., 2018), unfortunately no studies are done in other producing countries as Russia and China. The yield loss caused by *A. euteiches* could be as high as 70-80 % if the field is highly infected (Bogdan and Ag, 2019; Pfender and Hagedorn, 1982). As no chemical treatment or fully resistant cultivars are known so far (Quillévéré-Hamard et al., 2018), the crop rotation is the major strategy to avoid *A. euteiches* infestation, due to long time oospores conservation and broad legume host range, it's recommended to have legume rotation cycles of 10 years (Wu et al., 2018). The elucidation of *A. euteiches* pathogenicity mechanism is considered as an important step towards the breeding of resistant genotypes of leguminous crops (Desgroux et al., 2016).

A. euteiches has a wide range of hosts in *Fabaceae* family such as pea, alfalfa, trifolium, lentils, vetch etc. The studies of populations structures of *A. euteiches* showed the variability of pathogenicity and host preference of strains from both USA (Malvick et al., 2009) and french fields (Quillévéré-Hamard et al., 2018). Those data provide an idea of adaptation potential of the species and could be used as for detection of different isolates in the fields, however, no genomics data on different strains are available to understand the mechanisms of adaptation. *A. euteiches* can also infect the model legume *Medicago truncatula,* which allowed to gain molecular mechanisms of infection and resistance sources (Bonhomme and Jacquet, 2020).

Infection process of legumes including *M. truncatula* started with the encystment of flagellate zoospores in the close vicinity of the roots. After germination and once inside the root tissue, *A. euteiches* forms coenocytic hyphae which develop mainly extracellularly. After a few days, haploid antheridia and oogonia are formed in susceptible host. Oogonia are terminal, approximately spherical in shape and have a diameter ranging between 25 and 35 µm. Antheridia penetrate oogonia with fertilization tubes, which deliver male nuclei to the oogonia, resulting in the formation of diploid oospores (Scott, 1961). Tolerant *M. truncatula* lines restricts *A. euteiches* growth only to root cortex via pericycle cell division, lignin deposition and accumulation of phenolic compounds (Djébali et al., 2009).

Up to date there is no completely resistant genotype of the host plant were described. However, the genome wide association studies in Pea and *M. truncatula* demonstrated the quantitative resistance to *A. euteiches*. Pea QTL Ae-Ps7.6 explains over 50% of phenotypic variations using a collection of reference *A. euteiches* strains (Hamon et al., 2011, 2013). Combination of Ae-Ps7.6 with other QTLs delays symptoms' onset and slowdown root colonisation (Lavaud et al., 2016). The effect and stability of the QTL were validated using the large collection of *A. euteiches* strains from different regions of France (Quillévéré-Hamard et al., 2020), therefore the AeD990SW45-8-7 line, which harbours the combination of 4 major QTL Ae-Ps1.2, Ae-Ps2.2, Ae-Ps3.1 and Ae-Ps7.6 (Desgroux et al. 2016) might be used as a source of resistance in further breeding programs. GWAS studies on 157 lines of *M. truncatula* for resistance to *A. euteiches* identified two major loci on chromosome 3, both located in previously identified 135-kb *prAe1* locus (Djébali et al., 2009). The loci code for candidate F-box protein, and non-functional versions of these genes are related to more resistant genotypes, also significant SNPs were identified within an adenylate isopentenyltransferase (IPT) involved in cytokinin biosynthesis, and/or a MYB transcription factor regulated by gibberellin and abscisic acid (GAMYB) (Bonhomme et al., 2014, 2019).

Two genotypes Jemalong A17 and F83005.5 (commonly referred as A17 and F83) are routinely used as partially resistant and susceptible genotypes against *A. euteiches* infection. As depicted in **Figure 8**, using *in vitro* system, at 21 days after the infection *A. euteciches* hyphae reach the central cylinder of the roots in susceptible genotype, while in resistant genotype hyphae restricted only to a root cortex tissue. In comparison to susceptible genotype, in partially resistant *M. truncatula* division of pericycle cells is reinforced and phenolic antimicrobial compounds are accumulated **(Figure 8 b,c).** The cell wall of *A. euteiches* is composed in chitooligosaccharides (Badreddine et al., 2008), which allows staining with Wheat Germ Agglutinin to visualise hyphae localisation within infected roots. Microscopical studies showed that *A. euteiches* develops as intercellular filamentous microorganism and do not develop any haustoria-like structures (**Figure 8c**).

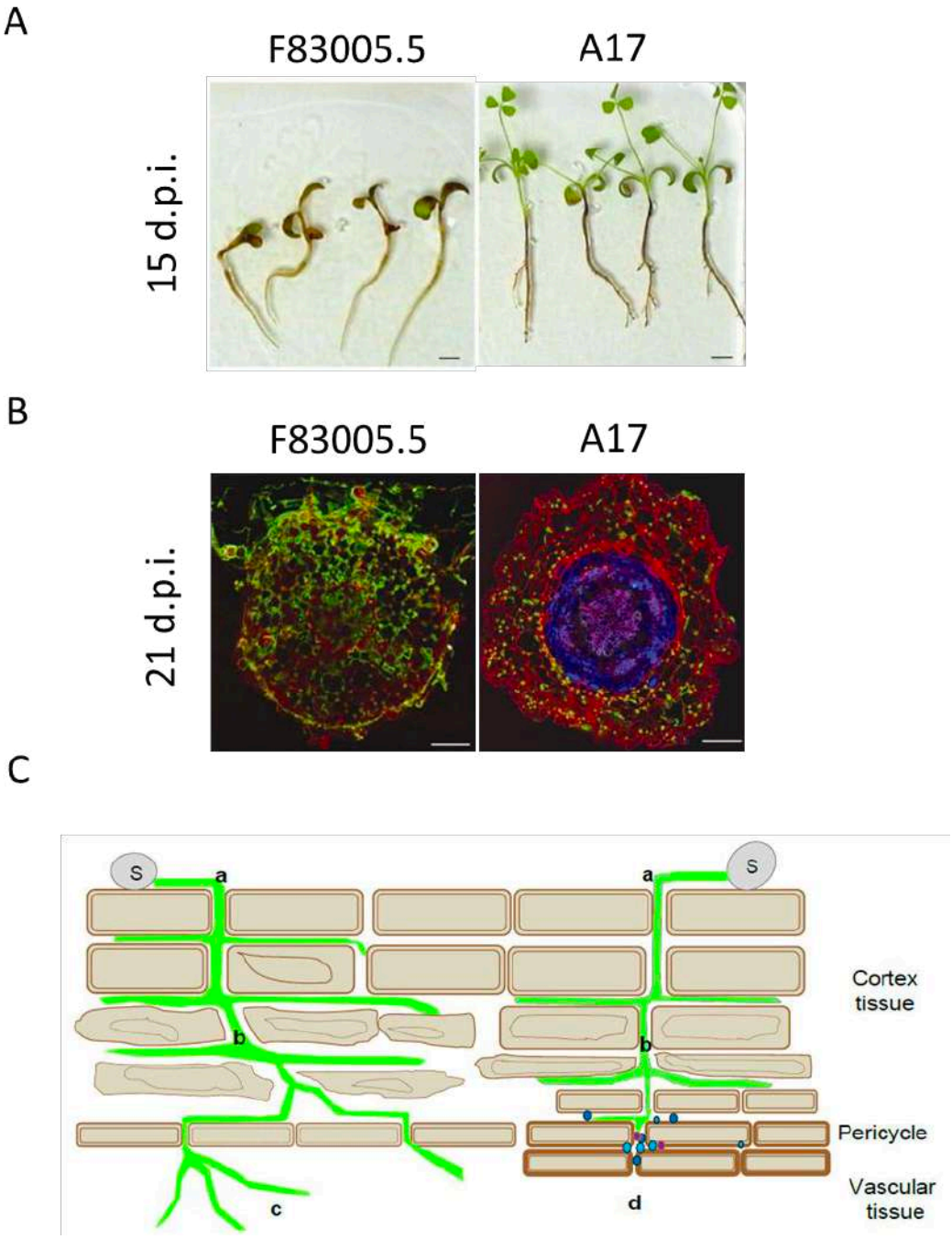

Figure 8. Infection model in the *Aphanomyces euteiches/Medicago truncatula* pathosystem. (A) Macroscopic symptoms of *M. truncatula* susceptible line F83005.5 and partially resistant line A17 infected with *A. euteiches* spores in *in vitro* conditions. Pictures were taken at 15 days post inoculation (dpi). Adapted from Djébali et al., 2009. (B) Cross-sections of infected roots showing full invasion (F83005.5) and partial invasion (A17) by *A. euteiches* (in green). Plant cell walls are coloured in red. A17 plants produced antimicrobial phenolic compounds (in blue) in the central cylinder. Pictures were taken at 21 dpi. Adapted from Djébali et al., 2009. (C) Scheme of a transversal section of a root infected by *A. euteiches* (in green).

1.7.2. *A. euteiches* effectors

The first genome annotation of *ATTC201684* strain of *A.euteiches* was published by our group in 2018 and was assembled by combining Illumina and 454 reads. Genome size was estimated to 57 Mb. The genome contains 19548 gene models with 6% being predicted secreted. Secretome encodes over 300 putative secreted carbohydrate-active enzymes (CAZy) and carbohydrate-binding modules. They include protein families targeting plant-specific polysaccharides (e.g. hemicellulases: GH 10, 11, CE4 families and pectinases: GH 28, PL1, 3, 4 families), which might be involved in penetration of plant cell wall (Lanver et al., 2014). Interestingly, animal pathogen *A. astaci* lacks those plant-specific families in its secretome (Gaulin et al., 2018). In contrast to Peronosporales oomycetes *A. euteiches* has no RxLR effectors, while it encodes a large set of CRN effectors (>160) and Small Secreted Proteins (>500). Functional studies on CRN and SSP effector candidate (**Fig. 9**) identified that AeCRN13 effector, is a DNA-binding nuclear-localized effector thanks to a HNH-endonuclease domain (Ramirez-Garcés et al., 2016) which triggers DNA-damage within roots to facilitate infection. One of the *A. euteiches* SSP (AeSSP1256) was shown during my PhD to enhance host susceptibility by hijacking *a M. truncataula* host DEAD-box RNA helicase that participate to ribosome pathway (Camborde et al., 2022; Gaulin et al., 2018).

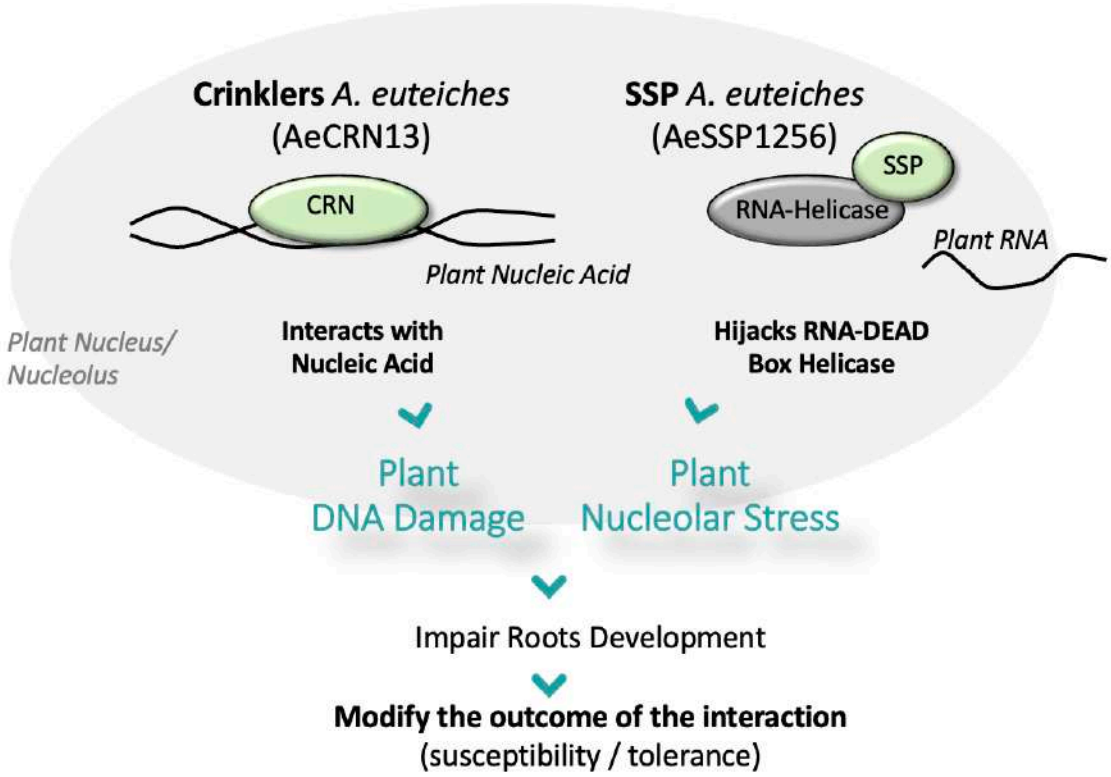

Figure 9. Schematic representation of functional activity of two functionally characterized *A. euteiches* effectors AeCRN13 (Ramirez-Garcés et al., 2016) and AeSSP1256 (Camborde et al., 2022). Both of the effectors target host nuclei. AeCRN13 is able to interact with host nucleic acid and induce plant DNA damage, AeSSP1256 hijacks RNA helicase from binding to plant RNA and cause nucleolar stress. Activity of both these effectors lead to the impaired root development and are able to enhance susceptibility of the host plant.

1.8 Scope of the thesis

The global aim of the PhD thesis, in the frame of the European Project 'PROTECTA', was to develop original experimental approaches for identification of effector molecules from *A. euteiches* starting from prediction of the effectors using 'omics' data to functional characterization.

In this context, the **Chapter II** of this manuscript is a review article describing biology, pathogenicity, economic impact and measures to counteract to *Aphanomyces* pathogens in agri- and aquaculture. The review article was written in collaboration with PhDs from PROTECTA project as equal first co-authors and published in Fungal Biology (Becking et al., 2021).

The presence of a high-quality reference genome is the important prerequisite for the development of the omics-based techniques of effectors identification. Thus, I performed PacBio-based genome assembly and annotation of a reference strain *ATCC201684 A. euteiches* previously sequenced by 454 and Illumina technology (Gaulin et al., 2018). The genome composition, repeat content and satellite DNA were identified in the genome. The analysis of gene-coding sequences was focused on the secretome. Then to evaluate whether secreted proteins and especially the SSP may participate to *A. euteiches* legume preference I performed a comparative analysis with four strains of *A. euteiches* with different host preferences, sequenced with Illumina technology. I highlighted that secreted proteins with a conserved domain form a core secretome of *A. euteiches,* while Small Secreted Proteins (SSPs) are mainly found as singletons and may participate to legume preference. The work was published in Journal of Fungi (**Chapter III,** Kiselev et al., 2022).

Upon *A. euteiches* genome annotation, we notice a large set of predicted extracellular proteins with expanded proteases. Thus, to confirm the prediction, I developed an assay to identify the active proteases implicated in the infection, in an international collaboration with a plant chemetics group (Prof. van der Hoorn) from University of Oxford (UK) and a mass spec specialist in Germany (Dr. Kaschani). I spent 2 months in the lab in UK in 2021 to set up on original system on *Pisum sativum*, to extract and characterize apoplastic proteases from *A euteiches* present during the interaction using Activity-Based Protein Profiling assay (ABPP). This 'in vivo' strategy, supports the genomics annotation and lead to the identification of a large set of pathogen's proteases present in the apoplastic fluid of the infected plants. Among them a novel class of modular proteases unique within *Aphanomyces* genus. Transient expression in *N. benthamiana* leaves confirm the apoplastic localisation of those original

modular proteases, suggesting a new role for this set of extracellular proteins during *A. euteiches* infection. (**Chapter IV**, presented as a submitted article where I'm first author).

In parallel, since numerous effectors are predicted to be intracellular and since our research team is focused on studying of nuclear localized effectors, I obtained from the local Research Federation (FRAIB, Fédération de Recherche Agrobiosciences, Interactions et Biodiversité) in the frame of the Young Scientists (JS, Jeunes Scientifiques) call a financial support to develop a system to directly characterize *A. euteiches* proteins present in the nuclei of *M. truncatula* upon roots infection. We developed a flow cytometry-based approach (FACS) in collaboration with Mickael Bourges from I2BC Cytometry platform in Paris and Prof. L. Bonhomme in Clermont-Ferrand to identify the *A. euteiches* proteins translocated into host nuclei during the infection. The analysis revealed in total 27 putative effectors, among them two homologous to known effectors from fungi and oomycete were identified and three novel SSP unrelated to the known AeSSP1256 were identified. Among 10 proteins tested for a subcellular 8 were shown to be localized in nuclei and 6 induced cytotoxicity in *N. benthamiana* leaves. This proof-of-concept approach showed that the developed technic could be used to identify the proteins implicated in the infection. The ready for submission to peer-review journal first-author publication is presented in **Chapter V.**

Finally, those two novels methods (ABPP, and FACS) developed in the frame of my PhD could be transferred to any plant pathogens in order to directly identify secreted proteins that could act as microbial pathogenicity factors.

During my PhD, I also participate to various work of the team related to 'omics' approach as the annotation of a long-read sequenced genome of the oomycete *Pythium oligandrum* (manuscript in preparation), the analysis of expression data from A17/F83 genotype of *Medicago* infected by *A. euteiches* to identify key genes that are differentially express in susceptible and tolerant line (manuscript in preparation) and identify by mining RNASeq data of *Medicago truncatula* genes those that are misregulated in the presence of the pathogen or the AeSSP1256 effector (Camborde and Kiselev et al., New Phytol 2022, Annex of this manuscript).

This PhD manuscript is therefore organised into four chapters, each presented as the published or submitted publication in peer-journal, followed by a general discussion

2. Chapter II - Pathogenicity of animal and plant parasitic *Aphanomyces spp* and their economic impact on aquaculture and agriculture (Becking et al., 2022)

The first chapter of my PhD is dedicated to the review of the recent advances in research of *Aphanomyces* genus. This genus is far less studied compared to the famous pathogens from *Phytophthora* genus or compared to the fungal plant pathogens, such as *Magnaporthe, Botrytis, Fusarium* etc. However, it represents the interesting opportunities for comparative studies of the adaptation to the hosts, since within the genus there are pathogens of various plant species, vertebrates, insects as well as saprotrophic organisms. In the review we focused on four major pathogens from *Aphanomyces* genus, which are *A. euteiches* – pathogen of leguminous plants, *A. cochlioides* – pathogen of sugarbeet, *A. invadans* – pathogen of fish, *A. astaci* - pathogen of crayfish. Therefore, the reviewed species represent the threats of agri- and aquaculture.

The last review of the biology of *A. euteiches* was done by our group in 2007, at the time no knowledge about the genomics and functions of the effectors were present. Here we reviewed the knowledge generated during last 15 years. The major advances were the publication of the genome sequence of *A. euteiches, A. invadans* and *A. astaci,* the identification of their effector repertoire and functional characterization of several effectors.

The last decades also signified the disease outbreaks caused by *Aphanomyces* genus in the different parts of the world. Outbreaks of *A. invadans* caused Epizootic ulcerative syndrome threaten the Asiatic food production by the multimillion dollars yearly losses, the root rot disease caused by *A. euteiches* was firstly detected in Australia. Therefore, we paid a special attention to a reviewing of spatial distribution of the *Aphanomyces* species over the world, and it could be postulated that these pathogens present almost ubiquitously in the production areas of their hosts.

The very little control of the *Aphanomyces* caused diseases could be achieved using the classical measures, such as chemical treatment or vaccination. For agriculture the long crop rotation is necessary to prevent the infestation is needed. To control the disease the use of resistant genotypes is a promising approach for sustainable food production. We reviewed the recent research in the development of the resistant cultivars.

ELSEVIER

British Mycological Society promoting fungal science

journal homepage: www.elsevier.com/locate/fbr

Review

Pathogenicity of animal and plant parasitic *Aphanomyces* spp and their economic impact on aquaculture and agriculture

Thomas BECKING[a,1], *Andrei KISELEV*[b,1], *Valentina ROSSI*[c,d,1], *David STREET-JONES*[e,1], *Frédéric GRANDJEAN*[a,**], *Elodie GAULIN*[b,*]

[a]*Laboratoire Ecologie et Biologie des Interactions, UMR CNRS 7267, Université de Poitiers, 86073, Poitiers, France*
[b]*Laboratoire de Recherche en Sciences Végétales, Université de Toulouse, CNRS, UPS, Toulouse INP, France*
[c]*MariboHilleshög Research AB, Säbyholmsvägen 24, S-26191, Landskrona, Sweden*
[d]*Department of Plant Protection Biology, Swedish University of Agricultural Sciences, Box 102, SE-23053, Alnarp, Sweden*
[e]*Aberdeen Oomycete Laboratory, Institute of Medical Sciences, University of Aberdeen, Foresterhill, Aberdeen, UK*

ARTICLE INFO

Article history:
Received 11 March 2021
Received in revised form
28 June 2021
Accepted 14 August 2021

Keywords:
Aphanomyces
Crayfish
Crayfish plague
Epizootic ulcerative syndrome
Fish
Pea
Root rot
Sugarbeet

ABSTRACT

Parasitic *Aphanomyces* species are a global threat to agri- and aquaculture, causing multi-million USD damage every year. Via the global trade, *Aphanomyces* has spread across all continents with exception of South America and Antarctica, and has become a major problem in pea, sugar beet, fish and crayfish production. The widespread *A. euteiches* and *A. cochlioides* induce root rot diseases in leguminous species and sugar beet respectively. The fish pathogen *A. invadans* is the causative agent of Epizootic Ulcerative Syndrome in various fish species whilst *A. astaci* infects crayfishes causing crayfish plague. *Aphanomyces* have developed an efficient transmission and infection mechanism which allows a rapid colonization and disruption of the host's infected tissues. This review presents an overview on the current research on *Aphanomyces* genus. We summarise the latest research efforts on four pathogenic *Aphanomyces* species, shedding light on the biology of these microorganisms, the pathogenicity factors of these parasites, the diseases which they cause, their distribution and finally the strategies to control the diseases.

1. Introduction

One of the major threats for both agriculture and aquaculture industries are the pathogenic oomycetes, a group known to be responsible for many outbreaks of natural host population (van West, 2006). These oomycetes, which belong to the Stramenopile Kingdom, are filamentous eukaryotic microorganisms that have spread in both terrestrial and aquatic

* *Corresponding author.*
** *Corresponding author.*
E-mail addresses: frederic.grandjean@univ-poitiers.fr (F. Grandjean), gaulin@lrsv.ups-tlse.fr (E. Gaulin).
[1] Co-authors: contributed equally to the work.
https://doi.org/10.1016/j.fbr.2021.08.001
1749-4613/

ecosystems (Beakes et al., 2012). Morphologically and ecologically similar to fungus, this phylum was historically considered as a basal fungal lineage (Lévesque, 2011), however genetic studies revealed that they are phylogenetically related to brown algae (Baldauf et al., 2000; Gleason et al., 2018). The most studied and notorious species belong to the genus *Phytophthora*, such as *Phytophthora infestans*, responsible for the Irish potato famine (Erwin and Ribeiro, 1996; Haas et al., 2009), *Phytophthora palmivora*, the causative agent of the cocoa black pod (Drenth et al., 2013) or *Phytophthora sojae* which is mainly destructive to soybean (Erwin and Ribeiro, 1996; Tyler, 2007). Beside this famous oomycete genus, other devastating pathogens have been identified, such as those belonging to the genus *Aphanomyces*. Much less studied than *Phytophthora* genus (more than 4,900 articles versus less than 350 articles referenced in Pubmed, consulted in 01–2021), the genus *Aphanomyces* appears to be an economically major threat that can affect both plants and aquatic animals (Diéguez-Uribeondo et al., 2009).

Here we reviewed the recent studies about four *Aphanomyces* species causing devastating diseases in agri- and aquaculture. We firstly present the biology of these four species and their distribution in the world, before depicting pathogenicity factors involved in host adaptation. We then discuss the economic impact of *Aphanomyces* spp. and recent advances in management of the diseases. To conclude we propose perspectives for further studies of *Aphanomyces* spp.

2. Biology of *Aphanomyces* genus

Aphanomyces is a monophyletic genus within Saprolegniales order, it has unique features in its lifecycle and host range. In this section we review the phylogenetic position of *Aphanomyces* genus, describe the different lifestyles and focus on the host range of parasitic species.

Phylogeny

Phylogenetic studies placed the *Aphanomyces* genus in the Saprolegnian lineage, an order that includes also numerous pathogenic species in both plants and aquatic animals (Diéguez-Uribeondo et al., 2009), such as the fish pathogen *Saprolegnia*, also known as "cotton mould" (Hulvey et al., 2007). This lineage is in contrast with the Peronosporalean lineage, which mainly includes plant pathogenic species and diverged from the Saprolegnian lineage in the Early Mesozoic era (Riethmuller et al., 2002; Beakes et al., 2012; Jiang and Tyler, 2012; Matari and Blair, 2014). Phylogenetic analysis revealed that the *Aphanomyces* genus appears to be monophyletic (Leclerc et al., 2000; Diéguez-Uribeondo et al., 2009) and is clustered in three major lineages, composed by plant pathogens, aquatic animal pathogens, and saprotrophic or opportunistic parasites, respectively (Diéguez-Uribeondo et al., 2009) (Fig. 1). To date around 40 *Aphanomyces* species are described occurring in various ecological niches and ranging from highly specialized parasites to saprotrophic species developing on plant residues or dead animals (Scott, 1961; Dick, 2001; Johnson et al., 2002).

Aphanomyces *host range*

The pathogenic species belonging to the genus *Aphanomyces* are known to infect a wide range of different hosts. Depending on the species considered, the host spectrum varies from plants to vertebrates, and also invertebrates.

On one hand, many plant taxa are susceptible to infection by *Aphanomyces* species. The plant pathogen *Aphanomyces euteiches*, is specialized on perennial or annual plants of the Fabaceae family, including peas (*Pisum sativum* L.), alfalfa (*Medicago sativa* L.), common bean (*Phaseolus vulgaris* L.), broad bean (*Vicia faba* L.), red and white clover (*Trifolium pratense* L.

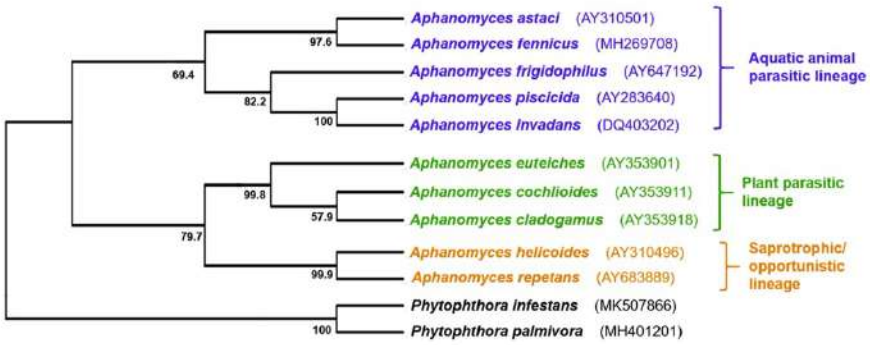

Fig. 1 – Cladogramm of *Aphanomyces* species showing the three major lineages based on the host category. The phylogeny is based on 5.8S ribosomal RNA gene with a 691 nucleotides alignment length. Phylogenetic reconstruction was performed with PhyML 3.0 (Guindon et al., 2010), under the GTR + G substitution model [assessed with jModelTest 2.1.7, (Darriba et al., 2012)] and was tested with the Bootstrap method (1,000 replicates). The identifier written between brackets correspond to the NCBI accession number.

and *T. repens* L., respectively) (Gaulin et al., 2007). Another oomycete plant parasite, *Aphanomyces cochlioides* is specialized to parasitize roots of sugar beet (*Beta vulgaris* L.), spinach (*Spinacia oleracea* L.), cockscomb (*Celosia argentea* L.), and other various species of Chenopodiaceae and Amaranthaceae (Scott, 1961).

On the other hand, several animal taxa are susceptible to infection by *Aphanomyces* species. Firstly *Aphanomyces invadans*, the causative agent of the Epizootic Ulcerative Syndrome (EUS), has been reported to interact with more than 160 species of fish (Herbert et al., 2019). It may infect a wide range of estuarine and freshwater fish species (Chinabut, 1998; Blazer et al., 1999) and is especially virulent to catfish (Roberts et al., 1993) and murrels (Chondar and Rao, 1996). Secondly *Aphanomyces astaci* the causative agent of the crayfish plague, is known to associate with crayfish species from Asia, Australia and Europe. *A. astaci* is an obligate parasite specialized on freshwater crayfish (Söderhäll and Cerenius, 1999; Diéguez-Uribeondo, 2006). This oomycete is known to have a North American origin, and could occasionally also be harboured by other decapods such as freshwater crabs or shrimps (Putra et al., 2018; Svoboda et al., 2017; Martín-Torrijos et al., 2021a). *Aphanomyces frigidophilus* is known to infect the eggs of several salmonid species (Ballesteros et al., 2006). The impact of these pathogens is major since they may cause the devastation of both natural and cultured stocks of freshwater animals (Söderhäll and Cerenius, 1999; Collas et al., 2016). Lastly, *Aphanomyces sinensis* is a pathogen known to infect the Japanese turtle *Pelodiscus sinensis*, causing small whitish maculae on the carapace (Takuma et al., 2011). These four *Aphanomyces* species are the most notable animal-pathogenic members of the genus. Of these, *A. invadans* and *A. astaci* have by far the greatest economic impact – both of which cause significant losses within the global aquaculture industry (Iberahim et al., 2018; CABI, 2020a). Hence, the primary focus in terms of animal-pathogenic *Aphanomyces* shall be upon these two species.

In several other species belonging to the *Aphanomyces* genus, some are predominantly saprotrophic (i.e., *Aphanomyces laevis*, *Aphanomyces stellatus*, *Aphanomyces helicoides* or *Aphanomyces repetans*), but may turn as opportunistic pathogens with no host specialization (Royo et al., 2004; Patwardhan et al., 2005).

Life cycle

The typical life cycle of *Aphanomyces* spp. includes both asexual and sexual phases for the plant pathogens while sexual reproduction in animal pathogens is rare or completely absent (Diéguez-Uribeondo et al., 2009).

Sexual reproduction involves specialized reproductive structures, oogonia and antheridia, in which meiosis occurs and gametes are formed. The oogonium produces one to several oospheres, cellular structures containing haploid nuclei (Malloch, 2007). Antheridia are structures in which male nuclei are formed (Dick, 1969; Malloch, 2007). *Aphanomyces* species such as *A. euteiches* and *A. cochlioides* are homothallic, presenting male and female reproductive structures on the same thallus. Fertilization begins when antheridia develop a fertilization tube which penetrates the oogonium. Male nuclei pass through this tube and enter the oogonium where they fuse within the oospheres to produce a diploid (Malloch, 2007).

In phytopathogenic *Aphanomyces* spp. fertilization of the oogonium results in the formation of oospores, thick-walled zygotes, 18–25 μm in size, which function as resting spores to survive unfavourable winter conditions (Heffer, 2002; Wu et al., 2018). They are produced in plant infected tissue and are released in the soil when the plant degrades (Heffer, 2002). Oospores can remain dormant in the soil for years in the absence of a host, representing a long-lived source of inoculum (Papavizas and Ayers, 1974; Gaulin et al., 2007). Under warm and moist soil conditions oospore germination is stimulated by the host exudates (Dyer and Windels, 2003). Oospores form a germ tube which develops vegetative hyphae that can directly infect the host (Dyer and Windels, 2003).

In the asexual stage of plant pathogenic species, vegetative hyphae differentiate to sporangia in which motile uninucleate zoospores are produced. Primary zoospores equipped with an anterior "tinsel" flagellum and a posterior "whiplash" flagellum is released in the soil (Walker and van West, 2007). After evacuation from the zoosporangium primary zoospores encyst and give rise to secondary zoospores (Papavizas and Ayers, 1974; Sivachandra Kumar et al., 2020). Secondary zoospores which also present an anterior and posterior flagellum are motile for a longer period and are determinant for a successful infection (Walker and van West, 2007). Zoospores swim in water film around soil particles through the root surface where in a few minutes they adhere, encyst developing a germ tube, penetrate and colonize the tissue (van West et al., 2003). The invasion events of *A. euteiches* in pea roots have been described by Papavizas and Ayers (1974). The germ tube invades the host tissue in the intercellular spaces within 2 h. In some cases, it enters the cell wall with the formation of an appressorium-like structure. Within a few hours *A. euteiches* penetrates the host cortical cells and develops hyphae that rapidly spread mainly in the intercellular spaces of the root cortex and eventually colonize the entire root system (Wu et al., 2018). Antheridia and oogonia are formed in the invaded tissue within few days, likewise in sugar beet once *A. cochlioides* zoospores have encysted on the root surface the resulting germ tubes penetrate the host directly or via appressoria (Islam et al., 2003) leading to a rapid infection within 30–40 min after the zoospores adhesion to the root surface (Islam, 2010). The presence of *A. cochlioides* mycelia has been observed in the intercellular spaces of the cortex (Papavizas and Ayers, 1974).

In animal pathogenic species zoospores are produced from clusters of primary cysts at the hyphal tips. As soon as the primary spores are ejected, they immediately cluster around the sporangial opening and form an achlyoid cluster or "spore ball" at the apical tip of the sporangia from where secondary flagellated zoospores are released (Vrålstad et al., 2011a). Secondary zoospores swim in the water column and adhere on the surface of a suitable host. Once they have settled, they discard flagella and encyst. Cysts subsequently germinate and develop a germ tube which penetrates the host (Vrålstad et al., 2011b). Hyphae invade deeper tissue or organs of a susceptible host, differentiate to zoosporangia which release zoospores prior to or just after the host's death (Vrålstad et al., 2011b).

Encysted zoospores of pathogenic *Aphanomyces* species have also the ability to release a new generation of zoospores instead of germinating. This event is known as repeated zoospore emergence (RZE) (Diéguez-Uribeondo et al., 2009). It has been observed that if encystment occurs in the absence of a favorable host, the crayfish pathogen *A. astaci* can produce three consecutive generations of new zoospores before the spore ceases to live (Cerenius and Söderhäll, 1984).

Distribution and diversity

Pathogenic *Aphanomyces* species are widely spread around the hemisphere with cases also reported in South-East Asia, Australia and South Africa (Fig. 2). Plant pathogenic *Aphanomyces* spp. are detected in the majority of regions where suitable crops are cultivated. Occurrence of crayfish pathogen *A. astaci* is mainly found in North America, Europe and Japan whereas fish pathogen *A. invadans* is spread around the world except for Europe and South America.

Aphanomyces euteiches

Since its first report in peas in Wisconsin by Drechsler in 1925 (Jones and Drechsler, 1925), *A. euteiches* has been reported as one of the major yield limiting factors in the US (Gossen et al., 2016), Canada (Wu et al., 2018) France (Quillévéré-Hamard et al., 2018) and Sweden (Levenfors et al., 2003). Cases of *A. euteiches* detection were also reported in Australia (van Leur et al., 2008), China, India, territory of former USSR, former Czechoslovakia, Poland, Italy, Germany (CABI, 2019) and the Netherlands (Oyarzun and van Loon, 1989) (Fig. 2). Unfortunately, no quantitative data on *A. euteiches* distribution is known for major producing countries as India, China and Russia.

A. euteiches has a broad host range within the family Fabaceae such as pea, alfalfa, trifolium, lentil, etc. (Gaulin et al., 2007; Malvick et al., 2009) and cause the greatest economic damage to pea and lentil crops (Gaulin et al., 2007; Malvick et al., 2009; Ma et al., 2020). The ability of different *A. euteiches* pea strains to infect plants was used to identify two pathotypes (I and III). While both pathotypes are present in North America, only the pathotype I is reported in France (Wicker et al., 2001). A recent study also indicates that pathotype I is prevalent in Canadian prairies (Kumar et al., 2021). *A. euteiches* strains isolated from alfalfa fields are designated as races: the less aggressive race 1 is able to infect susceptible alfalfa genotype Saranac, but not the tolerant genotype WAPH-1; the more aggressive race 2 genotype overcomes resistance of WAPH-1 and is able to infect both genotypes (Malvick et al., 2009; Grau et al., 1991; Malvick and Grau, 2001). Studies on *A. euteiches* isolates from US alfalfa fields demonstrate the emergence of new races (Seitz and Rouse, 2012) and the prevalence of the aggressive race 2, which represents around 45 % of all strains, while race 1 represents 11 % (Samac et al., 2017).

Aphanomyces cochlioides

It was 1929 when *A. cochlioides* was first identified as the causal agent of the black rot disease in sugar beet in Michigan (Dreschler, 1929). Despite the restricted host range, this pathogen has a worldwide distribution and its presence has been reported especially in major sugar beet producing areas in North America such as The River Valley of Minnesota, North Dakota, Nebraska and Wyoming, in Canada, Chile, Europe

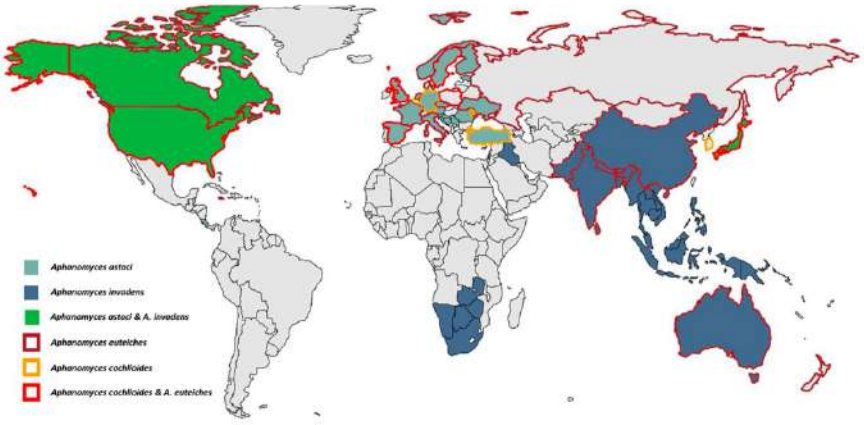

Fig. 2 – Occurrence of *A. astaci*, *A. invadans* *A. euteiches* and *A. cochlioides* worldwide. Countries are labelled in colours according to *Aphanomyces* species presence. *A. astaci* is actually founded in 24 countries (North America and Europe), and 28 countries have experienced an outbreak caused by *A. invadans* (North America, South Africa, South East of Asia and Oceania), 21 countries have experienced an outbreak caused by *A.euteiches* (North America, South America, Europe, Asia and Oceania) and 11 countries have experienced an outbreak caused by *A. cochlioides* (North America, Europe and Asia). To summarize, a total of 56 countries are known to have experienced an outbreak caused by one of the four species studied in this review. All these countries are listed in the supplementary table 1.

and Japan (Harveson, 2000; Beale et al., 2002). Although *A. cochlioides* represents a major constraint in sugar beet production, little attention has been given to the genotypic variation among *A. cochlioides* strains in comparison to the intensively-studied *A. euteiches*.

Aphanomyces invadans

A. invadans was first isolated in Japan (1971), from a freshwater fish farm (Egusa and Masuda, 1971). Over the past half-century, this fish-pathogenic oomycete has spread globally and has now been isolated from the continents of Asia, North America, Africa and Australia (OIE, 2016; Iberahim et al., 2018). Recently, molecular techniques for the identification of *A. invadans* have been developed and refined (Vandersea et al., 2006; Kamilya and Kollanoor, 2020). Therefore, the global distribution of *A. invadans* is closely monitored and currently listed in 28 countries.

A. invadans is a specialized pathogen of fish exclusively (Diéguez-Uribeondo et al., 2009), with over 125 species of fish currently known to be susceptible to infection (Kamilya and Baruah, 2014), a further 38 additional susceptible fish genera having been recognized since the authors' previous study (Baruah et al., 2012). To date, only one genotype of *A. invadans* has been recorded (OIE, 2016), with all isolates tested demonstrating fish pathogenicity – encompassing those from North America (Sosa et al., 2007), Europe (Oidtmann et al., 2008) and Asia (Yadav et al., 2014). Several *Aphanomyces* isolates were obtained from Malaysian fish farms and found to be non-pathogenic to fish under laboratory conditions, however these were not identified to species level (Afzali et al., 2013). This species propagates solely via asexual reproduction (Kiryu et al., 2005; Diéguez-Uribeondo et al., 2009). The lack of a sexual life stage has given rise to the global spread of *A. invadans*, as a single highly virulent clone, worldwide over the past 50 years (Lilley et al., 2003; Iberahim et al., 2020).

Aphanomyces astaci

A. astaci is originally a specific parasite of crayfish originating from the North American continent (Martín-Torrijos et al., 2021b). North American crayfish species are known to be healthy carriers, for example such as *Procambarus clarkii* (red swamp crayfish), *Pacifastacus leniusculus* (signal crayfish) and *Faxonius limosus* (spiny-cheek crayfish) (Souty-Grosset et al., 2006). For several decades, phylogenetic analyses have been performed to better describe and understand the relationship between *A. astaci* and its North American hosts. Thus, the Random Amplification of Polymorphic DNA–Polymerase Chain Reaction (PCR-RAPD) was the first molecular technique which enabled the description of the genetic diversity of *A. astaci*, and enabled the characterization of 5 distinct genetic groups. Group A was isolated from specimens of the native European crayfish *Astacus astacus*, and is probably related to the first introduction of *A. astaci* in Europe during the 19th century (Huang et al., 1994). Group B was isolated from signal crayfish *P. leniusculus* Swedish specimens (originally from Canada) (Huang et al., 1994), and appears to be responsible for many outbreaks in native European species so far (Cerenius et al., 2008). Group C was also isolated from *P. leniusculus* Swedish specimens (Huang et al., 1994); however, it has never been observed again since its detection (Söderhäll and Cerenius, 1999). Group D was isolated from introduced Spanish specimens of red swamp crayfish *P. clarkii* (Diéguez-Uribeondo et al., 1995), whereas group E was isolated from the spiny-cheek crayfish *F. limosus* introduced in Czech Republic (Kozubíková et al., 2011). Over the last ten years, the number of genotyping methods to characterize *A. astaci* has been constantly increasing, facilitating the identification of genotypes involved in outbreaks. In order to evaluate the genetic diversity of the pathogen *A. astaci*, studies have focused on the sequencing of chitinase genes (Makkonen et al., 2012a), but also Amplified Fragment Length Polymorphism (AFLP) markers (Rezinciuc et al., 2014), and recently on Single Nucleotide Polymorphisms (SNP) diversity based on mitochondrial DNA (Minardi et al., 2019). The genetic markers currently most used to characterize the pathogen strains responsible for outbreaks have focused on microsatellite sequencing (Grandjean et al., 2014) and mitochondrial haplotyping (Makkonen et al., 2018) approaches. It was possible to distinguish 4 mitochondrial haplogroups: a (corresponding to the RAPD-group A and C), b (corresponding to the RAPD-group B), d (corresponding to the RAPD-group D) and e (corresponding to the RAPD-group E) (Makkonen et al., 2018). These findings were also congruent with the genetic diversity observed on microsatellites, since the same genetic groups were found between RAPD initial markers: SSR-A, SSR-B, SSR-C, SSR-D and SSR-E corresponding to RAPD-groups A, B, C, D and E, respectively (Grandjean et al., 2014). Furthermore, these results underline the mitochondrial diversity observed within the different *A. astaci* strains, since 2 different mitochondrial haplotypes were described within the RAPD-group D (d1 and d2, Makkonen et al., 2018). The author also differentiated the *A. astaci* strains in 2 lineages: lineage 1 which includes a, b and e mitochondrial haplotypes (RAPD-groups A, B and E) and lineage 2 corresponding to the d1 and d2 mitochondrial haplotypes (RAPD-group D) (Makkonen et al., 2018). Recently, six new haplotypes have been characterized in North American species belonging to both lineage 1 (called usa1 and usa2) and lineage 2 (usa3 to usa6) (Martín-Torrijos et al., 2021b). The development of these different markers will increase our knowledge of the genetic diversity of *A. astaci* strains, which is still relatively unknown. Thus, microsatellite markers have allowed the characterization of a new genotype, isolated in North America from the rusty crayfish *Faxonius rusticus* (Panteleit et al., 2019). The newly described strain presented the same RAPD and mitochondrial haplogroup profiles as RAPD-group A. Although additional combination of chitinase-like markers attached this new strain to group C. All these results illustrate the complementarity of the different markers developed, as well as the need to use a combination of these approaches in order to better understand the diversity and the evolutionary history of *A. astaci*.

3. Pathogenicity determinants of *Aphanomyces* spp.

Pathogenic *Aphanomyces* spp. are distributed around the world and are able to infect various host ranges. In this section we review current knowledge of the factors which make the

Aphanomyces genus the global threat for agriculture and aquaculture.

Zoospores as a key pathogenicity factor

Oomycetes zoospores play a key role in the infection process and in the pathogen transmission from host to host (Walker and van West, 2007). Spore production rate is an important trait to determine the aggressiveness and the ability of the pathogen to disperse and successfully infect new hosts (Delmas et al., 2014). In plant pathogenic oomycetes zoospores motility is influenced by tactic and electrostatic signals generated by root exudates which drive the zoospores throughout a suitable infection site (Appiah et al., 2005). Attractants of *A. raphani* and *A. euteiches* zoospores such as indole-3-aldehyde and prunetin have been identified in cabbage seedlings and pea seedlings respectively (Yokosawa et al., 1986), while a potent attractant substance to *A. cochlioides* zoospores, cochliophilin A (5-hydroxy-6,7-methylenedioxyflavone, 1) has been isolated from one of its host roots *Spinacia oleracea* (Horio et al., 1992) and it is known to be present also in sugar beet roots. This flavonoid is considered a species-specific attractant compound since it has the capacity to attract *A. cochlioides* zoospores but it has no effect on zoospores motility of other *Aphanomyces* species (Islam and Tahara, 2001). When attracted by cochliophilin A, *Aphanomyces* zoospores encyst in few minutes and germinate within 30–60 min (Sakihama et al., 2004). Another important step towards a successful infection is the differentiation of zoospores from a motile form into cyst, the immobile form capable of infecting the host. Several studies have provided evidence that changes in cations concentration such as calcium (Byrt et al., 1982a, 1982b; Morris et al., 1995) and potassium (Appiah et al., 2005) play an important role in zoospores taxis and encystment of plant pathogenic oomycetes. Chemotaxis has been reported also on the animal pathogenic *A. astaci* where chemotactic responses were observed within few minutes mainly towards parts of the crayfish where the cuticle is soft such as the tip and the junction of the legs (Cerenius and Söderhäll, 1984). However, no recent studies have confirmed the role of chemotaxis in *A. astaci* zoospores attraction and information about zoospores motility in *A. invadans* and other animal pathogenic *Aphanomyces* species remains still unknown.

Genetic determinants of pathogenicity

When *Aphanomyces* starts colonization of the host, it has to cope with host immunity and defence reactions. Oomycetes widely exploit the repertoire of secreted proteins called effectors to modulate host physiology and immune reactions (Bozkurt et al., 2012). Based on subcellular localization within the host, effectors are reported as extracellular when they act within the apoplast while intracellular effectors are able to reach the intracellular space of the host cells (Gaulin et al., 2008; Schornack et al., 2010). These proteins are generally induced during infection and generally harbour a signal peptide to be secreted by the pathogen (Bozkurt et al., 2012). Availability of the whole genome sequence of four *Aphanomyces* strains allowed *in silico* prediction of putative secreted proteins in *A. astaci* and *A. invadans* (strain NJM9701) - animal pathogens; *A. euteiches* (strain ATCC201684) plant pathogen and *A. stellatus* (strain CBS 578.67) saprophyte (Gaulin et al., 2018; Iberahim et al., 2018). The genome size of *Aphanomyces* spp. are estimated at 50–70 Mb, having 16,000–25,000 predicted genes. Secreted proteins correspond respectively to 10 % and 6 % of the total proteome of plant and animal pathogens (Gaulin et al., 2018).

Extracellular effectors

A large majority of extracellular effectors concern cell wall degrading enzymes for plant pathogens such as *A. euteiches*. Indeed, to get through plant cell wall plant-associated pathogens release a set of cell-wall degrading enzymes (CWDE), which mostly consist of glycosyl hydrolases families (GH), GlycosylTransferases (GT), PolysaccharideLyases (PL) and Carbohydrate-Esterase (CE) also regrouped as CAZymes (Lombard et al., 2014). *A. euteiches* has over 300 secreted carbohydrate-active enzymes (CAZy) and carbohydrate-binding modules (Gaulin et al., 2018). They include protein families targeting plant-specific polysaccharides (e.g., hemicellulases: GH 10, 11, CE4 families and pectinases: GH 28, PL1, 3, 4 families), which might be involved in penetration of plant cell wall (Lanver et al., 2014). Interestingly, animal pathogen *A. astaci* lacks those plant-specific families in its secretome but harbours enzymes able to interact with chitinous exoskeleton of the crayfish (Gaulin et al., 2018). Indeed, during infection, chitinase may play a major role in the penetration of the hyphae through the chitinous wall following spore germination (Söderhäll et al., 1978). While several species of *Aphanomyces* show chitinase activity in the presence of chitin, *A. astaci* has been shown to be capable of producing chitinases even in the absence of substrate (Andersson and Cerenius, 2002). However, to date, no strain-specific or genotype-specific expression has been found in the chitinase activities of *A. astaci* (Andersson and Cerenius, 2002). Moreover, it has been suggested that this expression pattern may be the result of an adaptation of the pathogen to a purely parasitic lifestyle (Unestam, 1966; Andersson and Cerenius, 2002). Genomic work has identified three major chitinase groups (CHI1, CHI2 and CHI3) existing in the different strains of *A. astaci*. Depending on the strain considered, these genes showed structural differences in their coding region, thus highlighting the variations in the epidemiological properties of the different genotypes studied (Makkonen et al., 2012a).

Whole genome sequencing of *A. invadans* (strain NJM9701) in 2014 has enabled initial exploration of the effector repertoire for this species (Makkonen et al., 2016). Recent analysis of effectors encoded within the genome indicate that *A. invadans* encodes a sizeable number of effector proteins, bearing more similarity to animal-pathogenic as opposed to plant-pathogenic saprolegniales (Iberahim et al., 2018). Firstly, CAZymes are thought to play an important part in *A. invadans* infection – although potentially not having such a pivotal role as during plant-pathogenic *Aphanomyces* infections. Specifically, key CAZyme gene families, encoding CE1-and CE10, are induced primarily in plant-pathogenic oomycetes (de Vries and de Vries, 2020). Also of considerable interest are those effector classes typically associated with pathogenic *Aphanomyces* species but lacking in *A. invadans*. Specifically, the *A. invadans* genome was found to lack two major

extracellular effectors: disintegrins and haemolysin-E (Iberahim et al., 2018). These peptides are key protease effectors often secreted by animal-pathogenic oomycetes, such as *Saprolegnia parasitica* (Banfield and Kamoun, 2013; Rzeszutek, 2019), both known to play a significant role in oomycete virulence via mediation of host-cell binding (Banfield and Kamoun, 2013). Proteases overall have long been recognized as key effectors of pathogenic oomycetes (Schornack et al., 2009). Recent analysis of extracellular protease products from A. *invadans* has found that, of these, serine proteases constitute the vast majority hence likely are of central importance to virulence (Majeed et al., 2017).

Intracellular effectors

Intracellular oomycete effectors, meaning molecules that are addressed within the cytoplasm of the host cell, were predicted years ago based on comparative genomics of known virulence genes of oomycetes genomes (Tyler, 2002). Two main protein families have been predicted based on the presence of RxLR or LxLFLAK amino acid motif after the predicted signal peptide in the plant pathogen *Phytophthora sp.* (Birch et al., 2008; Schornack et al., 2010). Hundreds of genes encoding RxLR and CRN effectors are predicted and characterized in Peronosporales oomycetes especially in *Phytophthora* genus (Rehmany et al., 2005; Schornack et al., 2010).

In plant pathogenic *Aphanomyces* no RxLRs were found during the genome analysis, but numerous CRNs were identified (Gaulin et al., 2018). In contrast the A. *invadans* genome was found to lack those two major classes of effectors (Iberahim et al., 2018), while around 31 CRN-like genes were identified in A. *astaci* (Gaulin et al., 2018). The first reported putative intracellular effector from A. *euteiches* AeCRN5 was described in 2010 (Schornack et al., 2010) although its function within the cell is still unknown. Another member of CRNs effectors in A. *euteiches*, AeCRN13, was found to target host nuclei and possesses DNA damage activity (Ramirez-Garcés et al., 2016). The triggered DNA damage response induces severe plant necrosis. Interestingly, the homolog of AeCRN13 from the batracian pathogen *Batrachochytrium dendrobatidis* also targets host nuclei and induces DNA-damage responses (DDR). It seems that nuclear targeting and DNA damage is an important strategy of pathogenesis for *Aphanomyces* spp. (Camborde et al., 2019). A third class of oomycete effectors was recently reported in the genus *Aphanomyces* (Gaulin et al., 2018). *Aphanomyces* SSPs for Small Secreted Proteins were named in analogy with fungal SSPs (Rep, 2005) and characterized as proteins with a signal peptide, <300 amino acids in size and without any functional domain predicted. In A. *euteiches* 296 SSPs are predicted, and numerous are organized in cluster (Gaulin et al., 2018). SSPs have also been detected in A. *astaci*. Functional studies have shown that SSPs from A. *euteiches* can target plant nuclei and modify activity of plant DEAD-box RNA helicase to enhance A. *euteiches* infection (Camborde et al., 2020). These effectors appear to be a promising area of research to improve our understanding of the molecular factors involved in the virulence of A. *euteiches*.

Recently, the intracellular chaperone Lhs1 has also been identified as an important modulator of virulence in A. *invadans* (Iberahim et al., 2020). This study of RNAi-based Lhs1 silencing demonstrated significantly reduced virulence in a *Galleria melonella* infection model, likely due to the role of Lhs1 as an important regulator in oomycete and fungal zoospore production (Chen et al., 2019; Iberahim et al., 2020). Due to limited knowledge of both extracellular and intracellular A. *invadans* effectors, further research in this field is warranted. Specific to A. *invadans*, a contemporary study successfully targeted the serine protease gene of this species using single-guide RNAs via the Crispr/Cas9 editing system (Majeed et al., 2018). Zoospores genetically edited in this manner did not produce clinical signs of EUS during *in vivo* infection trials of the ornamental fish *Trichogaster lalius* (Majeed et al., 2018), suggesting the viability of genome editing as a potential technique for combatting epizootic ulcerative syndrome specifically.

4. Economic impact of *Aphanomyces* spp.

Aphanomyces spp. cause a dramatic economic impact on various sectors of agri- and aquaculture businesses. In general, it is very difficult to precisely calculate the impact caused by *Aphanomyces* spp. as it includes direct yield loss, implementation of protective measures such as crop rotation in the fields and conservation strategies in aquatic environments.

Damage to agriculture

Among the most relevant *Aphanomyces* species in agriculture special attention must be given to A. *euteiches* and A. *cochlioides* being responsible for the root rot disease in two of the most economically important crops such as pea and sugar beet, respectively. Pea is the second most important food legume crop in the world (Ali et al., 1994) and is cultivated primarily in Canada, Russia, the United States, France, and Australia (Tulbek et al., 2016). Sugar beet is a major crop in temperate regions providing about 20 % of sugar worldwide and it dominates the market in the European Union and the United States (Finkenstadt, 2014). Although crop losses caused by these two species can be difficult to estimate, the majority of yield loss in pea and sugar beet can be attributed to root rot rather than other diseases (Papavizas and Ayers, 1974). Very raw estimation of pea yield loss due to root rot complex is around 10 % (Allmaras et al., 1998), which in the current market could cost up to 600 million US dollars (transparency market research). The root rot disease complex of legumes is usually an association of A. *euteiches* with *Fusarium* spp., *Pythium* spp. and *Rhizoctonia solani*. This complex triggers damping-off, root rot and reduces root development and nitrogen fixation (Gossen et al., 2016). A. *euteiches* is present in over 90 % of fields diagnosed with root rot in Canada (Wu et al., 2018). The yield loss caused by A. *euteiches* could be as high as 70–80 % in heavily infested fields (Pfender and Hagedorn, 1982; Bogdan, 2019). A. *cochlioides* has a great impact on sugar beet production and has a world-wide distribution representing a big threat in many areas of the United States, Europe and Asia (CABI, 2020b). About 51 % of 293.000 ha of sugar beet field was estimated to be infested with A. *cochlioides* in Minnesota and North Dakota in 1999 (Beale et al., 2002). In USA 42.8 million dollars per year is lost to A. *cochlioides* with current management practices such as application of the

fungicide Tachigaren on seeds, whereas 243.5 million dollar is lost when no treatment or agronomic practices are used (information given by the Beet Sugar Development Foundation, BSDF, 2020). *A. cochlioides* is also often part of a root rot complex in association with *Fusarium* spp and *Rhizoctonia solani* (Harveson and Rush, 2002).

Damage to aquaculture

A. invadans is the causative agent of Epizootic Ulcerative Syndrome (EUS) (Huchzermeyer and Van der Waal, 2012), a seasonal oomycete disease affecting both wild and farmed fish within fresh and brackish water (OIE, 2016). EUS due to *A. invadans* is economically devastating to aquaculture at a global level, with losses from this disease at infected farms frequently reaching one hundred percent (Iberahim et al., 2018). While no worldwide data exists from the past three decades, within the Asia–Pacific region alone the most recent estimates indicate that EUS caused a loss of circa USD 110 million between the late 1980s and early 1990s (Lilley et al., 1998; Majeed et al., 2017).

Since 1990, the global aquaculture industry has expanded enormously (FAO, 2020). In 1990, the global output of the aquaculture sector was circa 14 million tons (FAO, 1991) and has since increased fivefold to 81.8 million tons in 2018 (FAO, 2020). Furthermore, the region with greatest recent growth in aquaculture, warmwater Asia, is also the region that is most susceptible to *A. invadans* (FAO, 2020). Due to both above factors, alongside minimal effective treatment options, contemporary global aquaculture losses to EUS are likely huge. Nationally, culturing of major carps in India (Pradhan et al., 2008; Kamilya and Kollanoor, 2020) and various snakeheads (*Channa* sp.) in Thailand (Lilley et al., 2003; Arshad and Arockiarai, 2020) are most adversely impacted by EUS. Non-Asian countries tend to provide a less suitable climate and temperature for *A. invadans*, hence outbreaks in aquaculture non-Asian countries are often less costly (Kamilya and Kollanoor, 2020). Within North America, *A. invadans* is often present in freshwater bodies (Saylor et al., 2010). However, EUS outbreaks seldom occur and a 2010 mass mortality in Florida of 300 captive snakehead fish (*Channa marulius*) was highly unusual (Saylor et al., 2010).

The source of introduction of the crayfish plague pathogen *A. astaci* in Europe during the 19th century was never established. This pathogen has caused devastating damage to native European crayfish populations, mainly concerning the species *Austropotamobius pallipes* (white-clawed crayfish), *Austropotamobius torrentium* (stone crayfish), *A. astacus* (noble crayfish) and *Pontastacus leptodactylus* (narrow-clawed crayfish) (Holdich et al., 1995; Westman, 1995; Alderman, 1996; Machino and Diéguez-Uribeondo, 1998). Nevertheless, data on the real economic impact of this disease are rather unknown. Historically, native European crayfish have been widely used as a food source (especially in poor areas, since the catch was not regulated), mainly through the cropping of the native species *A. astacus* and *P. leptodactylus* (CABI, 2020a). However, the crayfish plague has drastically reduced the production of native species, reducing stocks by up to 90 % in some countries, mainly in Scandinavia, Germany, Spain and Turkey (Lodge et al., 2000). For instance, data from the beginning of the 20th century report that noble crayfish *A. astacus* exports from Sweden dropped from 90 tons in 1908 to only 30 tons in 1910 (Brinck, 1975). Similarly, in Finland, exports fell from 16 million *A. astacus* individuals in 1880 to less than 2 million in 1910 (Westman, 1991). The economic impact of the crayfish plague is best described since its introduction in Turkey in the 1980s, where fished crayfish stocks declined from 8,000 tons in 1984 to less than 500 tons between 1990 and 1994 as a result of the disease (Ackefors, 2000). Thus, even though no native European species has been extinguished by the disease, the range and local abundance of populations has drastically decreased due to *A. astaci* (CABI, 2020a). *A. astaci* is moreover considered as one of the "100 of the World's Worst Invasive Alien Species", according to the Global Invasive Species Database (Lowe et al., 2000).

Another direct economic impact of *A. astaci* to consider is the cost of native crayfish conservation strategies, which are directly impacted by the spread of crayfish plague through the European continent. Currently, crayfish plague has been detected and potentially implicated in outbreaks in at least 20 countries, spreading over 3,500 km from North (Finland) to South (Spain) and over 3,000 km from East (Turkey) to West (Spain) (Ungureanu et al., 2020), highlighting its presence and impact throughout entire Europe. Furthermore, over the past 20 years, the cost of conservation programs has reached several million US dollars to the economies of most European countries (CABI, 2020a). However, the budget allocated to the conservation of native European crayfish has never been recorded to our knowledge.

5. Diseases caused by *Aphanomyces* spp. and management strategies

The next section reported on the diseases due to *Aphanomyces* spp. and strategies to limit the impact of the microorganism on agri and aquaculture.

Aphanomyces *root rot in peas, alfalfas and lentils*

A. euteiches induces root rot of the host plant and dramatically decreases the yield or even induces death of plants in the fields. Legumes are susceptible to *A. euteiches* throughout their life cycle and the first symptoms can be seen 3–4 days after infection (Papavizas and Ayers, 1974). The primary inoculum of *A. euteiches* in the field is oospores, which keep germination ability for ten years (Schren, 1960). The most favourable conditions for *A. euteiches* pea infection appears in wet periods, when moisture in soil induces massive production of swimming zoospores and their spread within the field (Hoch and Mitchell, 1973; Gaulin et al., 2007; Wu et al., 2018). At early-stages of infection *A. euteiches* induces softened and water-soaked zones on roots (Hughes and Grau, 2007). At the later stages of infection, roots impair in function and in nodulation therefore secondary symptoms appear such as chlorosis, necrosis and wilting of the foliage (Papavizas and Ayers, 1974; Hughes and Grau, 2007) (Fig. 3A).

No efficient chemical protection against *A. euteiches* is known; in addition it seems that effective fungicides against individual soilborne pathogens as *Aphanomyces* spp. are less

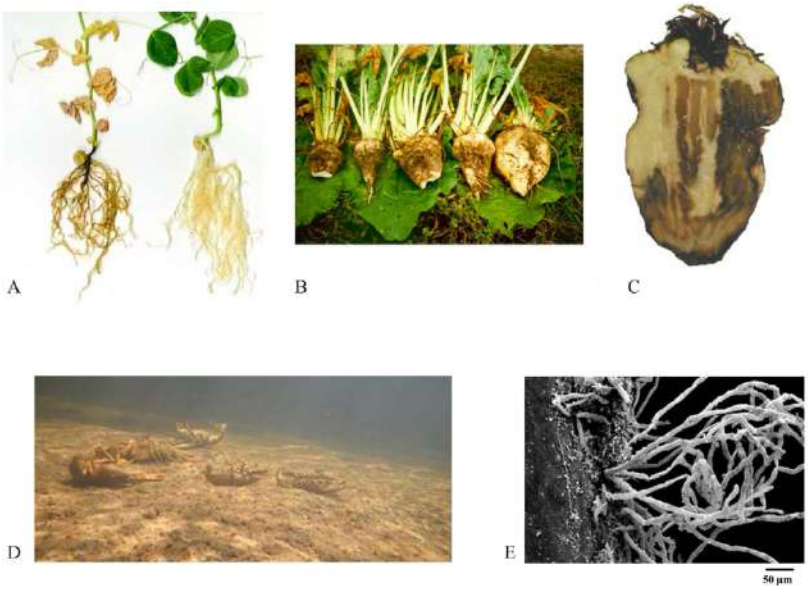

Fig. 3 – Symptoms of diseases induced by *Aphanomyces* genus. (A) *A. euteiches* root rot symptoms on dry pea (*Pisum sativum*) cv. Cameor. At 34 days after inoculation with zoospore suspension at root level, *A. euteiches* induces browning of roots; impaired root growth and induces yellowing of leaves Left: infected. Right: control, non-infected (pictures, A. Kiselev, LRSV, France). (B,C) *A. cochlioides* root rot on sugar beet: dark-brown and scabby lesions on sugar beet roots infected in field and longitudinal section of a sugar beet root with water-soaked lesions (pictures provided by Maribo Hilleshög Research AB, Sweden). (D, E) White-clawed crayfish mass mortality in Lucelle brook (France) (Collas et al., 2016) and *A. astaci* hypha (in white) in naive infected crayfish (pictures from scanning electron microscope provided by UMR CNRS 7267 France).

efficient against soilborne pathogens complexes (You et al., 2020). Without chemical control available, several microorganisms have been tested for biological control of *A. euteiches*. Promising effects have been observed *in vitro*, but slight effects on root rot emergence are generally observed in field conditions (Wakelin et al., 2012; King and Parke, 2013). Thereby crop management remains the most effective tool to limit legumes root rot. One recommendation to improve management of *A. euteiches* root rot in legumes field is crop rotation with different periods to diminish the pathogen level in soils overtime. Nevertheless the diversity of alternative hosts in combination with the extraordinary longevity of *A. euteiches* oospores in soil reduces the efficiency of this method (Schren, 1960; Moussart et al., 2009). Another recommendation is to seed plants into soil rich in phosphorus, as it delays disease development (Bødker et al., 1998). Finally there are DNA tests to check the presence of *A. euteiches* in suspect soils, root tissues or seeds (Gangneux et al., 2014). While improved procedures and reproducibility of DNA testing are needed, these tools are useful for implementing disease management practices when the pathogen is present.

For the past two decades, the obtention of resistant pea cultivars has been considered as a major objective in France to secure the yields (Quillévéré-Hamard et al., 2021). The strategy of the pea breeding program launched in 1995 relies on pyramidizing of different genetic loci from partially resistant pea lines (Gritton, 1990; Kraft, 1992; Pilet-Nayel et al., 2017). The first Quantitative Trait Loci (QTL) of resistance were described in some pea accessions by Pilet-Nayel et al., in 2002 and 2005, and the first varieties with partial *A. euteiches* resistance were registered in 2012 (McGee et al., 2012). Genome-wide association mapping using 175 lines of pea validated 52 QTL of small size-intervals associated with resistance to *A. euteiches* (Desgroux et al., 2016). Among them six major QTL were verified. These studies along with the availability of GenoPea SNP Array (Tayeh et al., 2015) will facilitate the development of resistant cultivars. One of the major QTLs in pea is Ae-Ps7.6 which explains over 50 % of phenotypic variations using a collection of reference *A. euteiches* strains (Hamon et al., 2011, 2013). Combination of Ae-Ps7.6 with other QTLs delays symptom onset and slows down root colonization (Lavaud et al., 2016). The effect and stability of the QTL were validated using the large collection of *A. euteiches* strains from different regions of France (Quillévéré-Hamard et al., 2021), therefore the AeD990SW45-8-7 line, which harbours the combination of 4 major QTL Ae-Ps1.2, Ae-Ps2.2, Ae-Ps3.1

and Ae-Ps7.6 might be used as a source of resistance in further pea breeding programs (Desgroux et al., 2016). In alfalfa, there are at least two significant races (*i.e*, race1 and race2) that are detrimental to the crop. Alfalfa resistant cultivars to race 1 were released in the 1990's (Grau, 1992), but the resistance was rapidly overcome by the pathogen leading to the discovery of the race 2 and the development of race2-resistant alfalfa cultivars. By now *A. euteiches* isolates able to knock out race1 and race2-resistance have been identified in the US (Samac et al., 2012; Seitz and Rouse, 2012). The emergence of a putative new race of the pathogen reveals the difficulties to obtain alfalfa cultivars displaying a durable resistance to *Aphanomyces* root rot. In lentil, the first QTL mapping and genome-wide association studies identify seven QTL clusters and 15 putative genes within the cluster associated with *Aphanomyces* resistance (Ma et al., 2020). This finding, in association with image-based phenotyping approaches on roots (Marzougui et al., 2019), will enhance the development of lentil cultivars with partial resistance to *A. euteiches*.

The complete genome sequence of reference pea 'Cameor' line became available in 2019 (Kreplak et al., 2019) and chromosome-level genome of alfalfa in 2020 (Chen et al., 2020). There are no doubts that these resources will facilitate research in resistance mechanisms of these crops and transfer of knowledge previously obtained using closely related model legume *Medicago truncatula*. As a legume model *M. truncatula* offers various techniques for molecular studies such as high-quality genome, transient and stable transformation, and fast generation cycle (Bruijn, 2020). An *in vitro* system which allows to test susceptibility of 157 *M. truncatula* lines against *A. euteiches* and demonstrates natural variation of susceptibility was reported (Djébali et al., 2009; Bonhomme et al., 2014). From the study one susceptible (F83005.5) and two tolerant lines (Jemalong A17 and DZA45.15) were selected for molecular studies (Badis et al., 2015; for review see Jacquet and Bonhomme, 2019) to decipher tolerant mechanisms. One of the major features of tolerant Jemalong A17 line is the development of 'ring of lignin' which protects central cylinder from invasion of *A. euteiches* into vascular tissue and therefore ensures the maintenance of nutrient and water supply in the plant (Djébali et al., 2009). Pathogen attack induces complex remodelling of the host metabolism such as phenolic compounds. One of the most induced genes of the tolerant A17 *M. truncatula* line under *A. euteiches* infection is isoliquiritigenin 2'-O-methyltransferase transforming isoliquirtigenin to 2'-O-methylisoliquirtigenin. The latter was shown to inhibit *A. euteiches* zoospores germination by 72–86 % (Badis et al., 2015). Genome-wide association studies of quantitative resistance to *A. euteiches* identified two major loci on the chromosome 3 of *M. truncatula* (Djébali et al., 2009). A candidate gene encoding an F-box protein was characterized as a negative regulator of resistance to *A. euteiches* (Bonhomme et al., 2014). In addition significant SNPs were identified within an adenylate isopentenyltransferase (IPT) involved in cytokinin biosynthesis, and/or a MYB transcription factor regulated by gibberellin and abscisic acid (GAMYB) (Bonhomme et al., 2014; Jacquet and Bonhomme, 2019). Thus the integration of genomic and genetic technologies with adapted breeding designs will accelerate legume improvement needed to counter *Aphanomyces* root rot.

Aphanomyces root rot in sugar beet

A. cochlioides is the causal agent of the black root rot in sugar beet. The disease can lead to the loss of entire sugar beet fields and to a drastic reduction of sugar yield (Papavizas and Ayers, 1974; Taguchi et al., 2010). The infection can occur in two separate phases during the sugar beet life cycle: an early, acute phase, known as damping-off, on 2- to 5-week-old seedlings and a chronic phase, later in the season on mature roots (Papavizas and Ayers, 1974). The acute phase generally occurs in post-emergence and it is favoured by warm soil temperature (20–30 °C) and moist conditions (Panella and Lewellen, 2005). Infected hypocotyls turn into a dark, thin thread (Harveson, 2006) and seedlings may fall over and die (Taguchi et al., 2009). If warm and wet conditions persist in the soil, the damage can lead to total crop failure (Luterbacher et al., 2005) but if the soil dries and temperature decreases, young roots may recover by developing later roots and survive (Papavizas and Ayers, 1974). The chronic phase occurs on older plants in late June to August (Buchholtz, 1944). Infected roots appear soft and water-soaked and are characterized by a dark brown discoloration on the affected area (Papavizas and Ayers, 1974) (Fig. 3B, C). Roots can be severely stunted and often show rotted, tasselled root tip (Windels, 2000). The infection, when severe, results in the death of the plants, however older roots that recover from damping-off infection or that are infected in a later stage can survive but are characterized by reduced yield and low sugar content (Windels, 2000). While the effects of *Aphanomyces* damping-off can be overcome by the application of fungicides such as hymexazol, no effective strategies have been developed for the control of the chronic phase of the black rot disease (Taguchi et al., 2010). Cultivation practices such as early planting, enhanced drainage or application of "spent lime" (calcium carbonate) in sugar beet field as pH adjustment in the soil can help to reduce the effect of *Aphanomyces* on sugar beet yield (Bresnahan et al., 2001; Brantner and Chanda, 2016). However, in highly infested soils these practices are inadequate for economic yields. Crop rotation is also not efficient because of the persistence of the pathogen in the soil (Takenaka and Ishikawa, 2013). The development of resistant varieties remains the only valuable solution to control the disease but the genetic basis of resistance to *A. cochlioides* is still unclear. Bockstahler et al., (1950) indicated that the resistance to *Aphanomyces* is heritable and dominant, but important details such as number, map position and products of resistance genes remain unknown (Taguchi et al., 2009). Taguchi et al., (2010) have identified a single dominant gene, *Acr1* (*A. cochlioides* resistance 1) that confers resistance to *Aphanomyces* root rot in both greenhouse conditions and in *Aphanomyces*-infested field and such gene has been located on chromosome III in sugar beet genome. Several genes and major QTLs associated with the resistance to important sugar beet diseases such as Rhizomania and Cercospora leaf spot have been mapped on the same chromosome (Barzen et al., 1997; Schäfer-Pregl et al., 1999; Scholten et al., 1999; Setiawan et al., 2000; Gidner et al., 2005; Grimmer et al., 2007) highlighting the importance of *Acr1* in sugar beet breeding to *Aphanomyces*-caused disease.

Epizootic ulcerative syndrome (EUS) caused by A. invadans

A. invadans typically infects the juvenile and young adult stages of fishes, with no documented pathogenicity towards larvae and fry (OIE, 2016). The severity of EUS infection varies considerably depending on culture conditions of affected fish. Mortality and morbidity within a typical aquaculture scenario, snakehead species (*Channa* sp.), are both highest (exceeding 50 %) when water temperatures remain between 18 and 22 °C for an extended time (OIE, 2016). Therefore, protracted periods of low (sub-22 °C) temperature throughout summer alongside heavy rainfall appear to be the major environmental factors which increase severity of EUS outbreaks.

Characteristic external clinical signs of EUS are uniform across the majority of affected species and in order of diagnostic significance include: dermal ulceration, erratic swimming and inappetence, with increasing symptoms as the disease progresses (Blazer et al., 2002; Saylor et al., 2010). Due to the non-specific external clinical signs, a molecular approach to diagnosis involving PCR-based internal transcribed spacer sequencing (Vandersea et al., 2006; Kamilya and Kollanoor, 2020) is used to positively identify *A. invadans* at fish farm outbreaks. Nonetheless, the characteristic dermal ulceration caused by *A. invadans* has been deemed an appropriate presumptive diagnosis for EUS (Bondad-Reantaso, 1992). Death, generally caused by internal mycosis or loss of osmotic balance, typically occurs within 1–4 days post-infection (Saylor et al., 2010). Internal clinical signs of EUS are similarly uniform across infected fish species: mycotic granulomas form as *A. invadans* hyphae penetrate through dermal tissue and into the target organ of the host – skeletal muscle (OIE, 2016). Mycotic granulomas, the typical internal pathology associated with EUS, may also be present throughout other internal organs.

EUS is a highly difficult disease to treat within commercial aquaculture; therefore the most common approach currently undertaken by farmers is immediate destruction of infected stock (Herbert et al., 2019). No antibiotic treatments are commercially available for *A. invadans* (Iberahim et al., 2018). Furthermore, the two chemotherapeutics with demonstrated efficacy against *A. invadans*, malachite green and formalin, are tightly regulated globally and hazardous to human health and the environment (Srivastava et al., 2004; Iberahim et al., 2018). Use of malachite green in aquaculture is currently prohibited worldwide (Zhou et al., 2019).

However, recent *in vitro* testing of antifungals against *A. invadans* has yielded encouraging results. Formalin, KMn04 and Fluconazole show considerable inhibitory action against zoospore germination and hyphal growth of *A. invadans* at 10 ppm, 100 ppm and 1 ppm respectively (Paria et al., 2020). The activity of KMn04 and Fluconazole against *A. invadans* had been little-studied, with these candidates currently showing the greatest promise in the search for chemical EUS treatments.

Regarding immunostimulants, use of pro- and prebiotics for disease management in aquaculture is an emerging field (Verschuere et al., 2000), with strong potential in the shrimp sector and industry-wide (Lara-Flores, 2011; Kumar et al., 2016). Regarding *A. invadans*, two recent immunostimulant trials have demonstrated efficacy as in-feed treatments for EUS (Devi et al., 2019a, 2019b).

Crayfish plague caused by A. astaci

When a native European crayfish population is affected by *A. astaci*, one of the first observable symptoms is often the presence of numerous crayfish visible in broad daylight (whereas crayfish are most often active at night). Indeed, clinical symptoms at the individual level are manifested by behavioural changes (such as changes in feeding behaviour, in swimming movement, lethargy), as well as the appearance of visible lesions (Fig. 3E) on the cuticle (CABI, 2020a). However, these lesions are not specific to aphanomycosis and may be caused by mechanical injury or infection with other fungal or bacterial pathogens (Persson and Söderhäll, 1983). However, unless aquatic environments are particularly monitored, the first sign of infection at the population level is the presence of many dead crayfish observed (Fig. 3D), with no mortality in other aquatic animal species (which could be possibly due to pollution effect or to a less specific pathogen) (Alderman et al., 1987). Currently, the most reliable and commonly used diagnostic techniques are based on PCR tests, either followed by a sequencing step (Oidtmann et al., 2006) or directly by real time PCR approaches from the cuticle of dead individuals found in the wild (Vrålstad et al., 2009). In recent years, the development of techniques based on environmental DNA (eDNA) has been a promising tool for the detection of plague directly in water samples, allowing an early management of this pathogen potentially present in aquatic systems, as well as a better understanding of the spread of this disease in the natural environment (Strand et al., 2014; Wittwer et al., 2018, 2019).

These recent detection techniques have made it possible to identify several populations of native European crayfish (*A. astacus*, *P. leptodactylus* and *A. torrentium*) that are chronically infected by the crayfish plague, notably in Finland, Turkey, Slovenia or Spain (Jussila et al., 2011; Kokko et al., 2012; Kušar et al., 2013; Maguire et al., 2016, Martín-Torrijos et al., 2017). When it was verified, it turns out that haplogroups A and B were involved in these chronical infections (Maguire et al., 2016). These observations raised the question of the potential virulence of the different strains of *A. astaci*, but also the question of the potential immunological resistance developed by natural populations of European crayfish. Thus, following infections carried out in a controlled environment using *A. astacus* crayfish to estimate mortality rates, it was also shown that RAPD-groups B and E were more virulent than the RAPD-group A (Becking et al., 2015; Makkonen et al., 2012b) A recent study revealed resistance and susceptibility of European crayfish to *A. astaci* could depend on the population origin (Jussila et al., 2020). In the case of resistant North American crayfish, they have developed immune defences that prevent a fatal *A. astaci* infection (Cerenius et al., 2003).

6. Conclusion and perspectives

Aphanomyces genus comprises a vast number of species including both plant and animal pathogenic species and saprophytic species (Diéguez-Uribeondo et al., 2009). Due to

their remarkable economic impact on agriculture and aquaculture systems, their worldwide distribution, species belonging to this genus have been receiving growing attention from the oomycete research community with a major focus on pathogenicity and host resistance mechanisms.

To secure the production of economically important *Aphanomyces* spp. hosts we suggest several directions for further studies:

- Enhance our understanding of *Aphanomyces* spp. pathogenesis on molecular level and elucidate the role of effectors and their interaction with the host during infection;
- Exploit the natural variation of resistance against *Aphanomyces* spp. in commercial breeding;
- For plant pathogenic species, begin studying the role of soil microbiome in stimulation or protection against *Aphanomyces*-induced diseases.
- For animal pathogenic species, combine the analysis of *Aphanomyces* spp. effectors with the immunological response of the host to better understand and control the spread of those pathogens in natural environments.

Declaration of competing interest

The authors declare that they have no conflict of interest.

The manuscript has been read and approved by all of the authors.

Acknowledgements

The authors would like to thanks the Office Français de la Biodiversité (AFB) under grant agreement No 150656 and the European Union's Horizon 2020 Research and Innovation programme under grant agreement No 766048.

Appendix A. Supplementary data

Supplementary data to this article can be found online at https://doi.org/10.1016/j.fbr.2021.08.001.

REFERENCES

Ackefors, H.E., 2000. Freshwater crayfish farming technology in the 1990s: a European and global perspective. Fish Fish. 1, 337–359.

Afzali, S.F., Hassan, M.D., Abdul-Rahim, A.M., Sharifpour, I., Sabri, J., 2013. Isolation and identification of *Aphanomyces* species from natural water bodies and fish farms in Selangor, Malaysia. Malays. Appl. Biol. 42, 21–31.

Alderman, D.J., 1996. Geographical spread of bacterial and fungal diseases of crustaceans. Rev. Sci. Tech. 15, 603–632.

Alderman, D.J., Polglase, J.L., Frayling, M., 1987. *Aphanomyces astaci* pathogenicity under laboratory and field conditions. J. Fish. Dis. 10, 385–393.

Ali, S.M., Sharma, B., Ambrose, M.J., 1994. Current status and future strategy in breeding pea to improve resistance to biotic and abiotic stresses. In: Muehlbauer, F.J., Kaiser, W.J. (Eds.), Expanding the Production and Use of Cool Season Food Legumes: A Global Perspective of Persistent Constraints and of Opportunities and Strategies for Further Increasing the Productivity and Use of Pea, Lentil, Faba Bean, Chickpea and Grasspea in Different Farming Systems, Current Plant Science and Biotechnology in Agriculture. Springer Netherlands, Dordrecht, pp. 540–558.

Allmaras, R., Fritz, V.A., Pfleger, F.L., Copeland, S.M., 1998. Common root rot of pea (*Pisum sativum* L.): oat pre-crop and traffic compaction effects in fine-textured mollisols. In: Root Demographics and Their Efficiencies in Sustainable Agriculture, Grasslands and Forest Ecosystems. Springer, pp. 285–294.

Andersson, M.G., Cerenius, L., 2002. Analysis of chitinase expression in the crayfish plague fungus *Aphanomyces astaci*. Dis. Aquat. Org. 51, 139–147.

Appiah, A.A., Van West, P., Osborne, M.C., Gow, N.A., 2005. Potassium homeostasis influences the locomotion and encystment of zoospores of plant pathogenic oomycetes. Fungal Genet. Biol. 42, 213–223.

Arshad, P.E., Arockiaraj, J., 2020. Pathogenicity and pathobiology of Epizootic Ulcerative Syndrome (EUS) causing fungus *Aphanomyces invadans* and its immunological response in fish. Rev. Fish. Sci Aquac. 28, 358–375.

Badis, Y., Bonhomme, M., Lafitte, C., Huguet, S., Balzergue, S., Dumas, B., Jacquet, C., 2015. Transcriptome analysis highlights preformed defenses and signaling pathways controlled by the prAe1 quantitative trait locus (QTL), conferring partial resistance to *Aphanomyces euteiches* in *Medicago truncatula*. Mol. Plant Pathol. 16, 973–986.

Baldauf, S.L., Roger, A.J., Wenk-Siefert, I., Doolittle, W.F., 2000. A kingdom-level phylogeny of eukaryotes based on combined protein data. Science 290, 972–977.

Ballesteros, I., Martin, M., Diéguez-Uribeondo, J., 2006. First isolation of *Aphanomyces frigidophilus* (Saprolegniales) in Europe. Mycotaxon 95, 335–340.

Banfield, M.J., Kamoun, S., 2013. Hooked and Cooked: A Fish Killer Genome Exposed. PLoS Genet. 9 (6)e1003590.

Baruah, A., Saha, R.K., Kamilya, D., 2012. Inter-species transmission of the epizootic ulcerative syndrome (EUS) pathogen, *Aphanomyces invadans*, and associated physiological responses. Israeli J. Aquacult. 64, 9.

Barzen, E., Stahl, R., Fuchs, E., Borchardt, D.C., Salamini, F., 1997. Development of coupling-repulsion-phase SCAR markers diagnostic for the sugar beet Rz1 allele conferring resistance to rhizomania. Mol. Breed. 3, 231–238.

Beakes, G.W., Glockling, S.L., Sekimoto, S., 2012. The evolutionary phylogeny of the oomycete "fungi. Protoplasma 249, 3–19.

Beale, J.W., Windels, C.E., Kinkel, L.L., 2002. Spatial distribution of *Aphanomyces cochlioides* and root rot in sugar beet fields. Plant Dis. 86, 547–551.

Becking, T., Mrugała, A., Delaunay, C., Svoboda, J., Raimond, M., Viljamaa-Dirks, S., Petrusek, A., Grandjean, F., Braquart-Varnier, C., 2015. Effect of experimental exposure to differently virulent *Aphanomyces astaci* strains on the immune response of the noble crayfish *Astacus astacus*. J. Invertebr. Pathol. 132, 115–124.

Birch, P.R., Boevink, P.C., Gilroy, E.M., Hein, I., Pritchard, L., Whisson, S.C., 2008. Oomycete RXLR effectors: delivery, functional redundancy and durable disease resistance. Curr. Opin. Plant Biol. 11, 373–379.

Blazer, V.S., Lilley, J.H., Schill, W.B., Kiryu, Y., Densmore, C.L., Panyawachira, V., Chinabut, S., 2002. *Aphanomyces invadans* in

Atlantic Menhaden along the East Coast of the United States. J. Aquat. Anim. Health 14, 1–10.
Blazer, V.S., Vogelbein, W.K., Densmore, C.L., May, E.B., Lilley, J.H., Zwerner, D.E., 1999. *Aphanomyces* as a cause of ulcerative skin lesions of menhaden from Chesapeake Bay tributaries. J. Aquat. Anim. Health 11, 340–349.
Bockstahler, H.W., Hogaboam, G.J., Schneider, C.L., 1950. Further studies on the inheritance of black root resistance in sugar beets. Proc. Am. Soc. Sugar Beet Technol. 104–107.
Bødker, L., Kjøller, R., Rosendahl, S., 1998. Effect of phosphate and the arbuscular mycorrhizal fungus *Glomus intraradices* on disease severity of root rot of peas (*Pisum sativum*) caused by *Aphanomyces euteiches*. Mycorrhiza 8, 169–174.
Bogdan, J., 2019. *Aphanomyces* Root Rot in Pulse Crops.
Bondad-Reantaso, M.G., 1992. Environmental monitoring of the epizootic ulcerative syndrome (EUS) in fish from Munoz, Nueva Ecija in the Philippines. Dis. Asian Aquacult. I 475–490.
Bonhomme, M., André, O., Badis, Y., Ronfort, J., Burgarella, C., Chantret, N., Prosperi, J.-M., Briskine, R., Mudge, J., Debéllé, F., Navier, H., Miteul, H., Hajri, A., Baranger, A., Tiffin, P., Dumas, B., Pilet-Nayel, M.-L., Young, N.D., Jacquet, C., 2014. High-density genome-wide association mapping implicates an F-box encoding gene in *Medicago truncatula* resistance to *Aphanomyces euteiches*. New Phytol. 201, 1328–1342.
Bozkurt, T.O., Schornack, S., Banfield, M.J., Kamoun, S., 2012. Oomycetes, effectors, and all that jazz. Curr. Opin. Plant Biol. 15, 483–492.
Brantner, J.R., Chanda, A.K., 2016. Addition of supplemental spent lime to previously limed soil for control of *Aphanomyces* root rot on sugarbeet. In: Phytopathology. Amer. Phytopathological Soc, pp. 80–87.
Bresnahan, G.A., Dexter, A.G., Windels, C.E., Brantner, J.R., Luecke, J.L., 2001. Influence of soil pH on *Aphanomyces cochlioides* in sugarbeet. Sugarbeet Res. Ext. Rep. 32, 264–268.
Brinck, P., 1975. Crayfish in Sweden. Freshw. Crayfish 2, 77–85.
Bruijn, F.J. de (Ed.), 2020. The Model Legume *Medicago truncatula*. John Wiley & Sons, Ltd.
Buchholtz, W.F., 1944. The sequence of infection of a seedling stand of sugar beets by *Pythium debaryanum* and *Aphanomyces cochlioides*. Phytopathology 34, 490–496.
Byrt, P.N., Irving, H.R., Grant, B.R., 1982a. The effect of organic compounds on the encystment, viability and germination of zoospores of *Phytophthora cinnamomi*. Microbiology 128, 2343–2351.
Byrt, P.N., Irving, H.R., Grant, B.R., 1982b. The effect of cations on zoospores of the fungus *Phytophthora cinnamomi*. Microbiology 128, 1189–1198.
CABI, 2020a. Invasive Species Compendium. Datasheet on the crayfish plague. URL. https://www.cabi.org/isc/datasheet/87335.
CABI, 2020b. Invasive Species Compendium. Datasheet on *Aphanomyces cochlioides*. URL. https://www.cabi.org/isc/datasheet/6405.
CABI, 2019. Invasive Species Compendium. Datasheet on *Aphanomyces euteiches*. URL. https://www.cabi.org/isc/datasheet/6408.
Camborde, L., Kiselev, A., Pel, M.J.C., Leru, A., Jauneau, A., Pouzet, C., Dumas, B., Gaulin, E., 2020. A DEAD BOX RNA helicase from *Medicago truncatula* is hijacked by an RNA-binding effector from the root pathogen *Aphanomyces euteiches* to facilitate host infection. bioRxiv. https://doi.org/10.1101/2020.06.17.157404.
Camborde, L., Raynaud, C., Dumas, B., Gaulin, E., 2019. DNA-damaging effectors: new players in the effector arena. Trends Plant Sci. 24, 1094–1101.
Cerenius, L., Bangyeekhun, E., Keyser, P., Söderhäll, I., Söderhäll, K., 2003. Host prophenoloxidase expression in freshwater crayfish is linked to increased resistance to the crayfish plague fungus. *Aphanomyces astaci*. Cell. Microbiol. 5, 353–357.
Cerenius, L., Lee, B.L., Söderhäll, K., 2008. The proPO-system: pros and cons for its role in invertebrate immunity. Trends Immunol. 29, 263–271.
Cerenius, L., Söderhäll, K., 1984. Chemotaxis in *Aphanomyces astaci*, an arthropod-parasitic fungus. J. Invertebr. Pathol. 43, 278–281.
Chen, H., Zeng, Y., Yang, Y., Huang, L., Tang, B., Zhang, H., Hao, F., Liu, W., Li, Youhan, Liu, Y., Zhang, X., Zhang, R., Zhang, Y., Li, Yongxin, Wang, K., He, H., Wang, Z., Fan, G., Yang, H., Bao, A., Shang, Z., Chen, J., Wang, W., Qiu, Q., 2020. Allele-aware chromosome-level genome assembly and efficient transgene-free genome editing for the autotetraploid cultivated alfalfa. Nat. Commun. 11, 2494.
Chen, L., Geng, X., Ma, Y., Zhao, J., Chen, W., Xing, X., Shi, Y., Sun, B., Li, H., 2019. The ER lumenal Hsp70 pProtein FpLhs1 is important for conidiation and plant infection in *Fusarium pseudograminearum*. Front. Microbiol. 10.
Chinabut, S., 1998. Epizootic ulcerative syndrome: information up to 1997. Fish Pathol. 33, 321–326.
Chondar, S.L., Rao, P.S., 1996. Epizootic Ulcerative Syndrome Disease to Fish and its Control: a Review. World Aquaculture, p. 77.
Collas, M., Becking, T., Delpy, M., Pflieger, M., Bohn, P., Reynolds, J., Grandjean, F., 2016. Monitoring of white-clawed crayfish *Austropotamobius pallipes* population during a crayfish plague outbreak followed by rescue. Knowl. Manag. Aquat. Ecosyst. 1.
Darriba, D., Taboada, G.L., Doallo, R., Posada, D., 2012. jModelTest 2: more models, new heuristics and parallel computing. Nat. Methods 9, 772, 772.
de Vries, S., de Vries, J., 2020. A Global Survey of Carbohydrate Esterase Families 1 and 10 in Oomycetes. Front. Genet. 11, 756.
Delmas, C.E., Mazet, I.D., Jolivet, J., Delière, L., Delmotte, F., 2014. Simultaneous quantification of sporangia and zoospores in a biotrophic oomycete with an automatic particle analyzer: disentangling dispersal and infection potentials. J. Microbiol. Methods 107, 169–175.
Desgroux, A., L'anthoëne, V., Roux-Duparque, M., Rivière, J.-P., Aubert, G., Tayeh, N., Moussart, A., Mangin, P., Vetel, P., Piriou, C., 2016. Genome-wide association mapping of partial resistance to *Aphanomyces euteiches* in pea. BMC Genom. 17, 124.
Devi, G., Harikrishnan, R., Paray, B.A., Al-Sadoon, M.K., Hoseinifar, S.H., Balasundaram, C., 2019a. Comparative immunostimulatory effect of probiotics and prebiotics in Channa punctatus against *Aphanomyces invadans*. Fish Shellfish Immunol. 86, 965–973.
Devi, G., Harikrishnan, R., Paray, B.A., Al-Sadoon, M.K., Hoseinifar, S.H., Balasundaram, C., 2019b. Effects of aloe-emodin on innate immunity, antioxidant and immune cytokines mechanisms in the head kidney leucocytes of Labeo rohita against *Aphanomyces invadans*. Fish Shellfish Immunol. 87, 669–678.
Dick, M.W., 2001. The peronosporomycetes. In: Systematics and Evolution. Springer, pp. 39–72.
Dick, M.W., 1969. Morphology and taxonomy of the Oomycetes, with special reference to Saprolegniaceae, Leptomitaceae and Pythiaceae. New Phytol. 68, 751–775.
Diéguez-Uribeondo, J., 2006. The dispersion of the *Aphanomyces astaci*-carrier *Pacifastacus leniusculus* by humans represents the main cause of disappearance of the indigenous crayfish *Austropotamobius pallipes* in Navarra. Bull. Fr. Peche Piscic. 1303–1312.
Diéguez-Uribeondo, J., García, M.A., Cerenius, L., Kozubíková, E., Ballesteros, I., Windels, C., Weiland, J., Kator, H., Söderhäll, K., Martín, M.P., 2009. Phylogenetic relationships among plant and animal parasites, and saprotrophs in *Aphanomyces* (Oomycetes). Fungal Genet. Biol. 46, 365–376.
Diéguez-Uribeondo, J., Huang, T.-S., Cerenius, L., Söderhäll, K., 1995. Physiological adaptation of an *Aphanomyces astaci* strain

isolated from the freshwater crayfish *Procambarus clarkii*. Mycol. Res. 99, 574–578.
Djébali, N., Jauneau, A., Ameline-Torregrosa, C., Chardon, F., Jaulneau, V., Mathé, C., Bottin, A., Cazaux, M., Pilet-Nayel, M.-L., Baranger, A., Aouani, M.E., Esquerré-Tugayé, M.-T., Dumas, B., Huguet, T., Jacquet, C., 2009. Partial Resistance of *Medicago truncatula* to *Aphanomyces euteiches* is associated with protection of the root stele and is controlled by a major QTL rich in proteasome-related Genes. MPMI (Mol. Plant-Microbe Interact.) 22, 1043–1055.
Drechsler, C., 1929. The beet water mold and several related root. J. Agric. Res. 38, 309.
Drenth, A., Torres, G.A., López, G.M., 2013. *Phytophthora palmivora*, la causa de la Pudrición del cogollo en la palma de aceite. Revista Palmas 34, 87–94.
Dyer, A.T., Windels, C.E., 2003. Viability and maturation of *Aphanomyces cochlioides* oospores. Mycologia 95, 321–326.
Egusa, S., Masuda, N., 1971. A new fungal of *Plecoglossus altivelis*. Fish Pathol. 6, 41–46.
Erwin, D.C., Ribeiro, O.K., 1996. *Phytophthora* Diseases Worldwide. American Phytopathological Society (APS Press).
FAO, 2020. The State of World Fisheries and Aquaculture 2020: Sustainability in action, La situation mondiale des pêches et de l'aquaculture (SOFIA). FAO, Rome, Italy.
FAO, 1991. The State of Food and Agriculture 1991. Food & Agriculture Org.
Finkenstadt, V.L., 2014. A review on the complete utilization of the sugarbeet. Sugar Tech 16, 339–346.
Gangneux, C., Cannesan, M.A., Bressan, M., Castel, L., Moussart, A., Vicré-Gibouin, M., Driouich, A., Trinsoutrot-Gattin, I., Laval, K., 2014. A sensitive assay for rapid detection and quantification of *Aphanomyces euteiches* in soil. Phytopathology 104, 1138–1147.
Gaulin, E., Bottin, A., Jacquet, C., Dumas, B., 2008. *Aphanomyces euteiches* and Legumes. In: Oomycete Genetics and Genomics: Diversity, Interactions, and Research Tools, pp. 345–360.
Gaulin, E., Jacquet, C., Bottin, A., Dumas, B., 2007. Root rot disease of legumes caused by *Aphanomyces euteiches*. Mol. Plant Pathol. 8, 539–548.
Gaulin, E., Pel, M.J.C., Camborde, L., San-Clemente, H., Courbier, S., Dupouy, M.-A., Lengellé, J., Veyssiere, M., Le Ru, A., Grandjean, F., Cordaux, R., Moumen, B., Gilbert, C., Cano, L.M., Aury, J.-M., Guy, J., Wincker, P., Bouchez, O., Klopp, C., Dumas, B., 2018. Genomics analysis of *Aphanomyces* spp. identifies a new class of oomycete effector associated with host adaptation. BMC Biol. 16, 43.
Gidner, S., Lennefors, B.-L., Nilsson, N.-O., Bensefelt, J., Johansson, E., Gyllenspetz, U., Kraft, T., 2005. QTL mapping of BNYVV resistance from the WB41 source in sugar beet. Genome 48, 279–285.
Gleason, F.H., Lilje, O., Lange, L., 2018. What has happened to the "aquatic phycomycetes" (sensu Sparrow)? Part II: Shared properties of zoosporic true fungi and fungus-like microorganisms. Fungal Biol. Rev. 32, 52–61.
Gossen, B.D., Conner, R.L., Chang, K.-F., Pasche, J.S., McLaren, D.L., Henriquez, M.A., Chatterton, S., Hwang, S.-F., 2016. Identifying and managing root rot of pulses on the northern great plains. Plant Dis. 100, 1965–1978.
Grandjean, F., Vrålstad, T., Dieguez-Uribeondo, J., Jelić, M., Mangombi, J., Delaunay, C., Filipova, L., Rezinciuc, S., Kozubikova-Balcarova, E., Guyonnet, D., 2014. Microsatellite markers for direct genotyping of the crayfish plague pathogen *Aphanomyces astaci* (Oomycetes) from infected host tissues. Vet. Microbiol. 170, 317–324.
Grau, C.R., Muehlchen, A.M., Tofte, J.E., Smith, R.R., 1991. Variability in virulence of *Aphanomyces euteiches*. Plant Dis. 75, 1153–1156.
Grau, C.R., 1992. Registration of WAPH-1 alfafa germplasm with resistance to *Aphanomyces* root rot. Crop Sci. 32, 287–288.
Grimmer, M.K., Trybush, S., Hanley, S., Francis, S.A., Karp, A., Asher, M.J.C., 2007. An anchored linkage map for sugar beet based on AFLP, SNP and RAPD markers and QTL mapping of a new source of resistance to Beet necrotic yellow vein virus. Theor. Appl. Genet. 114, 1151–1160.
Gritton, E.T., 1990. Registration of five root rot resistant germplasm lines of processing pea. Crop Sci. 30, 1166–1167.
Guindon, S., Dufayard, J.-F., Lefort, V., Anisimova, M., Hordijk, W., Gascuel, O., 2010. New algorithms and methods to estimate maximum-likelihood phylogenies: assessing the performance of PhyML 3.0. Syst. Biol. 59, 307–321.
Haas, B.J., Kamoun, S., Zody, M.C., Jiang, R.H., Handsaker, R.E., Cano, L.M., Grabherr, M., Kodira, C.D., Raffaele, S., Torto-Alalibo, T., 2009. Genome sequence and analysis of the Irish potato famine pathogen *Phytophthora infestans*. Nature 461, 393–398.
Hamon, C., Baranger, A., Coyne, C.J., McGee, R.J., Le Goff, I., L'Anthoëne, V., Esnault, R., Rivière, J.-P., Klein, A., Mangin, P., McPhee, K.E., Roux-Duparque, M., Porter, L., Miteul, H., Lesné, A., Morin, G., Onfroy, C., Moussart, A., Tivoli, B., Delourme, R., Pilet-Nayel, M.-L., 2011. New consistent QTL in pea associated with partial resistance to *Aphanomyces euteiches* in multiple French and American environments. Theor. Appl. Genet. 123, 261–281.
Hamon, C., Coyne, C.J., McGee, R.J., Lesné, A., Esnault, R., Mangin, P., Hervé, M., Le Goff, I., Deniot, G., Roux-Duparque, M., Morin, G., McPhee, K.E., Delourme, R., Baranger, A., Pilet-Nayel, M.-L., 2013. QTL meta-analysis provides a comprehensive view of loci controlling partial resistance to *Aphanomyces euteiches* in four sources of resistance in pea. BMC Plant Biol. 10 (13), 45.
Harveson, R.M., 2000. First report of *Aphanomyces* root rot of sugar beet in Nebraska and Wyoming. Plant Dis. 84, 596, 596.
Harveson, R.M., Rush, C.M., 2002. The influence of irrigation frequency and cultivar blends on the severity of multiple root diseases in sugar beets. Plant Dis. 86, 901–908.
Harveson, R.M., 2006. Identifying and distinguishing seedling and root rot diseases of sugar beets. Plant Health Prog. 7, 39.
Heffer, V., Powelson, M., Johnson, K., 2002. Oomycetes. The Plant Health Instructor.
Herbert, B., Jones, J.B., Mohan, C.V., Perera, R.P., 2019. Impacts of epizootic ulcerative syndrome on subsistence fisheries and wildlife. Rev. Sci. Tech. Off. Int. Epiz 38, 459–475.
Hoch, H.C., Mitchell, J.E., 1973. The effects of osmotic water potentials on *Aphanomyces euteiches* during zoosporogenesis. Can. J. Bot. 51, 2.
Holdich, D.M., Reader, J.P., Rogers, W.D., Harlioglu, M., 1995. Interactions between three species of crayfish (*Austropotamobius pallipes*, *Astacus leptodactylus* and *Pacifastacus leniusculus*). Freshw. Crayfish 10, 46–56.
Horio, T., Kawabata, Y., Takayama, T., Tahara, S., Kawabata, J., Fukushi, Y., Nishimura, H., Mizutani, J., 1992. A potent attractant of zoospores of *Aphanomyces cochlioides* isolated from its host, *Spinacia oleracea*. Experientia 48, 410–414.
Huang, T., Cerenius, L., Söderhäll, K., 1994. Analysis of genetic diversity in the crayfish plague fungus, *Aphanomyces astaci*, by random amplification of polymorphic DNA. Aquaculture 126, 1–9.
Huchzermeyer, K.D., Van der Waal, B.C., 2012. Epizootic ulcerative syndrome: exotic fish disease threatens Africa's aquatic ecosystems. J. S. Afr. Vet. Assoc. 83, 39–46.
Hughes, T.J., Grau, C.R., 2007. *Aphanomyces* root rot (common root rot) of legumes. *Aphanomyces* root rot (common root rot) of legumes. The Plant Health Instructor. https://doi.org/10.1094/PHI-I-2007-0418-01.
Hulvey, J.P., Padgett, D.E., Bailey, J.C., 2007. Species boundaries within Saprolegnia (Saprolegniales, Oomycota) based on

morphological and DNA sequence data. Mycologia 99, 421–429.
Iberahim, N.A., Sood, N., Pradhan, P.K., van den Boom, J., van West, P., Trusch, F., 2020. The chaperone Lhs1 contributes to the virulence of the fish-pathogenic oomycete *Aphanomyces invadans*. Fungal Biol. 124, 1024–1031.
Iberahim, N.A., Trusch, F., Van West, P., 2018. *Aphanomyces invadans*, the causal agent of Epizootic Ulcerative Syndrome, is a global threat to wild and farmed fish. Fungal Biol. Rev. 32, 118–130.
Islam, M.T., 2010. Ultrastructure of *Aphanomyces cochlioides* zoospores and changes during their developmental transitions triggered by the host-specific flavone cochliophilin A. J. Basic Microbiol. 50, S58–S67.
Islam, M.T., Ito, T., Tahara, S., 2003. Host-specific plant signal and G-protein activator, mastoparan, trigger differentiation of zoospores of the phytopathogenic oomycete *Aphanomyces cochlioides*. In: Roots: The Dynamic Interface between Plants and the Earth. Springer, pp. 131–142.
Islam, M.T., Tahara, S., 2001. Chemotaxis of fungal zoospores, with special reference to *Aphanomyces cochlioides*. Biosci. Biotechnol. Biochem. 65, 1933–1948.
Jacquet, C., Bonhomme, M., 2019. Deciphering resistance mechanisms to the root rot disease of legumes caused by *Aphanomyces euteiches* with *Medicago truncatula* genetic and genomic resources. In: Bruijn, F.J. de (Ed.), The Model Legume *Medicago truncatula*. John Wiley & Sons, Ltd, pp. 307–316.
Jiang, R.H., Tyler, B.M., 2012. Mechanisms and evolution of virulence in oomycetes. Annu. Rev. Phytopathol. 50, 295–318.
Johnson, T.W., Seymour, R.L., Padgett, D.E., 2002. Biology and Systematics of the Saprolegniaceae. University of North Carolina at Wilmington, Dept. of Biological Sciences, Wilmington, N.C.
Jones, F.R., Drechsler, C., 1925. Root rot of peas in the United States caused by *Aphanomyces euteiches*. J. Agric. Res. 30, 293–325.
Jussila, J., Maguire, I., Kokko, H., Tiitinen, V., Makkonen, J., 2020. Narrow-clawed crayfish in Finland: *Aphanomyces astaci* resistance and genetic relationship to other selected European and Asian populations. Knowl. Manag. Aquat. Ecosyst. 30.
Jussila, J., Makkonen, J., Vainikka, A., Kortet, R., Kokko, H., 2011. Latent crayfish plague (*Aphanomyces astaci*) infection in a robust wild noble crayfish (*Astacus astacus*) population. Aquaculture 321, 17–20.
Kamilya, D., Baruah, A., 2014. Epizootic ulcerative syndrome (EUS) in fish: history and current status of understanding. Rev. Fish Biol. Fish. 24, 369–380.
Kamilya, D., Kollanoor, R., 2020. Epizootic Ulcerative Syndrome (*Aphanomyces invadans*). In: Climate change and infectious diseases. CABI, pp. 291–302.
Kiryu, Y., Blazer, V.S., Vogelbein, W.K., Kator, H., Shields, J.D., 2005. Factors influencing the sporulation and cyst formation of *Aphanomyces invadans*, etiological agent of ulcerative mycosis in Atlantic menhaden, *Brevoortia tyrannus*. Mycologia 97, 569–575.
Kokko, H., Koistinen, L., Harlioğlu, M.M., Makkonen, J., Aydın, H., Jussila, J., 2012. Recovering Turkish narrow clawed crayfish (*Astacus leptodactylus*) populations carry *Aphanomyces astaci*. Knowl. Manag. Aquat. Ecosyst. 12.
Kozubíková, E., Viljamaa-Dirks, S., Heinikainen, S., Petrusek, A., 2011. Spiny-cheek crayfish *Orconectes limosus* carry a novel genotype of the crayfish plague pathogen *Aphanomyces astaci*. J. Invertebr. Pathol. 108, 214–216.
Kraft, J.M., 1992. Registration of 90-2079-2131, and 90-2322 PEA Germplasms. Crop Sci. 32, 1076.
Kreplak, J., Madoui, M.-A., Cápal, P., Novák, P., Labadie, K., Aubert, G., Bayer, P.E., Gali, K.K., Syme, R.A., Main, D., Klein, A., Bérard, A., Vrbová, I., Fournier, C., d'Agata, L., Belser, C., Berrabah, W., Toegelová, H., Milec, Z., Vrána, J., Lee, H., Kougbeadjo, A., Térézol, M., Huneau, C., Turo, C.J., Mohellibi, N., Neumann, P., Falque, M., Gallardo, K., McGee, R., Tar'an, B., Bendahmane, A., Aury, J.-M., Batley, J., Le Paslier, M.-C., Ellis, N., Warkentin, T.D., Coyne, C.J., Salse, J., Edwards, D., Lichtenzveig, J., Macas, J., Doležel, J., Wincker, P., Burstin, J., 2019. A reference genome for pea provides insight into legume genome evolution. Nat. Genet. 51, 1411–1422.
King, E.B., Parke, J.L., 1993. Biocontrol of *Aphanomyces* root rot and *Pythium* damping-off by *Pseudomonas cepacia* AMMD on four pea cultivars. Plant Dis. 77, 1185–1188.
Kumar, N.T.S., Caudillo-Ruiz, K.B., Chatterton, S., Banniza, S., 2021. Characterization of *Aphanomyces euteiches* pathotypes infecting peas in Western Canada. Plant Dis. https://doi.org/10.1094/PDIS-04-21-0874-RE. Online ahead of print.
Kumar, V., Roy, S., Meena, D.K., Sarkar, U.K., 2016. Application of probiotics in shrimp aquaculture: importance, mechanisms of action, and methods of administration. Rev. Fish. Sci Aquac. 24, 342–368.
Kušar, D., Vrezec, A., Ocepek, M., Jenčič, V., 2013. *Aphanomyces astaci* in wild crayfish populations in Slovenia: first report of persistent infection in a stone crayfish *Austropotamobius torrentium* population. Dis. Aquat. Org. 103, 157–169.
Lanver, D., Berndt, P., Tollot, M., Naik, V., Vranes, M., Warmann, T., Münch, K., Rössel, N., Kahmann, R., 2014. Plant surface cues prime *Ustilago maydis* for biotrophic development. PLoS Pathog. 10e1004272.
Lara-Flores, M., 2011. The use of probiotic in aquaculture: an overview. Int. Res. J. Microbiol. 2, 471–478.
Lavaud, C., Baviere, M., Le Roy, G., Hervé, M.R., Moussart, A., Delourme, R., Pilet-Nayel, M.-L., 2016. Single and multiple resistance QTL delay symptom appearance and slow down root colonization by *Aphanomyces euteiches* in pea near isogenic lines. BMC Plant Biol. 16, 166.
Leclerc, M.C., Guillot, J., Deville, M., 2000. Taxonomic and phylogenetic analysis of Saprolegniaceae (Oomycetes) inferred from LSU rDNA and ITS sequence comparisons. Antonie Leeuwenhoek 77, 369–377.
Levenfors, J.P., Wikström, M., Persson, L., Gerhardson, B., 2003. Pathogenicity of *Aphanomyces* spp. from different leguminous crops in Sweden. Eur. J. Plant Pathol. 109, 535–543.
Lévesque, C.A., 2011. Fifty years of oomycetes—from consolidation to evolutionary and genomic exploration. Fungal Divers. 50, 35.
Lilley, J.H., Callinan, R.B., Chinabut, S., Kanchanakhan, S., MacRae, I.H., Phillips, M.J., 1998. Epizootic Ulcerative Syndrome (EUS) Technical Handbook.
Lilley, J.H., Hart, D., Panyawachira, V., Kanchanakhan, S., Chinabut, S., Söderhäll, K., Cerenius, L., 2003. Molecular characterization of the fish-pathogenic fungus *Aphanomyces invadans*. J. Fish. Dis. 26, 263–275.
Lodge, D.M., Taylor, C.A., Holdich, D.M., Skurdal, J., 2000. Nonindigenous crayfishes threaten North American freshwater biodiversity: lessons from Europe. Fisheries 25, 7–20.
Lombard, V., Golaconda Ramulu, H., Drula, E., Coutinho, P.M., Henrissat, B., 2014. The carbohydrate-active enzymes database (CAZy) in 2013. Nucleic Acids Res. 42, D490–D495.
Lowe, S., Browne, M., Boudjelas, S., De Poorter, M., 2000. 100 of the World's Worst Invasive Alien Species: a Selection from the Global Invasive Species Database. Invasive Species Specialist Group Auckland, New Zealand.
Luterbacher, M.C., Asher, M.J.C., Beyer, W., Mandolino, G., Scholten, O.E., Frese, L., Biancardi, E., Stevanato, P., Mechelke, W., Slyvchenko, O., 2005. Sources of resistance to diseases of sugar beet in related Beta germplasm: II. Soil-borne diseases. Euphytica 141, 49–63.
Ma, Y., Marzougui, A., Coyne, C.J., Sankaran, S., Main, D., Porter, L.D., Mugabe, D., Smitchger, J.A., Zhang, C., Amin, M.N.,

Rasheed, N., Ficklin, S.P., McGee, R.J., 2020. Dissecting the genetic architecture of *Aphanomyces* root rot resistance in lentil by QTL mapping and genome-wide association study. Int. J. Mol. Sci. 20, 2129.

Machino, Y., Diéguez-Uribeondo, J., 1998. Un cas de peste des écrevisses en France dans le bassin de la Seine. Astaciculteur Fr. 54, 2–11.

Maguire, I., Jelić, M., Klobučar, G., Delpy, M., Delaunay, C., Grandjean, F., 2016. Prevalence of the pathogen *Aphanomyces astaci* in freshwater crayfish populations in Croatia. Dis. Aquat. Org. 118, 45–53.

Majeed, M., Kumar, G., Schlosser, S., El-Matbouli, M., Saleh, M., 2017. *In vitro* investigations on extracellular proteins secreted by *Aphanomyces invadans*, the causative agent of epizootic ulcerative syndrome. Acta Vet. Scand. 59, 78.

Majeed, M., Soliman, H., Kumar, G., El-Matbouli, M., Saleh, M., 2018. Editing the genome of *Aphanomyces invadans* using CRISPR/Cas9. Parasites Vectors 11, 554.

Makkonen, J., Jussila, J., Kokko, H., 2012a. The diversity of the pathogenic Oomycete (*Aphanomyces astaci*) chitinase genes within the genotypes indicate adaptation to its hosts. Fungal Genet. Biol. 49, 635–642.

Makkonen, J., Jussila, J., Kortet, R., Vainikka, A., Kokko, H., 2012b. Differing virulence of *Aphanomyces astaci* isolates and elevated resistance of noble crayfish *Astacus astacus* against crayfish plague. Dis. Aquat. Org. 102, 129–136.

Makkonen, J., Jussila, J., Panteleit, J., Keller, N.S., Schrimpf, A., Theissinger, K., Kortet, R., Martín-Torrijos, L., Sandoval-Sierra, J.V., Diéguez-Uribeondo, J., Kokko, H., 2018. MtDNA allows the sensitive detection and haplotyping of the crayfish plague disease agent *Aphanomyces astaci* showing clues about its origin and migration. Parasitology 145, 1210–1218.

Makkonen, J., Vesterbacka, A., Martin, F., Jussila, J., Diéguez-Uribeondo, J., Kortet, R., Kokko, H., 2016. Mitochondrial genomes and comparative genomics of *Aphanomyces astaci* and *Aphanomyces invadans*. Sci. Rep. 6, 36089.

Malloch, D., 2007. The Oomycota. Mycology Web Pages. URL. http://website.nbm-nb.ca/mycologywebpages/NaturalHistoryOfFungi/Oomycota.html.

Malvick, D.K., Grau, C.R., 2001. Characteristics and frequency of *Aphanomyces euteiches* races 1 and 2 associated with alfalfa in the Midwestern United States. Plant Dis. 85, 740–744.

Malvick, D.K., Grünwald, N.J., Dyer, A.T., 2009. Population structure, races, and host range of *Aphanomyces euteiches* from alfalfa production fields in the central USA. Eur. J. Plant Pathol. 123, 171.

Martín-Torrijos, L., Campos Llach, M., Pou-Rovira, Q., Diéguez-Uribeondo, J., 2017. Resistance to the crayfish plague, *Aphanomyces astaci* (Oomycota) in the endangered freshwater crayfish species, *Austropotamobius pallipes*. PloS One 12e0181226.

Martín-Torrijos, L., Correa-Villalona, A.J., Azofeifa-Solano, J.C., Villalobos-Rojas, F., Wehrtmann, I.S., Diéguez-Uribeondo, J., 2021a. First Detection of the Crayfish Plague Pathogen *Aphanomyces astaci* in Costa Rica: European Mistakes Should Not Be Repeated. Front. Ecol. Evol. 9.

Martín-Torrijos, L., Martínez-Ríos, M., Casabella-Herrero, G., Adams, S.B., Jackson, C.R., Diéguez-Uribeondo, J., 2021b. Tracing the origin of the crayfish plague pathogen, *Aphanomyces astaci* , to the Southeastern United States. Sci. Rep. 11, 9332.

Marzougui, A., Ma, Y., Zhang, C., McGee, R.J., Coyne, C.J., Main, D., Sankaran, S., 2019. Advanced imaging for quantitative evaluation of *Aphanomyces* root rot resistance in lentil. Front. Plant Sci. 16, 383.

Matari, N.H., Blair, J.E., 2014. A multilocus timescale for oomycete evolution estimated under three distinct molecular clock models. BMC Evol. Biol. 14, 101.

McGee, R.J., Coyne, C.J., Pilet-Nayel, M.-L., Moussart, A., Tivoli, B., Baranger, A., Hamon, C., Vandemark, G., McPhee, K., 2012. Registration of pea germplasm lines partially resistant to *Aphanomyces* root rot for breeding fresh or freezer pea and dry pea types. J. Plant Registrations 6, 203–207.

Minardi, D., Studholme, D.J., Oidtmann, B., Pretto, T., Van Der Giezen, M., 2019. Improved method for genotyping the causative agent of crayfish plague (*Aphanomyces astaci*) based on mitochondrial DNA. Parasitology 146, 1022–1029.

Morris, B.M., Reid, B., Gow, N.A.R., 1995. Tactic response of zoospores of the fungus *Phytophthora palmivora* to solutions of different pH in relation to plant infection. Microbiology 141, 1231–1237.

Moussart, A., Wicker, E., Le Delliou, B., Abelard, J.-M., Esnault, R., Lemarchand, E., Rouault, F., Le Guennou, F., Pilet-Nayel, M.-L., Baranger, A., Rouxel, F., Tivoli, B., 2009. Spatial distribution of *Aphanomyces euteiches* inoculum in a naturally infested pea field. Eur. J. Plant Pathol. 123, 153–158.

Oidtmann, B., Geiger, S., Steinbauer, P., Culas, A., Hoffmann, R.W., 2006. Detection of *Aphanomyces astaci* in North American crayfish by polymerase chain reaction. Dis. Aquat. Org. 72, 53–64.

Oidtmann, B., Steinbauer, P., Geiger, S., Hoffmann, R.W., 2008. Experimental infection and detection of *Aphanomyces invadans* in European catfish, rainbow trout and European eel. Dis. Aquat. Org. 82, 195–207.

OIE, 2016. Manual of Diagnostic Tests for Aquatic Animals, seventh edition, p. 2016.

Oyarzun, P., van Loon, J., 1989. *Aphanomyces euteiches* as a component of the complex of foot and root pathogens of peas in Dutch soils. Neth. J. Plant Pathol. 95, 259–264.

Panella, L., Lewellen, R.T., 2005. Registration of FC301, monogerm, O-type sugarbeet population with multiple disease resistance. Crop Sci. 45, 2666–2667.

Panteleit, J., Horvath, T., Jussila, J., Makkonen, J., Perry, W., Schulz, R., Theissinger, K., Schrimpf, A., 2019. Invasive rusty crayfish (*Faxonius rusticus*) populations in North America are infected with the crayfish plague disease agent (*Aphanomyces astaci*). Freshw. Sci. 38, 425–433.

Papavizas, G.C., Ayers, W.A., 1974. *Aphanomyces* species and their root diseases in pea and sugarbeet –a review, vol. 1485. Agricultural Research Service, United States Department of Agriculture technical bulletin, p. 158.

Paria, A., Dev, A.K., Pradhan, P.K., Kumar, R., Rathore, G., Sood, N., 2020. Evaluation of therapeutic potential of selected antifungal chemicals and drugs against *Aphanomyces invadans*. Aquaculture 529, 735643.

Patwardhan, A., Gandhe, R., Ghole, V., Mourya, D., 2005. Larvicidal activity of the fungus *Aphanomyces* (oomycetes: Saprolegniales) against *Culex quinquefasciatus*. Magnesium (ppm) 243, 238.

Persson, M., Söderhäll, K., 1983. *Pacifastacus leniusculus Dana* and its resistance to the parasitic fungus *Aphanomyces astaci Schikora*. Freshw. Crayfish 5, 292–298.

Pfender, W.F., Hagedorn, D.J., 1982. *Aphanomyces euteiches f. sp. phaseoli*, a causal agent of bean root and hypocotyl rot. Phytopathology 72, 306–310.

Pilet-Nayel, M., Muehlbauer, F., McGee, R., Kraft, J., Baranger, A., Coyne, C., 2002. Quantitative trait loci for partial resistance to *Aphanomyces* root rot in pea. Theor. Appl. Genet. 106, 28–39.

Pilet-Nayel, M.-L., Moury, B., Caffier, V., Montarry, J., Kerlan, M.-C., Fournet, S., Durel, C.-E., Delourme, R., 2017. Quantitative resistance to plant pathogens in pyramiding strategies for durable crop protection. Front. Plant Sci. 8, 1838.

Pilet-Nayel, M.L., Muehlbauer, F.J., McGee, R.J., Kraft, J.M., Baranger, A., Coyne, C.J., 2005. Consistent quantitative trait loci in pea for partial resistance to *Aphanomyces euteiches* isolates from the United States and France. Phytopathology 95, 1287–1293.

Pradhan, P.K., Mohan, C.V., Shankar, K.M., Kumar, B., 2008. Infection experiments with *Aphanomyces invadans* in advanced fingerlings of four different carp species. Diseases in Asian Aquaculture VI. Manila: Fish Health Section. Asian Fish. Soc. 105–114.

Putra, M.D., Bláha, M., Wardiatno, Y., Krisanti, M., Yonvitner, Jerikho, R., Kamal, M.M., Mojžišová, M., Bystrický, P.K., Kouba, A., Kalous, L., Petrusek, A., Patoka, J., 2018. *Procambarus clarkii* (Girard, 1852) and crayfish plague as new threats for biodiversity in Indonesia. Aquat. Conserv. Mar. Freshw. Ecosyst. 28, 1434–1440.

Quillévéré-Hamard, A., Le Roy, G., Lesné, A., Le May, C., Pilet-Nayel, M.-L., 2021. Aggressiveness of diverse French *Aphanomyces euteiches* isolates on pea Near-Isogenic-Lines differing in resistance QTL. Phytopathology 111, 695–702.

Quillévéré-Hamard, A., Le Roy, G., Moussart, A., Baranger, A., Andrivon, D., Pilet-Nayel, M.-L., Le May, C., 2018. Genetic and pathogenicity diversity of *Aphanomyces euteiches* populations from pea-growing regions in France. Front. Plant Sci. 9, 1673.

Ramirez-Garcés, D., Camborde, L., Pel, M.J.C., Jauneau, A., Martinez, Y., Néant, I., Leclerc, C., Moreau, M., Dumas, B., Gaulin, E., 2016. CRN13 candidate effectors from plant and animal eukaryotic pathogens are DNA-binding proteins which trigger host DNA damage response. New Phytol. 210, 602–617.

Rehmany, A.P., Gordon, A., Rose, L.E., Allen, R.L., Armstrong, M.R., Whisson, S.C., Kamoun, S., Tyler, B.M., Birch, P.R.J., Beynon, J.L., 2005. Differential recognition of highly divergent downy mildew avirulence gene alleles by RPP1 resistance genes from two *Arabidopsis* lines. Plant Cell 17, 1839–1850.

Rep, M., 2005. Small proteins of plant-pathogenic fungi secreted during host colonization. FEMS Microbiol. Lett. 253, 19–27.

Rezinciuc, S., Galindo, J., Montserrat, J., Diéguez-Uribeondo, J., 2014. AFLP-PCR and RAPD-PCR evidences of the transmission of the pathogen *Aphanomyces astaci* (Oomycetes) to wild populations of European crayfish from the invasive crayfish species, *Procambarus clarkii*. Fungal Biol. 118, 612–620.

Riethmuller, A., Voglmayr, H., Goker, M., Weiß, M., Oberwinkler, F., 2002. Phylogenetic relationships of the downy mildews (Peronosporales) and related groups based on nuclear large subunit ribosomal DNA sequences. Mycologia 94, 834–849.

Roberts, R.J., Willoughby, L.G., Chinabut, S., 1993. Mycotic aspects of epizootic ulcerative syndrome (EUS) of Asian fishes. J. Fish. Dis. 16, 169–183.

Royo, F., Andersson, G., Bangyeekhun, E., Múzquiz, J.L., Söderhäll, K., Cerenius, L., 2004. Physiological and genetic characterisation of some new *Aphanomyces* strains isolated from freshwater crayfish. Vet. Microbiol. 104, 103–112.

Rzeszutek, E., Diaz-Moreno, S., Bullone, V., 2019. Identification and characterization of the chitin synthase genes from the fish pathogen *Saprolegnia parasitica*. Front. Microbiol. 10, 2873.

Sakihama, Y., Shimai, T., Sakasai, M., Ito, T., Fukushi, Y., Hashidoko, Y., Tahara, S., 2004. A photoaffinity probe designed for host-specific signal flavonoid receptors in phytopathogenic Peronosporomycete zoospores of *Aphanomyces cochlioides*. Arch. Biochem. Biophys. 432, 145–151.

Samac, D.A., Seitz, V., Ristow, P., Rouse, D., 2012. *Aphanomyces* root rot: widespread distribution of race 2. Forage Focus 8–9.

Samac, D.A., Bucciarelli, B., Dornbusch, M., Miller, S., Yu, L.-X., 2017. Identification of Markers Associated with Race-specific Resistance to *Aphanomyces* Root Rot in Alfalfa, Poster at the 2017 APS Meeting.

Saylor, R.K., Miller, D.L., Vandersea, M.W., Bevelhimer, M.S., Schofield, P.J., Bennett, W.A., 2010. Epizootic ulcerative syndrome caused by *Aphanomyces invadans* in captive bullseye snakehead *Channa marulius* collected from south Florida, USA Dis. Aquat. Org. 88, 169–175.

Schäfer-Pregl, R., Borchardt, D.C., Barzen, E., Glass, C., Mechelke, W., Seitzer, J.F., Salamini, F., 1999. Localization of QTLs for tolerance to *Cercospora beticola* on sugar beet linkage groups. Theor. Appl. Genet. 99, 829–836.

Scholten, O.E., De Bock, T.S., Klein-Lankhorst, R.M., Lange, W., 1999. Inheritance of resistance to beet necrotic yellow vein virus in *Beta vulgaris* conferred by a second gene for resistance. Theor. Appl. Genet. 99, 740–746.

Schornack, S., Huitema, E., Cano, L.M., Bozkurt, T.O., Oliva, R., Damme, M.V., Schwizer, S., Raffaele, S., Chaparro-Garcia, A., Farrer, R., Segretin, M.E., Bos, J., Haas, B.J., Zody, M.C., Nusbaum, C., Win, J., Thines, M., Kamoun, S., 2009. Ten things to know about oomycete effectors. Mol. Plant Pathol. 10, 795–803.

Schornack, S., van Damme, M., Bozkurt, T.O., Cano, L.M., Smoker, M., Thines, M., Gaulin, E., Kamoun, S., Huitema, E., 2010. Ancient class of translocated oomycete effectors targets the host nucleus. Proc. Natl. Acad. Sci. U. S. A. 107, 17421–17426.

Schren, A.L., 1960. Germination of oospores of *Aphanomyces euteiches* embedded in plant debris. Phytopathology 50, 274–277.

Scott, W.W., 1961. A monograph of the genus *Aphanomyces*. Tech. Bull. Virginia Agricult. Experiment Stat. 151.

Seitz, V., Rouse, D., 2012. Evidence for *Aphanomyces euteiches*, Race 3 on *Alfalfa*. In: North American Alfalfa Improvement Conferences Proceedings. http://naaic.org.

Setiawan, A., Koch, G., Barnes, S.R., Jung, C., 2000. Mapping quantitative trait loci (QTLs) for resistance to *Cercospora* leaf spot disease (*Cercospora beticola* Sacc.) in sugar beet (*Beta vulgaris* L.). Theor. Appl. Genet. 100, 1176–1182.

Sivachandra Kumar, N.T., Cox, L., Armstrong-Cho, C., Banniza, S., 2020. Optimization of zoospore production and inoculum concentration of *Aphanomyces euteiches* for resistance screening of pea and lentil. J. Indian Dent. Assoc. 42, 419–428.

Söderhäll, K., Cerenius, L., 1999. The crayfish plague fungus: history and recent advances. Freshw. Crayfish 12, 11–35.

Söderhäll, K., Svensson, E., Unestam, T., 1978. Chitinase and protease activities in germinating zoospore cysts of a parasitic fungus, *Aphanomyces astaci*, Oomycetes. Mycopathologia 64, 9–11.

Sosa, E.R., Landsberg, J.H., Kiryu, Y., Stephenson, C.M., Cody, T.T., Dukeman, A.K., Wolfe, H.P., Vandersea, M.W., Litaker, R.W., 2007. Pathogenicity studies with the fungi *Aphanomyces invadans*, *Achlya bisexualis*, and *Phialemonium dimorphosporum*: induction of skin ulcers in striped mullet. J. Aquat. Anim. Health 19, 41–48.

Souty-Grosset, C., Holdich, D.M., Noël, P.-Y., Reynolds, J.-D., Haffner, P., 2006. Atlas of Crayfish in Europe. Muséum National d'Histoire Naturelle, Paris.

Srivastava, S., Sinha, R., Roy, D., 2004. Toxicological effects of malachite green. Aquat. Toxicol. 66, 319–329.

Strand, D.A., Jussila, J., Johnsen, S.I., Viljamaa-Dirks, S., Edsman, L., Wiik-Nielsen, J., Viljugrein, H., Engdahl, F., Vrålstad, T., 2014. Detection of crayfish plague spores in large freshwater systems. J. Appl. Ecol. 51, 544–553.

Svoboda, J., Mrugała, A., Kozubíková-Balcarová, E., Petrusek, A., 2017. Hosts and transmission of the crayfish plague pathogen *Aphanomyces astaci*: a review. J. Fish. Dis. 40, 127–140.

Taguchi, K., Ogata, N., Kubo, T., Kawasaki, S., Mikami, T., 2009. Quantitative trait locus responsible for resistance to *Aphanomyces* root rot (black root) caused by *Aphanomyces cochlioides* Drechs. in sugar beet. Theor. Appl. Genet. 118, 227–234.

Taguchi, K., Okazaki, K., Takahashi, H., Kubo, T., Mikami, T., 2010. Molecular mapping of a gene conferring resistance to *Aphanomyces* root rot (black root) in sugar beet (*Beta vulgaris* L.). Euphytica 173, 409–418.

Takenaka, S., Ishikawa, S., 2013. Biocontrol of sugar beet seedling and taproot diseases caused by *Aphanomyces cochlioides* by

Pythium oligandrum treatments before transplanting. Jpn. Agric. Res. Q.: JARQ 47, 75–83.
Takuma, D., Wada, S., Kurata, O., Hatai, K., Sano, A., 2011. *Aphanomyces sinensis* sp. nov., isolated from juvenile soft-shelled turtle, *Pelodiscus sinensis*, in Japan. Mycoscience 52, 119–131.
Tayeh, N., Aubert, G., Pilet-Nayel, M.-L., Lejeune-Hénaut, I., Warkentin, T.D., Burstin, J., 2015. Genomic tools in pea breeding programs: status and perspectives. Front. Plant Sci. 6.
Tulbek, M., Lam, R., Wang, C., Asavajaru, P., Lam, A., 2016. Pea: a sustainable vegetable protein crop. In: Sustainable Protein Sources. Academic Press, pp. 145–162.
Tyler, B.M., 2007. *Phytophthora sojae*: root rot pathogen of soybean and model oomycete. Mol. Plant Pathol. 8, 1–8.
Tyler, B.M., 2002. Molecular basis of recognition between *Phytophthora* pathogens and their Hosts. Annu. Rev. Phytopathol. 40, 137–167.
Unestam, T., 1966. Studies on the crayfish plague fungus *Aphanomyces astaci*. Physiol. Plantarum 19, 1110–1119.
Ungureanu, E., Mojžišová, M., Tangerman, M., Ion, M.C., Pârvulescu, L., Petrusek, A., 2020. The spatial distribution of *Aphanomyces astaci* genotypes across Europe: Introducing the first data from Ukraine. Freshw. Crayfish 25.
van Leur, J.A.G., Southwell, R.J., Mackie, J.M., 2008. *Aphanomyces* root rot on fababean in northern NSW. Australas. Plant Dis. Notes 3, 8–9.
van West, P., Appiah, A.A., Gow, N.A., 2003. Advances in research on oomycete root pathogens. Physiol. Mol. Plant Pathol. 62, 99–113.
van West, P., 2006. *Saprolegnia parasitica*, an oomycete pathogen with a fishy appetite: new challenges for an old problem. Mycologist 20, 99–104.
Vandersea, M.W., Litaker, R.W., Yonnish, B., Sosa, E., Landsberg, J.H., Pullinger, C., Moon-Butzin, P., Green, J., Morris, J.A., Kator, H., 2006. Molecular assays for detecting *Aphanomyces invadans* in ulcerative mycotic fish lesions. Appl. Environ. Microbiol. 72, 1551–1557.
Verschuere, L., Rombaut, G., Sorgeloos, P., Verstraete, W., 2000. Probiotic bacteria as biological control agents in aquaculture. Microbiol. Mol. Biol. Rev. 64, 655–671.
Vrålstad, T., Johnsen, S.I., Fristad, R.F., Edsman, L., Strand, D., 2011a. Potent infection reservoir of crayfish plague now permanently established in Norway. Dis. Aquat. Org. 97, 75–83.
Vrålstad, T., Johnsen, S.I., Taugbøl, T., 2011b. NOBANIS–Invasive alien species fact sheet–Aphanomyces astaci. From: Online Database of the European Network on Invasive Alien Species–NOBANIS. www.nobanis.org.
Vrålstad, T., Knutsen, A.K., Tengs, T., Holst-Jensen, A., 2009. A quantitative TaqMan® MGB real-time polymerase chain reaction based assay for detection of the causative agent of crayfish plague *Aphanomyces astaci*. Vet. Microbiol. 137, 146–155.
Wakelin, S.A., Walter, M., Jaspers, M., Stewart, A., 2012. Biological control of *Aphanomyces euteiches* root rot of pea with spore-forming bacteria. Australas. Plant Pathol. 31, 401–407.
Walker, C.A., van West, P., 2007. Zoospore development in the oomycetes. Fungal Biol. Rev. 21, 10–18.
Westman, K., 1995. Introduction of alien crayfish in the development of crayfish fisheries; experience with signal crayfish (*Pacifastacus leniusculus* (*Dana*)) in Finland and the impact on the native noble crayfish (*Astacus astacus* (*L.*)). Freshw. Crayfish 10, 1–17.
Westman, K., 1991. The crayfish fishery in Finland–its past, present and future. Finn. Fish. Res. 12, 187–216.
Wicker, E., Rouxel, F., 2001. Specific behaviour of French *Aphanomyces euteiches Drechs.* Populations for virulence and aggressiveness on pea, related to isolates from Europe, America and New Zealand. Eur. J. Plant Pathol. 107, 919–929.
Windels, C.E., 2000. *Aphanomyces* root rot on sugar beet. Plant Health Prog. 1, 8.
Wittwer, C., Stoll, S., Strand, D., Vrålstad, T., Nowak, C., Thines, M., 2018. eDNA-based crayfish plague monitoring is superior to conventional trap-based assessments in year-round detection probability. Hydrobiologia 807, 87–97.
Wittwer, C., Stoll, S., Thines, M., Nowak, C., 2019. eDNA-based crayfish plague detection as practical tool for biomonitoring and risk assessment of *A. astaci*-positive crayfish populations. Biol. Invasions 21, 1075–1088.
Wu, L., Chang, K.-F., Conner, R.L., Strelkov, S., Fredua-Agyeman, R., Hwang, S.-F., Feindel, D., 2018. *Aphanomyces euteiches*: A threat to Canadian field pea production. Engineering 4, 542–551.
Yadav, M.K., Pradhan, P.K., Sood, N., Chaudhary, D.K., Verma, D.K., Debnath, C., Sahoo, L., Chauhan, U.K., Punia, P., Jena, J.K., 2014. Innate immune response of Indian major carp, Labeo rohita infected with oomycete pathogen *Aphanomyces invadans*. Fish Shellfish Immunol. 39, 524–531.
Yokosawa, R., Kuninaga, S., Sekizaki, H., 1986. *Aphanomyces euteiches* zoospore attractant isolated from pea root; prunetin. Japan. J. Phytopathol. 52, 809–816.
You, M.P., Lamichhane, J.R., Aubertot, J.N., Barbetti, M., 2020. Understanding why effective fungicides against individual soilborne pathogens are ineffective with soilborne pathogen complexes. Plant Dis. 104, 904–920.
Zhou, Y., Li, X., Pan, Z., Ye, B., Xu, M., 2019. Determination of Malachite green in fish by a modified MOF-based electrochemical sensor. Food Anal. Methods 12, 1246–1254.

3. Chapter III - A Comprehensive Assessment of the Secretome Responsible for Host Adaptation of the Legume Root Pathogen *Aphanomyces euteiches* (Kiselev et al., 2022)

The soil borne oomycete pathogen *Aphanomyces euteiches* cause root rot diseases that threaten the production of important legume crops such as pea and alfalfa. Various *A. euteiches* pathotypes show differential quantitative virulence on pea or alfalfa. However, the molecular basis of host adaptation is not known. In this study we re-sequenced a pea strain of *A. euteiches* using long reads technology to generate a high-quality genome reference for the *Aphanomyces* genus. To explore whether the secretome may participate to host preference, we performed Illumina sequencing of four strains of *A. euteiches* that display contrasted specificity for pea or alfalfa and isolated from different geographical areas. We identified that the core secretome of *A. euteiches* is characterized by a large portfolio of secreted proteases and carbohydrate-active enzymes (CAZymes). In contrast, small secreted proteins (SSP) less than 300 amino acid residues without functional domain can contribute to legume preference.

Journal of *Fungi*

MDPI

Article

A Comprehensive Assessment of the Secretome Responsible for Host Adaptation of the Legume Root Pathogen *Aphanomyces euteiches*

Andrei Kiselev, Hélène San Clemente, Laurent Camborde, Bernard Dumas and Elodie Gaulin *

Laboratoire de Recherche en Sciences Végétales (LRSV), Université de Toulouse, CNRS, UPS, Toulouse INP, 31320 Toulouse, France; kiselev@lrsv.ups-tlse.fr (A.K.); sancle@lrsv.ups-tlse.fr (H.S.C.); camborde@lrsv.ups-tlse.fr (L.C.); dumas@lrsv.ups-tlse.fr (B.D.)
* Correspondence: gaulin@lrsv.ups-tlse.fr (E.G.)

Abstract: The soil-borne oomycete pathogen *Aphanomyces euteiches* causes devastating root rot diseases in legumes such as pea and alfalfa. The different pathotypes of *A. euteiches* have been shown to exhibit differential quantitative virulence, but the molecular basis of host adaptation has not yet been clarified. Here, we re-sequenced a pea field reference strain of *A. euteiches* ATCC201684 with PacBio long-reads and took advantage of the technology to generate the mitochondrial genome. We identified that the secretome of *A. euteiches* is characterized by a large portfolio of secreted proteases and carbohydrate-active enzymes (CAZymes). We performed Illumina sequencing of four strains of *A. euteiches* with contrasted specificity to pea or alfalfa and found in different geographical areas. Comparative analysis showed that the core secretome is largely represented by CAZymes and proteases. The specific secretome is mainly composed of a large set of small, secreted proteins (SSP) without any predicted functional domain, suggesting that the legume preference of the pathogen is probably associated with unknown functions. This study forms the basis for further investigations into the mechanisms of interaction of *A. euteiches* with legumes.

Keywords: oomycete; *Aphanomyces*; secretome; effector; legume; adaptation; SSP; pathogenicity

Citation: Kiselev, A.; San Clemente, H.; Camborde, L.; Dumas, B.; Gaulin, E. A Comprehensive Assessment of the Secretome Responsible for Host Adaptation of the Legume Root Pathogen *Aphanomyces euteiches*. *J. Fungi* **2022**, *8*, 88. https://doi.org/10.3390/jof8010088

Academic Editor: Ana Cristina Esteves

Received: 1 December 2021
Accepted: 14 January 2022
Published: 17 January 2022

1. Introduction

The *Aphanomyces* genus belongs to the order Saprolegniales, which includes filamentous eukaryotic pathogens that are encountered in different terrestrial and aquatic ecosystems [1,2]. This genus includes about 45 species that infect plants, animals (fish, crustaceans) and agricultural crops [1,3–6]. Thus, it is of great interest to study *Aphanomyces* to reveal the evolutionary mechanisms that allow host adaptation. *Aphanomyces euteiches* is a soil-borne phytopathogenic oomycete with a wide spectrum of leguminous hosts and affects legumes such as pea, lentil and alfalfa [1,7,8]. Due to its soil-borne nature and the production of oospores that stay viable for up to 10 years in the soil, long-term crop rotation has so far been the measure used to avoid *A. euteiches* infection [1]. *A. euteiches* induces root rot, which causes seedlings' damping-off, yield decrease or even the death of the plant. This oomycete is highly virulent, mainly due to the production of a large number of motile biflagellate zoospores, which can move in liquid film in the soil and infect a whole field in a short time, leading to a complete loss of yield [2]. Several *A. euteiches* "pathotypes and/or races" have been identified based on their virulence on various legume hosts, such as pea or alfalfa [9–11]. Legume resistance against the pathogen is quantitatively mediated by diverse quantitative trait loci (QTL) that target different stages in the lifecycle of the pathogen [12,13]. However, the molecular basis for the adaptation of *A. euteiches* to various host legumes remains to be clarified.

Filamentous eukaryotic plant pathogens such as oomycetes secrete myriad proteins called effectors that modulate the host physiology and immune responses and enable

parasitic infection [14–17]. Therefore, genomics studies on oomycetes involve exploring the organization and constitution of the complete set of secreted proteins defining the secretome [18,19]. This identification is facilitated by the fact that in eukaryotes, most of the secreted proteins follow the general secretory pathway, via a small N-terminal amino acid sequence known as the signal peptide [20]. In addition, oomycete effectors can be predicted due to the presence of a conserved amino acid motif generally in the Nter region. This motif has been detected in the RxLR and Crinkler families, which include hundreds of members [21–25]. Oomycete-secreted proteins include catalytic and non-catalytic proteins that function in ways that alter the plant cell wall, metabolism, nucleic acid integrity, signaling cascade, RNA-silencing and immune responses [15,26–34]. Thus, the prediction of the secretome opens up a new research area targeted toward understanding how secreted proteins function within the host cell to promote disease and thereby help the pathogen to adapt to the host.

Long-read-based sequencing technology routinely allows to obtain reads over 10 kb in length and significantly outperforms the Illumina short-read sequencing, where only reads of up to 600 base pairs can be obtained [35]. Using this advanced technique, numerous resequencing studies on filamentous pathogenic eukaryotes such as fungi and oomycetes have been undertaken. Long-read sequencing allows to obtain a continuous assembly, which can help to resolve localization of repeated regions and to improve gene annotations, notably for large families of genes such as effectors, which are often located in repeat-rich regions [36]. One example is the resequencing of the oomycete *Phytophthora parasitica* that helped to identify a new class of repeats corresponding to satellite DNA, which could not be identified in a short-read-based assembly [37]. Using long-read technology has helped to resolve the organization of repeated pathogenicity loci in the wheat fungal pathogen *Pyrenophora tritici* [38]. Resequencing a genome using long-read technology can also help to unravel the secretome, as demonstrated by the identification of a biosynthetic cluster of secondary metabolites that take part in the infection process of the fungal phytopathogen *Colletotrichum higginsianum* [39]. Further to this, in *Puccinia triticina*, genome resequencing allowed the prediction of a variety of new effectors [40].

In our previous study, we reported for the first time the 57 Mb genome assembly of the *A. euteiches* ATCC201684 strain based on a combination of Illumina and Roche 454 sequencing technologies. We estimated genome size of 61 Mb, predicted 19,548 genes and provided the first overview of the *A. euteiches* genome [41]. A comparative analysis with Illumina sequenced the crayfish pathogen *Aphanomyces astaci*, the saprotroph *Aphanomyces stelattus* and other well-studied oomycete phytopathogens such as *Phytophthora* was performed. The analysis detected a large set of Crinklers (CRNs), as well as a new family of secreted proteins called SSPs (small secreted proteins) unique to the *Aphanomyces* genus [41]. These SSPs are less than 300 residues in length and do not contain any predicted functional domain. This suggests that *Aphanomyces* spp. may develop its own original mechanism to achieve host invasion, one that is different from that of other oomycetes, such as the potato late blight oomycete *Phytophthora infestans*.

In this work, we first aimed to produce a long-read-based genome assembly of the *A. euteiches* ATCC201684 strain, generating a high-quality assembly in terms of contiguity and completeness. We identified 23,027 genes, of which 1515 (~6,5%) were further predicted to encode secreted proteins, and resolved the repeated regions. Long-read sequencing allowed us to provide the first-ever mitochondrial genome assembly for this plant pathogen. Four additional *A. euteiches* strains collected in different geographical areas and speciated to different legumes were subjected to Illumina sequencing. Through comparative analysis, we identified the core, accessory and specific secretomes of *A. euteiches*. We found that all the secretomes were closely related with respect to the functional classes of secreted proteins, but the 'non-core' secretomes were highly enriched in SSPs. This finding suggests that legume preference is linked to variation in the secretome content that has an unknown function. This work provides a useful resource for further studies on *A. euteiches*-plant interactions. Moreover, as the only plant pathogenic Saprolegniales species with a high-

quality genome assembly, our work is also important to gain an increased understanding of oomycetes' pathogenicity.

2. Materials and Methods

2.1. Aphanomyces ssp. Growth and DNA Preparation

A. euteiches ATCC201684, RB84, MF1, NC1 and Ae109 strains were grown for four days in a liquid YG medium (2.5% yeast extract, 5% glucose) at 23 °C in the dark. Mycelia were harvested and DNA extracted from ground mycelia using Macherey-Nagel Nucleobond RNA/DNA for the ATCC201684 strain and using our previously reported protocol for the other strains [41].

2.2. Genomes Sequencing, Assembly and Annotation

The preparation of all the libraries and sequencing was performed at the GeT-PlaGe core facility in Toulouse, France (https://get.genotoul.fr/en/). For ATCC201684, the library preparation was carried out according to the "Shared Protocol-30 kb Template Preparation/BluePippin Size Selection System". A NanoDrop100 spectrophotometer (QIAGEN, Frederick, MD, USA), a Qubit (Life Technologies, Carlsbad, CA, USA) and a Fragment analyzer (AATI) were used to analyze the purity, integrity, quality and concentration of DNA. Genomic DNA was further purified using a BluePippin DNA size selection system (Sage Science, Beverly, MA, USA). Sequencing using PacBio SMRT technology to obtain long-reads was performed at the GeT-PlaGe core facility using 10 SMRTcells on a PacBio RSII Instrument. The raw sequencing reads were evaluated for their GC content distribution, quality distribution, base composition and average quality score at each position, and stored in NG6 [42]. The reads were de novo assembled using the RS Hierarchical Genome Assembly Process in SMRT analysis version 2.3.0 software (Pacific Biosciences, Menlo Park, CA, USA). For the RB84, Ae109, MF1 and NC1 strains, DNA-seq libraries were prepared using an Illumina TruSeq DNA v.2 Library Prep Kit following the manufacturer's instructions. An Agilent Bioanalyzer was used to assess the quality of the libraries, and the libraries were quantified by qPCR using the Kapa Library Quantification Kit. DNA-seq experiments were performed on an Illumina HiSeq2000 Sequencer using a paired-end read-length of 2 × 100 pb with the HiSeq v.3 Reagent Kit at the GeT-PlaGe core facility in Toulouse. All the reads were quality-checked and stored in NG6 [42]. The reads of Ae109, RB84, MF1 and NC1 were assembled using MaSurCa [43] and the assembly metrics were calculated using assemblathon_stats.pl script (http://korflab.ucdavis.edu/datasets/Assemblathon/Assemblathon2/Basic_metrics/assemblathon_stats.pl).

Proteomes were predicted using the Augustus-based Braker 2 pipeline [44] trained with predicted proteins from a previous assembly, and RNASeq reads of zoospores and mycelium from *A. euteiches* [41]. Proteomes predictions were benchmarked using BUSCO software with the Stramenopiles reference gene set [45]. Repeated sequences were *de novo* identified using the RepeatModeller pipeline and the repeated sequence was then masked in the genome using RepeatMasker 4.1.0 (http://www.repeatmasker.org).

Satellite DNA was predicted using the bioinformatics algorithm as described in a previous publication [37]. Tandem Repeat Finder [46] was used to find tandemly repeated sequences in the genome; the resulting sequences were sorted by size to keep the ones with sizes from 100 bp to 500 bp. The monomeric sequences were blasted [47] against the genome (-perc_identity 85 -qcov_hsp_perc 90). The monomeric sequences that occurred less than 100 times were excluded from the analysis. Blastclust pairwise analysis was used to cluster monomeric sequences (identifying at 75%) to form families. Sequences of families were loaded into CLC Main Workbench software (Qiagen) to obtain the consensus sequence of the family. Sequences were aligned using ClustalW and the Neighbor-Joining method was used to build and visualize the phylogenetic tree in CLC Main Workbench software. All the data were stored in AphanoDB in August 2021 (https://www.polebio.lrsv.ups-tlse.fr/aphanoDB/) [48].

2.3. Mitochondrial Genome Assembly

A random subsample of 10% of self-corrected PacBio reads was used in the perl-based software Organelle_PBA (https://github.com/aubombarely/Organelle_PBA) as described in [49] to generate a circular contig. The *Aphanomyces astaci* mitochondrial genome (NCBI RefSeq: NC_032051, [50]) was used as the reference. Gene annotation was done on the MITOS webserver in May 2021 (http://mitos.bioinf.uni-leipzig.de) with further manual curation. The contig was visualized using the OGDRAW webtool [51].

2.4. Functional Characterization of Genome

Predicted proteins were assigned to protein families (PFAMs) and GO terms using InterProScan [52]. Secreted proteins were identified as reported in [53] using SignalP v.5 [54]. Proteins predicted with a transmembrane domain using TMHMM 2.0 [55] were excluded.

2.5. Comparative Analyses

The whole-genome alignment of the new and existing assemblies was performed with the LAST algorithm (http://last.cbrc.jp) and visualized in the D-genies tool (http://dgenies.toulouse.inra.fr). The protein predictions were compared with OrthoFinder v.2.5 using the DIAMOND engine for a sequence similarity search [56], and then they were visualized as a Venn diagram using the Bioinformatics & Evolutionary Genomics Venn diagram custom draw tool (http://bioinformatics.psb.ugent.be/webtools/Venn/). Based on the OrthoFinder results, the secreted proteins of the five strains were divided into three groups: core—from orthogroups containing orthologs of all five strains; accessory—from orthogroups containing orthologs of 2–4 strains; singletons—from orthogroups containing proteins without orthologs in other strains. For comparative studies, proteomes of *Phytophthora infestans* T30-4, *Saprolegnia parasitica* CBS223-65 and *Aphanomyces invadans* NJM9701 were downloaded from the FungiDB repository [57] and functional characterization of proteins was performed using the same procedure as for *A. euteiches*.

2.6. Small, Secreted Proteins' (SSPs') Prediction and Classification

To identify the SSPs, we selected secreted proteins of less than 300 amino acids in size. Proteins with a predicted functional domain were excluded based on previously reported InterProScan (v.5.48) results [52] using the following applications: TIGRFAM, PANTHER, Pfam, PIRSF, PRINTS, ProSitePatterns, ProSiteProfiles, SMART and SUPERFAMILY. To calculate the amino acid enrichment, we determined the distribution of amino acid frequency in the total proteome and calculated the third quartile of each amino acid (e.g., 75% of the total proteome has a lower share of the amino acid). We set a cutoff of 1.5× (third quartile) as enrichment. The phylogenetic tree was based on multiple alignments of SSPs from all the analyzed strains using Clustal Omega on the EBI website (https://www.ebi.ac.uk/Tools/msa/clustalo/). The tree was imported into iTOL software for visualization (https://itol.embl.de/).

3. Results

3.1. Genomic Features of the A. euteiches ATCC201684 Strain Defined by PacBio Technology

The *A. euteiches* ATCC201684 strain was originally isolated from infected pea in Denmark, and in a previous report, we described how we generated a first genome assembly (version 1, V1) based on short-read sequencing technologies [41]. In this work, we aimed to improve the pathogen reference genome sequence using PacBio long-read technology to facilitate comparative genomic studies. Ten SMRT cells on PacBio RSII generated 1,414,231 total reads with a genome coverage of 146X and an average read length of 10.5 Mb. This resulted in a 72 Mb genome assembly (Table 1), the size of which was larger than the V1 assembly of 57 Mb (for an estimated genome size of 61 Mb), obtained by combining Illumina and 454 technologies. The GC content of around 47% was similar to the previous assembly. We improved the contiguity, as demonstrated by the big increase in N50 (N50 of

0.275 vs. 1.005 Mb). We generated a similar number of contigs, mainly because we obtained additional sequences present in rather small contigs (50–100 Mb in average; Figure 1). Indeed, we detected that the 49 largest contigs of V2 cover the full size of the V1 assembly, as depicted in Figure 1b, showing that a long-read assembly allows the detection of new contigs with putative new coding sequences. We identified that the additional V2 assembly contigs are distinct from the contigs aligned with the V1 version, with a lower gene content per Mb (329 vs. 112) and a higher percentage of repetition (16.8 vs. 64.6). The proteome was predicted by incorporating available expression data on *A. euteiches* previously generated by RNASeq technology [41,58]. We checked the completeness of the genome assembly using a Benchmarking Universal Single-Copy Ortholog (BUSCO) [45] based on 100 highly conserved Stramenopile proteins (100 proteins, odb10 dataset) and identified 98% complete genes, 2% fragmented genes and zero missing (Table 1). The two fragmented genes were EF-hand domain and mitochondrial-processing peptidase subunit beta, both of which harbor catalytic domains.

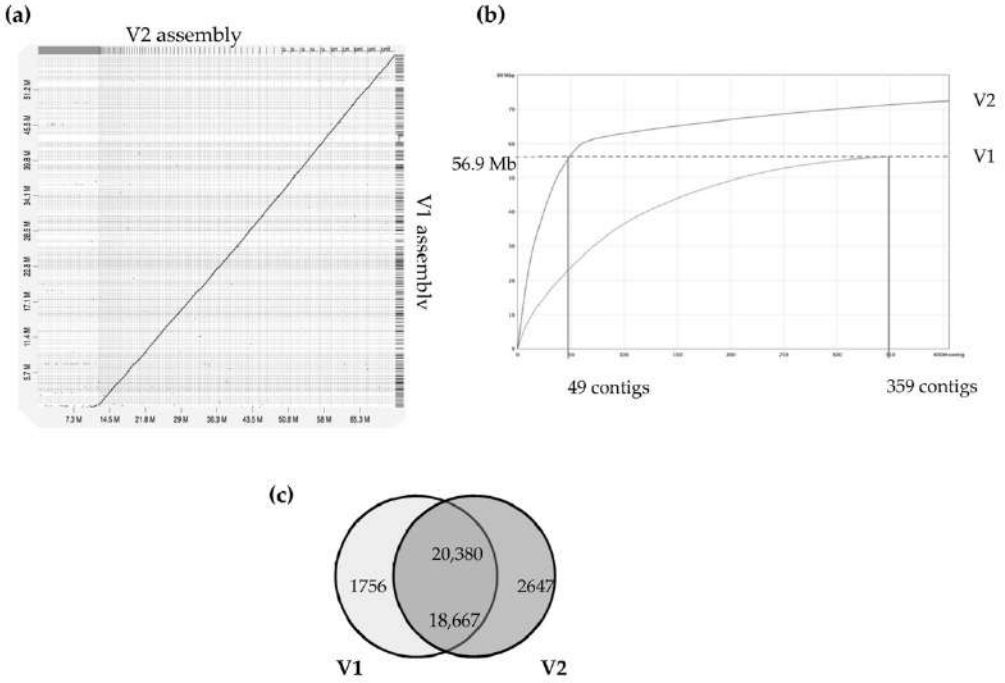

Figure 1. Comparison of version 1 and version 2 of *A. euteiches* genome assembly (ATCC201684 strain). A previous study using Illumina/454 technologies allowed the V1 assembly of the *A. euteiches* genome to be obtained [41]. This study provides the V2 assembly, obtained using long-read PacBio technology. (**a**) Dot-plot of pairwise whole-genome alignment of V1 and V2 assemblies. Note the additional sequence consisting of smaller contigs in V2 as compared to the V1 assembly. (**b**) Plot describing distribution of contigs by length for V1 and V2 assemblies. The 49 largest contigs of V2 cover the full size of the V1 genome. Additional contigs are present in V2. (**c**) Venn diagram of pairwise protein comparison of V1 and V2 (% ident > 75%, coverage > 75%). Shared part represents number of pairwise hits from V2 (upper number) and V1 (lower number).

Table 1. Summary of *A. euteiches* ATCC201684 genome assemblies, annotation statistics and completeness evaluation.

Genome Version	Version V1 [Ref] Illumina/454	Version V2 (This Study) PacBio
Total contig length (Mb)	56.9	72
GC content (%)	47.69	47.27
Protein-coding genes	20,623	23,027
Average exons per gene	3.7	3.5
Mean gene size (kb)	1503	1447
N50 (kbp)	275,164	1,005,788
N90 (kbp)	69	39
Gene density (nb genes/Mb)	343	320
Coverage	146x	148x
Number of scaffolds	349	420
BUSCO complete/ fragmented/duplicated /missing	83.1%/3.8% (Alveolata-Stramenopiles dataset)	98%/2%/0%/0% (Stramenopiles dataset)

A total of 23,027 genes from the *A. euteiches* V2 (this study) were identified (Table S1a), representing an increase of 2404 genes when compared with V1. Comparison of proteomes from both assemblies showed that over 20,000 proteins from V2 (88.5%) had protein models identical (identifying at $\geq$ 75%) to those in V1. In our work, 2647 new protein models were predicted and 1756 protein models from V1 were not supported in V2 (Figure 1c). Among the new set of predicted proteins, only around 25% (i.e., 647 proteins) harbor a predicted PFAM domain mainly related to nucleic acid interactions, such as 'integrase', 'endonuclease', 'transposase', 'RNAse', 'Helicase' and 'CENPB DNA-binding' (Table S1b).

All the data were stored in an updated version of the AphanoDB database in August 2021 (https://www.polebio.lrsv.ups-tlse.fr/aphanoDB/) [48]. This resource is dedicated to "omics" studies on the *Aphanomyces* genus and provides tools such as a genome browser, gene annotation facilities and Basic Local Alignment Search Tool (BLAST) to facilitate analysis [48].

3.2. Repeat Content and Satellite DNA in A. euteiches ATCC201684

We identified that close to 25% of the whole genome sequence of *A. euteiches* was represented as repeated sequences (Table S1c). This high level of repetition was not detected in our previous study where we used an Illumina/454 assembly [41]. As depicted in Figure 2, the most abundant repeat types were the LINEs repeats, which accounted for 3.7 Mb, and the LTR elements, which accounted for 2 Mb. To compare the levels of the different repeats in *A. euteiches* with those in other oomycetes, we selected three plant pathogenic oomycete genomes sequenced with long-read technology (*Plasmopara viticola* [58], *Bremia lactucae* [59], *Phytophthora sojae* [60]) and also included the *Phytophthora infestans* genome sequence [21]. When compared with the other oomycetes, the proportions of the different repeat types differed in *A. euteiches*, with it having the smallest size of repeated sequence and the largest portion of LINEs. Using the rolling-circles mechanism, we found that 1.5 Mb of the repeated sequences were predicted to be replicated. This has not been detected in other oomycetes (Figure 2, Table S1d).

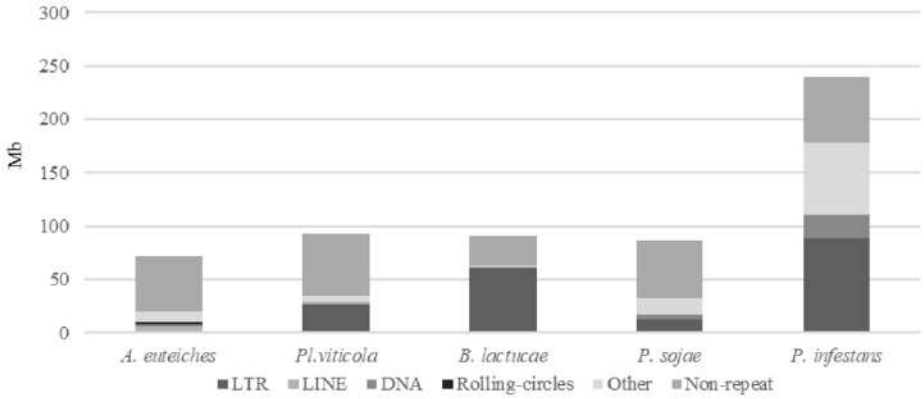

Figure 2. Repeats and non-repeated sequence distribution in plant pathogenic oomycete genomes as compared to *A. euteiches*. Three plant pathogenic oomycetes (*Plasmopara viticola*, *Bremia lactucae*, *Phytopthora sojae*) sequenced with long-read technology and the *P. infestans* genome were used to compare repeats and non-repeated sequences' distribution within the legume pathogen *A. euteiches* ATCC201684. Families of repeats are indicated with a grey color. Data are available in ST1c-d.

The large proportion of repeated regions in the *A. euteiches* genome prompted us to look for putative tandemly repeated sequences varying in size, copy number and sequence conservation, which could correspond to putative satellite DNA. The latter was recently reported following genome resequencing by long-read technology of the oomycete *Phytophthora parasitica* [37]. Based on the report by Panabières et al. [37], we searched for tandemly repeated sequences with monomer sizes ranging from 100 to 500 bp. The monomeric sequences were used to perform BlastN searches against the *A. euteiches* genome to identify the number of occurrences in the genome; the ones with more than 100 occurrences were kept for further analysis. We used blastclust pairwise comparison to group the tandem repeats into clusters based on sequence similarity. Our analysis revealed 41 families (AeSat) of tandem repeats matching satellite DNA criteria (Table S1e). As previously described for *Phytophthora*, the GC content might vary significantly between satellite DNA families, from 39% to 63% for the *A. euteiches* genome. The number of copies varied from 106 to more than 3000 for the four most-represented AeSat (i.e., AeSat1–AeSat4). In these regions, no coding sequences were identified, but for ten AeSat, we identified similarities with known transposable elements (TE), such as DNA/Harbinger, DNA/Helitron, NonLTR/Tad1, LTR/Gypsy and IntegratedVirus/DNAV (Table S1e). Sequence homologs of the two abundant families PpSat1 and PpSat2 from *P. parasitica* [37] were identified in *A. euteiches*. To unravel the relationship among satellite DNA families, a phylogenetic tree was constructed including PpSat1 and PpSat2 from *P. parasitica* [37] (Figure 3). The topology of the tree suggests diversification in AeSat families, with high copy number (i.e., >1000) families clustered into a central location group.

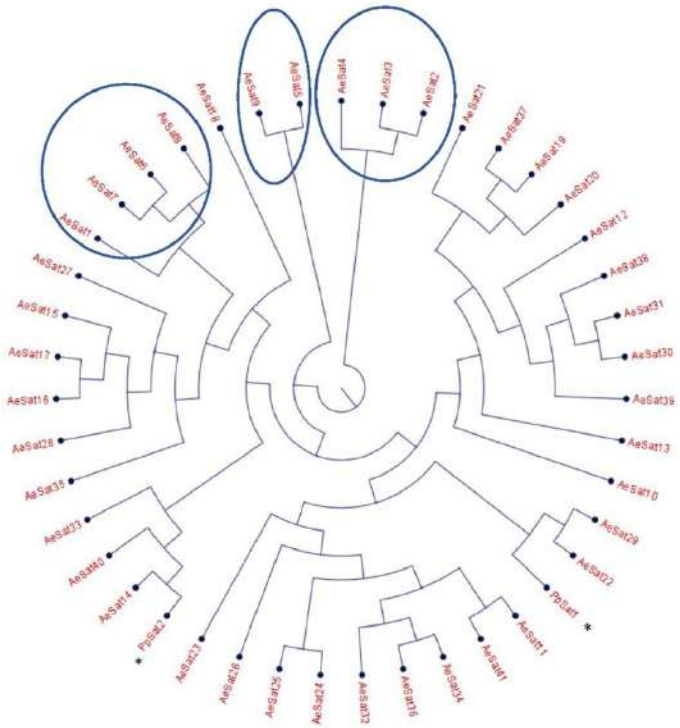

Figure 3. Phylogenetic tree of satellite DNA families from *A. euteiches*. Phylogenetic tree of the 41 satellite DNA families from *A. euteiches*, including the DNA satellite from *P. parasitica* * (PpSat1 and PpSat 2 [37]). HC = high number of copies of DNA satellite families (>1000 copies in the genome).

3.3. Mitochondrial Genome of *A. euteiches* ATCC201684

From the obtained long-read sequences, we assembled the mitochondrial genome (mtDNA) of the *A. euteiches* ATCC201684 strain. As depicted in Figure 4, the circular genome is 47 kb in size and is predicted to encode 40 protein-coding genes, 4 ribosomal RNA genes and 35 tRNA genes (Table S1f). The genes are encoded by both strands. As previously reported for mitogenomes of oomycetes [61], a bias in A/T usage is observed for the GC content around 22%. Using the available mitochondrial genome information (Table S1g), we compared the mitogenome content of *A. euteiches* with those of two other Saprolegniales (*Aphanomyces astaci* and *Saprolegnia ferax*) and one Peronosporale (*Phytophthora infestans*). The mitogenome size of *A. euteiches* is similar to that of the other Saprolegniales and larger than that of Peronosporale (e.g., 39.8 kb for *P. infestans vs.* 46.9 kb), as previously reported [50,62]. The gene content of mtDNA from *A. euteiches* is similar to those in other Saprolegniales and Peronosporales. A duplication of ribosomal RNA is observed in the Saprolegniales when compared with *P. infestans* (4 vs. 2). A secY gene that encodes for the central subunit of the secretory channel SecYEG, which enables the secretion of proteins across a membrane in their unfolded version, is present in the mitogenome of *A. euteiches* as it is in the other oomycetes.

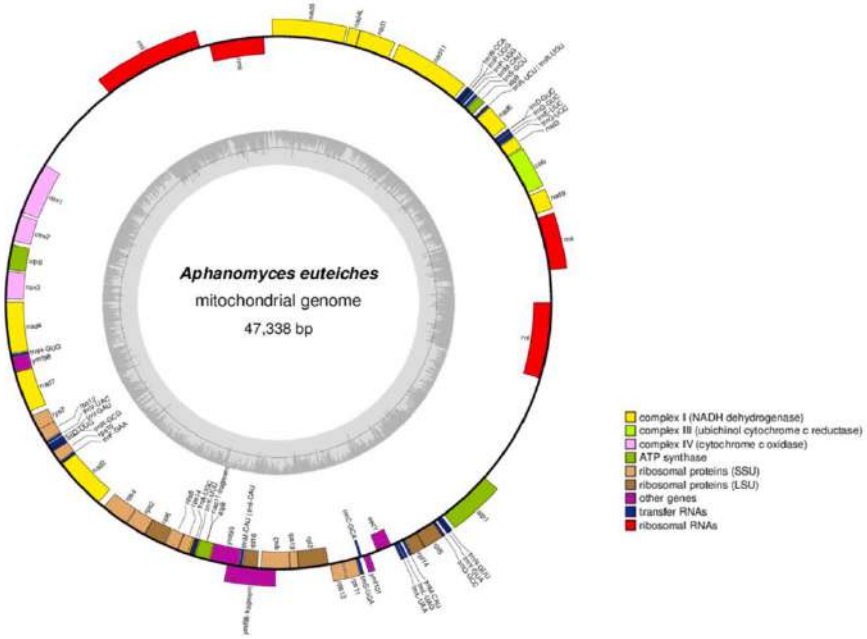

Respiratory chain: (n=19)
Complex I : nad1, nad2, nad3, nad4, nad5, nad6, nad7, nad9, 2*nad11, nad4L
Complex III: cob
Complex IV: cox1, cox2, cox3
Complex V:, atp1, atp6, atp8, atp9
Ribosomal RNAs (n=4) : 2*rRNAs, 2*rRNAl
Ribosomal proteins (n=16): rsp2, rps3, rps4, rps7, rps12, rps8, rps10, rps14, rps13, rps19, rpl16, rpl2, rpl5, rpl6, rps11, rpl 14
Transfer RNAs (n=35): trnS-UGA, trnL-UAA, trnL-UAG, trnL-UAG, trnM-CAU, trnG-GCC, trnG-GCC, trnY-GUA, trnN-GUU, trnG-UCC, trnE-UUC, trnD-GUC, trnD-GUC, trnD-GUC, trnR-UCU | trnR-UGU, trnS-GCU, trnM-CAU, trnM-CAU, trnP-UGG, trnP-UGG, trnW-CCA, trnH-GUG, trnH-GUG, trnV-UAC, trnI-GAU, trnI-GAU, trnQ-UUG, trnQ-UUG, trnR-GCG, trnR-GCG, trnF-GAA, trnA-UGC, trnK-UUU, trnM-CAU | trnI-CAU, trnC-GCA
Other (unidentified open reading-frames) (n=4): 2*ymf98, ymf99, ymf101
Import protein (n=1): secY

Figure 4. Circular map of the mitochondrial genome of *A. euteiches*. Protein coding genes, tRNA and rRNA are shown on the outer colored ring. Genes encoded on both strands are listed below. The inner ring shows the GC density.

3.4. Functional Annotation of A. euteiches ATCC201684 Genome

The whole predicted proteome of *A. euteiches* was searched for the presence of PFAM domains. In total, 12,978 predicted proteins (56%) were found to harbor a PFAM domain (Table S1a). The most frequent were proteins containing Ankyrin and WD40 repeats, protein kinase domains and ABC-transporters, as shown in Figure 5. The genome of *A. euteiches* is also characterized by a large set of proteins containing domains related to nucleic acids such as the FYVE zinc finger, endonuclease and reverse transcriptase. We then searched the whole-proteome for putative secreted proteins, to predict the *A. euteiches* secretome. We identified 2106 proteins with a signal peptide (~9% total proteome) using SignalP V5 [54]. Among these, 1515 do not have a predicted transmembrane domain (6.5% of the proteome) and 591 contain at least one transmembrane region (TM; 2.5 % of the proteome). We annotated the CRN effectors as reported by [21] using the hmm-profile of the conserved N-ter domain constructed on CRN genes from the V1 assembly of the *A. euteiches* genome [41].

We predicted 234 CRN effectors, with less than 4% harboring a predicted signal peptide (i.e., 8 CRNs; Table S1h). In accordance with the V1 genome assembly and transcriptomic analyses, we did not detect any RxLR coding genes in *A. euteiches*. Among the secreted proteins without a predicted functional domain, we identified 568 small secreted proteins (SSP) with sizes of less than 300 amino acid residues and without any functional domains, as detected by an InterProScan search. This expands the original SSP repertoire detected in the V1 version of the genome. To confirm the putative role of SSPs as effectors, we performed an analysis using EffectorP v2. Around 80% of the SPPs (453 proteins) were predicted as effectors, among which 78% (351 proteins) were predicted as cytoplasmic effectors, 19% (88 proteins) as apoplastic effectors and 3% (15 proteins) as apoplastic or cytoplasmic effectors (Table S1i).

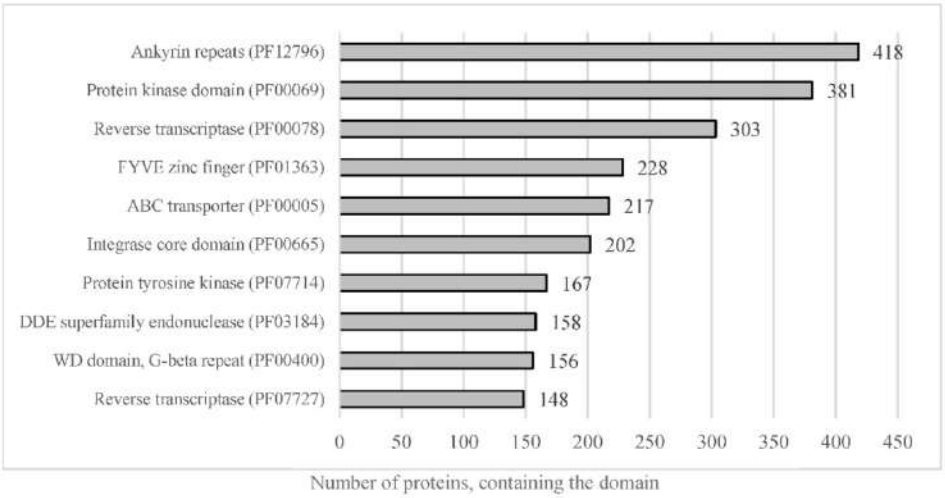

Figure 5. Representation of the most abundant PFAM predicted domain in the proteome of *A. euteiches*. When considering the number of proteins containing the most-present PFAM domains in total proteome, of the 23,027 total predicted proteins, around 56% harbor a PFAM domain.

3.5. Secretome Features of A. euteiches ATCC201684 Strain

To gain an overview of the *A. euteiches* secretome's composition and compare it with that of the other oomycetes, we identified and annotated the secretomes of two Saprolegniales, namely, the fish pathogens *Aphanomyces invadans* and *Saprolegnia parasitica*, and the distant Peronosporale plant pathogen *Phytophthora infestans* (Table S2a–c). We searched for the most represented PFAM-containing proteins and divided them into five classes (>15 proteins per class, Table S2d). The carbohydrate-active enzymes (CAZymes) class included secreted proteins that play a role in polysaccharides' degradation in the host as well as in remodeling the oomycete cell wall. The protease and inhibitors class included secreted proteolytic proteins that take part in the alteration of the host immune system and in protecting against host lytic enzymes. The adhesion class comprised secreted proteins with adhesive capacity to different substrates such as cellulose and chitin and/or catalytic activity. The toxicity/elicitors class corresponded to secreted proteins that are known to trigger a host response or to be toxic to the host cells (i.e., elicitins, NLPs). The class labeled 'others' included all other secreted proteins known to play a role in host interaction (i.e., calcineurin-like phosphoesterase, tyrosinase). CRN and SSP families were not included in the analysis due to the absence of PFAM domains in a large majority of these proteins. Figure 6 presents the PFAM-containing proteins in the whole-proteome

in each class with respect to the number that is expected to be secreted (Table S2k). We observe that a common trait of the oomycetes' secretome is the 'proteases and inhibitors' class, which presents the most-enriched terms in Saprolegniales and Peronosporales with respect to the total protein content, but this is not the case for *A. euteiches*. The 'adhesion' class is a common trait among the four oomycete species, with an enrichment of PAN-Apple-containing proteins within this category such as the CBEL cell wall glycoprotein of *Phytophthora* sp., which contributes to plant adhesion and the cell wall architecture [63]. Overall, we notice that the phylogenetically distant *P. infestans* presents a distinctly different secretome profile compared to Saprolegniales species, characterized by the enrichment of toxic/elicitors proteins and protease-inhibiting Kazal domains. The Saprolegniales species, despite their different host preferences (plants vs. fish), show common features in their secretome profile such as enrichment in both adhesion domains and in several proteolytic domains. *A. euteiches* and *S. parasitica* secretomes seem more diverse in terms of their PFAM domains related to the different classes, as compared to *A. invadans*, and present an increase in proteolytic enzymes included in the 'protease and inhibitor' class. The *A. euteiches* secretome is also highly enriched in carbohydrate-binding proteins, especially with respect to proteins containing cellulose-binding domains (CBM1); this high number is a distinguishing feature that stands out when compared to the other species. Finally, the secretomes of plant pathogens share the CAZymes class as a unique and common feature.

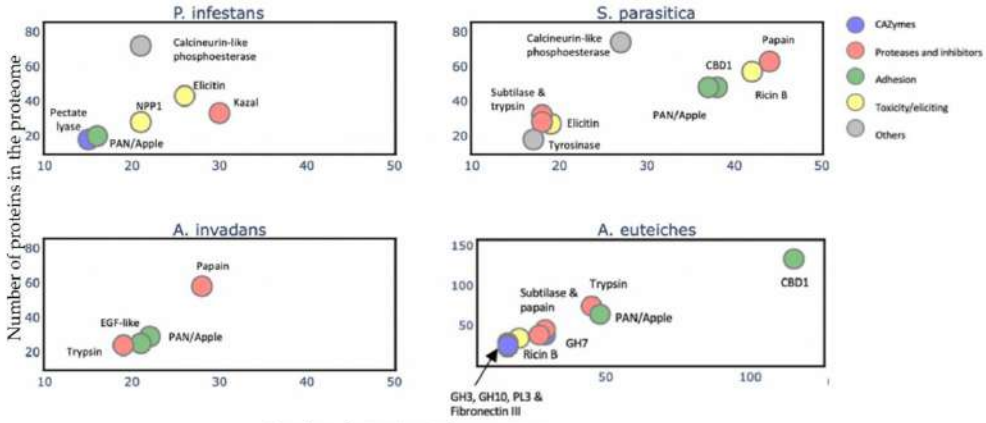

Figure 6. Comparison of *A. euteiches* secretome content with three other oomycetes. PFAM domains were searched in secreted proteins of two plant pathogens *Phytophthora infestans* (Peronosporale) and *Aphanomyces euteiches* (Saprolegniale) and two fish pathogens *Saprolegnia parasitica* and *Aphanomyces invadans* (Saprolegniale). Five classes of PFAM-containing proteins were identified. A PFAM domain present in more than 15 secreted proteins per class is represented as a colored circle and its name indicated above the circle. Arrow indicates overlaying circles. All selected PFAM domains were significantly enriched (Fisher's exact test, $p<0,05$) with an enrichment coefficient (predicted secreted *vs.* expected secreted) over five for each class.

3.6. Illumina Sequencing of Four Strains of *A. euteiches* with Differential Legumes Preference

To decipher the putative variability in legume pathogenicity genes within the *A. euteiches* lineage, we performed whole-genome sequencing of four strains of *A. euteiches* using Illumina technology. We selected strains with varied geographical origins and distinct host-spectra within legumes (Table 2). The RB84 strain, as the reference ATCC201684 strain, was isolated in Europe from pea fields and belongs to pathotype I according to pathogenicity tests performed with various genotypes of pea [64,65]. Both strains have a

broad spectrum of hosts within the legumes but have a preference for pea [66]. The Ae109 strain, which was originally isolated from a pea field in the US and was subsequently shown to also be virulent in alfalfa, belongs to pathotype III. The MF1 and NC1 strains isolated in Wisconsin and North Carolina (US) vary in aggression and belong, respectively, to Race 1 and Race 2 of *A. euteiches* [52]. Race 1 is relatively widespread throughout the alfalfa-producing region in the US (Wisconsin and Minnesota) and Race 2 appeared in the 1990s after alfalfa failed to resist Race 1. Race 2 is considered to be more virulent than Race 1 and its prevalence is reported in US alfalfa fields and represents around 45% of all strains, with Race 1 representing 11% [67,68]. All the strains have been used in the implementation of GWAS on pea, or on the legume model *Medicago truncatula*, to characterize the genomic loci controlling resistance to *A. euteiches* [13,69,70].

Table 2. Origin and host spectrum of *A. euteiches* strains.

A. euteiches Strain	Isolated from	Origin	Host-Spectrum within Legumes *	References
ATCC201684	Pea	Denmark	Broad: pea, alfalfa	[41,71]
RB84	Pea	France	Broad: pea, alfalfa, bean, lentil, vetch	[66]
Ae109	Pea	USA	Narrow: pea, alfalfa	[9,70,72]
MF1	Alfalfa	USA	Narrow: alfalfa but not pea	[67,73]
NC1	Alfalfa	USA	Narrow: alfalfa but not pea	[10,73]

* All the strains can interact with the model legume *M. truncatula*.

We obtained four draft assemblies of 52–59 Mbp in size and with N50 values of 11 to 29 kbp (Table 3). The genomes had a GC content of about 47%, similar to the reference ATC201684 strain. Although the higher number of contigs in the NC1 strain suggests a slightly more fragmented assembly when compared to the three other strains, the level of genome completeness obtained using BUSCO analysis is similar for all the strains. We annotated around 22,000 protein-coding genes/strain except for the NC1 strain, which had 19,911. The proportion of secreted proteins is similar to that in the ATCC201684 reference strain and varies from 5.9% to 6.3% of the total proteome size (Table S3a–f).

Table 3. Assembly statistics of four near-complete *A. euteiches* genome sequences.

Description	NC1	MF1	RB84	109
Assembly size (Mb)	52.04	59.75	59.39	58.41
N50 (bp)	11.661	24.852	29.237	21.846
Scaffold count	15.477	7.808	7.095	6.495
GC content (%)	47.73	47,46	47.45	47.43
Protein-coding gene count	19.911	22.012	21.892	21.546
Number of secreted proteins (%)	1.190 (5.9%)	1.344 (6.1%)	1.324 (6%)	1.369 (6.3%)
BUSCO score for Stramenopiles (%) (complete/duplicated/fragmented/missing)	100/0/0/0	98/2/0/0	97/0/0/3	100/0/0/0

Next, we examined the phylogenetic relationship between the strains. We performed an OrthoFinder search to identify orthogroups (OG) of the proteins, to construct a Species Tree from all Genes (STAG) [74]. To identify the positions of newly sequenced strains within the oomycetes, we used the sequences of the two Saprolegniales fish pathogens (*Aphanomyces invadans* and *Saprolegnia parasitica*) and also included the Peronosporale plant pathogen *Phytophthora infestans* (Figure 7). The five strains of *A. euteiches* were grouped and formed a clade together with *A. invadans* within the Saprolegniales. Within the *A. euteiches* lineage, two subgroups were detected: one corresponding to European strains isolated

from pea fields (ATCC201684 and RB84) and the other including strains isolated in the US (MF1, NC1 and Ae109), with the position of the NC1 strain being distinct within the subgroup.

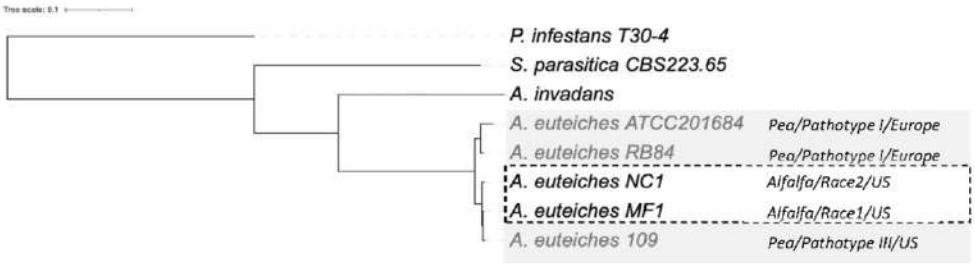

Figure 7. Phylogenetic relationship between the six sequenced *A. euteiches* strains. The maximum likelihood tree was built using Species Tree from All Genes (STAG) method from OrthoFinder. *A. euteiches*, *S. parasitica* and *P. infestans* were used as outgroups of different degrees of relativeness. MC1 and NC1 were identified as race 1 and race 2 (hatched square) based on their virulence on the Saranac and WAPH-1 alfalfa genotypes, while the ATCC201684, RB84 and Ae109 strains (grey square) were included in the 'pathotype' based on their aggressiveness against a pea collection. The geographical origins of the strains are indicated.

3.7. Comparative Analysis of Functional Domains in Secretomes of A. euteiches Strains

To check if the variation in the secretome content could be correlated to the host legume preference, we searched for shared and accessory secreted proteins in the five strains. To this end, the five secretomes were combined (totaling 6742 secreted proteins) and clustered using OrthoFinder. Proteins from the secretome were assigned to 1597 OrthoGroups (OG; Figure 8a, Table S3g). We defined a 'core' set of 659 OGs, where each OG had sequences from all the five secretomes analyzed, totaling 3970 secreted proteins. The accessory secretome was defined as OGs, which had proteins from two to four strains and comprised 604 OGs that encoded 2394 secreted proteins. A set of 378 secreted proteins in the form of 'singletons' clustered into 334 OGs with sequences from a single strain. Around 58% of the accessory secretome was shared by the four strains and less than 15% was specific to one strain (Figure 8b). A closer view of the OG distribution (Figure 8c) identified around 100 shared accessory OGs for the US strains (MF1/NC1/Ae109) and 94 for the European strains (ATCC201684/RB84). At the host level, 13 OGs were shared by the 'pea' strains (Ae109/ATCC201684/RB84) while 23 were shared by the 'alfalfa' strains (MF1, NC1) (Table S3h).

We then searched for the main functions that were present in the core and the accessory secretomes of *A. euteiches* by grouping the secreted proteins, based on their predicted PFAM domains, into classes as described above, except for the 'toxic/elicitor' class that we split into 'toxic' and 'cysteine-rich' classes for better visualization (Figure 9, Table S3i). CRNs and SSPs were not considered in this analysis either due to the absence of a predicted signal peptide or a PFAM domain. Around one-third of the secreted proteins of the core secretome (1186 of 3970) were predicted to be enzymes with activity against peptides (proteases) or cell-wall components (CAZymes).

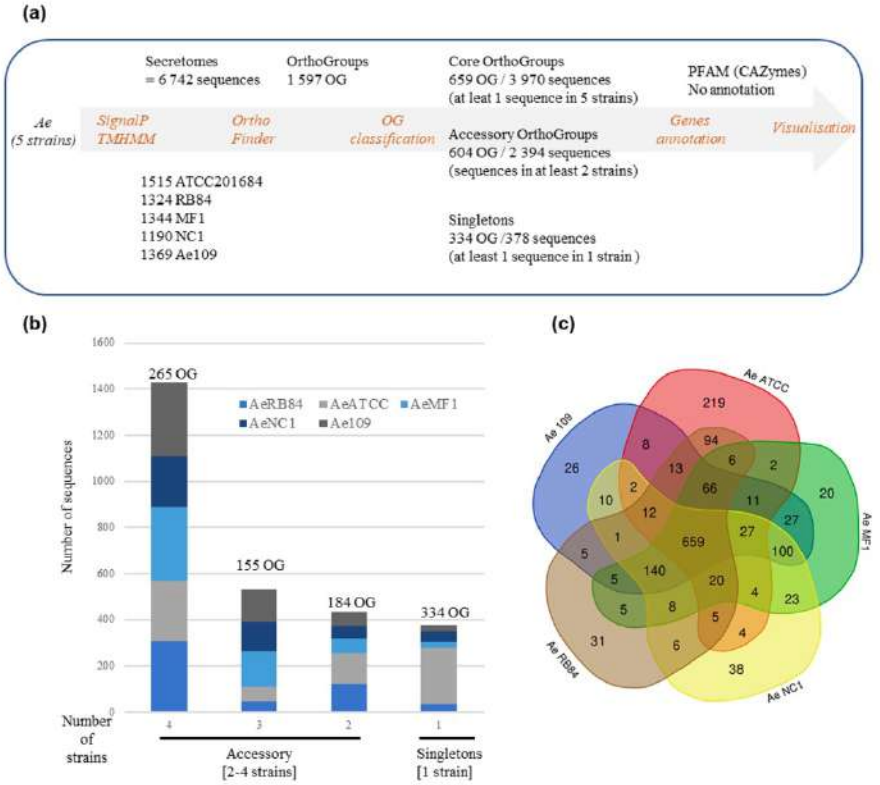

Figure 8. Comparative analysis of secretome of five *A. euteiches* strains with different host preference and geographical origins. (**a**) Pipeline used for comparative analysis of *A. euteiches* strains. (**b**) Distribution of sequences by *A. euteiches* strain (color-coded) found in accessory and singleton orthogroups. Number of orthogroups (OGs) is indicated. (**c**) Venn diagram depicting number of OGs per *A. euteiches* strain.

In Figure 9, where the number of secreted proteins containing PFAM domains in the core (left column) and accessory secretomes (right columns) is shown, proteases can be seen to be largely distributed in the core secretome. The principal members of the core secretome are found to be families of metalloproteases M12A (astacin), M13 and M8 (leishmmanolysin), the serine proteases S10 (carboxypeptidase), S8/S53 (subtilisin) and S28 and the trypsin families. Cysteine protease families have a lower representation except for the C1A family (papain-type), while the C69 and C19 families are absent from the core secretome. We noticed the presence of Kazal serine protease inhibitors, which are known to be involved in the pathogenicity of *Phytophthora infestans* [75]. Cell wall-degrading enzymes, illustrated by CAZymes, constitute another major trait of the core secretome of *A. euteiches*. The most representative CAZymes families are present, including enzymes implicated in plant cell-wall degradation, such as polygalacturonases (family GH28) and cellulases (family GH5, GH6 and GH7), except for GH11 (xylanase), GH20 (hexosaminidase), GH63 (α-glucosidase) and PL1 (pectin lyase). We confirmed the presence of GH62 (α-l-arabinofuranosidase), not reported in other oomycetes except in *S. parasitica* [41,76]. In addition to the large proportion of 'ricin' and 'necrosis-inducing' domains that are known to trigger cell necrosis [77–79], the core secretome contains adhe-

sive and cysteine-rich proteins involved in oomycetes' pathogenicity, such as elicitin and CBM1 [30,80,81], or sterol binding CAP proteins that have recently been reported to be virulence factors in animal and plant pathogenic fungi [82].

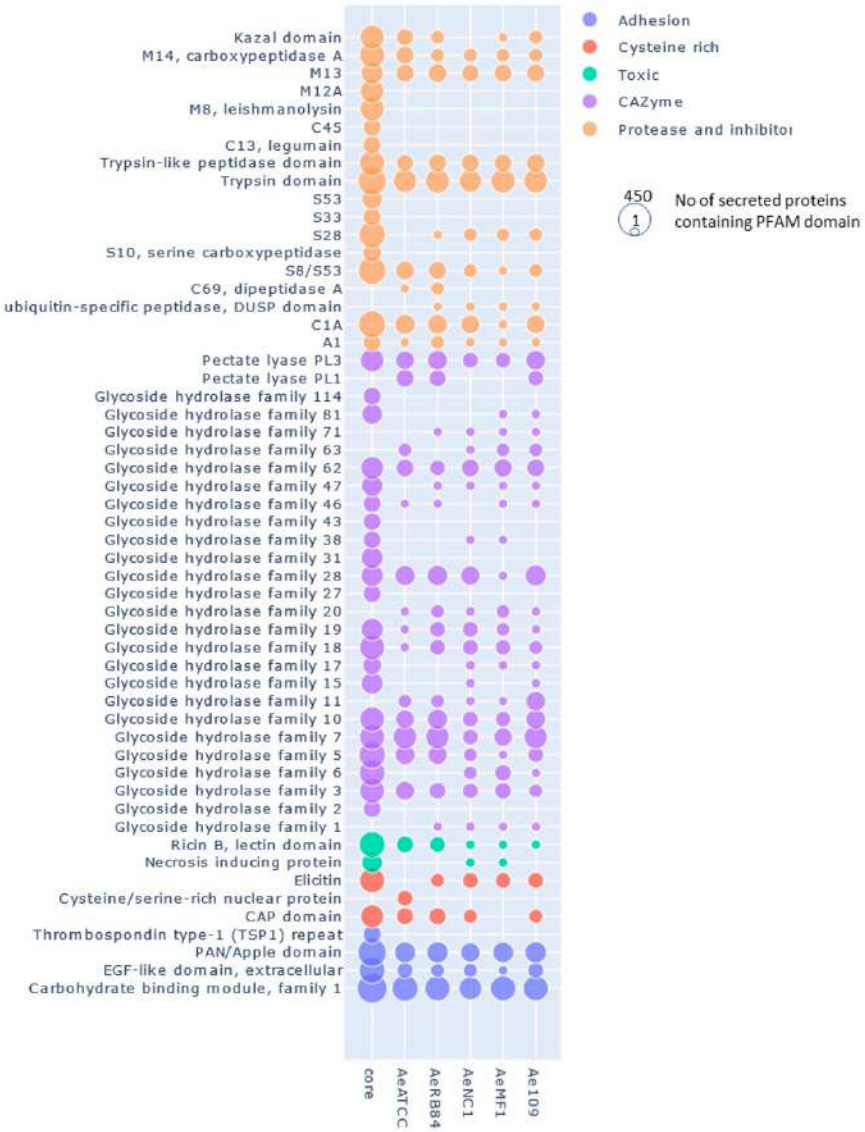

Figure 9. Distribution of secreted proteins containing a PFAM domain in the core and accessory secretome of *A. euteiches*. The first 'core' column represents the number of secreted proteins containing PFAM domains found in core orthogroups; the other columns represent the numbers of accessory and singleton orthogroups. The size of the circle corresponds to the log10 + 1 number of secreted proteins with a PFAM domain.

In the 'non-core' secretome, the large majority of the secreted proteins displayed a predicted function that was already detected in the 'core' secretome. This is illustrated with S8/S53 proteases, GH62 or PL3 for CAZymes and PAN/Apple or CBM1 for adhesion (Figure 9), depicting the variation in the structural organization of the secreted proteins. We see that the five strains display species-specific proteins in the 'accessory' secretomes, as exemplified by the CAZymes GH11 and GH20. However, the NC1 strain contains no specific GH 46 (chitosanases) or Kazal-protease inhibitor and the MF1 strain is devoid of specific CAP secreted proteins. The difference between the European (ATCC201684/RB84) and the US (MF1/NC1/Ae109) 'accessory' secretome is the presence of specific C69 peptidases (present in European strains and absent in US ones) and GH6 and GH17 (cellulase) secreted proteins (absent in European strains and present in US ones).

3.8. Small Secreted Proteins (SSPs) with Unknown Function as Legume Adaptation Proteins

In the core genome, around 60% of the secreted proteins match a PFAM domain, while the accessory and singleton secretomes are characterized by a large representation of secreted proteins without any functional annotation (Figure 10, Table S3a–d).

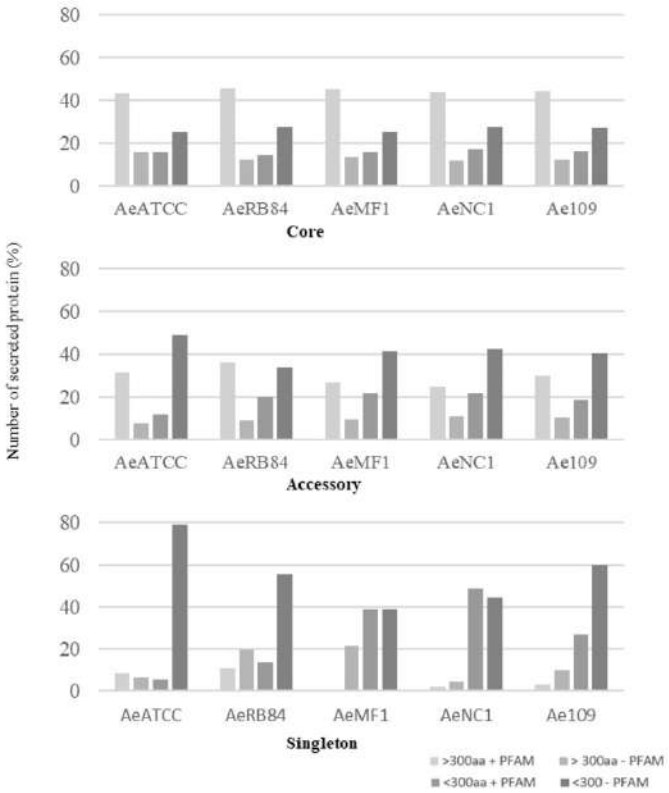

Figure 10. Size distribution of secreted proteins in the core, accessory and singleton secretomes of *A. euteiches* spp. *A. euteiches* spp. secreted proteins with (+) or without (−) a predicted PFAM domain are classified in two categories based on their size: larger than 300 amino acids (>300 aa) or less than 300 residues (<300 aa).

Among these, SSPs are less present in the 'core' secretome (44% for SSP vs. 58% for the total secretome) and are widely distributed in the 'accessory' and 'singleton' secretomes of the five strains. The higher occurrence of SSPs in 'accessory' and 'singleton' secretomes of *A. euteiches* as compared to the core proteome indicates that these secreted proteins could participate in deciding legume preference. The task was then to identify classes within SSPs to find the corresponding structural regularities. The SSPs were first examined for the presence of conserved motifs or domains, as previously reported for RxLR and CRN effectors of oomycetes [21,24]. No conserved pattern was defined but we observed amino acid-enriched protein sequences in the SSPs. We consider as 'enriched' an amino acid with a 1.5-fold higher frequency than the third quartile value in the whole proteome of the strain. When plotting the amino acid enrichment on a phylogenetic tree of *A. euteiches* SPPs from the five strains, we see that clustered SPPs correspond to G-rich, T-rich and D-rich secreted proteins and account for 40–50 % of the total SSP set (Figure 11a).

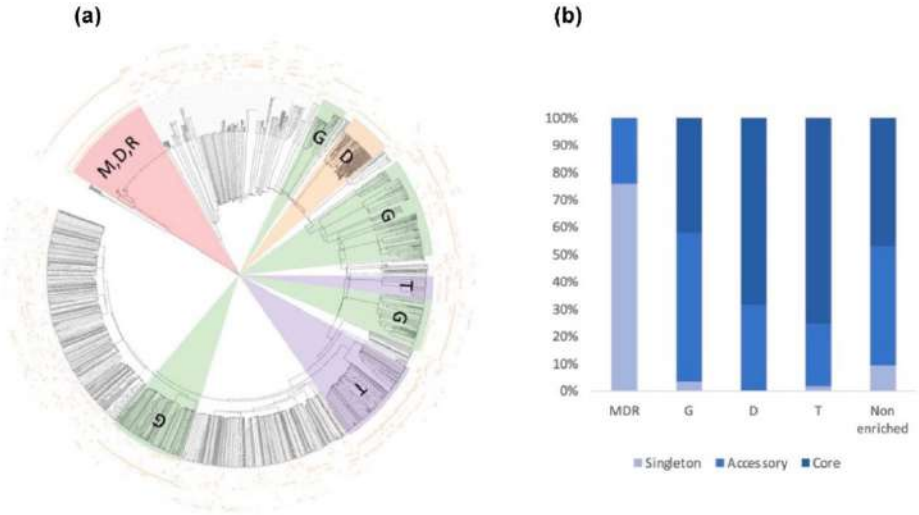

Figure 11. Consensus tree and class distribution of small, secreted proteins (SSP) within five strains of *A. euteiches*. (**a**) UPGMA consensus tree of 2010 SSPs from five strains of *A. euteiches* (RB84, Ae109, MF1, NC1, ATCC201684) based on whole protein amino acid sequence alignment using ClustalOmega (inner circle). Outside circles represent amino acid enrichment with one amino acid per circle (color = enriched, blank = non-enriched value). Colored ranges represent SSP classes with similar amino acid enrichment patterns. Green = G-rich, orange = D-rich, purple = T-rich, pink = MDR-rich. (**b**) Distribution of SSP classes (G-rich, D-rich, T-rich, MDR-rich, non-enriched) between core, accessory and singleton secretomes (in percent) of *A. euteiches*.

Oddly, the long-read sequenced pea strain ATCC201684 is characterized by a large set of MDR-rich SPPs, not represented in the other Illumina-sequenced strains. These specific SSPs are tandemly repeated in the genome of the ATCC strain, while only one copy is detected in the Illumina sequenced strain, except for NC1, thus probably explaining the few sequences detected in the other *A. euteiches* species. While the distribution of SPPs within the five strains is almost similar, without considering the atypical MDR-rich class, the core secretome of *A. euteiches* contains T- and D-rich SSPs in contrast to the 'non-core' secretome characterized by G-rich SSPs (Figure 11b). This particular distribution of enriched-SSP suggests that they probably participate through an unknown function in the adaptation of *A. euteiches* to its environment.

4. Discussion

The mechanisms of pathogen adaptation to quantitative resistance in plants are largely unknown. In this paper, taking advantage of the availability of several *A. euteiches* strains adapted to pea or alfalfa, we investigated genetic variations that could be correlated with host preference, using a comparative genomics approach.

To obtain a high-quality 71 Mb genome assembly, we first re-sequenced, using PacBio, the ATCC201684 *A. euteiches* strain that we previously sequenced with a combination of Illumina and 454 technologies [41]. In this work, we improved the assembly and identified a large number of repetitive sequences as well as the presence of satellite DNA, as previously reported for the *Phytophthora parasitica* genome when re-sequenced by the long-read approach [37]. In addition, we assembled the first mitochondrial genome (mtDNA) for a Saprolegniales plant pathogen. The mitochondrial eukaryotic genome performs key functions in cells, such as the synthesis of nucleotides, and also contains the machinery for oxidative phosphorylation and electron transport, which are required for the production of energy [61]. The circular mitochondrial genome of *A. euteiches* is 47 kb in size. This size is similar to the genome size reported for other Saprolegniales such as *Aphanomyces astaci* and *Aphanomyces invadans* (49 kb) [50] and is different from those of Peronosporales (38 kb [83]) and Pythiales (55 kb [84]). This work reveals that the mitochondrial gene contents of plant and animal pathogenic Saprolegniales are very similar. In addition, the availability for the first time of the *A. euteiches* mtDNA offers us the possibility of developing new markers [83] and enables the detection of the pathogen with greater sensitivity [85] for root rot diagnostics.

A total of 23,027 protein-coding genes were identified in the V2 assembly of the *A. euteiches* genome, which is a significantly higher number than in V1. Among the newly predicted proteins present in the V2 assembly, 44% do not possess a putative functional PFAM domain, while the rest harbor PFAMs related to nucleic acid modification (i.e., integrase, endonuclease, transposase, etc.). Overall, the proteome exhibits numerous ankyrin repeats and WD-40 repeats. The ankyrin repeat is one of the most frequently observed amino acid motifs in protein databases, probably because this protein-protein interaction motif is involved in a diverse set of cellular functions [86]. Similarly, in eukaryotes, WD-40 repeat proteins generally mediate supramolecular interactions and participate in the assembly of complexes involved in different cellular processes [87]. These features may explain the large representation of ankyrin and WD40 repeats in the *A. euteiches* proteome. The expansion of the kinome (a set of protein kinases) observed in the *A. euteiches* genome has already been detected in the fish oomycete pathogen *Saprolegnia parasitica*, where these proteins are presumed to act as cell surface receptors [88]. The genome of *A. euteiches* encodes over 200 ABC transporters, a large proportion of which are commonly present in oomycetes [89]. Unlike fungi, oomycetes, in general, including *A. euteiches*, do not possess a set of detoxifying enzymes; notably, they are missing P450 enzymes. Therefore, the ABC transporters might counteract antimicrobial compounds, such as flavonoids [90]. The large repertoire of ABC transporters can also improve resistance to synthetic chemicals (e.g., fungicides), which complicates the application of chemicals to protect crops [91].

The secretome of plant-associated eukaryotic filamentous organisms such as fungi and oomycetes corresponds to secreted proteins that alter the environment to acquire nutrients or modify the host to facilitate invasion (effectors). Here, we predicted 1515 proteins, which corresponds to 6.5% of the *A. euteiches* ATCC201684 whole proteome. While we detected a larger set of Crinklers and SSPs in V2, we ascertained the absence of putative RxLR, which is predominant effectors in Peronosporales [92]. By looking for the major secretome components in *A. euteiches* and three other oomycetes, we confirmed the previous observation that the *A. euteiches* secretome is distinct from that of the animal pathogenic *Aphanomyces* [41] in harboring a large set of enzymes implicated in plant cell-wall deconstruction. The *A. euteiches* secretome is highly distinct from the one predicted in the plant pathogen *P. infestans*, which preferentially contains necrosis-inducing molecules (i.e., elicitin, NPP) and protease inhibitors (i.e., Kazal). Taken together, the PacBio long-read

assembly of the ATCC201684 strain thus provides a high-quality reference genome for the *Aphanomyces* genus.

A. euteiches was initially considered as a pathogen of pea [6], but now we know that it can infect alfalfa, clover, dry beans and lentils, though not lupine or soybean [6,13]. To probe the molecular basis underlying the legume preference of *A. euteiches*, we compared the draft genomes of four strains of the pathogen (RB84, Ae109, MF1, NC1) from different geographical areas (Europe, US) with different pathogenicity traits on pea and alfalfa. Our phylogenetic analysis revealed that the strains MF1 and NC1 are closely related and are slightly distant from Ae109. The US strains are distant from the European strains (RB84, ATCC201684), suggesting an early divergence. The content of *A. euteiches* secretomes appears to be largely shared among all strains, with few gains/losses of secreted proteins. The 'core' secretome shares a number of properties, such as a large set of enzymatic proteins targeting carbohydrates and proteins. This set includes CAZymes, which are involved in the breakdown or binding of plant cell-wall carbohydrates such as cellulases and cellulose-binding proteins except for GH20 (hexosaminidase), GH63 (α-glucosidase) and PL1 (pectin lyase). We previously reported the enrichment of carbohydrate-binding and glycosyl hydrolases (GH) in the ATCC201684 strain [41,93], and the current work highlights the fact that the GH of CAZymes is a major trait of the *A. euteiches* 'core' secretome. This is in agreement with other studies that have identified a large repertoire of GH in oomycetes, with *Phytophthora* species tending to have the highest number as compared to other oomycete taxa [60,94–96]. Oomycetes produce CAZymes as a part of their arsenal for the supply of nutrition and to invade their preferential hosts. The GH repertoire may be linked to the oomycete lifestyle [19], with obligate biotrophic species having a reduced number and diversity of these proteins [97].

Another trait of the 'core' *A. euteiches* secretome is the presence of secreted cysteine and serine proteases except for C69 peptidases. The production of secreted proteases as a component of virulence in oomycetes that infect animals has received greater attention than plant pathogens. Secreted proteases have been proposed to be involved in the digestion of the host barrier, such as the crayfish cuticle in the case of *Aphanomyces astaci* [98], or the human epidermis in the case of *Pythium insidiosum* [99]. However, it is assumed that proteolysis of plant substrates is a strategy employed by plant pathogens during the infection process [100,101], meaning most of the proteases predicted in *Phytophthora sp.* contribute to pathogen virulence [102,103]. A previous study reported elevated pathogen-derived protease activity in pea tissues infected by *A. euteiches* (MN174 strain), whereas this activity was not required for saprophytic growth [104]. Thus, we propose that the core proteases of *A. euteiches* may act as potential pathogenicity factors.

The 'non-core' secretome of *A. euteiches* displays secreted proteins with functional activities reported in the 'core' secretome, depicting variation in the protein architecture rather than in its activity. Nevertheless, the two categories of CAZymes GH11(xylanases) and GH20 (hexosaminidases) are distinct characteristics of the 'non-core' secretome of *A. euteiches*. Xylanases are involved in the degradation of plant hemicellulose, and GH11 has been reported to participate in increasing the virulence of certain phytopathogenic fungi such as *Botrytis cinerea* or *M. oryzae* [105,106]. Interestingly, the soil-borne fungus *Verticillium dahliae* secretes a GH11(Vd424Y), essential for virulence, that targets the plant nucleus rather than the cell wall, suggesting an unknown function for fungal GH11 during host infection [107]. GH11s are not functionally characterized in oomycetes, but their presence in the 'non-core' secretome of *A. euteiches* in combination with GH62 (α-l-arabinofuranosidases) from the core secretome, probably provides improved access to the xylan backbone of plant hemicellulose, as reported for fungi [108]. GH20s, which degrade chitooligosaccharides (COS) into GlcNAc monomers [109], have been suggested as putative virulence factors shared by animal pathogenic oomycetes (Saprolegniales proteomes) but absent in phytopathogenic oomycetes [110]. The presence of chitooligosaccharides (COS) in the cell wall of *A. euteiches* [111,112] in contrast to other phytopathogenic oomycetes (Peronosporales), suggests the structural or protective role of GH20 for phytopathogenic *Aphanomyces* species.

Only minor content variations due to the presence/absence of secreted proteins allow us to distinguish the *A. euteiches* strains based on their geographical origin or legume preference. The US strains are characterized by the presence of specific cellulases (GH6, GH17), while the European strains harbor C69 peptidases. The presence of a specific set of secreted proteins could be related to the soil composition of the fields, with different histories of legumes in the US and Europe. The possibility of deciding the host preference based on compounds released by legumes roots has been suggested for closely related legume root-infecting *Phytophthora* species [113]. In addition, the use of partially resistant alfalfa cultivars in the US could also contribute to the diversity of *A. euteiches* as it could allow the selection of better-adapted strains such as NC1.

Finally, the 'non-core' secretome shows a higher abundance of small secreted proteins (SSP) with unknown functions as compared to the 'core' secretome. It is suspected that SSPs may play a role in the host adaptation of fungi but this aspect remains unclear [114]. However, their importance in the successful interaction with the host has been reported for various fungal symbionts and pathogens [114–117]. The presence of large variations in the gene number of SSPs within phytopathogenic fungi suggested that the molecular function of SSPs could be linked to the different infection strategies developed by such microorganisms [114]. In *Leptosphaeria maculans*, the expression of SSPs is regulated during plant infection and is also influenced by physical parameters such as the presence of antibiotics from prokaryotes in the rhizosphere [117]. This suggests that fungal SSPs, in addition to their role in plant interaction, may participate in ecological niche colonization by shaping plant-associated microbial interactions [118]. In a previous article, we reported the presence of SSPs in oomycetes [41]; here, we propose that SSPs may participate in determining the host preference. The classification of SSPs from *A. euteiches* into three groups based on their amino acid composition may help to unravel their unknown function. This is exemplified with AeSSP1256, a 'core SPP' from the G-rich class, which hijacks a *Medicago truncatula* RNA-helicase from its nucleic target and promotes *A. euteiches* roots' infection [119].

In conclusion, this study provides a high-quality genome reference for *A. euteiches* at the nuclear and mitochondrial levels. Our comparative secretome analysis of *A. euteiches* species with different legume preferences mainly identified secreted proteins shared between species. The microbial molecular determinants of legumes' preferences remain elusive, although this work sheds light on the presence of a certain degree of specificity at the level of SSPs' repertoire.

Supplementary Materials: The following are available online at https://www.mdpi.com/article/10.3390/jof8010088/s1, Table S1: *A. euteiches* (pea strain ATCC201684) genome annotation (PacBio); Table S2: Oomycete secretomes; Table S3: *A. euteiches* strains' annotation (Ae109, RB84, MF1, NC1 strains, Illumina).

Author Contributions: Conceptualization, A.K., L.C., B.D. and E.G.; data curation, A.K., H.S.C. and E.G.; formal analysis, A.K., L.C. and E.G.; funding acquisition, E.G.; investigation, A.K., L.C., B.D. and E.G.; methodology, A.K. and E.G.; project administration, E.G.; resources, A.K. and E.G.; software, A.K. and H.S.C.; supervision, E.G.; validation, H.S.C.; writing—original draft, A.K., H.S.C. and E.G. All authors have read and agreed to the published version of the manuscript.

Funding: This research was funded by the European Union's Horizon 2020 research program under grant no. 766048 (MSCA-ITN-2017 PROTECTA).

Institutional Review Board Statement: Not applicable.

Informed Consent Statement: Not applicable.

Data Availability Statement: Assemblies, sequencing and annotation are available in the publicly accessible repository AphanoDB v2.0, updated in August 2021 (http://www.polebio.lrsv.ups-tlse.fr/aphanoDB/). The genome assembly of *A. euteiches* ATCC201684 (Illumina/545 combination) is also available via the EMBL | European Nucleotide Archive (ENA) (https://www.ebi.ac.uk/ena/browse) under study number PRJEB24016. For the other genome assemblies, data are currently under

submission at ENA as follows: ATCC201684 (PacBio); PRJNA769534 | MF1; PRJNA767766 | NC1; PRJNA767769 | RB84; PRJNA767773 | Ae109; PRJNA767593.

Acknowledgments: The authors would like to thank the GeT-PlaGe core facility in Toulouse, France (https://get.genotoul.fr/en/). Editorial assistance from R. Bacsa is acknowledged.

Conflicts of Interest: The authors declare no conflict of interest. The funders had no role in the design of the study; in the collection, analyses, or interpretation of data; in the writing the manuscript, or in the decision to publish the results.

References

1. Gaulin, E.; Jacquet, C.; Bottin, A.; Dumas, B. Root rot disease of legumes caused by *Aphanomyces euteiches*. *Mol. Plant. Pathol.* **2007**, *8*, 539–548. [CrossRef] [PubMed]
2. Becking, T.; Kiselev, A.; Rossi, V.; Street-Jones, D.; Grandjean, F.; Gaulin, E. Pathogenicity of animal and plant parasitic *Aphanomyces spp* and their economic impact on aquaculture and agriculture. *Fungal Biol. Rev.* 2021, *in press*. [CrossRef]
3. Svoboda, J.; Mrugała, A.; Kozubíková-Balcarová, E.; Petrusek, A. Hosts and transmission of the crayfish plague pathogen *Aphanomyces astaci*: A review. *J. Fish Dis.* **2017**, *40*, 127–140. [CrossRef]
4. Iberahim, N.A.; Trusch, F.; van West, P. *Aphanomyces invadans*, the causal agent of epizootic ulcerative syndrome, is a global threat to wild and farmed fish. *Fungal Biol. Rev.* **2018**, *32*, 118–130. [CrossRef]
5. Patwardhan, A.; Gandhe, R.; Ghole, V.; Mourya, D. Larvicidal activity of the fungus *Aphanomyces* (oomycetes: Saprolegniales) against Culex quinquefasciatus. *J. Commun. Dis.* **2005**, *37*, 269–274. [PubMed]
6. Papavizas, G.C.; Ayers, W.A. *Aphanomyces Species and Their Root Diseases in Pea and Sugar Beet*; Technical Bulletin; Agricultural Research Service of the U.S. Department of Agriculture: Washington, DC, USA, 1974.
7. Levenfors, J.P.; Fatehi, J. Molecular characterization of *Aphanomyces* species associated with legumes. *Mycol. Res.* **2004**, *108*, 682–689. [CrossRef] [PubMed]
8. Bazghaleh, N.; Prashar, P.; Woo, S.; Vandenberg, A. Microorganisms effects of lentil genotype on the colonization of beneficial *Trichoderma* species and biocontrol of *Aphanomyces* Root Rot. *Microorganisms* **2020**, *8*, 1290. [CrossRef] [PubMed]
9. Wicker, E.; Hullé, M.; Rouxel, F. Pathogenic characteristics of isolates of *Aphanomyces euteiches* from pea in France. *Plant Pathol.* **2001**, *50*, 433–442. [CrossRef]
10. Malvick, D. *Aphanomyces euteiches* Race 2 in central Illinois alfalfa fields. *Plant Dis.* **2002**, *86*, 560. [CrossRef]
11. Chatterton, S.; Bowness, R.; Harding, H.W. First report of root rot of field pea caused by *Aphanomyces euteiches* in Alberta, Canada. *Plant Dis.* **2015**, *99*, 288. [CrossRef]
12. Lavaud, C.; Baviere, M.; Le Roy, G.; Hervé, M.R.; Moussart, A.; Delourme, R.; Pilet-Nayel, M.-L. Single and multiple resistance QTL delay symptom appearance and slow down root colonization by *Aphanomyces euteiches* in pea near isogenic lines. *BMC Plant Biol.* **2016**, *16*, 166. [CrossRef]
13. Bonhomme, M.; Fariello, M.I.; Navier, H.; Hajri, A.; Badis, Y.; Miteul, H.; Samac, D.A.; Dumas, B.; Baranger, A.; Jacquet, C.; et al. A local score approach improves GWAS resolution and detects minor QTL: Application to *Medicago truncatula* quantitative disease resistance to multiple *Aphanomyces euteiches* isolates. *Heredity* **2019**, *123*, 517–531. [CrossRef]
14. Khan, M.; Seto, D.; Subramaniam, R.; Desveaux, D. Oh, the places they'll go! A survey of phytopathogen effectors and their host targets. *Plant J.* **2018**, *93*, 651–663. [CrossRef]
15. Rocafort, M.; Fudal, I.; Mesarich, C.H. Apoplastic effector proteins of plant-associated fungi and oomycetes. *Curr. Opin. Plant Biol.* **2020**, *56*, 9–19. [CrossRef]
16. Kanja, C.; Hammond-Kosack, K.E. Proteinaceous effector discovery and characterization in filamentous plant pathogens. *Mol. Plant Pathol.* **2020**, *21*, 1353–1376. [CrossRef]
17. Camborde, L.; Raynaud, C.; Dumas, B.; Gaulin, E. DNA-damaging effectors: New Players in the effector arena. *Trends Plant Sci.* **2019**, *24*, 1094–1101. [CrossRef]
18. Chepsergon, J.; Motaung, T.E.; Bellieny-Rabelo, D.; Moleleki, L.N. Organize, don't agonize: Strategic success of *Phytophthora* species. *Microorganisms* **2020**, *8*, 917. [CrossRef]
19. McGowan, J.; Fitzpatrick, D.A. Recent advances in oomycete genomics. *Adv. Genet.* **2020**, *105*, 175–228.
20. Vincent, D.; Rafiqi, M.; Job, D. The Multiple Facets of Plant–fungal interactions revealed through plant and fungal secretomics. *Front. Plant Sci.* **2020**, *10*, 1626. [CrossRef]
21. Haas, B.; Kamoun, S.; Zody, M.C.; Jiang, R.H.; Handsaker, R.E.; Cano, L.M.; Grabherr, M.; Kodira, C.D.; Raffaele, S.; Torto-Alalibo, T.; et al. Genome sequence and analysis of the Irish potato famine pathogen *Phytophthora infestans*. *Nature* **2009**, *461*, 393–398. [CrossRef]
22. Torto, T.A.; Li, S.; Styer, A.; Huitema, E.; Testa, A.; Gow, N.A.; van West, P.; Kamoun, S. EST mining and functional expression assays identify extracellular effector proteins from the plant pathogen Phytophthora. *Genome Res.* **2003**, *13*, 1675–1685. [CrossRef] [PubMed]
23. Rehmany, A.P.; Gordon, A.; Rose, L.E.; Allen, R.L.; Armstrong, M.R.; Whisson, S.C.; Kamoun, S.; Tyler, B.M.; Birch, P.R.J.; Beynon, J.L. Differential recognition of highly divergent downy mildew avirulence gene alleles by RPP1 resistance genes from two *Arabidopsis* lines. *Plant Cell* **2005**, *17*, 1839. [CrossRef] [PubMed]

24. Schornack, S.; van Damme, M.; Bozkurt, T.O.; Cano, L.M.; Smoker, M.; Thines, M.; Gaulin, E.; Kamoun, S.; Huitema, E. Ancient class of translocated oomycete effectors targets the host nucleus. *Proc. Natl. Acad. Sci. USA* **2010**, *107*, 17421–17426. [CrossRef] [PubMed]
25. Tyler, B.M.; Tripathy, S.; Zhang, X.; Dehal, P.; Jiang, R.H.Y.; Aerts, A.; Arredondo, F.D.; Baxter, L.; Bensasson, D.; Beynon, J.L.; et al. *Phytophthora* genome sequences uncover evolutionary origins and mechanisms of pathogenesis. *Science* **2006**, *313*, 1261–1266. [CrossRef]
26. Ramirez-Garces, D.; Camborde, L.; Pel, M.J.; Jauneau, A.; Martinez, Y.; Neant, I.; Leclerc, C.; Moreau, M.; Dumas, B.; Gaulin, E. CRN13 candidate effectors from plant and animal eukaryotic pathogens are DNA-binding proteins which trigger host DNA damage response. *New Phytol.* **2016**, *210*, 602–617. [CrossRef]
27. Liang, X.; Bao, Y.; Zhang, M.; Du, D.; Rao, S.; Li, Y.; Wang, X.; Xu, G.; Zhou, Z.; Shen, D.; et al. A *Phytophthora capsici* RXLR effector targets and inhibits the central immune kinases to suppress plant immunity. *New Phytol.* **2021**, *232*, 264–278. [CrossRef]
28. Stam, R.; Motion, G.B.; Martinez-Heredia, V.; Boevink, P.C.; Huitema, E. A conserved Oomycete CRN effector targets tomato TCP14-2 to enhance virulence. *Mol. Plant Microbe Interact.* **2021**, *34*, 309–318. [CrossRef]
29. Qiao, Y.; Shi, J.; Zhai, Y.; Hou, Y.; Ma, W. *Phytophthora* effector targets a novel component of small RNA pathway in plants to promote infection. *Proc. Natl. Acad. Sci. USA* **2015**, *112*, 5850–5855. [CrossRef]
30. Gaulin, E.; Drame, N.; Lafitte, C.; Torto-Alalibo, T.; Martinez, Y.; Ameline-Torregrosa, C.; Khatib, M.; Mazarguil, H.; Villalba-Mateos, F.; Kamoun, S.; et al. Cellulose binding domains of a *Phytophthora* cell wall protein are novel pathogen-associated molecular patterns. *Plant Cell* **2006**, *18*, 1766–1777. [CrossRef]
31. Du, Y.; Chen, X.; Guo, Y.; Zhang, X.; Zhang, H.; Li, F.; Huang, G.; Meng, Y.; Shan, W. *Phytophthora* infestans RXLR effector PITG20303 targets a potato MKK1 protein to suppress plant immunity. *New Phytol.* **2021**, *229*, 501–515. [CrossRef]
32. Lin, K.; Limpens, E.; Zhang, Z.; Ivanov, S.; Saunders, D.G.; Mu, D.; Pang, E.; Cao, H.; Cha, H.; Lin, T.; et al. Single nucleus genome sequencing reveals high similarity among nuclei of an endomycorrhizal fungus. *PLoS Genet.* **2014**, *10*, e1004078. [CrossRef]
33. Huang, J.; Lu, X.; Wu, H.; Xie, Y.; Peng, Q.; Gu, L.; Wu, J.; Wang, Y.; Reddy, A.S.N.; Dong, S. *Phytophthora* effectors modulate genome-wide alternative splicing of host mRNAs to reprogram plant immunity. *Mol. Plant* **2020**, *13*, 1470–1484. [CrossRef]
34. Turnbull, D.; Yang, L.; Naqvi, S.; Breen, S.; Welsh, L.; Stephens, J.; Morris, J.; Boevink, P.C.; Hedley, P.E.; Zhan, J.; et al. RXLR effector AVR2 up-regulates a brassinosteroid-responsive bHLH transcription factor to suppress immunity. *Plant Physiol.* **2017**, *174*, 356–369. [CrossRef]
35. Rhoads, A.; Au, K.F. PacBio sequencing and its applications. *Genom. Proteom. Bioinform.* **2015**, *13*, 278–289. [CrossRef]
36. Fouché, S.; Oggenfuss, U.; Chanclud, E.; Croll, D. A devil's bargain with transposable elements in plant pathogens. *Trends Genet.* 2021, *in press*. [CrossRef]
37. Panabières, F.; Rancurel, C.; da Rocha, M.; Kuhn, M.-L. Characterization of two satellite DNA families in the genome of the Oomycete plant pathogen *Phytophthora parasitica*. *Front. Genet.* **2020**, *11*, 557. [CrossRef]
38. Moolhuijzen, P.; See, P.T.; Moffat, C.S. PacBio genome sequencing reveals new insights into the genomic organisation of the multi-copy ToxB gene of the wheat fungal pathogen *Pyrenophora tritici-repentis*. *BMC Genom.* **2020**, *21*, 645. [CrossRef]
39. Dallery, J.-F.; Lapalu, N.; Zampounis, A.; Pigné, S.; Luyten, I.; Amselem, J.; Wittenberg, A.H.J.; Zhou, S.; de Queiroz, M.V.; Robin, G.P.; et al. Gapless genome assembly of *Colletotrichum higginsianum* reveals chromosome structure and association of transposable elements with secondary metabolite gene clusters. *BMC Genom.* **2017**, *18*, 667. [CrossRef]
40. Wu, J.Q.; Dong, C.; Song, L.; Park, R.F. Long-Read–Based de novo Genome Assembly and Comparative genomics of the wheat leaf rust pathogen *Puccinia triticina* identifies candidates for three avirulence genes. *Front. Genet.* **2020**, *11*, 521. [CrossRef]
41. Gaulin, E.; Pel, M.J.C.; Camborde, L.; San-Clemente, H.; Courbier, S.; Dupouy, M.A.; Lengellé, J.; Veyssiere, M.; Le Ru, A.; Grandjean, F.; et al. Genomics analysis of *Aphanomyces spp.* identifies a new class of oomycete effector associated with host adaptation. *BMC Biol.* **2018**, *16*, 43. [CrossRef]
42. Mariette, J.; Escudié, F.; Allias, N.; Salin, G.; Noirot, C.; Thomas, S.; Klopp, C. NG6: Integrated next generation sequencing storage and processing environment. *BMC Genom.* **2012**, *13*, 462. [CrossRef] [PubMed]
43. Zimin, A.V.; Marçais, G.; Puiu, D.; Roberts, M.; Salzberg, S.L.; Yorke, J.A. The MaSuRCA genome assembler. *Bioinformatics* **2013**, *29*, 2669–2677. [CrossRef] [PubMed]
44. Hoff, K.J.; Stanke, M. Predicting genes in single genomes with AUGUSTUS. *Curr. Protoc. Bioinform.* **2018**, *65*, e57. [CrossRef] [PubMed]
45. Manni, M.; Berkeley, M.R.; Seppey, M.; Simao, F.A.; Zdobnov, E.M. BUSCO update: Novel and streamlined workflows along with broader and deeper phylogenetic coverage for scoring of eukaryotic, prokaryotic, and viral genomes. *Mol. Biol. Evol.* **2021**, *38*, 4647–4654. [CrossRef]
46. Benson, G. Tandem repeats finder: A program to analyze DNA sequences. *Nucleic Acids Res.* **1999**, *27*, 573–580. [CrossRef]
47. Altschul, S.F.; Gish, W.; Miller, W.; Myers, E.W.; Lipman, D.J. Basic local alignment search tool. *J. Mol. Biol.* **1990**, *215*, 403–410. [CrossRef]
48. Madoui, M.A.; Gaulin, E.; Mathe, C.; Clemente, H.S.; Couloux, A.; Wincker, P.; Dumas, B. AphanoDB: A genomic resource for *Aphanomyces* pathogens. *BMC Genom.* **2007**, *8*, 471. [CrossRef]
49. Soorni, A.; Haak, D.; Zaitlin, D.; Bombarely, A. Organelle_PBA, a pipeline for assembling chloroplast and mitochondrial genomes from PacBio DNA sequencing data. *BMC Genom.* **2017**, *18*, 49. [CrossRef]

50. Makkonen, J.; Vesterbacka, A.; Martin, F.; Jussila, J.; Diéguez-Uribeondo, J.; Kortet, R.; Kokko, H. Mitochondrial genomes and comparative genomics of *Aphanomyces astaci* and *Aphanomyces invadans*. *Sci. Rep.* **2016**, *6*, 36089. [CrossRef]
51. Greiner, S.; Lehwark, P.; Bock, R. OrganellarGenomeDRAW (OGDRAW) version 1.3.1: Expanded toolkit for the graphical visualization of organellar genomes. *Nucleic Acids Res.* **2019**, *47*, W59–W64. [CrossRef]
52. Blum, M.; Chang, H.Y.; Chuguransky, S.; Grego, T.; Kandasaamy, S.; Mitchell, A.; Nuka, G.; Paysan-Lafosse, T.; Qureshi, M.; Raj, S.; et al. The InterPro protein families and domains database: 20 years on. *Nucleic Acids Res.* **2021**, *49*, D344–D354. [CrossRef]
53. Sperschneider, J.; Dodds, P.N.; Gardiner, D.M.; Manners, J.M.; Singh, K.B.; Taylor, J.M. Advances and challenges in computational prediction of effectors from plant pathogenic fungi. *PLoS Pathog.* **2015**, *11*, e100480. [CrossRef]
54. Almagro Armenteros, J.J.; Tsirigos, K.D.; Sønderby, C.K.; Petersen, T.N.; Winther, O.; Brunak, S.; von Heijne, G.; Nielsen, H. SignalP 5.0 improves signal peptide predictions using deep neural networks. *Nat. Biotechnol.* **2019**, *37*, 420–423. [CrossRef]
55. Krogh, A.; Larsson, B.; Von Heijne, G.; Sonnhammer, E.L.L. Predicting transmembrane protein topology with a hidden markov model: Application to complete genomes. *J. Mol. Biol.* **2001**, *305*, 567–580. [CrossRef]
56. Emms, D.M.; Kelly, S. OrthoFinder: Phylogenetic orthology inference for comparative genomics. *Genome Biol.* **2019**, *20*, 1–14. [CrossRef] [PubMed]
57. Basenko, E.Y.; Pulman, J.A.; Shanmugasundram, A.; Harb, O.S.; Crouch, K.; Starns, D.; Warrenfeltz, S.; Aurrecoechea, C.; Stoeckert, C.J.; Kissinger, J.C.; et al. FungiDB: An integrated bioinformatic resource for Fungi and Oomycetes. *J. Fungi* **2018**, *4*, 39. [CrossRef]
58. Fang, Y.; Coelho, M.A.; Shu, H.; Schotanus, K.; Thimmappa, B.C.; Yadav, V.; Chen, H.; Malc, E.P.; Wang, J.; Mieczkowski, P.A.; et al. Long transposon-rich centromeres in an oomycete reveal divergence of centromere features in Stramenopila-Alveolata-Rhizaria lineages. *PLoS Genet.* **2020**, *16*, e1008646. [CrossRef]
59. Fletcher, K.; Gil, J.; Bertier, L.D.; Kenefick, A.; Wood, K.J.; Zhang, L.; Reyes-Chin-Wo, S.; Cavanaugh, K.; Tsuchida, C.; Wong, J.; et al. Genomic signatures of heterokaryosis in the oomycete pathogen *Bremia lactucae*. *Nat. Commun.* **2019**, *10*, 2645. [CrossRef]
60. Dussert, Y.; Mazet, I.D.; Couture, C.; Gouzy, J.; Piron, M.-C.; Kuchly, C.; Bouchez, O.; Rispe, C.; Mestre, P.; Delmotte, F. A High-quality grapevine downy mildew genome assembly reveals rapidly evolving and lineage-specific putative host adaptation genes. *Genome Biol. Evol.* **2019**, *11*, 954–969. [CrossRef]
61. Zardoya, R. Recent advances in understanding mitochondrial genome diversity. *F1000Research* **2020**, *9*, F1000 Faculty Rev-270. [CrossRef]
62. Avila-Adame, C.; Gómez-Alpizar, L.; Zismann, V.; Jones, K.M.; Buell, C.B.; Ristaino, J.B. Mitochondrial genome sequences and molecular evolution of the Irish potato famine pathogen, *Phytophthora infestans*. *Current Genet.* **2006**, *49*, 39–46. [CrossRef] [PubMed]
63. Gaulin, E.; Jauneau, A.; Villalba, F.; Rickauer, M.; Esquerré-Tugayé, M.-T.; Bottin, A. The CBEL glycoprotein of *Phytophthora parasitica var-nicotianae* is involved in cell wall deposition and adhesion to cellulosic substrates. *J. Cell Sci.* **2002**, *115*, 4565–4575. [CrossRef] [PubMed]
64. Wicker, E.; Rouxel, F. Specific behaviour of french *Aphanomyces euteiches* Drechs. Populations virulence and aggressiveness on pea, related to isolates from Europe, America and New Zealand. *Eur. J. Plant Pathol.* **2001**, *107*, 919–929. [CrossRef]
65. Wicker, E.; Moussart, A.; Duparque, M.; Rouxel, F. Further contributions to the development of a differential set of pea cultivars (*Pisum sativum*) to investigate the virulence of isolates of *Aphanomyces euteiches*. *Eur. J. Plant Pathol.* **2003**, *109*, 47–60. [CrossRef]
66. Moussart, A.; Onfroy, C.; Lesne, A.; Esquibet, M.; Grenier, E.; Tivoli, B. Host status and reaction of *Medicago truncatula* accessions to infection by three major pathogens of pea (*Pisum sativum*) and alfalfa (*Medicago sativa*). *Eur. J. Plant Pathol.* **2006**, *117*, 57–69. [CrossRef]
67. Malvick, D.K.; Grau, C.R. Characteristics and frequency of *Aphanomyces euteiches* Races 1 and 2 associated with alfalfa in the Midwestern United States. *Plant Dis* **2001**, *85*, 740–744. [CrossRef]
68. Samac, D. The Ongoing Race to Find Aphanomyces euteiches Resistance. Available online: http://hayandforage.com/print-article-1002-permanent.html (accessed on 1 November 2021).
69. Desgroux, A.; L'Anthoëne, V.; Roux-Duparque, M.; Rivière, J.-P.; Aubert, G.; Tayeh, N.; Moussart, A.; Mangin, P.; Vetel, P.; Piriou, C.; et al. Genome-wide association mapping of partial resistance to *Aphanomyces euteiches* in pea. *BMC Genom.* **2016**, *17*, 124. [CrossRef]
70. Hamon, C.; Baranger, A.; Miteul, H.; Lecointe, R.; Le Goff, I.; Deniot, G.; Onfroy, C.; Moussart, A.; Prosperi, J.-M.; Tivoli, B.; et al. A complex genetic network involving a broad-spectrum locus and strain-specific loci controls resistance to different pathotypes of *Aphanomyces euteiches* in *Medicago truncatula*. *Theor. Appl. Genet.* **2009**, *120*, 955–970. [CrossRef]
71. Grau, C.R.; Muehlchen, A.M.; Tofte, J.E. Variability in virulence of *Aphanomyces euteiches*. *Plant Dis.* **1991**, *75*, 1153–1156. [CrossRef]
72. Malvick, D.K.; Grau, C.R.; Percich, J.A. Characterization of *Aphanomyces euteiches* strains based on pathogenicity tests and random amplified polymorphic DNA analyses. *Mycol. Res.* **1998**, *10*, 465–475. [CrossRef]
73. Malvick, D.K.; Grünwald, N.J.; Dyer, A.T. Population structure, races, and host range of *Aphanomyces euteiches* from alfalfa production fields in the central USA. *Eur. J. Plant Pathol.* **2009**, *123*, 171–182. [CrossRef]
74. Emms, D.M.; Kelly, S. STAG: Species tree inference from all Genes. *bioRxiv* **2018**, 267914. [CrossRef]
75. Tian, M.; Huitema, E.; da Cunha, L.; Torto-Alalibo, T.; Kamoun, S. A Kazal-like extracellular serine protease inhibitor from *Phytophthora infestans* targets the tomato pathogenesis-related protease P69B. *J. Biol. Chem.* **2004**, *279*, 26370–26377. [CrossRef]

76. Contesini, F.J.; Liberato, M.V.; Rubio, M.V.; Calzado, F.; Zubieta, M.P.; Riaño-Pachón, D.M.; Squina, F.M.; Bracht, F.; Skaf, M.S.; Damasio, A.R. Structural and functional characterization of a highly secreted α-l-arabinofuranosidase (GH62) from *Aspergillus nidulans* grown on sugarcane bagasse. *Biochim. Biophys. Acta-Proteins Proteom.* **2017**, *1865*, 1758–1769. [CrossRef]
77. Askani, L.; Schumacher, S.; Fuchs, R. Sequence and gene expression analysis of recently identified NLP from *Plasmopara viticola*. *Microorganisms* **2021**, *9*, 1453. [CrossRef]
78. Seidl, M.F.; Van Den Ackerveken, G. Activity and phylogenetics of the broadly occurring family of microbial Nep1-Like proteins. *Annu. Rev. Phytopathol.* **2019**, *57*, 367–386. [CrossRef]
79. Soliman, S.S.M.; Baldin, C.; Gu, Y.; Singh, S.; Gebremariam, T.; Swidergall, M.; Alqarihi, A.; Youssef, E.G.; Alkhazraji, S.; Pikoulas, A.; et al. Mucoricin is a ricin-like toxin that is critical for the pathogenesis of mucormycosis. *Nat. Microbiol.* **2021**, *6*, 313–326. [CrossRef]
80. Kharel, A.; Islam, M.T.; Rookes, J.; Cahill, D. How to unravel the key functions of cryptic Oomycete elicitin proteins and their role in plant disease. *Plants* **2021**, *10*, 1201. [CrossRef]
81. Larroque, M.; Barriot, R.; Bottin, A.; Barre, A.; Rouge, P.; Dumas, B.; Gaulin, E. The unique architecture and function of cellulose-interacting proteins in oomycetes revealed by genomic and structural analyses. *BMC Genom.* **2012**, *13*, 605. [CrossRef]
82. Schneiter, R.; Di Pietro, A. The CAP protein superfamily: Function in sterol export and fungal virulence. *Biomol. Concepts* **2013**, *4*, 519–525. [CrossRef] [PubMed]
83. Yuan, X.; Feng, C.; Zhang, Z.; Zhang, C. Complete mitochondrial genome of *Phytophthora nicotianae* and identification of molecular markers for the Oomycetes. *Front. Microbiol.* **2017**, *8*, 1484. [CrossRef]
84. Tangphatsornruang, S.; Ruang-areerate, P.; Sangsrakru, D.; Rujirawat, T.; Lohnoo, T.; Kittichotirat, W.; Patumcharoenpol, P.; Grenville-Briggs, L.J.; Krajaejun, T. Comparative mitochondrial genome analysis of *Pythium insidiosum* and related oomycete species provides new insights into genetic variation and phylogenetic relationships. *Gene* **2016**, *575*, 34–41. [CrossRef] [PubMed]
85. Kulik, T.; Bilska, K.; Żelechowski, M. Promising Perspectives for Detection, Identification, and Quantification of plant pathogenic Fungi and Oomycetes through targeting mitochondrial DNA. *Int. J. Mol. Sci.* **2020**, *21*, 2645. [CrossRef] [PubMed]
86. Mosavi, L.K.; Cammett, T.J.; Desrosiers, D.C.; Peng, Z. The ankyrin repeat as molecular architecture for protein recognition. *Protein Sci.* **2004**, *13*, 1435–1448. [CrossRef] [PubMed]
87. Jain, B.; Pandey, S. WD40 Repeat Proteins: Signalling scaffold with diverse functions. *Protein J.* **2018**, *37*, 391–406. [CrossRef]
88. Jiang, R.H.; de Bruijn, I.; Haas, B.J.; Belmonte, R.; Lobach, L.; Christie, J.; van den Ackerveken, G.; Bottin, A.; Bulone, V.; Diaz-Moreno, S.M.; et al. Distinctive expansion of potential virulence genes in the genome of the oomycete fish pathogen *Saprolegnia parasitica*. *PLoS Genet.* **2013**, *9*, e1003272. [CrossRef]
89. Levesque, C.A.; Brouwer, H.; Cano, L.; Hamilton, J.P.; Holt, C.; Huitema, E.; Raffaele, S.; Robideau, G.P.; Thines, M.; Win, J.; et al. Genome sequence of the necrotrophic plant pathogen *Pythium ultimum* reveals original pathogenicity mechanisms and effector repertoire. *Genome Biol.* **2010**, *11*, R73. [CrossRef]
90. Ah-Fong, A.M.V.; Shrivastava, J.; Judelson, H.S. Lifestyle, gene gains and loss, and transcriptional remodeling cause divergence in the transcriptomes of *Phytophthora infestans* and *Pythium ultimum* during potato tuber colonization. *BMC Genom.* **2017**, *18*, 764. [CrossRef]
91. Judelson, H.; Senthil, G. Investigating the role of ABC transporters in multifungicide insensitivity in *Phytophthora infestans*. *Mol. Plant Pathol.* **2006**, *7*, 17–29. [CrossRef]
92. Boevink, P.C.; Birch, P.R.J.; Turnbull, D.; Whisson, S.C. Devastating intimacy: The cell biology of plant–*Phytophthora* interactions. *New Phytol.* **2020**, *228*, 445–458. [CrossRef]
93. Gaulin, E.; Madoui, M.A.; Bottin, A.; Jacquet, C.; Mathé, C.; Couloux, A.; Wincker, P.; Dumas, B. Transcriptome of *Aphanomyces euteiches*: New oomycete putative pathogenicity factors and metabolic pathways. *PLoS ONE* **2008**, *3*, e1723. [CrossRef]
94. Ospina-Giraldo, M.; Griffith, J.; Laird, E.; Mingora, C. The CAZyome of *Phytophthora* spp.: A comprehensive analysis of the gene complement coding for carbohydrate-active enzymes in species of the genus *Phytophthora*. *BMC Genom.* **2010**, *11*, 525. [CrossRef]
95. Faure, C.; Veyssière, M.; Boëlle, B.; Clemente, H.S.; Bouchez, O.; Lopez-Roques, C.; Chaubet, A.; Martinez, Y.; Bezouška, K.; Suchánek, M.; et al. Long-Read Genome Sequence of the sugar beet rhizosphere mycoparasite *Pythium oligandrum*. *G3 Genes | Genomes | Genetics* **2020**, *10*, 431. [CrossRef]
96. Blackman, L.M.; Cullerne, D.P.; Hardham, A.R. Bioinformatic characterisation of genes encoding cell wall degrading enzymes in the *Phytophthora parasitica* genome. *BMC Genom.* **2014**, *15*, 785. [CrossRef] [PubMed]
97. Klein, J.L.; Neilen, M.; Van Verk, M.; Dutilh, B.E.; Van Den Ackervekenid, G. Genome reconstruction of the non-culturable spinach downy mildew *Peronospora effusa* by metagenome filtering. *PLoS ONE* **2020**, *15*, e0225808. [CrossRef] [PubMed]
98. Bangyeekhun, E.; Cerenius, L.; Söderhäll, K. Molecular cloning and characterization of two serine proteinase genes from the crayfish plague fungus, *Aphanomyces astaci*. *J. Invertebr. Pathol.* **2001**, *77*, 206–216. [CrossRef]
99. Ravishankar, J.P.; Davis, C.M.; Davis, D.J.; MacDonald, E.; Makselan, S.D.; Millward, L.; Money, N.P. Mechanics of solid tissue invasion by the mammalian pathogen *Pythium insidiosum*. *Fungal Genet. Biol.* **2001**, *34*, 167–175. [CrossRef]
100. Godson, A.; Hoorn, R.A.L.; van der Hoorn, R.A. The front line of defence: A meta-analysis of apoplastic proteases in plant immunity. *J. Exp. Bot.* **2021**, *72*, 3381. [CrossRef]
101. Jashni, M.K.; Mehrabi, R.; Collemare, J.; Mesarich, C.H.; de Wit, P.J.G.M. The battle in the apoplast: Further insights into the roles of proteases and their inhibitors in plant–pathogen interactions. *Front. Plant Sci.* **2015**, *6*, 584. [CrossRef]

102. Zhang, Q.; Li, W.; Yang, J.; Xu, J.; Meng, Y.; Shan, W. Two *Phytophthora* parasitica cysteine protease genes, PpCys44 and PpCys45, trigger cell death in various *Nicotiana spp.* and act as virulence factors. *Mol. Plant Pathol.* **2020**, *21*, 541. [CrossRef]
103. Jashni, M.; Dols, I.; Iida, Y.; Boeren, S.; Beenen, H.; Mehrabi, R.; Collemare, J.; de Wit, P. Synergistic action of a metalloprotease and a serine protease from *Fusarium oxysporum* f. sp. lycopersici cleaves chitin-binding tomato chitinases, reduces their antifungal activity, and enhances fungal virulence. *Mol. Plant Microbe Interact.* **2015**, *28*, 996–1008. [CrossRef] [PubMed]
104. Weiland, J.J. Production of protease isozymes by *Aphanomyces cochlioides* and *Aphanomyces euteiches*. *Physiol. Mol. Plant Pathol.* **2004**, *65*, 225–233. [CrossRef]
105. Brito, N.; Espino, J.J.; González, C. The endo-beta-1,4-xylanase xyn11A is required for virulence in *Botrytis cinerea*. *Mol. Plant. Microbe. Interact.* **2006**, *19*, 25–32. [CrossRef] [PubMed]
106. Nguyen, Q.B.; Itoh, K.; Van Vu, B.; Tosa, Y.; Nakayashiki, H. Simultaneous silencing of endo-β-1,4 xylanase genes reveals their roles in the virulence of *Magnaporthe oryzae*. *Mol. Microbiol.* **2011**, *81*, 1008–1019. [CrossRef]
107. Liu, L.; Wang, Z.; Li, J.; Wang, Y.; Yuan, J.; Zhan, J.; Wang, P.; Lin, Y.; Li, F.; Ge, X. *Verticillium dahliae* secreted protein Vd424Y is required for full virulence, targets the nucleus of plant cells, and induces cell death. *Mol. Plant Pathol.* **2021**, *22*, 1109–1120. [CrossRef]
108. De Vries, R.P.; Kester, H.C.M.; Poulsen, C.H.; Benen, J.A.E.; Visser, J. Synergy between enzymes from *Aspergillus* involved in the degradation of plant cell wall polysaccharides. *Carbohydr. Res.* **2000**, *327*, 401–410. [CrossRef]
109. Olivera, I.E.; Fins, K.C.; Rodriguez, S.A.; Abiff, S.K.; Tartar, J.L.; Tartar, A. Glycoside hydrolases family 20 (GH20) represent putative virulence factors that are shared by animal pathogenic oomycetes, but are absent in phytopathogens. *BMC Microbiol.* **2016**, *16*, 1–11. [CrossRef]
110. Seidl, V. Chitinases of filamentous fungi: A large group of diverse proteins with multiple physiological functions. *Fungal Biol. Rev.* **2008**, *22*, 36–42. [CrossRef]
111. Nars, A.; Lafitte, C.; Chabaud, M.; Drouillard, S.; Mélida, H.; Danoun, S.; Le Costaouëc, T.; Rey, T.; Benedetti, J.; Bulone, V.; et al. *Aphanomyces euteiches* cell wall fractions containing novel glucan-chitosaccharides induce defense genes and nuclear calcium oscillations in the plant host *Medicago truncatula*. *PLoS ONE* **2013**, *8*, e75039. [CrossRef]
112. Badreddine, I.; Lafitte, C.; Heux, L.; Skandalis, N.; Spanou, Z.; Martinez, Y.; Esquerré-Tugayé, M.T.; Bulone, V.; Dumas, B.; Bottin, A. Cell wall chitosaccharides are essential components and exposed patterns of the phytopathogenic oomycete *Aphanomyces euteiches*. *Eukaryot. Cell* **2008**, *7*, 1980–1993. [CrossRef]
113. Hosseini, S.; Heyman, F.; Olsson, U.; Broberg, A.; Funck Jensen, D.; Karlsson, M. Zoospore chemotaxis of closely related legume-root infecting *Phytophthora* species towards host isoflavones. *Plant Pathol.* **2014**, *63*, 708–714. [CrossRef]
114. Kim, K.-T.; Jeon, J.; Choi, J.; Cheong, K.; Song, H.; Choi, G.; Kang, S.; Lee, Y.-H. Kingdom-wide analysis of fungal small secreted proteins (SSPs) reveals their potential role in host association. *Front. Plant Sci.* **2016**, *7*, 186. [CrossRef]
115. Daguerre, Y.; Basso, V.; Hartmann-Wittulski, S.; Schellenberger, R.; Meyer, L.; Bailly, J.; Kohler, A.; Plett, J.M.; Martin, F.; Veneault-Fourrey, C. The mutualism effector MiSSP7 of *Laccaria bicolor* alters the interactions between the poplar JAZ6 protein and its associated proteins. *Sci. Rep.* **2020**, *10*, 20362. [CrossRef]
116. Germain, H.; Joly, D.L.; Mireault, C.; Plourde, M.B.; Letanneur, C.; Stewart, D.; Morency, M.J.; Petre, B.; Duplessis, S.; Séguin, A. Infection assays in *Arabidopsis* reveal candidate effectors from the poplar rust fungus that promote susceptibility to bacteria and oomycete pathogens. *Mol. Plant Pathol.* **2018**, *19*, 191–200. [CrossRef]
117. Meyer, M.; Bourras, S.; Gervais, J.; Labadie, K.; Cruaud, C.; Balesdent, M.H.; Rouxel, T. Impact of biotic and abiotic factors on the expression of fungal effector-encoding genes in axenic growth conditions. *Fungal Genet. Biol.* **2017**, *99*, 1–12. [CrossRef] [PubMed]
118. Gaulin, E. Effector-mediated communication of filamentous plant pathogens with their hosts. *Adv. Bot. Res.* **2017**, *82*, 161–185.
119. Camborde, L.; Kiselev, A.; Pel, M.J.C.; Leru, A.; Jauneau, A.; Pouzet, C.; Dumas, B.; Gaulin, E. An oomycete effector targets a plant RNA helicase involved in root development and defense. *New Phytol.* 2022, *in press*. [CrossRef]

4. Chapter IV - Modular Extracellular Proteases Secreted by the Root Pathogen *Aphanomyces euteiches*

During the comparative genome analysis presented in chapter II, we notified that in the genome of *A. euteiches* there is a large repertoire of predicted secreted proteases. Previous studies highlighted the importance of plant apoplastic proteases in the immune responses and defence. However, very few studies focused on apoplastic proteases secreted by the pathogen. Here genome mining demonstrated that high proportion of the secreted proteases are tandemly repeated in the genome of *A. euteiches.* This supports the hypothesis of their involvement in the pathogenicity as previously the tandem repetition was shown for many effector proteins in oomycetes. Expression analysis of the *A. euteiches* genes showed the upregulation of trypsin, papain-like and zinc carboxypeptidases during the infection of model plant *M. truncatula.*

To validate the presence of *A. euteiches* secreted proteases in the apoplasm of infected roots we established a novel assay for identification of the active proteases. Activity Based Protein Profiling (ABPP) coupled with protein mass spectrometry. As Serine and Cysteine proteases were the most abundant in *A. euteiches* genome, for ABPP pull down experiments we have selected probes against serine and cysteine hydrolases. For the assay a natural host of *A. euteiches* ATCC201684 *Pisum sativum* was chosen.

The proteomics analysis revealed a dataset of 32 serine and cysteine proteases being active in infected pea roots. This set of proteases around 30% of proteases detected expressed in the RNASeq experiment. Among the identified proteins we found novel types of modular secreted proteases, which are composed of the proteolytic domain (PLCP or Subtillisin) and a 'binding' domain with affinity to either lipids (CAP, ML domains) or to carbohydrates (CBM1 domain). Whereas PLCP-ML proteins have homologs within all the Stramenopiles lineage, the other modular proteases were identified as unique to *Aphanomyces* genus.

The chapter is presented as a manuscript ready to be submitted to a Frontiers in Plant Science journal special research topic dedicated to root diseases of legume crops https://www.frontiersin.org/research-topics/35207/legume-root-diseases.

Modular extracellular proteases secreted by the root pathogen *Aphanomyces euteiches*

Andrei Kiselev[1], Laurent Camborde[1], Laura Ossorio Carballo[2], Farnusch Kaschani[3], Markus Kaiser[3], Renier van der Hoorn[2], Elodie Gaulin [1*]

[1] Laboratoire de Recherche en Sciences Végétales (LRSV), Université de Toulouse, CNRS, UPS, Toulouse INP, Auzeville-Tolosane, 31320 France

[2] The Plant Chemetics Laboratory, Department of Plant Sciences, University of Oxford, Oxford OX1 2JD, United Kingdom

[3] ZMB Chemical Biology, Faculty of Biology, University of Duisburg-Essen, Essen, Germany

*** Correspondence:**
Corresponding Author
elodie.gaulin@univ-tlse3.fr

Keywords: Aphanomyces, Root rot, plant pathogen, proteases, apoplasm, extracellular, Activity based protein profiling

Abstract

To successfully colonize the host, phytopathogens develop a large repertoire of components to combat host plant defense mechanisms and to be able to survive in adverse environmental conditions. Microbial proteases are predicted to be crucial components of these systems. In the present work we aimed to identify active secreted proteases from the oomycete *Aphanomyces euteiches*, causing root rot diseases on legumes. Genome mining and expression analysis highlighted the overrepresentation of microbial tandemly repeated proteases, which are upregulated during the host infection. Activity Based Protein Profiling (ABPP) on apoplastic fluids from pea roots infected by the pathogen, allows the mass spectrometry identification of 32 active extracellular microbial proteases. This dataset represents around 30% of the total serine and cysteine proteases genes expressed by *A. euteiches* during legume infection. In addition, ABPP points out 6 original modular secreted proteases form of a proteolytic domain (papain-like cysteine proteases PLCP or serine protease) associated to a non-catalytic domain that display 'binding' properties either for lipids (CAP, ML domains) or carbohydrates (CBM1 domain). Transient expression in *Nicotiana* leaves of selected modular extracellular proteases from *A. euteiches*, positively promote oomycete infection. This study is the first *in vivo* characterization of oomycete proteases present during host plant infection. It reveals original modular extracellular eukaryotic proteases as potential pathogenicity factors in *Aphanomyces* genus.

1. Introduction

Root rot diseases remain a major global threat to the productivity of agricultural crops. The term 'root rot' has been widely used to describe a group of diseases characterized by softening and necrosis of the roots, producing a broad spectrum of lesions with various color and size (Sharma et al., 2022). The widely spread Oomycetes and Fungi are the most prevalent soil-borne root rot pathogens (Gaulin et al., 2007; Dean et al., 2012). *Aphanomyces* root rot (ARR) disease is one of the major limitation factors in North American (Papavizas and Ayers, 1974; Wu et al., 2018) and European pea (Quillévéré-Hamard et al., 2018) cultivation areas, with some recent of disease in Australian faba bean cultures (Watson et al., 2013). Infected plants have brown water-soaked roots, which are impaired in the development, while the disease can cause from 26 to 86% of the yield loss in the infected field depending on cultivar (Conner et al., 2013). Resistance to ARR is known to be mediated by more than one gene and designed as quantitative resistance, providing only a partial resistance of pea against the invader (Quillévéré-Hamard et al., 2020). To limit outbreaks, cultural practices as crop rotations, due to the capacity of *A. euteiches* as numerous others root rot pathogen to survive on plant debris or form resting structures in the soil (Moussart et al., 2009), are recommended. While ARR can be caused by a single pathogen, there is evidence that different combinations of *A. euteiches* with others filamentous pathogens as *Fusarium* sp (fungi), *Rhizoctonia solani* (Fungi), *Pythium* spp (oomycete) or *Phytophthora* spp. (oomycete) may interact and infect the plant conjointly forming the pea root rot complex (PRRC) (Baćanović-Šišić et al., 2018; Chatterton et al., 2019)

Before entering the root cells, plant pathogens including *A. euteiches* may pass the apoplasm. Due to its extracellular nature, apoplasm is involved in the perception and transduction of environmental signals (for review see Farvardin et al., 2020). On plant microbe detection, plant cell wall is modified and the fluidic apoplasm become a harsh environment equipped by means of antimicrobial compounds and various type of enzymes to restrict pathogen infection (Jashni et al., 2015; Dora et al., 2022). Basically, to survive in plant apoplasm, phytopathogens depends on their ability to harvest nutriments, to hide from the host surveillance system and to attenuate host defense responses. Therefore, those pathogens produce (CWDE) and evolved molecular mechanisms to permit hiding, inhibition of defense-induced components, and detoxification/degradation of hosts components (Rocafort et al., 2020). Within the two-last category, secreted proteases are present in the extracellular space of infected plant tissues and originated from both the host and the pathogen (Jashni et al., 2015; Paulus et al., 2020).

Plant-secreted proteases are suspected to play major role during oomycete infection and numerous are highly upregulated during host colonization as exemplified with the aspartic protease StAsp from potato (Guevara et al., 2005) or the P69B serine protease from tomato (Tian et al., 2004). The P69B subtilase also catalytically activates the extracellular immune protease RcR3 in tomato against late blight disease (*Phytophthora infestans*) (Paulus et al., 2020), as others subtilases from different plant family. Silencing in *Nicotiana benthamiana* leaves of an extracellular C14 protease induced by *P. infestans*, enhances susceptibility against the pathogen (Kaschani et al., 2010). Thus, plant proteolytic activity may provide a robust apoplastic immunity, however, the defense function of most plant apoplastic proteases remain largely elusive.

Recent evidences showed that proteases from oomycetes might also play a role during plant invasion. Expression profile of *in-silico* identified metalloprotease from *P. infestans* pinpointed a dozen of enzymes that potentially affect virulence of the pathogen (Schoina et al., 2021). Knockout-mutants of two secreted cysteine proteases from *P. parasitica* (PpCys44, 45) present a reduced virulence during *N. benthamiana* infection, while overexpression of both proteases in the plant apoplasm triggers cell death (Zhang et al., 2020). In addition, a general counter-defense strategy used by invading oomycetes relies on the inhibition of host proteases. In *Phytophthora*, a large group of 'extracellular cystatin-like protease' (EPIC) are known to target RcR3 from tomato to inhibit its activity in apoplasm (Kaschani et al., 2010). Kazal serine protease inhibitors from *Phytophthora* also act as inhibitor of plant proteases as exemplified with EP1 and EPI10 that target tomato P69B subtilase (Tian et al., 2004, 2005). Genome mining of the fish pathogen *S. parasitica* linked the abundance of secreted proteases with an adaptation to animal hosts (Jiang et al., 2013). Gene editing of an extracellular serine subtilisine protease from *A. invadans* drastically reduced fish ulcerative symptoms (Majeed et al., 2018) and extracellular proteases from *S. parasitica* and *A. invadans* secreted in culture medium have been reported as active against fish immune IgM antigen, suggesting their contribution as virulence factors (Jiang et al., 2013; Majeed et al., 2017). In phytopathogenic *Phytophthora* species a critical role in pathogenicity for the serine, cysteine and metalloproteases is also predicted (Zhang et al., 2020; Schoina et al., 2021). Interestingly, the genome of A. *euteiches*, in addition to numerous CWDE, is characterized by a large representation of putative extracellular proteases as in the crayfish pathogen *Aphanomyces astaci* (Gaulin et al., 2018; Becking et al., 2021; Kiselev et al., 2022), suggesting a key role for infection.

To characterize oomycete enzymes contributing to virulence, Meijer et al., (2014) performed a proteome profiling of the secretome from *P. infestans* grown on plant-based media

and identified one aspartic protease, four cysteine proteases and two metalloproteases (Meijer et al., 2014). Similar studies of other *Phytophthora* species do not allow the identification of any proteases in the secretome (Severino et al., 2014; McGowan et al., 2020). This apparently contradicting results suggest that untargeted *in vitro* methods are may be not well adapted for protease identification. Activity-based protein profiling (ABPP) is a technique that uses highly selective active-site targeted chemical probes to label and characterize *in vivo*, active proteins including proteases (van der Hoorn et al., 2004; Kaschani et al., 2009). According to MEROPS database (Rawlings et al., 2018) proteases are classified according to their catalytic site and distributed into six major classes: cysteine proteases (C), serine proteases (S), aspartic proteases (A), metalloproteases (M), threonine peptidases (T), asparagine peptide lyases (N), mixed catalytic types (P) and unassigned families. For ABPP approach a set of various probes was developed to target different families of proteases including Papain-like cysteine proteases (PLCP), Serine hydrolases, proteasomes, matrix metalloproteases (van der Hoorn and Kaiser, 2012). In this context a proteolytic-based immune cascade involved in recognition of Avr2 of fungal pathogen *Cladosporium fulvum* (Paulus et al., 2020), or the role of secreted inhibitors from oomycete *P. infestans* (Kaschani et al., 2010) were characterized. This system was also successfully used to assign the functions of many plant secreted proteases (van der Hoorn, 2011).

Here we assessed whether the large repertoire of predicted *A. euteiches* proteases may play a role during host infection using an ABPP approach on infected-pea roots. We firstly precise the repertoire and genome organization of *A. euteiches* secreted proteases and evaluated their expression upon host infection. We set up an ABPP method on pea roots colonized by *A. euteiches*, to identify apoplastic active microbial proteases by LC-MS. We identified 32 microbial proteases; among them 7 papain-like cysteine proteases show original architecture due to the presence of ‘a binding domain’ in addition to the catalytic region. This work showed ABPP as an efficient *in vivo* tool to quickly support genomics prediction of microbial pathogenicity factors. It allows the identification of original oomycete modular cysteine 1A proteases, that *A. euteiches* secrete in the apoplastic host space to initiate disease process.

Results

A. euteiches encodes numerous secreted proteases, tandemly duplicated in the genome

We previously reported upon the genome annotation of the pea strain ATCC201684 from *Aphanomyces euteiches*, the large representation of secreted proteases as compared to the phytopathogen oomycete *Phytophthora infestans* (Gaulin et al., 2018; Kiselev et al., 2022)**.** Accordingly, the AphanoDB (https://www.polebio.lrsv.ups-tlse.fr/aphanoDB/), a database dedicated to the genus *Aphanomyces*, contains 518 proteins with a PFAM-based GO Peptidase activity (GO:0008233), with trypsin S1 as the largest family (74 genes) in *A. euteiches*. Among all the proteases, 151 proteins contain a predicted signal peptide (+SP) and no transmembrane domain (-TM) (**ST1**). Secreted proteases account for 28,5% of total set of proteases from *A. euteiches* indicating significant enrichment in the secretome (Fischer exact's test $p < 0,05$). As illustrated in **Figure 1A**, more than 80% of secreted proteases correspond to five families based on PFAM domains: serine proteases from S1, S8/S53, S28 (trypsin, subtilase and carboxypeptidase), papain-like cysteine proteases C1A (PLCPs) and metalloproteases M14. In all these five families the number of secreted proteases is greater than non-secreted, along with two families of metalloproteases M8 and M12A, consisting of 5 secreted and 1 non-secreted proteins each. The *A. euteiches* secretome has scarcely any carboxypeptidase (S10) X-Pro dipeptidyl-peptidase (S15), cysteine peptidases (C69 and C13) and aspartyl proteases (A1) and no M3 peptidases (**ST2**). Thus, the secretory repertoire of proteases in *A. euteiches* spans thirteen families among 281 described in MEROPS.

A

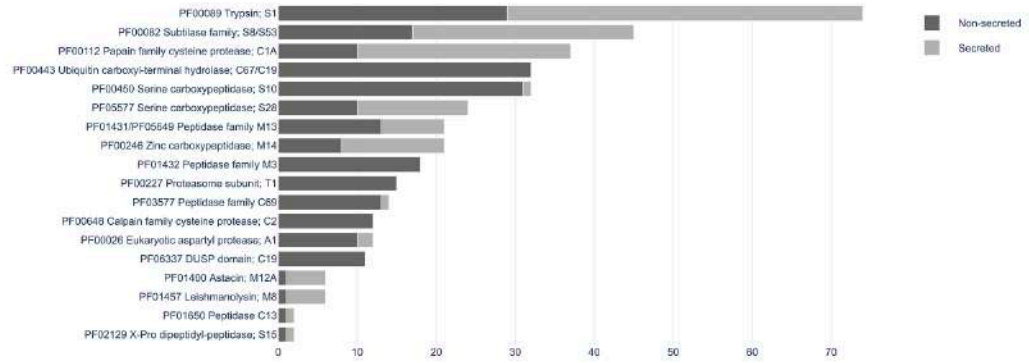

B

ID	Pfam-identified proteolytic domain	No of members per family	No of TR*/ No of genes/No of genes per repeat	% of TR genes
1	Trypsin; S1	37	8/19/2,4	50%
2	Papain; C1A	26	5/12/2,4	44%
3	Subtilase; S8/S53	24	6/14/2,3	50%
4	Serine carboxypeptidase; S28	14	2/5/2,5	35%
5	Zinc carboxypeptidase; M14	12	1/5/5	41%
6	Peptidase M13	8	0	0
7	Trypsin; S1	7	1/2/2	28%
8	Leishmanolysin; M8	5	1/4/4	66%
9	Astacin; M12	4	1/3/3	75%
10	Subtilase S8/S53 + pro-kumanolisin	2	0	0

*TR – tandem repeats

C

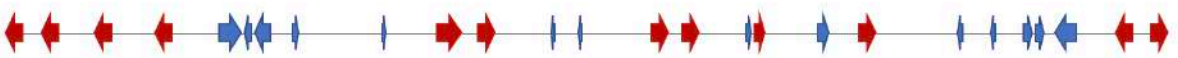

Ae201684P_13017 Ae201684P_13042

Figure 1. Mining of protease sequences from *A. euteiches* genome A). Repartition of proteolytic enzymes between secreted and non-secreted proteins in *A. euteiches* ATCC201684 genome. Proteolytic domains determined by InterProScan software against Pfam database. Secreted proteins (light-grey) correspond to proteins with a predicted signal peptide and without a predicted transmembrane domain. Data extraceted from AphanoDB (Madoui et al., 2007; Gaulin et al., 2018) database. **B).** Distribution of secreted proteolytic enzymes in multigene families and tandem repeats. Multigene families determined using Markov Cluster Algorithm (MCL) with a blast e-value < $1e^{-30}$, MCL inflation rate 1.5. Proteins considered in Tandem Repeats (TR), when having adjacent copy (blast e-value <$1e^{-80}$, coverage > 80%) **C).** A 97 kb genome region (between Ae201684P_13017 and Ae201684P_13042 genes) in 2,7 Mb contig of *A. euteiches* enriched in tandemly repeated secreted subtilases (multigene family 3). The cluster contains 25 genes, and red arrows indicate 12 secreted subtilases, while blue arrows correspond to various type of non-secreted proteins. See ST4 for the detailed description of proteins present in the cluster.

Since tandem duplication of genes is a driving force for the expansion of oomycete sequences related to pathogenicity (McGowan et al., 2019), we looked for genomic organisation of secreted proteases within *A. euteiches* genome. Markov cluster algorithm (MCL) grouped 138 secreted proteases (92%) from the genome sequence of *A. euteiches* into 10 multigene families (blast e-value < $1e^{-30}$, MCL inflation rate of 1,5), with size ranging from 2 members to 37 per family (average of 14) (**Figure 1B**). S1 trypsin proteases were grouped into two different subfamilies of 7 and 37 members, as well as subtilases formed two multigene families of 24 and 2 members while the other types of secreted proteases formed only a single multigene family per type. Only twelve secreted proteases do not present any paralog and considered as singletons (**ST3**). Tandemly repeated secreted proteases within each family we searched by looking for those having an adjacent copy (blast e-value <1e-80, coverage > 80%). For eight of ten families we found that a large proportion (over 28%) of the genes were tandemly replicated, while two small multigene families containing metallopeptidases M13 and Subtilases and pro-kumanolisin prodomain did not contain any tandem duplications. Tandem duplication rate of secreted proteases is between 33-60% in *A. euteiches*, while an average rate of 4-14% for whole genome in oomycetes is reported (McGowan et al., 2019).

The identification of multigene families with a high proportion of tandemly repeated genes prompted us to localize the family members in the genome of *A. euteiches.* We observed that for each multigene family there is a genome region consisting mainly of the family members. For the illustration we selected a 97 kb region in the contig 762, which encodes for 25 genes, among them 13 are secreted subtilases from the same multigene family (**Figure 1C**). Other genes from the cluster represent CYP450, endonuclease, Na/H exchanger, phosphatase, several Small Secreted Proteins (SSP) and proteins with unknown function (**ST4**). This genomic organisation of subtilases within *A. euteiches* was not detected in others oomycetes genomes using FungiDB or OGOB synteny searches (Basenko et al., 2018; McGowan et al., 2019), despite the presence of orthologous genes both in Saprolegniales and Peronosporales orders. The absence of the similar gene clusters in the animal pathogenic species from *Aphanomyces* genus support the hypothesis that duplications of secreted proteases happened during adaptation to the host plant. Altogether these data suggest that within *A. euteiches*, secreted proteases are pathogenicity factors that evolved through tandem duplication events which may offers the flexibility for a broad range pathogen as *A. euteiches.*

A. euteiches secreted proteases are induced during the infection

To identify whereas there is a transcriptional regulation of secreted proteases during infection of the host plant, we mined our previous dual RNAseq experiment consisting of three time points of infection (1, 3, 9 days post infection) of a susceptible *Medicago truncatula* F83005.5 line (Gaulin et al., 2018). 118 secreted proteases were expressed during among them 79 were differentially expressed (DE, adjusted p-value <0,05) in comparison to a mycelium grown on the synthetic media (**Figure 2, ST5**). The trypsin S1 and zinc carboxypeptidase M14 genes are highly express from 1 to 9 dpi post infection, as most of the papain C1A and carboxypeptidase M13 genes. Within the subtilases S8/S53 families, around 50% (17 genes) are differentially upregulated upon time, while five were downregulated. The proteases that are organized in tandemly repeated clusters (9 genes) do not present the same expression pattern, suggesting functional diversification of duplicated gene. The transcriptomics evidence of massively upregulated secreted proteases during infection of *M. truncataula* roots supports the role of these genes as pathogenicity factors of *A. euteiches.* In addition, various expression patterns observed within similar proteins of the same multigene family suggested an independent transcriptional regulation and function of tandemly repeated secreted proteases.

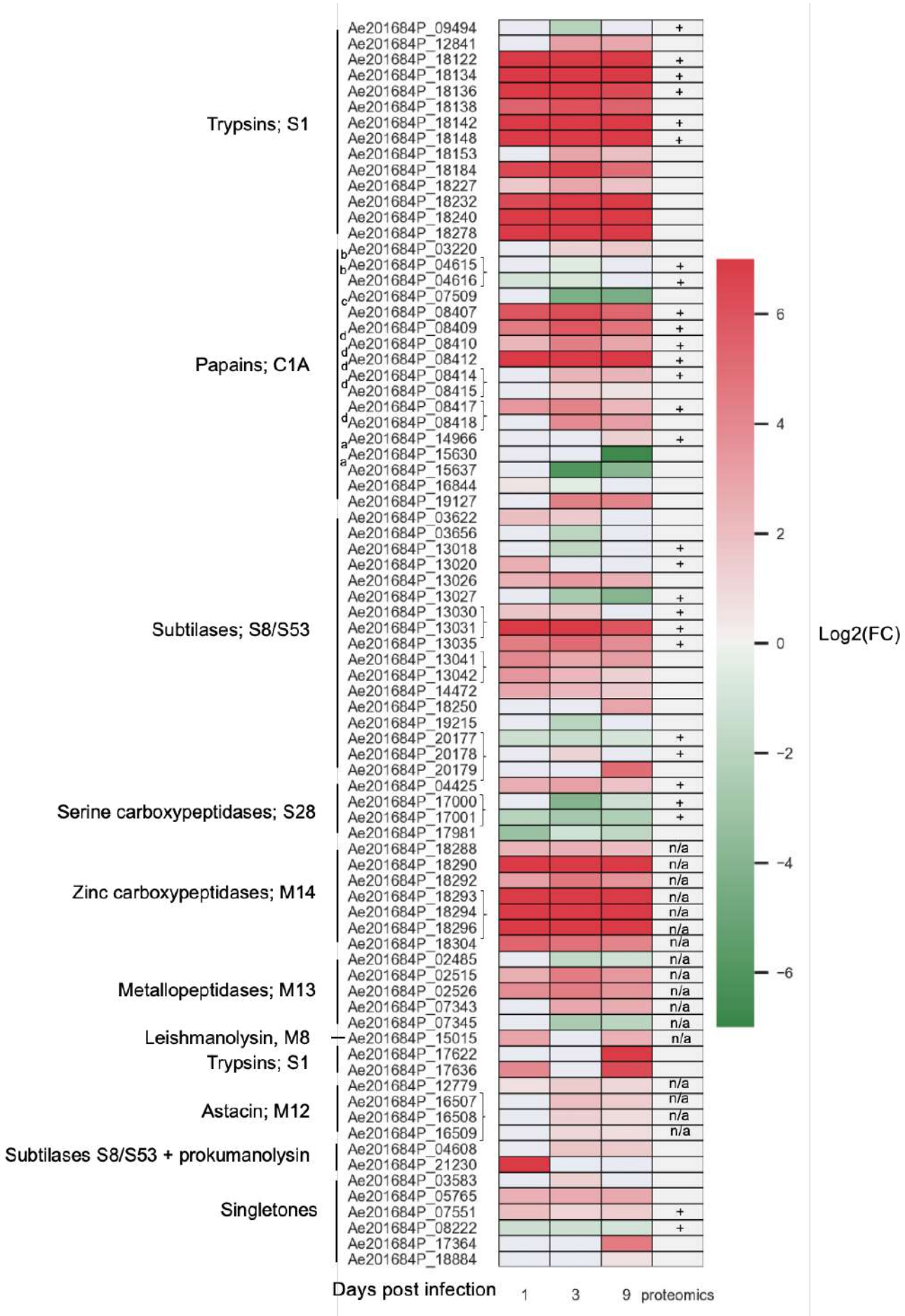
Trypsins; S1
Papains; C1A
Subtilases; S8/S53
Serine carboxypeptidases; S28
Zinc carboxypeptidases; M14
Metallopeptidases; M13
Leishmanolysin, M8
Trypsins; S1
Astacin; M12
Subtilases S8/S53 + prokumanolysin
Singletones
Ae201684P_09494
Ae201684P_12841
Ae201684P_18122
Ae201684P_18134
Ae201684P_18136
Ae201684P_18138
Ae201684P_18142
Ae201684P_18148
Ae201684P_18153
Ae201684P_18184
Ae201684P_18227
Ae201684P_18232
Ae201684P_18240
Ae201684P_18278
Ae201684P_03220
Ae201684P_04615
Ae201684P_04616
Ae201684P_07509
Ae201684P_08407
Ae201684P_08409
Ae201684P_08410
Ae201684P_08412
Ae201684P_08414
Ae201684P_08415
Ae201684P_08417
Ae201684P_08418
Ae201684P_14966
Ae201684P_15630
Ae201684P_15637
Ae201684P_16844
Ae201684P_19127
Ae201684P_03622
Ae201684P_03656
Ae201684P_13018
Ae201684P_13020
Ae201684P_13026
Ae201684P_13027
Ae201684P_13030
Ae201684P_13031
Ae201684P_13035
Ae201684P_13041
Ae201684P_13042
Ae201684P_14472
Ae201684P_18250
Ae201684P_19215
Ae201684P_20177
Ae201684P_20178
Ae201684P_20179
Ae201684P_04425
Ae201684P_17000
Ae201684P_17001
Ae201684P_17981
Ae201684P_18288
Ae201684P_18290
Ae201684P_18292
Ae201684P_18293
Ae201684P_18294
Ae201684P_18296
Ae201684P_18304
Ae201684P_02485
Ae201684P_02515
Ae201684P_02526
Ae201684P_07343
Ae201684P_07345
Ae201684P_15015
Ae201684P_17622
Ae201684P_17636
Ae201684P_12779
Ae201684P_16507
Ae201684P_16508
Ae201684P_16509
Ae201684P_04608
Ae201684P_21230
Ae201684P_03583
Ae201684P_05765
Ae201684P_07551
Ae201684P_08222
Ae201684P_17364
Ae201684P_18884
Days post infection
1
3
9
proteomics
n/a
Log2(FC)
6
4
2
0
−2
−4
−6

Figure 2. *Aphanomyces euteiches* differentially expressed genes coding for secreted proteases during *Medicago truncatula* infection. Three first columns of the heatmap represents log2(Fold Change) value of the significantly differentially expressed genes (DEG, p-value <0.05) during the time course of infection of *M. truncatula* roots (1, 3, 9 days pot infection) as compared to the free-living mycelium. The fourth column represents the identification of secreted proteases in activity-based proteome profiling proteomics (ABPP) experiment using probes against active serine and cysteine hydrolases (where '+' signifies that the protein was detected in proteomics experiment, blank cell signifies the protein was not detected in the proteomics experiment, 'n/a' signifies, that in proteomics experiment the probe used in the assay is not active against that catalytic core). Letter indexes next to a gene name represent the presence of an atypical binding domain within the secreted proteases: a) PAN domain (PF14295) b) ML domain (PF02221) c) Fungal cellulose binding domain (PF00734) d) cysteine rich secretory protein (PF00188). Braces on the right side of the gene name indicates adjacent tandemly repeated genes.

A. euteiches triggers root rot symptoms on pea in a semi-sterile infection system

To evaluate the contribution of secreted proteases during legume infection, we hypothesized the presence of *A. euteiches* extracellular proteases within the apoplasm of infected roots. We established a semi-sterile pathosystem using *Pisum sativum* to collect sufficient volume of apoplastic fluid (AF), after roots infection by *A. euteiches*. The growing system based on pots filled with zeolite as solid substrate and Fåhraeus media (Fåhraeus, 1957) as a nutritive solution is illustrated in **Figure 3A.** Root rot symptoms (root browning) were observed within 15 days after infection of the pea Precovil line by zoospores (**Figure 3B, C**). No death of emerged plantlets was recorded during the experiment. Cross sections of infected primary roots at 15 dpi in combination with specific staining of the pathogen using wheat-germ agglutin showed the intensive colonization of root tissues by the pathogen (**Figure 3D**). In addition, accumulation of phenolic compounds (visualized as blue fluorescence) within the root cortex induced by the presence of *A. euteiches* was recorded. This observation is reminiscent to the one detected upon infection of a tolerant line of the model legume *Medicago truncatula* (i.e. Jemalong A17) by the same strain of *A. euteiches* (Djébali et al., 2009). In *M. trunctaula* in addition, to the restriction of the pathogen into the root cortex, an additional layer of pericycle cells is detected at 15 dpi. Within *P. sativum*, at 15 dpi *A. euteiches* is also restricted to the root cortex and induced reinforcement of the pericycle cells (**Figure 3D**), suggesting a tolerant interaction with the Précovil line.

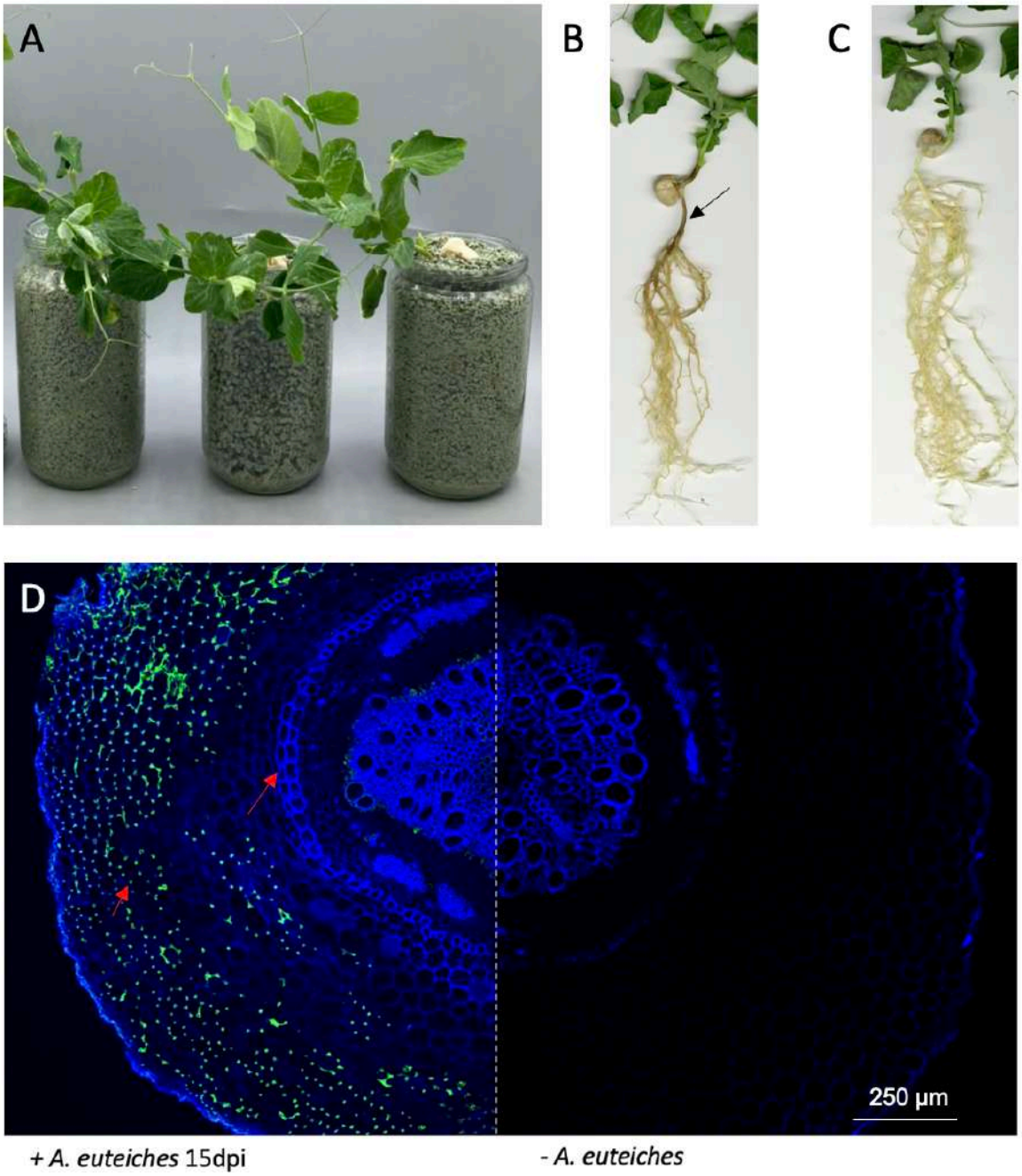

Figure 3. Interaction between *A. euteiches* and pea cv. *Précovil.* A). Photographs of culture pots filled with zeolite substrate and pea grown for 15 days (18h/6h day/night, 21^0C) Roots of infected and mock treated pea (**B, C** respectively) at 15 dpi with 10^5 zoospores. The black arrow points to root rot symptoms observed in infected roots. **D).** Cross sections of primary roots from infected (left) and mock treated (right) plants. The cross sections were stained with Wheat Germ Agglutinin-Alex Fluor 555 conjugate to stain *A. euteiches* hyphae (in green, lower arrow), and UV fluorescence of phenolic compounds (in blue) and pericycle cells reinforcement (upper arrow) in the infected root.

A. euteiches secretes active serine hydrolase and cysteine proteases into plant apoplasm during pea infection

To identify secreted proteases from *A. euteiches* present during *P. sativum* infection we used an Activity-Based Protein Purification (ABPP) assay and tandem mass spectrometry as outlined in **Figure 4**. Apoplastic fluid (AF) was isolated from infected and non-infected roots using vacuum infiltration with water followed by low-speed centrifugation. Two ml of the isolated AF was incubated with a cocktail of FP (labelling Serine proteases) and DCG-04 (labelling Cysteine proteases) probes fused to biotin tag. The similar volume was incubated without probes to further identify natively biotinylated proteins (NPC, No-Probe-Control). The FP-Biotin and DCG-04-Biotin probes are commercially available ABPP probes with a high affinity to the target proteins representing over 80% of the total arsenal of *A. euteiches* secreted proteases. Labelled and NPC samples were pulled down on streptavidin beads, digested with Trypsin and subjected for mass spectrometry protein identification.

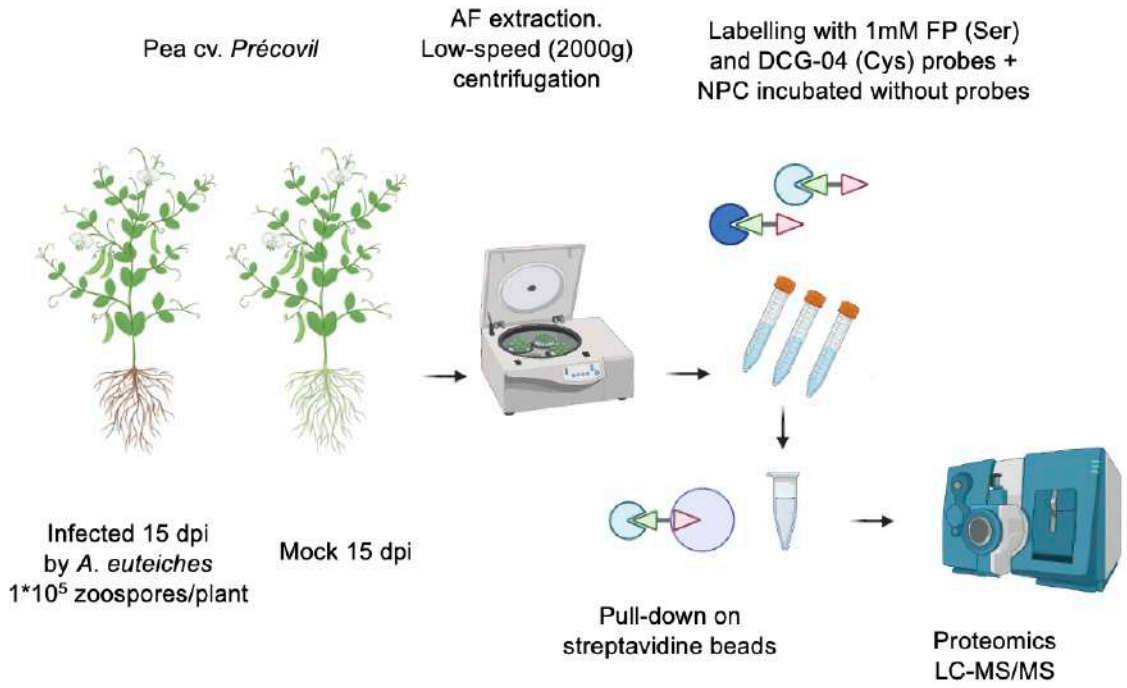

Figure 4. Schematic representation of the Activity-Based Protein Purification (ABPP) assay. Roots of *P. sativum* were inoculated with a zoospore suspension of *A. euteiches.* Apoplastic fluids (AF) were collected 15 days post infection (dpi) and labelled with a cocktail of FP-Biotin (serine proteases) and DCG04-Biotin (cysteine proteases) probes for a pull-down assay. Control samples (mock) correspond to non-inoculated roots. Apoplastic active serine and cysteine proteases were identified by LC-MS/MS analysis after pull down on streptavidin beads.

Protein identification by mass-spectrometry analysis was performed with MaxQuant software using the latest genome assembly of *A. euteiches* (Kiselev et al., 2022) and *P. sativum* (Kreplak et al., 2019). Protein identification revealed a total of 3 641 proteins groups (PG) (**Figure 5A**). PGs can represent several similar proteins, which are not distinguishable by detected peptides, and tandemly repeated *A. euteiches* proteins were often detected within one PG. The PGs containing *P. sativum* proteins were filtered out (525 PG), and 20 *A. euteiches* PGs identified in mock-treated samples were removed. For further analysis 274 PGs were kept, detected in at least three out of four replicates of the infected samples. From the resulted list **59** PGs were carrying the Serine or Cysteine hydrolase domain (**ST6**), while **52** of them were enriched in the 'probe' samples *vs* No-Probe-Control (p-value <0.05). Among the **52** PGs **26** were predicted as secreted and 3 proteins have no transcript within the RNAseq data, leading to a final set of **32** proteins. In addition, most of the corresponding genes are differentially expressed (28) at least at one time point during the infection of *M. truncatula.* (**Figure 2**). From the 115 annotated Cys and Ser hydrolases that could be labelled with the selected probes, 99 (~85%) have a transcript in at least one of the infection time point. Therefore, the ABPP-MS approach allows identification of 30% of the expressed sequence.

The set of the MS-identified secreted proteins consists of 4 PGs of subtilases that include 7 proteins, 4 PG of trypsines (6 proteins), 1 PG of Serine carboxypeptidase S10 (1 protein), 4 PG of Serine carboxypeptidase S28 (4 proteins), 5 PG of Papain-like cysteine proteases (PLCP) (5 proteins). Eight PG include 8 secreted modular proteins, in which an additional PFAM domain is associated to the proteolytic domain. Their correspond to: 1 PG of Subtilase + PAN domain (PF14295, 2 proteins), 2 PG of PLCP + Cysteine-rich secretory protein-CAP (PF00188, 2 proteins), 2 PG of PLCP + ML domain (PF02221) + Cathepsin (PF08246, 2 proteins) and 1 PG with PLCP + fungal cellulose binding domain (PF00734, 2 proteins).

All the MS-identified subtilases are present in the same gene cluster located in contig 762 presented in **Figure 1C**. For the trypsines, 7 out of 8 proteins are also originated from the same gene cluster in contig 60. A third cluster from contig 595 correspond to the PLCPs with or without additional PFAM domain. In addition to clustered proteases, two couples of tandemly repeated proteins were identified: carboxypeptidases (Ae201684P_17000 and _17001) and PLCPs-CAP proteins (Ae201684P_8414 and _8415). Both proteins of each repeats are identified as a separate PG indicating their presence in the sample. Altogether, this data supports the prediction of proteases gene clusters in *A. euteiches* genome and revealed the presence of active secreted proteases from the pathogen in the apoplasm during host infection.

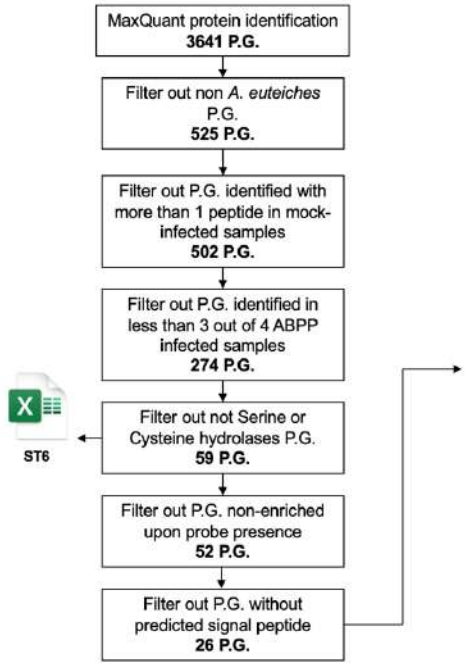

Pfam	No of Protein groups	Genes. *Genes listed in one line identified in same PG*	
PF00082 Subtilase family	4	Ae201684P_13042 Ae201684P_13035 Ae201684P_13031/18 Ae201684P_13030/27/20	Serine proteases
PF00089 Trypsin	4	Ae201684_18136 Ae201684_18122/42/48 Ae201684_18134 Ae201684_9494	Serine proteases
PF00450 Serine carboxypeptidase S10	1	Ae201684P_8222	Serine proteases
PF05577 Serine carboxypeptidase S28	4	Ae201684P_17000 Ae201684P_17001 Ae201684P_18544 Ae201684P_4425	Serine proteases
PF00082 Subtilase family/ PF14295 PAN domain	1	Ae201684P_20178/77	Serine proteases
PF00112 Papain family cysteine protease	5	Ae201684P_3220 Ae201684P_7551 Ae201684P_7509 Ae201684P_8409 Ae201684P_8417	Cysteine proteases
PF00112 Papain family cysteine protease/ PF08246 Cathepsin propeptide inhibitor domain	2	Ae201684P_16844 Ae201684P_14966	Cysteine proteases
PF00112 Papain family cysteine protease/ PF00188 Cysteine-rich secretory protein family	2	Ae201684P_8414 Ae201684P_8415	Cysteine proteases
PF00112 Papain family cysteine protease/ PF02221 ML domain / PF08246 Cathepsin propeptide inhibitor domain	2	Ae201684P_4616 Ae201684P_4615	Cysteine proteases
PF00112 Papain family cysteine protease/ PF00734 Fungal cellulose binding domain	1	Ae201684P_8407/12	Cysteine proteases

Figure 5. Data analysis workflow of secreted proteases from *A. euteiches* A). Downstream analysis of the MaxQuant assigned Protein Groups (PG). The number of PGs on each step is indicated in bold. **B).** List of the mass spectrometry identified extracellular serine and cysteine proteases from *A. euteiches* present in apoplastic fluid of pea, 15 days post infection. Gene IDs refer to AphanoDB nomenclature. Note that sequence present in one line of the table belong to the same PG.

A. euteiches produces modular extracellular serine and cysteine proteases during legume infection

Most families of fungal/oomycetes serine or cysteine proteases families correspond to single-domain protein (Muszewska et al., 2017). The identification by MS of modular extracellular proteases may suggest a specific function of these enzymes for *A. euteiches* invasion. Identified modular proteases harbour an additional binding domain consisting of a PAN Apple domain (PF14295) for subtilases and a ML lipid binding domain (PF02221), a CAP domain (PF00188) or a CBM1 cellulose binding domain (PF00734) for papain-like cysteine proteases (PCLP). PAN Apple and CBM1 has been suggested to mediate protein/carbohydrate or protein/protein interactions (Tordai et al., 1999), while CAP and ML domain are related to sterol and lipid binding capacities respectively (Inohara and Nuñez, 2002; Schneiter and Di Pietro, 2013). InterProScan domain architecture search revealed the large distribution within eukaryotes of modular PAN-trypsin proteases with an emphasis in animals, but the combination of PAN-domain with a subtilase (serine) domain is unique to *Aphanomyces* genus. While the extracellular modular cysteine protease C1A domain associated with a lipid-binding ML domain are present in several Stramenopila including oomycetes, yellow-green (Xanthophyceae, *Tribonema minus*) and brown algae (Phaeophyceae, *Ectocarpus siliculosus*), the other combinations are restricted to *Aphanomyces* genus for C1A:CBM1, and C1A:CAP, while secreted proteins with domains in reverse order, e.g CAP:C1A using IntrPro domain search were also detected in heterotrophic Amoebozoan slime moulds (*Planoprotselium fungivorum, Dictyostelium purpureum, Polysphondylium pallidum*). Subtilase:PAN/Apple domain architecture is abundant within *Aphanomyces* genus with variations from 1 to 4 PAN/Apple domains at C-term, also detected one example of the architecture in phytopathogenic oomycete *Pythium ultimum* and unicellular marine algae *Virtella brassicaformis*.

The gene cluster of PLCPs (contig 595) identified by MS displays the unique structure of modular cysteine proteases. Within a range of 50 kb it encodes 12 PLCPs genes, which have a conserved C1A (PLCP) domain at the Nterminal region associated with a variable Cterminal region consisting either CBM1, CAP or no domains (**Figure 6A**). The structural modelling and InterProScan analysis showed that the additional binding module is connected to the protease domain through a disordered linker, often represented as a PT-repeat. Multiple alignment of C1A domains (**Figure 6B**) of those proteins showed a very high similarity (~85%), suggesting a first duplication of the domain (gene) followed by the acquisition of the additional module

for modifying the initial function of the C1A domain. To predict whether the additional domain within modular PLCP may modulate the activity of the corresponding enzyme, we predict with AlphaFold-2 the structure of the catalytic and binding domains of each protease. The predicted 3D modelling was aligned with a reference structure of each domain. As depicted in **Figure 6C-E,** all the modular proteins keep a structural homology (RMSDE score <= 1) with the reference structure. Despite a slightly higher RMSDE score of ~4, the structural alignment of ML-domain revealed also a structural topology to the immunoglobulin (PDB 1AHM). According to the modelling results, the additional 'binding' domain detected in the extracellular PCLP of *A. euteiches* may serve for adhesion of a protease to a specific substrate to enhance its activity during infection.

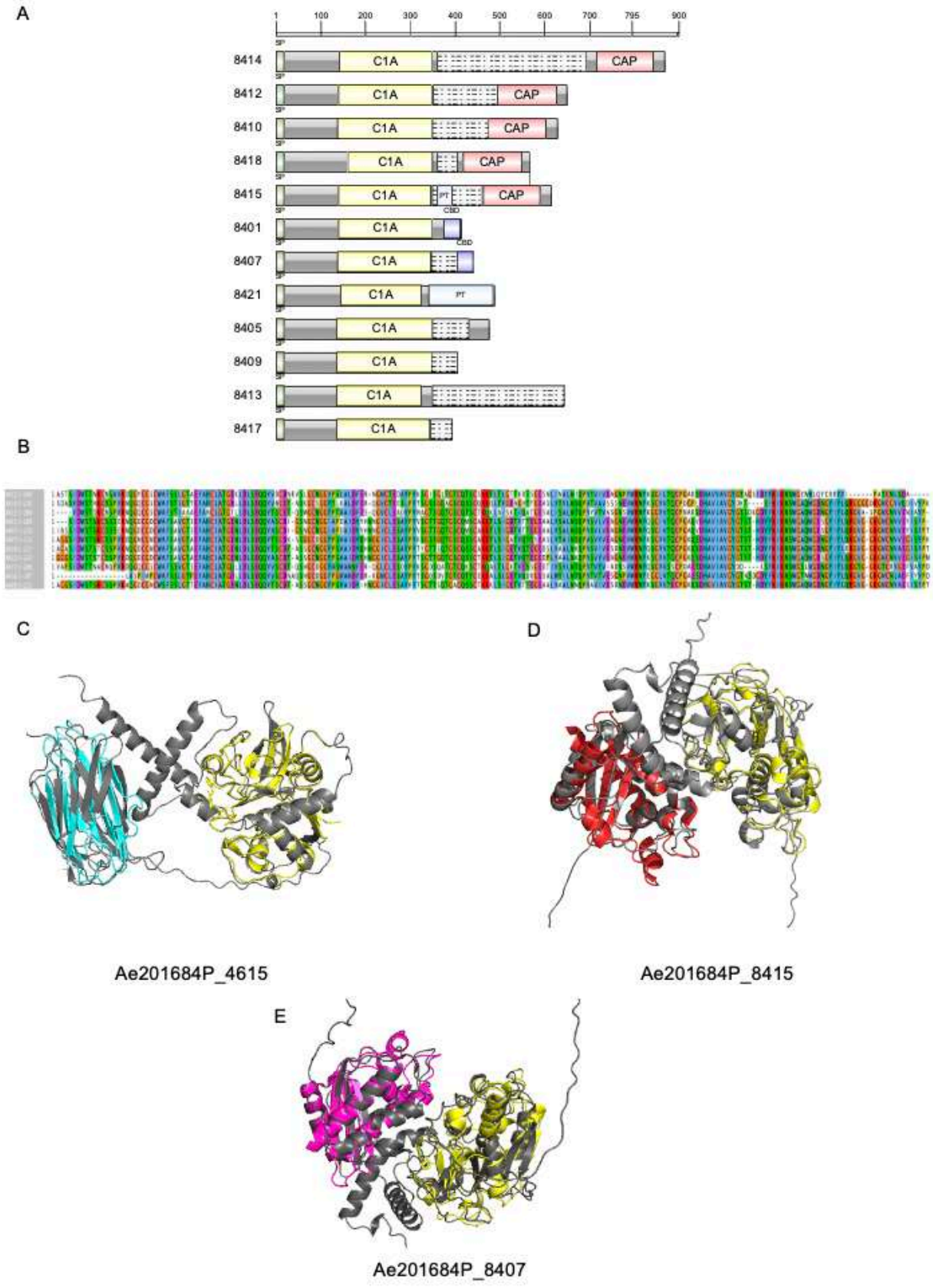

Figure 6. Domain architecture and 3D prediction of modular papain-like cysteine proteases (PLCP) from *A. euteiches* identified in pea apoplastic fluids A). Protein domain

architecture of the clustered PCLPs from *A. euteiches* on contig 595. C1A = cysteine protease domain type C1A (PF00112); CBM1 = carbohydrate-binding module (PF00734), CAP = Cysteine-rich secretory protein (PF00188), PT = PT-repeat (PF04886). Dashed-grey filled boxes – disorder prediction performed by InterProScan. **B)**. Multiple alignment of 12 proteins from clustered cysteine proteases encoded on contig 595 , performed with ClustalO algorithm and visualized with Jalview C-E PyMol generated representation of selected *A. euteiches* modular protein and a reference structure of a domain. Structures superposition 'align' Domain architecture of proteins from the cluster. **C).** Ae201684P_4615 (grey), Cysteine protease PDB 1BP4 (yellow), ML-domain PDB 1AHM (cyan). RMSD scores: C1A domains 0.674, ML-domains = 4.475. **D).** Ae201684P_8415 (grey), Cysteine protease PDB 1BP4 (yellow), CAP domain PDB 1SMB (red). RMSD scores: C1A domains 0.877, ML-domains = 1.077. E Ae201684P_8407 (grey), Cysteine protease PDB 1BP4 (yellow), CBM1 domain PDB 5X34 (magenta). RMSD scores: C1A domains 0.787, CBM1-domains = 0.937. Structural predictions were performed using AlphaFold2.

Discussion

The genome of *A. euteiches* is enriched in extracellular proteolytic enzymes consisting to trypsin (serine protease, S1 class) and papain proteases (cysteine protease, C1 class) (Kiselev et al., 2022). In this study, we precise the genomic organisation of these proteases sequences and characterize whether they are present and active during legume infection using an ABPP-MS approach. We have identified original modular PCLP and subtilisin extracellular proteases into the apoplasm of infected roots that may contribute to *A. euteiches* pathogenicity.

The curated annotation of the predicted proteases from the reference ATCC201684 long-read sequenced strain of *A. euteiches* ATCC201684 showed that up to 60% of secreted protease genes were found tandemly repeated and frequently organized in large clusters enriched in proteases (e.g. over 50% of genes within a cluster encode proteases). Of 20 oomycete species analysed, McGowan et al. identified that 40% of them display GO terms enrichment in terms linked to pathogenicity as 'catalytic activity, acting on protein' (GO:140096) and 'peptidase activity' (GO:0008233) (McGowan et al., 2019) in tandem duplicate genes. Tandem gene duplication in combination with homologous recombination are postulated to accelerate pathogenicity factors evolution within oomycete genomes (Haas et al., 2009; Fitzpatrick et al., 2010; Liang et al., 2020). In *A. euteiches,* we suspected neo-functionalization after tandemly duplication of the secreted cysteine protease family, due to the presence at the C-terminal part of the enzymes of various additional domain associated either to carbohydrate-binding capacity (CBM1, PAN-Apple) or sterol/lipid affinity (ML, CAP).

Whole expression analysis on *M. truncatula* roots infected by the pathogen, identified induction of Serine (trypsin, subtilisin), Papain-like Cysteine proteases (PLCP) and Zinc carboxypeptidases (M14) during the infection. Most of the secreted cysteine and serine proteases showed induced expression from the first day of infection, with increase in number of induced genes in 3 and 9 days after infection, suggesting a key role for plant invasion. The developed ABPP-MS assay on apoplastic fluid from pea roots infected by *A. euteiches* using probes that target serine (FP) and cysteine (DCG04) proteases, allows the identification of 32 *A. euteiches* extracellular active proteases. This set of active enzyme covers ~30% of total number of expressed genes during *M. truncatula* infection, showing the efficiency of ABBP assay to identify putative pathogenicity factors.

Several studies regarding plant-microbe interactions (van der Hoorn et al., 2004; Meijer et al., 2014) have reported the presence of plant proteases within infected tissues, and only few microbial proteases have been functionally characterized. Here we focused on a detection of

active serine and cysteine proteases, as the most abundant in *A. euteiches* genome, using well-characterized commercially available ABPP probes (FP for serine and DCG-04 for cysteine proteases). Thus, if oomycete identified cysteine/serine proteases take part to *A. euteiches* pathogenicity we can hypothesise their contribution in the degradation of host components like structural proteins from the plant cell wall. As example, the secreted SNP1 trypsin from *Parastagonospora (Stagnosphora) nodorum* is directly involved in the release of hydroxyproline from wheat cell wall (Carlile et al., 2000) probably from pathogenesis induced Hydrolyprolin-rich Glycoporteins (HRGPs) (Mazau and Esquerré-Tugayé, 1986). Alternatively, secreted cysteine/serine proteases from *A. euteiches* may counteract plant-defense proteins, be toxic for the root tissues or have a nutritional role for the pathogen. Although example is missing, the production of proteases and inhibitor of proteases by numerous plants during infection suggest that there is a need from the plant to limit such microbial activities. Accordingly, plant subtilase P69B cleaves cysteine-rich secreted protein PC2 from *P. infestans* to create immune peptides, while *P. infestans* secretes a Kazal-like inhibitor to prevent PC2 cleavage (Wang et al., 2021). Plant papain like cysteine proteases are also known to play an important role in the plant defence, and being targeted by proteins from pathogens (Paulus et al., 2020) as the tomato C14 PLCP is inhibited by cystatin-like EpiC1 and EpiC2B and Avrblb2 from *P. infestans* (Misas-Villamil et al., 2016).

The remarkable signature of the identified proteases in the apoplastic fluid of infected-pea roots, correspond to multidomain proteases with an additional 'binding domain' having affinity for carbohydrates or lipids/sterols. Eukaryotic proteases are rarely associated with a non-catalytic domain, but *A. euteiches* secreted several different combinations of modular proteases: cysteine proteases with CBM1, ML, CAP domains, serine proteases with PAN/Apple domain. All those proteases are expressed by the pathogen during roots infection of the model plant *M. truncatula* (Gaulin et al., 2018). While the extracellular modular cysteine protease C1A domain associated with a lipid-binding ML domain are present in several Stramenopila including oomycetes, yellow-green algae (Xanthophyceae, *Tribonema minus*) and brown algae (Phaeophyceae, *Ectocarpus siliculosus*), the other domain combinations (i,e C1A:CBM1 and C1A:CAP) are restricted to *Aphanomyces* genus.

Structural prediction of the modular C1A proteases of *A. euteiches* indicates that the additional domain does not form a lid structure or occluding loop that can cover the active site, suggesting the evolution of specialised functions for these cysteine proteases. Inappropriate activity of proteases can be deleterious to the cell or the organism that produce them, thus proteases activity is regulated to allow proteolysis event only in an adapted environment or

cellular compartment (For review see Kopitar-Jerala, 2012). Here we can suggest that the non-catalytic protease-associated domain found in *A. euteiches* correspond to regions responsible for regulation or targeting of the enzymes.

To conclude the ABPP approach allows the first characterization of microbial eukaryotic apoplastic proteases acting as pathogenicity factors during plant-pathogen interactions. This system can be easily translated into any other pathosystems and will facilitate the global challenge for the selection of microbial candidate genes for functional analysis. It highlighted the existence of original modular extracellular cysteine proteases produce by a root rot pathogen to enhance host infection.

Materials and methods

A. euteiches genome mining

Genome assembly (SRA accession SPR355760), predicted proteome sequence, expression data (RNASeq) of *A. euteiches* ATCC201684 were accessed through AphanoDB database (https://www.polebio.lrsv.ups-tlse.fr/aphanoDB/). The peptidases of *A. euteiches* were extracted as proteins harboring GO:0008233 and its child terms. To classify the genes into multigene families the Markov Clustering Algorithm was applied (inflation rate 1,5) to cluster pairwise blast results (e-value < 1 $1e^{-30}$). Tandemly repeated genes were identified as adjacent genes (blast e-value <1e-80, coverage > 80%). Microsynteny search was performed using OGOB browser (McGowan et al., 2019) and FungiDB (Basenko et al., 2018) resource using the best blast hit of the corresponding organism. Secreted proteases were identified as ones with a predicted signal peptide using SignalP v.5 (Almagro Armenteros et al., 2019) and without transmembrane helixes predicted using TMHMM v.2.0 (Krogh et al., 2001).

Whole expression analysis (RNASeq)

RNASeq reads of *M. truncatula* A17-Jemalong infected with *A. euteiches* ATCC201684 at 1, 3, 9 days post infection and *A. euteiches* mycelium were previously generated (Gaulin et al., 2018) and are accessible at NCBI SRA under reference SPR355760. The raw data were trimmed with TrimGalore (v.0.6.5) (https://github.com/FelixKrueger/TrimGalore) with cutadapt and FastQC options, and mapped to *M. truncatula* cv Jemalong A17 reference genome v.5.0 using Hisat2 (v.2.1.0) (Kim et al., 2019). Samtools (v.1.9) algorithms 'fixmate' and 'markdup' (Li et al., 2009) were used to clean alignments from duplicated sequences. Reads were counted with HTseq (v.0.9.1) (Anders et al., 2015) using the reference GFF file (Kiselev et al., 2022). The count files were normalized and differentially expressed genes (DEGs) were identified using the DESeq2 algorithm (Love et al., 2014).

Plant material, microbial strains and growth conditions

All experiments were carried out using *Précovil* variety of *Pisum sativum* produced by Vilmorin company (St Quentin Fallavier, France). For germination, seeds were sterilized 30 seconds in 96% EtOH, and 5 mins in 5% bleach solution. After germination seed were planted in 300ml sterile pots filled with zeolite (1-5 mm fraction) and Fahraeus media (Fåhraeus, 1957), supplemented with 5 mM NH_4NO_3 as a nitrogen supplement. Zoospores of *A. euteiches*

ATCC201684 were prepared as described elsewhere (Ramirez-Garcés et al., 2016). The plantelets were infected with 10^5 zoospores per plant 1 day after transfer to zeolite pots. Roots were harvested at 15 days after infection. Pea apoplastic fluid was extracted using a 3-times vacuum infiltration with ice-cold water (3 times * 10 mins, 2 Bar pressure). Infiltrated roots were dried by rolling into a paper towel, placed into 20 ml syringe and then into a 50 ml falcon tube, before centrifugation (4°C, 2000 rpm, slow acceleration/deceleration).

Microscopy

Primary and upper secondary roots of 15 dpi pea were collected for microscopic analysis. The primary root was placed directly on a holder and the secondary roots were embedded into 2,5% agarose and were sliced using a vibrating-blade microtome (Leica VT1000 S) to a thickness of 100 µm. To specifically stain *A. euteiches* hyphae, wheat germ agglutinin coupled to Alexa Fluor 488 conjugate (WGA-488, Invitrogen) was used. Briefly, specimens were stained in a 10 µg/ml staining solution for 5 minutes at room temperature and directly placed in a water drop on a microscope slide and directly observed at the confocal microscope. Imaging was performed by using a confocal laser scanning microscope (Leica TCS SP8) and the settings were operated in the LAS X software. Specimens were observed using a 10X dry objective (HC PL FLUOTAR 10x/0.30). A 405 nm diode laser was used to detect emitted auto-fluorescence from the sugar beet tissue collected in a wavelength range of 415-465 nm. An OPSL 488nm laser was used to detect the fluorophore Alexa Fluor 488 in a wavelength range of 500-565 nm. All images were processed in ImageJ version 1.53.

Labelling of active apoplastic hydrolases and affinity purification

Three ml of pea apoplastic fluid (AF) per treatment were labelled with 4 µM of FP-biotin (Sigma) and 4 µM DCG04 (MedKoo Biosciences) during 4 hours at room temperature and with a slow rotation (10 rpm). Reaction was buffered using 50 mM NaAc pH 5 and 5mM of dithiothreitol (DTT). No-probe control (NCP) samples were identical to labelled samples but instead of probes, an equal volume of DMSO was added to the 3 ml of AF. Labelling reactions were stopped by chloroform/methanol precipitation. 1:3:4 volumes of cold chloroform:water:methanol were added to the samples and mixed thoroughly. Precipitating samples were kept in the freezer at -20°C until next steps of the protocol were performed. Subsequently, samples were centrifugated at 3000xg for 30 minutes (4°C). The aqueous top

phase was removed without disturbing the interphase in which the proteins were present. Then 4 volumes of cold methanol were added, and samples were centrifuged again for 45 minutes at 3000xg (4°C). The supernatant was removed without disturbing the pellet and the precipitated proteins were left drying at room temperature. Precipitated proteins were resuspended with 2 ml of 1.2% sodium dodecyl sulphate (SDS) phosphate saline buffer (PBS) (Life Technologies, 18912-014) for at least 40 minutes. Then, samples were sonicated in a sonicating bath (ASK_REF) at maximum power for 10 minutes. A further 5 ml of PBS were added to the samples and proteins were denatured in a water bath at 90°C for five minutes. A further 3 ml of PBS were added to the samples to lower the SDS concentration below 0.2%. To enrich labelled proteins, 130 µl of PBS washed avidin beads (Sigma, A9207) were added to each sample, including the NPC. Beads were incubated with resuspended proteins for 1 hour at room temperature while rotating. Beads were then centrifugated for 1 minute at 400xg and supernatant was discarded. Avidin beads were then washed 5 times with 10 ml of 1% SDS PBS buffer to remove unspecific protein-beads interactions, and 3 times with 10 ml of ultra-pure HPLC-MS grade water. Avidin beads were transferred into 2 ml LoBind protein tubes (Eppendorf, Z666505-100EA).

On-bead digestion and peptide purification

250 µl of 8M Urea in 50 mM TrisHCl pH8 were added to the beads. Proteins reduced by adding 500mM of TCEP and incubating samples at 56°C for 30 minutes while shaking. Samples were then cooled down to room temperature before the alkylation step. 30 µl of 500mM chloroacetamide was added and alkylation was performed at 36°C for 30 minutes in dark. Samples were centrifuged at 2000 rpm for three minutes and the supernatant was removed. A vial of 20 µg of LysC endopeptidase enzyme (Wako, 125-02543) was resuspended into 1220 µl 1M urea in 50mM Tris-HCl pH. 80 µl of this resuspended LysC were added to each sample. Tubes were sealed with parafilm and LysC digestion was performed over night at 37°C while shaking. Next day, trypsin endopeptidase (Trypsin gold MS grade Promega V5280) was reconstituted following manufacturer's instructions in 50mM NaAc pH 5. 20 µg of reconstituted trypsin was added to 1200 µl 50 mM Tris-HCl pH8. 80 µl of the diluted trypsin was added to each sample (2 µg per sample) and incubated for at least 8 hours at 36°C.

After trypsin digestion, tryptic peptides present in the supernatant were recovered into a new Lobind protein tube. Prior to mass spectrometry analysis of the peptidic composition,

tryptic peptides were purified using 100 µl Agilent Bond Elut OMIX Pipette tips for micro extractions (Agilent, A57003100) using a 1 ml syringe coupled with a 1000 µl cut filter tip to push buffers and samples through the C18 column. Manufacturer's instructions were followed in this step.

LC-MS/MS

Experiments were performed on an Orbitrap Fusion Lumos instrument (Thermo) that was coupled to an EASY-nLC 1200 liquid chromatography (LC) system (Thermo). The LC was operated in the one-column mode. The analytical column was a fused silica capillary (75 µm × 46 cm) with an integrated PicoFrit emitter (New Objective) packed in-house with Reprosil-Pur 120 C18-AQ 1.9 µm resin (Dr. Maisch). The analytical column was encased by a column oven (Sonation) and attached to a nanospray flex ion source (Thermo). The column oven temperature was adjusted to 50 °C during data acquisition. The LC was equipped with two mobile phases: solvent A (0.1% formic acid, FA, in water) and solvent B (0.1% FA, 20% water and 80% acetonitrile, ACN). All solvents were of UPLC grade (Honeywell). Peptides were directly loaded onto the analytical column with a maximum flow rate that would not exceed the set pressure limit of 980 bar (usually around 0.6 – 0.8 µL/min). Peptides were subsequently separated on the analytical column by running a 140 min gradient of solvent A and solvent B (start with 8% B; gradient 8% to 35% B for 95 min; gradient 35% to 44% B for 20 min; gradient 44% to 100% B for 10 min and 100% B for 15 min) at a flow rate of 250 nl/min. The mass spectrometer was operated using Orbitrap Fusion Lumos Tune Application (version v3.3.2782.28) and Xcalibur (v4.3.73.11). The mass spectrometer was set in the positive ion mode. Precursor ion scanning was performed in the Orbitrap analyzer (FTMS; Fourier Transform Mass Spectrometry) in the scan range of m/z 375-1750 and at a resolution of 120000 with the internal lock mass option turned on (lock mass was 445.120025 m/z, polysiloxane) (Olsen et al., 2005). Product ion spectra were recorded in a data dependent fashion in the ion trap (ITMS) in a variable scan range and at a rapid scan rate. The ionization potential (spray voltage) was set to 2.3 kV and the ion transfer tube temperature to 275°C. Peptides were analyzed using a repeating cycle (cycle time = 3s) consisting of a full precursor ion scan (4.0×10^5 ions or 50 ms) and a variable number of product ion scans (1.0×10^4 ions, injection time set to "auto") where peptides are isolated based on their intensity in the full survey scan (threshold of 5000 counts) for tandem mass spectrum (MS2) generation that permits peptide sequencing and identification. Stepped Higher-energy collisional dissociation

(HCD) energy was set to 20, 35, 40% for the generation of MS2 spectra. During MS2 data acquisition dynamic ion exclusion was set to 25 seconds (mass tolerance ±10 ppm) and a repeat count of one. Ion injection time prediction, preview mode for the FTMS, monoisotopic precursor selection and charge state screening (charge states: 2 -6) were enabled.

Peptide and Protein Identification using MaxQuant

RAW spectra were submitted to an Andromeda (Cox et al., 2011) search in MaxQuant (2.0.2.0) using the default settings (Cox and Mann, 2008). Label-free quantification and match-between-runs was activated (Cox et al., 2014). The MS/MS spectra data were searched against the *Aphanomyces euteiches* database (Kiselev et al., 2022) and the *P. sativum* database (Kreplak et al., 2019). All searches included a contaminants database search (as implemented in MaxQuant, 245 entries). The contaminants database contains known MS contaminants and was included to estimate the level of contamination. Andromeda searches allowed oxidation of methionine residues (16 Da) and acetylation of the protein N-terminus (42 Da) as dynamic modifications and the static modification of cysteine (57 Da, alkylation with iodoacetamide). Enzyme specificity was set to "Trypsin/P" with two missed cleavages allowed. The instrument type in Andromeda searches was set to Orbitrap and the precursor mass tolerance was set to ±20 ppm (first search) and ±4.5 ppm (main search). The MS/MS match tolerance was set to ±0.5 Da. The peptide spectrum match FDR and the protein FDR were set to 0.01 (based on target-decoy approach). Minimum peptide length was 7 amino acids. For protein quantification unique and razor peptides were allowed. Modified peptides were allowed for quantification. The minimum score for modified peptides was 40. Label-free protein quantification was switched on, and unique and razor peptides were considered for quantification with a minimum ratio count of 2. Retention times were recalibrated based on the built-in nonlinear time-rescaling algorithm. Within parameter groups MS/MS identifications were transferred between LC-MS/MS runs with the "match between runs" (MBR) option in which the maximal match time window was set to 0.7 min and the alignment time window set to 20 min. The quantification is based on the "value at maximum" of the extracted ion current. At least two quantitation events were required for a quantifiable protein. Further analysis and filtering of the results was done in Perseus v1.6.10.0. (Tyanova et al., 2016). For quantification we combined related biological replicates to categorical groups and investigated only those proteins that were found in at least one categorical group in a minimum of 3 out of 4 biological replicates. Comparison of protein group quantities (relative quantification) between different

MS runs is based solely on the LFQ's as calculated by MaxQuant, MaxLFQ algorithm (Cox et al., 2014)

Supplementary Material

Supplementary tables and high-resolution figures are available on (published on a restricted access before the publication submission) https://doi.org/10.5281/zenodo.7134684

Data availability

The mass spectrometry proteomics data for the on-bead digestions have been deposited to the ProteomeXchange Consortium via the PRIDE (Vizcaíno et al., 2016) partner repository (https://www.ebi.ac.uk/pride/archive/) with the dataset identifier PXD035920.

During the review process the data can be accessed via a reviewer account (Username: reviewer_pxd035920@ebi.ac.uk; Password: EnN74xbG)

References

Almagro Armenteros, J. J., Tsirigos, K. D., Sønderby, C. K., Petersen, T. N., Winther, O., Brunak, S., et al. (2019). SignalP 5.0 improves signal peptide predictions using deep neural networks. *Nature Biotechnology* 37, 420–423. doi: 10.1038/s41587-019-0036-z.

Anders, S., Pyl, P. T., and Huber, W. (2015). HTSeq--a Python framework to work with high-throughput sequencing data. *Bioinformatics* 31, 166–169. doi: 10.1093/bioinformatics/btu638.

Baćanović-Šišić, J., Šišić, A., Schmidt, J. H., and Finckh, M. R. (2018). Identification and characterization of pathogens associated with root rot of winter peas grown under organic management in Germany. *Eur J Plant Pathol* 151, 745–755. doi: 10.1007/s10658-017-1409-0.

Basenko, E., Pulman, J., Shanmugasundram, A., Harb, O., Crouch, K., Starns, D., et al. (2018). FungiDB: An Integrated Bioinformatic Resource for Fungi and Oomycetes. *JoF* 4, 39. doi: 10.3390/jof4010039.

Becking, T., Kiselev, A., Rossi, V., Street-Jones, D., Grandjean, F., and Gaulin, E. (2021). Pathogenicity of animal and plant parasitic Aphanomyces spp and their economic impact on aquaculture and agriculture. *Fungal Biology Reviews*, S1749461321000397. doi: 10.1016/j.fbr.2021.08.001.

Carlile, A. J., Bindschedler, L. V., Bailey, A. M., Bowyer, P., Clarkson, J. M., and Cooper, R. M. (2000). Characterization of SNP1, a Cell Wall-Degrading Trypsin, Produced During Infection by *Stagonospora nodorum*. *MPMI* 13, 538–550. doi: 10.1094/MPMI.2000.13.5.538.

Chatterton, S., Harding, M. W., Bowness, R., Mclaren, D. L., Banniza, S., and Gossen, B. D. (2019). Importance and causal agents of root rot on field pea and lentil on the Canadian prairies, 2014–2017. *Canadian Journal of Plant Pathology* 41, 98–114. doi: 10.1080/07060661.2018.1547792.

Conner, R. L., Chang, K. F., Hwang, S. F., Warkentin, T. D., and McRae, K. B. (2013). Assessment of tolerance for reducing yield losses in field pea caused by Aphanomyces root rot. *Can. J. Plant Sci.* 93, 473–482. doi: 10.4141/cjps2012-183.

Cox, J., Hein, M. Y., Luber, C. A., Paron, I., Nagaraj, N., and Mann, M. (2014). Accurate Proteome-wide Label-free Quantification by Delayed Normalization and Maximal Peptide Ratio Extraction, Termed MaxLFQ. *Molecular & Cellular Proteomics* 13, 2513–2526. doi: 10.1074/mcp.M113.031591.

Cox, J., and Mann, M. (2008). MaxQuant enables high peptide identification rates, individualized p.p.b.-range mass accuracies and proteome-wide protein quantification. *Nat Biotechnol* 26, 1367–1372. doi: 10.1038/nbt.1511.

Cox, J., Neuhauser, N., Michalski, A., Scheltema, R. A., Olsen, J. V., and Mann, M. (2011). Andromeda: A Peptide Search Engine Integrated into the MaxQuant Environment. *J. Proteome Res.* 10, 1794–1805. doi: 10.1021/pr101065j.

Dean, R., Van Kan, J. A. L., Pretorius, Z. A., Hammond-Kosack, K. E., Di Pietro, A., Spanu, P. D., et al. (2012). The Top 10 fungal pathogens in molecular plant pathology: Top 10 fungal pathogens. *Molecular Plant Pathology* 13, 414–430. doi: 10.1111/j.1364-3703.2011.00783.x.

Dora, S., Terrett, O. M., and Sánchez-Rodríguez, C. (2022). Plant–microbe interactions in the apoplast: Communication at the plant cell wall. *The Plant Cell* 34, 1532–1550. doi: 10.1093/plcell/koac040.

Fåhraeus, G. (1957). The Infection of Clover Root Hairs by Nodule Bacteria Studied by a Simple Glass Slide Technique. *Microbiology* 16, 374–381. doi: 10.1099/00221287-16-2-374.

Farvardin, A., González-Hernández, A. I., Llorens, E., García-Agustín, P., Scalschi, L., and Vicedo, B. (2020). The Apoplast: A Key Player in Plant Survival. *Antioxidants* 9, 604. doi: 10.3390/antiox9070604.

Fitzpatrick, D. A., O'Gaora, P., Byrne, K. P., and Butler, G. (2010). Analysis of gene evolution and metabolic pathways using the Candida Gene Order Browser. *BMC Genomics* 11, 290. doi: 10.1186/1471-2164-11-290.

Gaulin, E., Jacquet, C., Bottin, A., and Dumas, B. (2007). Root rot disease of legumes caused by Aphanomyces euteiches. *Mol Plant Pathol* 8, 539–548. doi: 10.1111/j.1364-3703.2007.00413.x.

Gaulin, E., Pel, M. J. C., Camborde, L., San-Clemente, H., Courbier, S., Dupouy, M.-A., et al. (2018). Genomics analysis of Aphanomyces spp. identifies a new class of oomycete effector associated with host adaptation. *BMC Biol* 16, 43. doi: 10.1186/s12915-018-0508-5.

Guevara, M. G., Almeida, C., Mendieta, J. R., Faro, C. J., Veríssimo, P., Pires, E. V., et al. (2005). Molecular cloning of a potato leaf cDNA encoding an aspartic protease (StAsp) and its expression after P. infestans infection. *Plant Physiology and Biochemistry* 43, 882–889. doi: 10.1016/j.plaphy.2005.07.004.

Haas, B. J., Kamoun, S., Zody, M. C., Jiang, R. H., Handsaker, R. E., Cano, L. M., et al. (2009). Genome sequence and analysis of the Irish potato famine pathogen Phytophthora infestans. *Nature* 461, 393–398.

Inohara, N., and Nuñez, G. (2002). ML — a conserved domain involved in innate immunity and lipid metabolism. *Trends in Biochemical Sciences* 27, 219–221. doi: 10.1016/S0968-0004(02)02084-4.

Jashni, M. K., Dols, I. H. M., Iida, Y., Boeren, S., Beenen, H. G., Mehrabi, R., et al. (2015). Synergistic Action of a Metalloprotease and a Serine Protease from *Fusarium oxysporum* f. sp. *lycopersici* Cleaves Chitin-Binding Tomato Chitinases, Reduces Their Antifungal Activity, and Enhances Fungal Virulence. *MPMI* 28, 996–1008. doi: 10.1094/MPMI-04-15-0074-R.

Jiang, R. H. Y., de Bruijn, I., Haas, B. J., Belmonte, R., Löbach, L., Christie, J., et al. (2013). Distinctive expansion of potential virulence genes in the genome of the oomycete fish pathogen Saprolegnia parasitica. *PLoS Genet.* 9, e1003272. doi: 10.1371/journal.pgen.1003272.

Kaschani, F., Gu, C., Niessen, S., Hoover, H., Cravatt, B. F., and van der Hoorn, Renier. A. L. (2009). Diversity of Serine Hydrolase Activities of Unchallenged and Botrytis-infected Arabidopsis thaliana. *Molecular & Cellular Proteomics* 8, 1082–1093. doi: 10.1074/mcp.M800494-MCP200.

Kaschani, F., Shabab, M., Bozkurt, T., Shindo, T., Schornack, S., Gu, C., et al. (2010). An Effector-Targeted Protease Contributes to Defense against *Phytophthora infestans* and Is under Diversifying Selection in Natural Hosts. *Plant Physiology* 154, 1794–1804. doi: 10.1104/pp.110.158030.

Kim, D., Paggi, J. M., Park, C., Bennett, C., and Salzberg, S. L. (2019). Graph-based genome alignment and genotyping with HISAT2 and HISAT-genotype. *Nat Biotechnol* 37, 907–915. doi: 10.1038/s41587-019-0201-4.

Kiselev, A., San Clemente, H., Camborde, L., Dumas, B., and Gaulin, E. (2022). A Comprehensive Assessment of the Secretome Responsible for Host Adaptation of the Legume Root Pathogen Aphanomyces euteiches. *JoF* 8, 88. doi: 10.3390/jof8010088.

Kopitar-Jerala, N. (2012). The Role of Cysteine Proteinases and their Inhibitors in the Host-Pathogen Cross Talk. *CPPS* 13, 767–775. doi: 10.2174/138920312804871102.

Kreplak, J., Madoui, M.-A., Cápal, P., Novák, P., Labadie, K., Aubert, G., et al. (2019). A reference genome for pea provides insight into legume genome evolution. *Nat. Genet* 51, 1411–1422. doi: 10.1038/s41588-019-0480-1.

Krogh, A., Larsson, B., von Heijne, G., and Sonnhammer, E. L. L. (2001). Predicting transmembrane protein topology with a hidden markov model: application to complete genomes11Edited by F. Cohen. *Journal of Molecular Biology* 305, 567–580. doi: 10.1006/jmbi.2000.4315.

Li, H., Handsaker, B., Wysoker, A., Fennell, T., Ruan, J., Homer, N., et al. (2009). The Sequence Alignment/Map format and SAMtools. *Bioinformatics* 25, 2078–2079. doi: 10.1093/bioinformatics/btp352.

Liang, D., Andersen, C. B., Vetukuri, R. R., Dou, D., and Grenville-Briggs, L. J. (2020). Horizontal Gene Transfer and Tandem Duplication Shape the Unique CAZyme Complement of the Mycoparasitic Oomycetes Pythium oligandrum and Pythium periplocum. *Front. Microbiol.* 11, 581698. doi: 10.3389/fmicb.2020.581698.

Love, M. I., Huber, W., and Anders, S. (2014). Moderated estimation of fold change and dispersion for RNA-seq data with DESeq2. *Genome Biol* 15, 550. doi: 10.1186/s13059-014-0550-8.

Madoui, M.-A., Gaulin, E., Mathé, C., San Clemente, H., Couloux, A., Wincker, P., et al. (2007). AphanoDB: a genomic resource for Aphanomyces pathogens. *BMC Genomics* 8, 471. doi: 10.1186/1471-2164-8-471.

Majeed, M., Kumar, G., Schlosser, S., El-Matbouli, M., and Saleh, M. (2017). In vitro investigations on extracellular proteins secreted by Aphanomyces invadans, the causative agent of epizootic ulcerative syndrome. *Acta Vet. Scand* 59, 78.

Majeed, M., Soliman, H., Kumar, G., El-Matbouli, M., and Saleh, M. (2018). Editing the genome of Aphanomyces invadans using CRISPR/Cas9. *Parasites Vectors* 11, 554. doi: 10.1186/s13071-018-3134-8.

Mazau, D., and Esquerré-Tugayé, M. T. (1986). Hydroxyproline-rich glycoprotein accumulation in the cell walls of plants infected by various pathogens. *Physiological and Molecular Plant Pathology* 29, 147–157. doi: 10.1016/S0048-4059(86)80017-0.

McGowan, J., Byrne, K. P., and Fitzpatrick, D. A. (2019). Comparative Analysis of Oomycete Genome Evolution Using the Oomycete Gene Order Browser (OGOB). *Genome Biology and Evolution* 11, 189–206. doi: 10.1093/gbe/evy267.

McGowan, J., O'Hanlon, R., Owens, R. A., and Fitzpatrick, D. A. (2020). Comparative Genomic and Proteomic Analyses of Three Widespread Phytophthora Species: Phytophthora chlamydospora, Phytophthora gonapodyides and Phytophthora pseudosyringae. *Microorganisms* 8, 653. doi: 10.3390/microorganisms8050653.

Meijer, H. J. G., Mancuso, F. M., Espadas, G., Seidl, M. F., Chiva, C., Govers, F., et al. (2014). Profiling the Secretome and Extracellular Proteome of the Potato Late Blight Pathogen Phytophthora infestans. *Molecular & Cellular Proteomics* 13, 2101–2113. doi: 10.1074/mcp.M113.035873.

Misas-Villamil, J. C., Hoorn, R. A. L., and Doehlemann, G. (2016). Papain-like cysteine proteases as hubs in plant immunity. *New Phytol* 212, 902–907. doi: 10.1111/nph.14117.

Moussart, A., Wicker, E., Le Delliou, B., Abelard, J.-M., Esnault, R., Lemarchand, E., et al. (2009). Spatial distribution of Aphanomyces euteiches inoculum in a naturally infested pea field. *Eur J Plant Pathol* 123, 153–158. doi: 10.1007/s10658-008-9350-x.

Muszewska, A., Stepniewska-Dziubinska, M. M., Steczkiewicz, K., Pawlowska, J., Dziedzic, A., and Ginalski, K. (2017). Fungal lifestyle reflected in serine protease repertoire. *Sci Rep* 7, 9147. doi: 10.1038/s41598-017-09644-w.

Olsen, J. V., de Godoy, L. M. F., Li, G., Macek, B., Mortensen, P., Pesch, R., et al. (2005). Parts per Million Mass Accuracy on an Orbitrap Mass Spectrometer via Lock Mass Injection into a C-trap. *Molecular & Cellular Proteomics* 4, 2010–2021. doi: 10.1074/mcp.T500030-MCP200.

Papavizas, G. C., and Ayers, W. A. (1974). *Aphanomyces Species and Their Root Diseases in Pea and Sugarbeet: A Review*. Agricultural Research Service, U.S. Department of Agriculture.

Paulus, J. K., Kourelis, J., Ramasubramanian, S., Homma, F., Godson, A., Hörger, A. C., et al. (2020). Extracellular proteolytic cascade in tomato activates immune protease Rcr3. *Proc Natl Acad Sci USA* 117, 17409–17417. doi: 10.1073/pnas.1921101117.

Quillévéré-Hamard, A., Le Roy, G., Lesné, A., Le May, C., and Pilet-Nayel, M.-L. (2020). Aggressiveness of diverse French Aphanomyces euteiches isolates on pea Near-Isogenic-Lines differing in resistance QTL. *Phytopathology*. doi: 10.1094/PHYTO-04-20-0147-R.

Quillévéré-Hamard, A., Le Roy, G., Moussart, A., Baranger, A., Andrivon, D., Pilet-Nayel, M.-L., et al. (2018). Genetic and Pathogenicity Diversity of Aphanomyces euteiches Populations From Pea-Growing Regions in France. *Front. Plant Sci.* 9. doi: 10.3389/fpls.2018.01673.

Ramirez-Garcés, D., Camborde, L., Pel, M. J. C., Jauneau, A., Martinez, Y., Néant, I., et al. (2016). CRN13 candidate effectors from plant and animal eukaryotic pathogens are DNA-binding proteins which trigger host DNA damage response. *New Phytol* 210, 602–617. doi: 10.1111/nph.13774.

Rocafort, M., Fudal, I., and Mesarich, C. H. (2020). Apoplastic effector proteins of plant-associated fungi and oomycetes. *Current Opinion in Plant Biology* 56, 9–19. doi: 10.1016/j.pbi.2020.02.004.

Schneiter, R., and Di Pietro, A. (2013). The CAP protein superfamily: function in sterol export and fungal virulence. *BioMolecular Concepts* 4, 519–525. doi: 10.1515/bmc-2013-0021.

Schoina, C., Rodenburg, S. Y. A., Meijer, H. J. G., Seidl, M. F., Lacambra, L. T., Bouwmeester, K., et al. (2021). Mining oomycete proteomes for metalloproteases leads to identification of candidate virulence factors in *Phytophthora infestans*. *Mol Plant Pathol* 22, 551–563. doi: 10.1111/mpp.13043.

Severino, V., Farina, A., Fleischmann, F., Dalio, R. J. D., Di Maro, A., Scognamiglio, M., et al. (2014). Molecular Profiling of the Phytophthora plurivora Secretome: A Step towards Understanding the Cross-Talk between Plant Pathogenic Oomycetes and Their Hosts. *PLoS ONE* 9, e112317. doi: 10.1371/journal.pone.0112317.

Sharma, A., Rani, M., Lata, H., Thakur, A., Sharma, P., Kumar, P., et al. (2022). Global dimension of root rot complex in garden pea: Current status and breeding prospective. *Crop Protection* 158, 106004. doi: 10.1016/j.cropro.2022.106004.

Tian, M., Benedetti, B., and Kamoun, S. (2005). A Second Kazal-Like Protease Inhibitor from *Phytophthora infestans* Inhibits and Interacts with the Apoplastic Pathogenesis-Related Protease P69B of Tomato. *Plant Physiology* 138, 1785–1793. doi: 10.1104/pp.105.061226.

Tian, M., Huitema, E., da Cunha, L., Torto-Alalibo, T., and Kamoun, S. (2004). A Kazal-like Extracellular Serine Protease Inhibitor from Phytophthora infestans Targets the Tomato Pathogenesis-related Protease P69B. *Journal of Biological Chemistry* 279, 26370–26377. doi: 10.1074/jbc.M400941200.

Tordai, H., Bányai, L., and Patthy, L. (1999). The PAN module: the N-terminal domains of plasminogen and hepatocyte growth factor are homologous with the apple domains of

the prekallikrein family and with a novel domain found in numerous nematode proteins. *FEBS Letters* 461, 63–67. doi: 10.1016/S0014-5793(99)01416-7.

Tyanova, S., Temu, T., Sinitcyn, P., Carlson, A., Hein, M. Y., Geiger, T., et al. (2016). The Perseus computational platform for comprehensive analysis of (prote)omics data. *Nat Methods* 13, 731–740. doi: 10.1038/nmeth.3901.

van der Hoorn, R. A. L. (2011). Mining the active proteome of Arabidopsis thaliana. *Front. Plant Sci.* 2. doi: 10.3389/fpls.2011.00089.

van der Hoorn, R. A. L., and Kaiser, M. (2012). Probes for activity-based profiling of plant proteases. *Physiologia Plantarum* 145, 18–27. doi: 10.1111/j.1399-3054.2011.01528.x.

van der Hoorn, R. A. L., Leeuwenburgh, M. A., Bogyo, M., Joosten, M. H. A. J., and Peck, S. C. (2004). Activity Profiling of Papain-Like Cysteine Proteases in Plants. *Plant Physiology* 135, 1170–1178. doi: 10.1104/pp.104.041467.

Vizcaíno, J. A., Csordas, A., del-Toro, N., Dianes, J. A., Griss, J., Lavidas, I., et al. (2016). 2016 update of the PRIDE database and its related tools. *Nucleic Acids Res* 44, D447–D456. doi: 10.1093/nar/gkv1145.

Wang, S., Xing, R., Wang, Y., Shu, H., Fu, S., Huang, J., et al. (2021). Cleavage of a pathogen apoplastic protein by plant subtilases activates host immunity. *New Phytol* 229, 3424–3439. doi: 10.1111/nph.17120.

Watson, A., Browne, S. L., Snudden, M. G., and Mudford, E. M. (2013). Aphanomyces root rot of beans and control options. *Australasian Plant Pathol.* 42, 321–327. doi: 10.1007/s13313-012-0180-0.

Wu, L., Chang, K.-F., Conner, R. L., Strelkov, S., Fredua-Agyeman, R., Hwang, S.-F., et al. (2018). Aphanomyces euteiches: A Threat to Canadian Field Pea Production. *Engineering* 4, 542–551. doi: 10.1016/j.eng.2018.07.006.

Zhang, Q., Li, W., Yang, J., Xu, J., Meng, Y., and Shan, W. (2020). Two *Phytophthora parasitica* cysteine protease genes, *PpCys44* and *PpCys45* , trigger cell death in various *Nicotiana* spp. and act as virulence factors. *Molecular Plant Pathology* 21, 541–554. doi: 10.1111/mpp.12915.

5. Chapter V - FACS-based Screen for Identification of Nuclear Effectors from Phytopathogenic Filamentous Oomycetes *Aphanomyces euteiches*

Secreted proteins are among the main pathogenicity factors of filamentous pathogens such as oomycetes and fungi. They are targeting various components of host cells from cell wall degradation to transcription mechanism perturbation. Oomycetes are described as evolving two major groups of cytoplasmic the effectors: Crinklers (CRNs) (Schornack et al., 2010) and RxLRs (Morgan and Kamoun, 2007). Moreover, *in-planta* screenings of effector candidates demonstrated that over 50% of CRNs and RxLRs are localised in nuclei (Caillaud et al., 2012; Stam et al., 2013; Liu et al., 2018). Accordingly, we previously show that the N-terminal part of AeCRN5 from *A. euteiches*, allows the transfer of *Phytophthora* effector within the host cytoplasm (PNAS, Schornack 2010). In addition, we observed that the DNA-binding AeCRN13 effectors acts within the host nuclei to cause DNA-damage and facilitate oomycete infection (Ramirez-Garcés et al., 2016).

Recently our research group highlighted a third group of putative intracellular effectors called Small Secreted Proteins (SSP) in *A. euteiches*, characterized by the size of <300 amino acids, absence of detectable functional domain (Gaulin et al., 2018) and often, high enrichment in one or several amino acids (**Chapter III,** Kiselev et al 2022). Functional studies demonstrated that some of those SSPs are also localized within the nucleus and/or nucleolus when transiently express in presence or absence of their own signal peptide *in planta* (i;e *N benthamiana* leaves, *M. truncatula* roots). As evidence for AeSSP1256, the effector hijacks a DEAD-box RNA helicase from binding to RNA and cause mild growth delay of the roots and enhance plant susceptibility by perturbing ribosome-associated pathway (Gaulin et al., 2018; Camborde et al., 2022, **Annex I**).

All these findings mounted the interest in studying nuclear effectors which seems to be able to target either protein or nucleic acid from the host to perturb plant physiology To go further in the description of those original molecular mechanisms, and since we can hypothesize that the effectors may act synergic in combination with others effectors as reported for CRN63 and CRN115, which interaction needed to supress the host defence (Liu et al., 2011) or with hosts components, a robust experimental system to identify such microbial actors is required.

Indeed, the selection of effectors candidate for functional studies is currently supported by in silico prediction using bioinformatic software such as SignalP for signal peptide

detection (Almagro Armenteros et al., 2019), TMHMM for transmembrane domain detection (Krogh et al., 2001), effectorP (Sperschneider and Dodds, 2021) fo and several tools for prediction of nuclear localisation signal such as NLStradamus (Nguyen Ba et al., 2009) or cNLS-Mapper (Kosugi et al., 2009). Another layer of the identification of effector candidate exploits available genomics and transcriptomics resources (Gao et al., 2021). On the other site the information about the transcription profile of the effector gives a hint whereas a protein is expressed or induced during the infection process and at which stage (Chen et al., 2014; Gaulin et al., 2018). Finally, very few studies aimed in the direct detection of oomycete effector proteins through proteomics techniques. Existing studies indicates the presence of effectors of several classes within a plant-based media, where *Phytophthora* was grown (Meijer et al., 2014).

To fulfil this experimental gap, we developed a cell-sorting (FACS)-proteomics approach on infected-*M. truncatula* roots for proof of-concept of characterization of oomycete nuclear effector. Evolutionary large distance and availability of high-quality genomes of *Aphanomyces* and *Medicago* species allowed the accurate detection of proteins in the two-species proteomics. In the results part of the manuscript, we present the details of the technique and the list of the identified effector candidates. Among the proteins detected in proteomics analysis we firstly discovered *A. euteiches* RxLR-like protein, conserved aspartic-rich small secreted protein and present several effector candidates with a predicted enzymatic Pfam domain, including a very similar homolog of *Verticillium dahliae* Vd424Y nuclear effector, which carries glycoside hydrolase domain. Ten sequences have been further validated for their nuclear localization upon transient expression in *N. benthamiana* leaves, and six induced a cell death. In the discussion of the manuscript the way to improve the selectivity of the FACS to identify effector candidates as well as host-interacting proteins is presented.

Overall, the aim of this current study was to propose a flow cytometry coupled with proteomics approach to directly detect microbial effectors targeting host nuclei during the infection process. The chapter is presented as a future submitted manuscript.

FACS-based screen for identification of nuclear effectors from phytopathogenic filamentous oomycete *Aphanomyces euteiches*

Andrei Kiselev[1*], Laurent Camborde[1*], Mickael Bourges[2], Ludovic Bonhomme[3], Elodie Gaulin[1&]

[1] Laboratoire de Recherche en Sciences Végétales (LRSV), Université de Toulouse, CNRS, UPS, Toulouse INP, Auzeville-Tolosane, 31320 France

[2] Institute of Integrative Biology of the Cell (I2BC), CEA, CNRS, Université Paris-Saclay, 91198, Gif-sur-Yvette, France

[3] UMR 1095 Génétique Diversité Ecophysiologie des Céréales, INRAE, Université Clermont Auvergne 63000 Clermont-Ferrand, France

[*]Authors contributed equally to work

[&] Corresponding author gaulin@univ-tlse3.fr

Key Words

Effector, nucleus, FACS, *Aphanomyces*

Abstract

Filamentous eukaryotic pathogens produce a myriad of effector to threat the plant. Whole-genome sequences predict large repertoire of oomycete host-cell entering effectors but few of them are functionally proven. Here we describe an *in vivo* method to screen plant nuclear-localized proteins from the root rot pathogen of legume *Aphanomyces euteiches*. The method combines a cytometry enrichment of plant nuclei from infected *Medicago truncatula* roots with an LC/MS-MS identification of oomycete proteins. Twenty-five *A. euteiches* nuclear-targeting proteins have been identified. From ten *A. euteiches*-identified proteins, eight are nuclear localized upon transient expression in *Nicotiana benthamiana* leaves. This simple and efficient FACS-based method to identify oomycete nuclear effectors, will help unravel how root rot disease of legume is determined.

Introduction

Fungal and oomycetes plant pathogens are economically important due to the threat they pose to the production and yield of agricultural crops. It has been estimated that global agricultural production suffers an average annual loss of 15% due to plant diseases (Oerke, 2006; Lo Presti et al., 2015; Schwessinger et al., 2015). Effective control against microbial diseases depend on a better understanding of how the pathogens proliferate within the host plant and cause infection.

Filamentous plant pathogens secrete a panoply of proteins referred as 'effectors' to successfully facilitate infection. Apoplastic effectors are secreted outside the plant cell wall while intracellular proteinaceous effector exerts their function into the cytosol of the host plant or travel to others compartment as the nucleus (Wilson and McDowell, 2022). Within oomycetes, two major groups of intracellular effectors harbouring hundreds of members have been *in silico* predicted (Birch et al., 2008; Schornack et al., 2010; Fabro, 2022). The RxLR family firstly reported in *Phytophthora* species as the potato blight agent *Phytophthora infestans*, contains numerous members that target the nucleus, the cytosol or the endosplasmic reticulum. But to date only a dozen of *P. infestans* RxLR have been functionally characterized for their virulence activity (Petre et al., 2021; Zhou et al., 2022). Similarly, the CRN family predicted in plant and animal pathogenic oomycetes, in chytrid pathogenic fungi (Joneson et al., 2011; Ramirez-Garcés et al., 2016) and symbiotic fungi (Voß et al., 2018), present hundreds of members (Caillaud et al., 2012; Liu et al., 2018; Stam et al., 2013) which target intracellular space of the host cell including the nucleus and nucleoli. Another class of intracellular effector corresponding to hundreds small secreted proteins (SSP) less than 300 residues in size devoid of any predicted domain have been recently reported in *Aphanomyces* spp. including plant and crayfish pathogens (Gaulin et al., 2018), whilst SSPs were well described in true fungi (Kim et al., 2016). Within the legume pathogen *A. euteiches*, SPPs are classified in families based on the amino composition and are expected to contribute for legume preference of the pathogen (Kiselev et al., 2022). Only the nucleolar AeSSP1256 effector which hijacks a host DEAD-box RNA helicase from its RNA to enhance pathogen infection have been characterized (Camborde et al., 2022). To date, only a few pathogenic fungal/oomycete effectors have been experimentally studied, and their functions have been understood. Despite recent advances in the identification of the role played by individual effectors during host invasion, there are still many that require robust functional characterisation.

Pathogen effectors generally associate with host components as protein, or nucleic acid to function (Bozkurt et al., 2012; Camborde et al., 2019; Zhou et al., 2022). The availability of whole-genome sequences allows the prediction of large set of secreted proteins thanks to the detection of a N-terminal signal peptide (Sonah et al., 2016), even though numerous effectors are devoid of any conserved sequences (Giraldo et al., 2013; Yan et al., 2022). Current effector prediction pipelines provide thousand proteins per genome as putative candidate, which have to be reduced to a small set for functional validation. Further filtering or ranking in combination with expression analysis, GWAS approaches or comparative genomics are used for the prioritisation of effector (Hartmann et al., 2017), but can still provide hundreds of candidates and exclude by errors interesting candidates. Thus, we reasoned that the *in vivo* identification of microbial proteins within the plant cells during pathogen invasion would provide a powerful way for the prioritisation of intracellular effectors.

Here, as a proof of concept, we focus on the identification of nuclear-targeting proteins from the oomycete *Aphanomyces euteiches* present during colonization of *Medicago truncatula* legume roots. Genomes sequence of both partners allow proteins identification by mass spectrometry analysis (Hartmann et al., 2017) and nuclear effectors are already functionally characterized (i.e. SSP, CRN) (Ramirez-Garcés et al., 2016; Camborde et al., 2022). To limit the use of tagged-effectors and mimics natural host infection, we screened for all *A. euteiches* proteins present in the plant nuclei. Thus, a combination of fluorescence cell sorting technology (FACS) on *M. truncatula* roots infected by the parasite to collect plant nuclei followed by LC/MS-MS identification of nuclear proteins was set up. This unique method led to the identification of 25 microbial nuclear proteins, from which only 1.5% were predicted as effectors. Using live cell imaging we confirmed the nuclear localization of eight MS-identified proteins out of ten, following their transient expression in *N. benthamiana* leaves. This FACS-based screen method is an efficient way to quickly identify nuclear candidate effectors. It provides new insight into the complexity of molecular components deployed by oomycetes for host invasion and will help unravel how root rot disease of legume is determined.

Results

A nuclear-enrichment based protocol using cell-sorting (FACS) to collect *M. truncatula* nuclei from roots infected by the pathogen *A. euteiches*

To identify nuclear effectors from *A. euteiches*, we aimed to collect *M. truncatula* host nuclei from infected tissues Thus, we investigate whether the razor chopping method established to release nuclei in to suspension from plant tissues with sufficient yield for molecular studies (Galbraith et al., 1983), could provide a convenient approach for isolation of nuclei from root tissues. After zoospore inoculation of the pathogen, roots of the F83005.5 susceptible *M. truncatula* line were collected at 4, 7, 10 days and nuclear fraction were extracted by chopping roots in Gif Nuclear Buffer (GNB), before staining with propidium iodide as depicted in **Figure 1**. Mock samples correspond to roots treated with water and grown in the same conditions (in vitro, 4, 7, 10 days) before 'pooling' the samples. To enrich the infected sample in the nuclei from *M. truncatula*, cell sorting with a gain on PI intensity and side scattering channels to allows detection of different morphotypes of nuclei based on DNA quantity (PI intensity) and shape (Side Scattering) was performed. A clear separation of five nuclear types, corresponding to five datapoints clouds on the readout of infected samples. The identification of nuclei from a species was performed by a single species run, the PI intensity and Side scattering were conserved between single- and multispecies runs (**Figure S1**). Two peaks of nuclei of the pathogen and three peaks of the host plant *M. truncatula* nuclei representing different ploidy were identified as shown elsewhere (Bourge et al., 2018). We noticed that the amount of *A. euteiches* nuclei was several-fold higher, than the ones from *M. truncatula* during infection (**Table 1**).

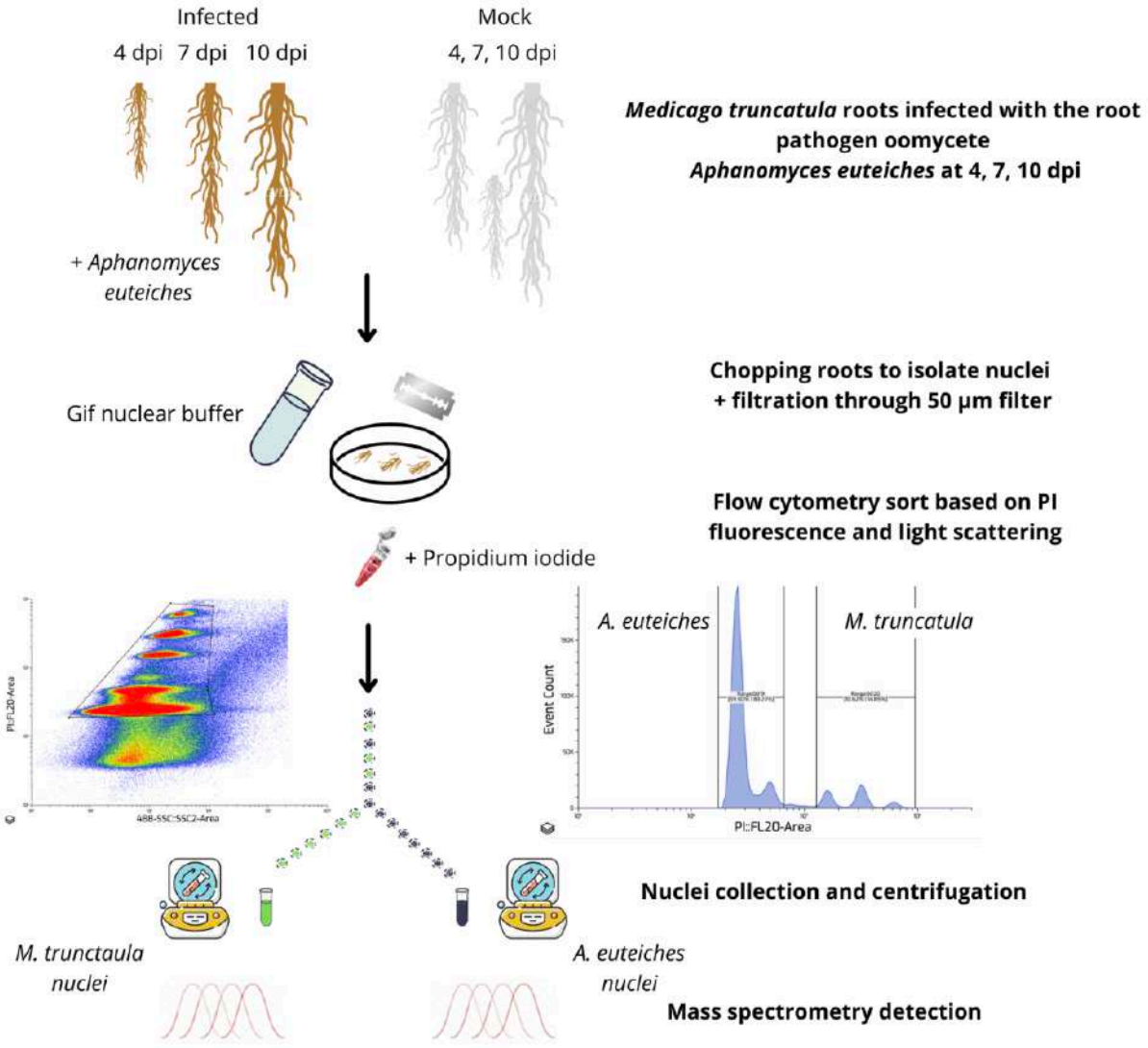

Figure 1. Experimental design combining purification of *M. truncatula* nuclei from roots infected by *A. euteiches* and mass spectrometry identification of nuclear proteins.

M. truncatula F830005 line was grown on M medium at 22°/18°C, 16h/8h day-night period for 3 days before inoculation with *A. euteiches* zoospores at a concentration of 10^4 zoospore / ml or with water (mock). Roots harbouring *Aphanomyces* root rot symptoms (i.e browning, yellowing) were harvested separately at 4, 7, 10 (dpi). The non-infected roots were pooled at 4, 7 and 10 days. Nuclear extraction was performed by chopping of the tissue and filtration through 50 µm filter (Bourge et al., 2018). *M. truncatula* and *A. euteiches* nuclei were separated by FACS after labelling with propidium iodide and collected by species separately. Collected nuclei were sedimented by centrifugation and digested with trypsin (one replicate / time point).

Samples were subjected to liquid chromatography tandem mass spectrometry (LC-MS/MS) analysis and peptide identification was performed using to identify putative nuclear proteins from *A. euteiches* and *M. truncatula.*

Table 1. Number of collected nuclei per sample

Sample	**Day**	***Mt* nuclei (thousands)**	***Ae* nuclei (thousands)**
M. truncatula mock	4, 7, 10 dpi (pool)	2090	-
M. truncatula infected with *A. euteiches*	4 dpi	864	2940
M. truncatula infected with *A. euteiches*	7 dpi	1570	4010
M. truncatula infected with *A. euteiches*	10 dpi	1760	3390

LC MS/MS analysis identifies A. euteiches proteins within nuclei of infected-M. truncatula roots

To detect the presence of *A. euteiches* proteins within the nuclei of *M. truncatula* during infection, all the samples were subjected to LC MS/MS qualitative analysis. In total, nine samples were subjected to proteomics analysis: 1 mock pool sample, 3 samples of *M. truncatula* nuclei from infected tissue (one per each dpi), 3 samples of *A. euteiches* nuclei from infected tissue (one per each dpi), 2 pooled samples from infected tissue (1 for *M. truncatula* and 1 for *A. euteiches* nuclei). For peptide identification the reference proteome *M. truncatula* A17 v5.1 (Pecrix et al., 2018) and *A. euteiches* ATCC201684 database (Kiselev et al, 2022, AphanoDB) were used. To detect misidentified proteins we removed all the *A. euteiches* assigned proteins within the list of all identified proteins in mock treated *M. truncatula* nuclei, where no *A. euteiches* proteins could be identified (**Table S1**). After that the analysis revealed in total 2305 putative nuclear proteins. The sample with the least number of the proteins was mock treatment 735 proteins, while the largest set was identified in 7 dpi sample of *A. euteiches* nuclei with 1600 proteins (raw data and analysis script are represented in **Supplementary File 1 (**'compar spectra' output corresponding to all spectra assigned to a given protein**), 2 and 3**, the correct list of identified proteins could be found in **Table S1**).

To assess whether the nuclear-enrichment based protocol using cell-sorting (FACS), allows the identification of predicted nuclear-targeting proteins we combined the use of four softwares for nuclear (PSORTII, NLStradamus, Predict NLS) or nucleolar localization (NoD) (Figure 2A). In total, around 50% of the detected proteins predicted to have Nuclear or Nucleolar localization signal. As depicted on **Fig 2B**, the largest proportion of the detected proteins in all samples is assigned to *M. truncatula* proteins, while the proportion of the nuclear *M. truncatula* proteins is diminished in *A. euteiches* nuclei samples (and vice-versa the *A. euteiches* proteins in *M. truncatula* nuclei samples, **Table S2**). These results signify the enrichment of nuclei of desired species in the respective samples, but not a clear separation of the nuclei from two species. This observation may also suggest that the host plant may transfer proteins within the pathogen, as recently illustrated for miRNA for plant pathogenic fungi (Kwon et al., 2021). In the control sample predicted nuclear proteins account for around 70% of total sequence (**Figure 2B**), the value is comparable with other studies (Howden et al., 2017; Goto et al., 2019) of plant nuclear proteomes, which signifies the correct extraction of the nuclear fraction. However, in infected samples we identified a two-fold increase of non-nuclear proteins from 215 proteins in control to 400-600 proteins in infected samples, while the number of nuclear proteins increased only for 17-21% from 522 proteins in control sample to 586-617 protein in infected samples (**Figure 2B**), which could be associated to the damage of the cells or to pathogen-induced protein translocation.

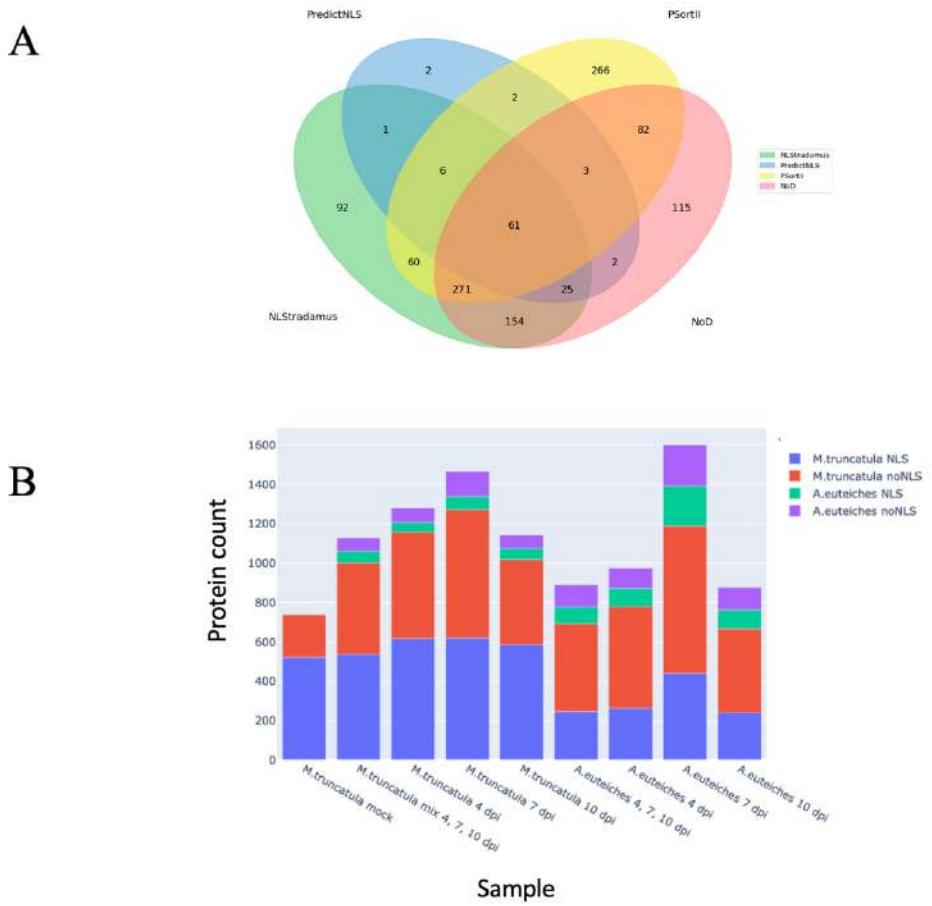

Figure 2. Identified nuclear proteins unequally distributed among the samples and signify a succsesful enrichment.

A. Venn diagramm of the Nuclear Localization Signal (NLS) predicted by four different algorithms: NLStradamus, PredictNLS, PSortII and NoD using all the proteins identified by LC MS/MS analysis **B**. Bar plot demonstrating the proportion of the proteins from each species in the samples and repartition by the presence of NLS detected by either software.

Putative effectors identification

To focus on the putative effectors within the list of identified proteins from *A. euteiches* we searched for the presence of a signal peptide (+SP) and the absence of a predicted transmembrane domain (-TM) in line with the initial hypothesis that secreted proteins from the pathogen are translocated into nuclei of the host. We identified 25 proteins as illustrated in Table 2, but we could not identify any *A. euteiches* proteins exclusively present in *M. truncatula* nuclei, all of the secreted proteins were identified in both host and pathogen's nuclei. We examined predicted function of this set of protein using PFAM and evaluated the size of the proteins, to identify plant process that may be affected by *A. euteiches* during roots colonization.

Around 50% of the identified proteins display a hydrolytic function against protein (i.e trypsin, subtilase, carboxypeptidase) or carbohydrate (i.e glycosyl-hydolase GH11, GH18, GH3 / pectate lyase). Ribosomal-related proteins are also present, as proteins with PFAM domain detected in known oomycetes effector or toxin (i.e Cellulose Binding Domain (CBD), PT repeat, Ricin, Lectin).

Table 2. List of *A. euteiches* proteins with a predicted Signal Peptide (+SP) and Nuclear Localization Signal (+NLS) and without Transmembrane Domain (-TM) present in nuclei of *M. truncatula* roots during infection. The last column of the table indicates in which sample the protein is detected (*Mt* – stands for *M. truncatula* nuclei samples, *Ae* – for *A. euteiches, pool* – for pooled samples of 4, 7, 10 dpi).

Gene name (AphanoDB nomnclature)	Protein length (aa)	Pfam domain or SSP	Gene Ontology	Sample, in which protein found
Ae201684P_312	627	PF04886 PT repeat RxLR-like	-	all
Ae201684P_455	233	PF00457 Glycosyl hydrolases family 11	GO:0004553 hydrolase activity, hydrolyzing O-glycosyl compounds / GO:0005975 carbohydrate metabolic process	Mt 7 dpi, Ae 4, 10 dpi
Ae201684P_1070	769	PF14310 Fibronectin type III-like domain / PF01915 Glycosyl hydrolase family 3 C-terminal domain / PF00933 Glycosyl hydrolase family 3 N terminal domain	GO:0004553 hydrolase activity, hydrolyzing O-glycosyl compounds / GO:0005975 carbohydrate metabolic process	all
Ae201684P_4392	194	- SSP	- -	Mt 7 dpi, Ae 4, 7, 10 dpi + pool
Ae201684P_5356	113	PF00428 60s Acidic ribosomal protein	-	all
Ae201684P_11034	272	- SSP	- -	Mt 7dpi + pool, Ae 10 dpi
Ae201684P_11036	304	- SSP	- -	Mt 4, 7, 10 dpi + pool. Ae 4, 10 dpi + pool
Ae201684P_11039	257	- SSP	- -	Mt 4, 7, 10 dpi + pool. Ae 4, 10 dpi + pool

Ae201684P_11833	115	PF00428 60s Acidic ribosomal protein	-	all
Ae201684P_11865	228	- SSP	- -	Mt 7, 10 dpi, Ae 7 dpi
Ae201684P_13031	489	PF00082 Subtilase family	GO:0004252 serine-type endopeptidase activity / GO:0006508 proteolysis	Mt 4, 7, 10 dpi + pool. Ae 4, 7 dpi + pool
Ae201684P_13261	498	PF13848 Thioredoxin-like domain / PF00085 Thioredoxin	GO:0005783 endoplasmic reticulum / GO:0016853 isomerase activity / GO:0045454 cell redox homeostasis	Mt 7 dpi, Ae 4, 7, 10 dpi + pool
Ae201684P_13653	534	PF00704 Glycosyl hydrolases family 18	GO:0008061 chitin binding / GO:0005975 carbohydrate metabolic process	Mt 4, 7, 10 dpi + pool. Ae 4, 7 dpi + pool
Ae201684P_13656	541	PF00704 Glycosyl hydrolases family 18	GO:0008061 chitin binding / GO:0005975 carbohydrate metabolic process	Mt 7 dpi + pool, Ae 4, 7 dpi + pool
Ae201684P_15812	595	PF00652 Ricin-type beta-trefoil lectin domain	-	Mt 7 dpi + pool, Ae 7 dpi + pool
Ae201684P_17584	781	PF00734 Fungal cellulose binding domain	GO:0030248 cellulose binding / GO:0005975 carbohydrate metabolic process / GO:0005576 extracellular region	Mt 7 dpi, Ae 7 dpi
Ae201684P_17878	259	PF03211 Pectate lyase	GO:0005576 extracellular region / GO:0030570 pectate lyase activity	Mt 4,7 dpi + pool, Ae 7 dpi + pool

Ae201684P_17885	259	PF03211 Pectate lyase	GO:0005576 extracellular region / GO:0030570 pectate lyase activity	all
Ae201684P_18103	432	PF13365 Trypsin-like peptidase domain	-	Mt 4, 7 dpi + pool, Ae 4, 7 dpi + pool
Ae201684P_18134	273	PF00089 Trypsin	GO:0004252 serine-type endopeptidase activity / GO:0006508 proteolysis	Mt 4, 7 + pool, Ae 4, 7, 10 + pool
Ae201684P_18136	273	PF00089 Trypsin	GO:0004252 serine-type endopeptidase activity / GO:0006508 proteolysis	all
Ae201684P_18138	273	PF00089 Trypsin	GO:0004252 serine-type endopeptidase activity / GO:0006508 proteolysis	all
Ae201684P_18184	268	PF00089 Trypsin	GO:0004252 serine-type endopeptidase activity / GO:0006508 proteolysis	Mt 7 dpi, Ae 7 dpi
Ae201684P_18290	381	PF00246 Zinc carboxypeptidase	GO:0006508 proteolysis / GO:0008270 zinc ion binding / GO:0004181 metallocarboxypeptidase activity	all
Ae201684P_19782	769	PF14310 Fibronectin type III-like domain / PF01915 Glycosyl hydrolase family 3 C-terminal domain / PF00933 Glycosyl hydrolase family 3 N terminal domain	GO:0004553 hydrolase activity, hydrolyzing O-glycosyl compounds / GO:0005975 carbohydrate metabolic process	all

A closer examination of the identified proteins highlighted Ae201684P_312 which shares a high similarity with RxLR effector from *Phytophthora spp.* Avr1b-1 (Shan et al., 2004). Sequence comparison of the two proteins revealed over 70% similarity of the C-term sequence, while N-ter where RxLR motif is located in Avr1b-1 protein is not conserved (**Figure 3A, C**). Blast search against *A. euteiches* proteome also identified Ae201684P_330 gene as another homolog of the RXLR Avr1b_1 protein. Another putative nuclear effector correspond to Ae201684P_455 protein, which is a homolog of a fungal effector from *Verticillium dahliae* Vd424 (Liu et al., 2021) that display a predicted GH11 endo-beta-xylanase domain (**Figure 3B, D**). To verify the similarity of the homologous on the structure levels, we predicted the 3D structure of *A. euteiches* putative effectors and their homologs using AlphaFold2

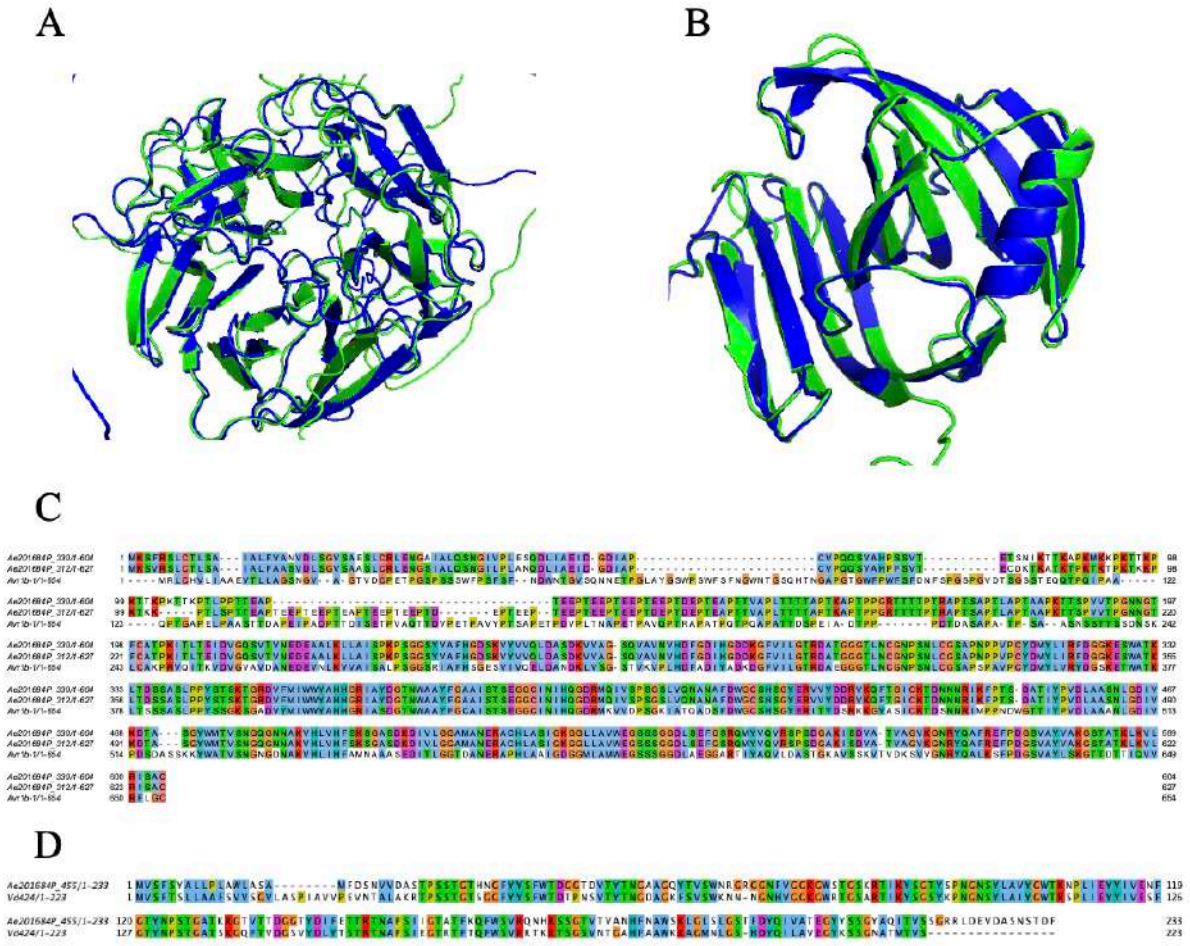

Figure 3. Two of identified putative effectors are homologous to previously characterized. A. Structural alignment of *A. euteiches* protein Ae201684P_312 (green) and *P. nicotiana* Avr1b-1 protein (blue) (only the structured part of the proteins is shown, disordered zones are not shown). B. Structural alignment of *A. euteiches* protein Ae201684P_455 (green) and *V. dahliae* Vd424 protein (blue). C. Sequence alignment of *A. euteiches* protein Ae201684P_312, Ae201684P_330 and *P. nicotiana* Avr1b-1 protein D. Sequence alignment of *A. euteiches* protein Ae201684P_455 and *V. dahliae* Vd424 protein.

To assess the significance of the experimental method for the identification of plant nuclear-targeting proteins from *A. euteiches*, we investigated their subcellular localization in *Nicotiana benthamiana* leaves. To select the candidates we used a previous expression analysis made by dual RNASeq on *A. euteiches/M. truncatula* (Gaulin et al., 2018) and the proteomics data. All of the selected secreted effectors are induced during the early stage of infection (1 dpi), while the expression at later stages differ between the proteins. In addition to Ae201684_312 which is an ortholog of *Phytophthora spp.* Avr1b RxLR-effector, we selected its homolog in *A. euteiches* genome Ae201684_330, which was not found in the proteomics assay, but which expression was induced during the early infection. Two last proteins and Ae201684P_13653 were the only, which were predicted to target nuclei. Four selected proteins harbour PFAM domains atypical for a nuclear-localization (i.e Ae201684P_13653 GH18, Ae201684P_455 GH11, Ae201684P_13031 Subtilase, Ae201684P_18136 Trypsin). Finally, we included for functional analysis three *A. euteiches* sequences, which were the only ones detected in the host nuclei and not detected in pathogen's, they encode no predicted signal peptide and are not differentially express during infection.

Table 3. PFAM domain, Expression profile, Signal Peptide, Transmembrane, nuclear localization prediction of the proteins selected for functional analysis. [a]Transcriptomics study published in Gaulin et al., 2018 [b]Protein not found in proteomics assay. Homologous to **Ae201684P_312**

Gene name	Functional domain PFAM	Expression profile[a]	Signal peptide (SP) / Transmembrane domain (TM) / NLS prediction	Localisation prediction software
Ae201684P_312[b]	PF04886 PT repeat Homologous to PnAvr1-b1	day 1 – UP, day3 – DOWN, day9 – UP	+SP-TM +NLS	NLStradamus, NoD, PSortII
Ae201684P_330	No domain. Homologous to PnAvr1-b1	day 1 – UP, day3 – DOWN, day9 – UP	+SP-TM +NLS	NLStradamus, NoD, PSortII
Ae201684P_455	PF00457 Glycosyl hydrolases family 11	day 1 – UP, day3 – UP, day9 – DOWN	+SP-TM - NLS	

Ae201684P_4392	SSP	day 1 – UP, day3 – DOWN, day9 – DOWN	+SP-TM - NLS	-
Ae201684P_13031	PF00082 Subtilase family	day 1 – UP, day3 – DOWN, day9 – DOWN	+SP-TM -NLS	-
Ae201684P_13653	PF00704 Glycosyl hydrolases family 18	day 1 – UP, day3 – DOWN, day9 – UP	+SP-TM -NLS	NoD
Ae201684P_18136	PF00089 Trypsin	day 1 – UP, day3 – UP, day9 – DOWN	+SP-TM - NLS	-
Ae201684P_17714	No domain	Expression in mycelia	- SP - TM -NLS	-
Ae201684P_19945	No domain	Expression in mycelia	- SP - TM -NLS	-
Ae201684P_7331	No domain	Expression in mycelia	- SP - TM -NLS	-

To elucidate the localization of ten candidates within the plant cell, mCherry fusion constructs were obtained and transiently expressed using *Agrobacterium tumefaciens* in leaves of *N. benthaminana*. Western-blot analyses one day after treatment revealed that all mCherry-fusion proteins were present (**Supplemental Figure S2**) despite some proteolytic cleavage of the tag. Seven candidates, including two without a predicted signal peptide (Ae201684P_19945 and Ae201684P_7331) demonstrated nucleo-cytoplasmic accumulation as evidence by mCherry fluorescence pattern. The remaining three candidates are either excluded from the nucleus (Ae201684P_18136 Tryspin) or present primarily in plastids and nucleoplasm (Ae201684P_ 17714 (unknown function). Interestingly, two similar proteins Ae201684P_330 and Ae201684P_312 showed contrary localization in nucleus and in cytoplasm respectively (Figure 4). This confocal analysis shows that eight of ten microbial candidates detected by proteomics approach from cell-sorting separated nuclei localize to the plant nucleus even in the absence of a predicted NLS or signal peptide within the amino acid sequence. These results support the experimental approach to identify putative oomycete effector targeting host nucleus.

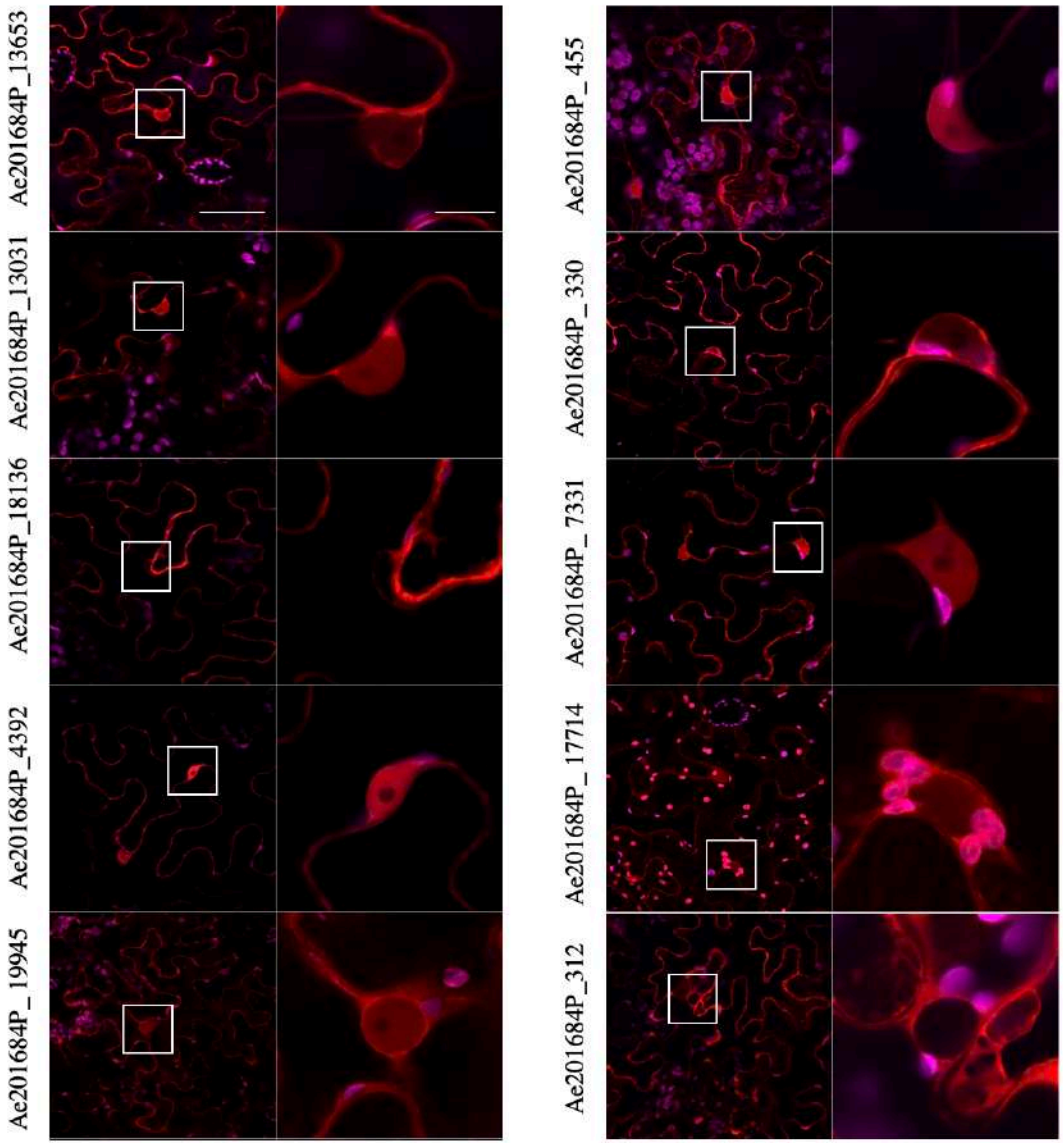

Figure 4. Localization of mCherry fusion *A. euteiches* candidate in *Nicotiana benthamiana* leaves. Ten *A. euteiches* putative nuclear-localized candidates identified by LC MS/MS analysis were evaluated for their subcellular localization after overexpression in *N. benthamiana* leaves using *A. tumefaciens*. One day after treatment, fluorescence patterns revealed the nucleo-cytoplasmic accumulation for eight candidates, while Ae201684P_18136, Ae201684P_312 are excluded from nuclei and Ae201684P_ 17714 targets plastids and nucleoplasm. mCherry was excitated by the laser at 552 nm (red) and chloroplast autofluorescence (magenta) reads at 680-720 nm. Left images represents the view of a whole epidermal cell of *N. benthamiana,* white square indicates the zone containing nuclei, right image represents zoom into the marked zone. Scale bar: 50 µm (left image) and 10 µm (right image).

All *N. benthamiana* leaves overexpressing the different mCherry-fusion candidates displayed a necrotic area within 10 days after treatment, with the exception of Ae201684P_18136, Ae201684P_13653 and Ae201684P_312 excluded from the nuclei (**Figure 5**). Therefore, most of the plant nuclear-localized proteins from *A. euteiches* are able to trigger cytotoxic effect when overexpressed in *N. benthamianna* leaves, suggesting that they may act as effectors during *M. truncatula* infection. By comparison of two homologous proteins Ae201684P_330 and Ae201684P_312 it's thought that a nuclear localisation is indispensable for a cytotoxic action of the proteins.

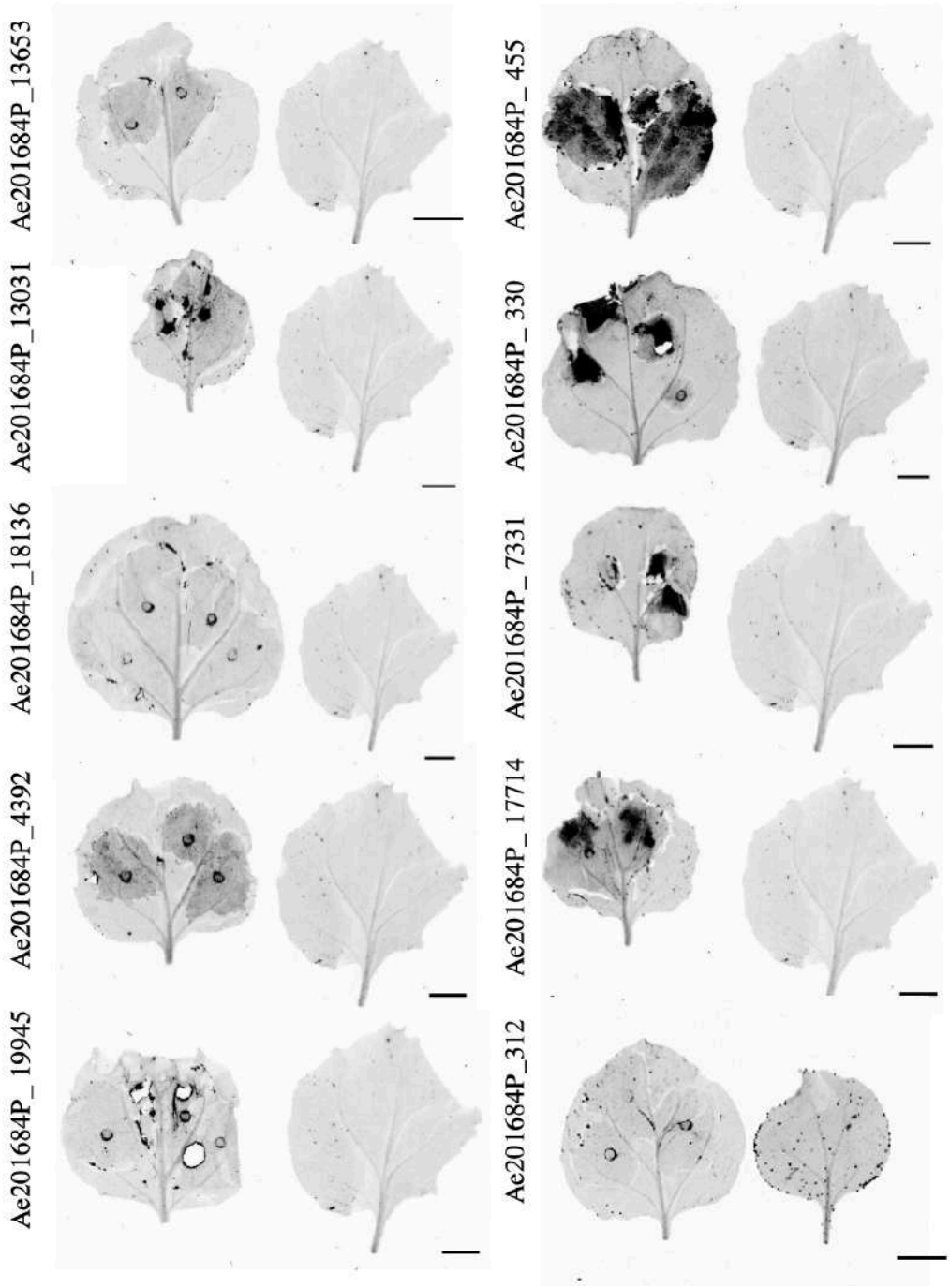

Figure 5. Phenotype induced by overexpression of ten candidate effectors

N. benthamiana leaves overexpressing the *A. euteiches* candidates (left) or not-treated (right) were analysed by image scanning using ChemiDoc (Bio-Rad) imaging system seven days after treatment by *A. tumefaciens* to visualise necrotic area (dark area) using 555 nm light source and by reading the chloroplast autofluorescence at far-red (600-720 nm) spectrum.

Discussion

In the present work we attempted to address one of the major questions in the field of molecular plant-pathogen interaction: which of myriads predicted effectors are present as proteins during the infection? Therefore this work will contribute to the 8th of top-10 questions in plant-microbe interactions (Harris et al., 2020). The available genomes of plant pathogens provide the important resource for comparative genomics and evolutionary studies contributing greatly to understanding of the pathogenesis, however such studies generate hundreds of putative effectors, which are difficult to select for further functional studies. Application of transcriptomics assays greatly helps to reduce a number of the effectors to study; however, the presence of the transcript doesn't necessarily guarantee the presence of the protein, especially secreted, in the pathosystem. Here we employed fluorescence-assisted nuclei sorting from infected roots to separate host (*M. truncatula*) and pathogen's (*A. euteiches*) nuclei from the infected roots, combine with a LC MS/MS approach to identify oomycete plant nuclear-targeting proteins.

To provide a quick experimental system with a restricted number of steps for nuclei isolation we tested the chopping method on *M. truncatula* roots infected by the pathogen, initially developed on non-infected leaves samples (Bourge et al., 2018). For proteomics analysis, samples corresponding to small part of *in vitro* roots harbouring browning symptoms were collected for cell sorting. Although this method does not allow a complete separation of nuclei from both partners, the chopping approach of *in vitro* tissues is a fast and easy experimental method to collect enough nuclei for LC MS/MS detection of nuclear proteins. For future studies we could recommend to apply more strict gating parameters during the sorting process. The recent development of single cell proteomics (Specht et al., 2021) should also bring the developed assay to the next level of purity of the samples since the number of sorted nuclei could be greatly reduced or even visual selection of nuclei could be performed during the sample preparation before proteomics analysis.

Within the analysis more than 2 300 putative nuclear proteins were characterized using the proteome sequence of *M. truncatula* or *A. euteiches*. In the mock water-treated samples around 70% of the identified proteins were predicted as nuclear, which is a comparable value with other plant nuclear proteome studies (Howden et al., 2017; Goto et al., 2019). The highest number of proteins was observed in nuclei from roots tissues in contact during 7 days with the pathogen. Overall, we observed during the analysis, a higher number of non-nuclear proteins in infected samples. Indeed, an increase of around 20% of the number of nuclear proteins, while

non-nuclear proteins increased by 60%, was recorded upon comparison of mock and infected-tissues. This might represent the dynamic response of nuclear proteome against stress in *M. truncatula* (Narula et al., 2013), which can include the mechanisms of protein relocation from mitochondria or plastids to nuclei (Krupinska et al., 2020) or as a sign of unfolded protein response, as a conservative pathway of plant defence reaction (Wahyu Indra Duwi Fanata et al., 2013).

To identify the putative plant nuclear-targeting proteins from *A. euteiches*, the analysis was restricted to secreted proteins with a predicted signal peptide and without any predicted transmembrane domain (+SP -TM) This filtering method allows the characterization of 23 protein groups representing 17 secreted proteins with either catalytic activity against protein/ carbohydrate or binding capacity. While nuclear proteases as well as Glycosyl-Hydrolase are not described up reported to now with the exception of the *Verticillium dahliae* effector (Liu et al., 2021), the identification of this set of proteins suggest a unique role during infection. In addition, we detected a RxLR-like protein, similar the virulence Avr1b-1 protein from *Phytophthora* spp (Shan et al., 2004). But devoid of the conserved N-ter part. Finally, five small secreted proteins (SSP) with unknown predicted PFAM domains were recovered.

To confirm the subcellular localization of the identified proteins, candidates were selected based on their expression profile during *M. truncatula* infection (i.e early, late) and the presence of predicted motif that could allow an extracellular localisation and three candidates without any predicted signal have been added. Transient expression in *Nicotiana benthamiana* leaves, revealed the cytotoxic activity for most of them with the exception of Ae201684P_18136 (trypsin), Ae201684P_13653 (GH18). The proteins, which are the homologs of the known effectors as Ae201684P_455 (homolog of nuclear localized Vd424 (GH11) induced very intense cell death symptoms. Intriguingly Ae201684P_330 (Avr1b-1-like) also induce necrotic effect in contrast to its paralog Ae201684P_312 (Avr1b-1-like). In addition, we identified necrotic activity for the tested SSP while up to now these effectors were not reported as necrotic-inducing protein when transiently express *in planta* (Gaulin et al., 2018; Camborde et al., 2022). Fluorescence pattern indicates the presence of most of the candidates within the nuclei of *N. benthamiana* leaves, with the exception of Ae201684P_17714 (-SP -TM), Ae201684P_18136 (trypsin) and Ae201684P_312 (Avr1b-1-like). Although, we cannot exclude putative contaminations from cytosolic material, a combination of cell sorting and LC MS/MS analysis is a fast and efficient method to recover

oomycete plant nuclear-targeting proteins. Future studies will aim to evaluate the effector capacity of this set of candidates.

This work provides an original and efficient tool to quickly screen for putative nuclear-targeting proteins from filamentous plant pathogen that may act as effector during interaction. It also reveals the complexity of the deployed nuclear proteins repertoire of phytopathogenic oomycete and give new insights of pathogenesis mechanisms at the root level.

Materials and Methods

Biological Material

All experiments were carried out using of *Medicago truncatula* F83005.5 genotype and *Aphanomyces euteiches* ATCC201684 strain.

A. euteiches was grown on Corn Meal Agar medium (CMA) at 22°C. For zoospore preparation the agar disks were transferred into Peptone glucose liquid medium and were grown at 22^0C for four days. On the fifth day the culture was washed 5-7 times with sterile commercially available mineral water Volvic and incubated in water overnight. The next day zoospore concentration was measured using hemocytometer slides as previously described (Camborde et al., 2021). Seeds of *M. truncatula* were incubated 1 min in concentrated H_2SO_4, then washed in sterile water, disinfected in 2.5% bleach solution and incubated on 1% Agar plate at 10°C in the dark. The germinated seeds were inoculated after two days with a zoospore solution of *A.* euteiches 3-µl drops of a 10^5 cell·ml^{-1} zoospore as described in (Badreddine et al., 2008).

Flow Cytometry

M. truncatula and *A. euteiches* nuclei were collected from infected-roots as described by (Bourge et al., 2018). Briefly, 4, 7 and 10 days after infection, around 5 g of infected roots with a blackish-brown appearance were chopped with a razor blade in a Petri dish with a Gif Nuclear Buffer (GNB : 45 mM $MgCl_2$, 30 mM Sodium-Citrate, 60 mM MOPS pH 7.0, 1%, PVP 10.000, 0.1% Triton X-100, 10 mM sodium metabisulfite $S_2O_5Na_2$). The nuclear suspension was filtered through 50-µm filter to remove plants and oomycete debris, before adding propidium iodide (50µg/ml; Sigma-Aldrich ref 81845) to stain nucleic acid.

After 5-min incubation at room temperature, fluorescence intensity of propidium iodide was collected using a MoFlo Astrios_EQ© cytometer (Beckman Coulter, Roissy, France) equipped with a 561-nm solid state laser for excitation and 614/20-nm filter for emission. To specifically identified *M. truncatula* nuclei within the heterogeneous non-purified suspension, gating was first performed on SSC-Height vs PI-Area dot plot to allow detection of different morphotypes of nuclei (*A. euteiches vs M. truncatula*), then doublets were discarded from a PI-Area vs PI-Height dot plot. Finally, DNA content of nuclei were gated on PI-area histograms.

1.5 x 10^6 isolated nuclei were sorted in PuraFlow sheath fluid (Beckman Coulter) at 25 psi (pounds per square inch), with a 100-micron nozzle. We performed sorting with ~43 kHz drop drive frequency, plates voltage of 4000-4500 V and an amplitude of 30-50 V. Sorting was performed in purity mode. After sorting, nuclei samples were centrifuged at 2500 rpm for 20 min at 4°C, the supernatant was discarded and the pelleted nuclei were denaturated by addition of 4X Laemmlli solution.

Mass Spectrometry Identification

Denaturated proteins were digested using trypsin and tryptic peptides were analyzed by tandem mass spectrometry. Proteins were identified with X!TandemPipeline (Langella et al., 2017), at least two peptides mapped onto the protein sequence with the maximum protein e-value of 10^{-4}. As a reference proteome published *M. truncatula* A17 v5.1 genome (Pecrix et al., 2018) and synthetic *A. euteiches* database was used composed of published proteome (Kiselev et al, 2022) combined with all possible Open Reading Frames (getorf) and Stringtie-assembled transcripts of transcriptomics assays (Gaulin et al., 2018). For final protein identification only sequences of the published proteome, as usage of ORFs and transcripts didn't add new outputs.

Detection of nuclear and nucleolar localisation signals was performed as previously described in Howden et al., 2017 the scripts from the publication deposited in https://github.com/remco-stam/howden-et-al were uploaded to a local Galaxy server.

Molecular cloning and *Agrobacterium*-mediated transformation

The 10 selected genes Ae201684_13653, Ae201684_13031, Ae201684_18136, Ae201684_4392, Ae201684_455, Ae201684_330, Ae201684_312, Ae201684_17714, Ae201684_19945 and Ae201684_7331 (sequence available at AphanoDB http://www.polebio.lrsv.ups-tlse.fr/aphanoDB/) were synthetized by GeneCust to be cloned in Golden Gate (GG) assembly. When necessary, sequences were domesticated from GG restriction enzyme sites and designed as « B3-B4 » GG nomenclature, without signal peptide and stop codon to allow C-terminal tag fusion, using Golden Braid 4.0 (https://gbcloning.upv.es/gbclasses/). All sequences were flanked with BsmBI sites, GCGCCGTCTCGCTCGA upstream of ATG codon and GGTTCGTGAGCGAGACGGCGC instead of the stop codon, and subcloned by BsmBI-V2 (NEB #R0739S) digestion in pUPD2 vector (Addgene #68161). Then each new vector was included in a GG assembly (Engler et al., 2014) containing the backbone plasmid pICH47742 (Addgene #48001), pICH51288 for

2x35s Cauliflower Mosaic Virus (CaMV) promoter + 5'UTR (Tobacco Mosaic Virus) (Addgene #50269), pICSL50004 for mCherry C-term fusion (Addgene #50316), and pICH41414 for 3'UTR and terminator sequence 35s from CaMV. Around 100ng of each plasmid were mixed with 20U of BsaI-HF®v2 (NEB #R3733S), 400U of T4 DNA ligase (NEB #M0202S) in T4 ligase buffer, and placed in thermocycler for 25 cycles of 5 min 37°C/16°C alternance, then 5 min at 80°C. 10 µl of 10-beta Competent *E. coli* (NEB #C3019H) were transformed with 4 µl of GG assembly reaction according to the manufacturer's recommendations. After plating on selective LB, transformants were confirmed by PCR, cultured on liquide LB with appropriate antibiotics and sequenced for validation. Plasmids were transformed into *Agrobacterium tumefaciens* (GV3101::pMP90) by electroporation and *Agrobacterium tumefaciens*-transformed strains were syringe-infiltrated into *N. benthamiana* as described by Gaulin et al. (2002). To verify the expression of a target proteins the total protein extract of the transfected leaves was used for a standard Western Blot procedure using anti-mCherry antibody (Sigma, H3663).

Confocal Fluorescence Microscopy

Leaf disks (diameter 10 mm) of the transfected area were collected 24h after agroinfiltration and were used immediately for confocal microscopy to detect subcellular localization of the tested proteins. Imaging was performed by using a confocal laser scanning microscope (Leica TCS SP8) and the settings were operated in the LAS X software. Specimens were observed using a 10X dry objective (HC PL FLUOTAR 10x/0.30). An OPSL 552 nm laser was used to detect the fluorescence of mCherry tag in a wavelength range of 680-720 nm. All images were processed in ImageJ version 1.53.

Cell death image acquisition

Whole leaves of *N. benthamiana* expressing candidate effectors 5 days after agroinfiltration were used for detection of effector-induced cell death as described in (Xi et al., 2021). Briefly, images of the transfected leaves were acquired using ChemiDoc MP Bio-Rad equipped with fluorescence reader, chlorophyll fluorescence was excited at 550 nm and read at 600-720 nm nm, dark areas with low chlorophyll emission designates necrotic areas. All images were processed in ImageJ version 1.53.

Supplementary materials

Supplementary materials are available for download here (published under restricted access upon the submission to a journal) https://doi.org/10.5281/zenodo.7134705

References

Badreddine, I., Lafitte, C., Heux, L., Skandalis, N., Spanou, Z., Martinez, Y., et al. (2008). Cell Wall Chitosaccharides Are Essential Components and Exposed Patterns of the Phytopathogenic Oomycete *Aphanomyces euteiches*. *Eukaryot Cell* 7, 1980–1993. doi: 10.1128/EC.00091-08.

Birch, P. R., Boevink, P. C., Gilroy, E. M., Hein, I., Pritchard, L., and Whisson, S. C. (2008). Oomycete RXLR effectors: delivery, functional redundancy and durable disease resistance. *Curr. Opin. Plant Biol* 11, 373–379. doi: 10.1016/j.pbi.2008.04.005.

Bourge, M., Brown, S. C., and Siljak-Yakovlev, S. (2018). Flow cytometry as tool in plant sciences, with emphasis on genome size and ploidy level assessment. *GenApp* 2, 1. doi: 10.31383/ga.vol2iss2pp1-12.

Bozkurt, T. O., Schornack, S., Banfield, M. J., and Kamoun, S. (2012). Oomycetes, effectors, and all that jazz. *Current Opinion in Plant Biology* 15, 483–492. doi: 10.1016/j.pbi.2012.03.008.

Caillaud, M., Piquerez, S. J. M., Fabro, G., Steinbrenner, J., Ishaque, N., Beynon, J., et al. (2012). Subcellular localization of the *Hpa* RxLR effector repertoire identifies a tonoplast-associated protein HaRxL17 that confers enhanced plant susceptibility. *The Plant Journal* 69, 252–265. doi: 10.1111/j.1365-313X.2011.04787.x.

Camborde, L., Kiselev, A., Pel, M. J. C., Le Ru, A., Jauneau, A., Pouzet, C., et al. (2022). An oomycete effector targets a plant RNA helicase involved in root development and defense. *New Phytologist* 233, 2232–2248. doi: 10.1111/nph.17918.

Camborde, L., Raynaud, C., Dumas, B., and Gaulin, E. (2019). DNA-Damaging Effectors: New Players in the Effector Arena. *Trends in Plant Science* 24, 1094–1101. doi: 10.1016/j.tplants.2019.09.012.

Carotenuto, G., Volpe, V., Russo, G., Politi, M., Sciascia, I., Almeida-Engler, J., et al. (2019). Local endoreduplication as a feature of intracellular fungal accommodation in arbuscular mycorrhizas. *New Phytol* 223, 430–446. doi: 10.1111/nph.15763.

Fabro, G. (2022). Oomycete intracellular effectors: specialised weapons targeting strategic plant processes. *New Phytologist* 233, 1074–1082. doi: 10.1111/nph.17828.

Gaulin, E., Pel, M. J. C., Camborde, L., San-Clemente, H., Courbier, S., Dupouy, M.-A., et al. (2018). Genomics analysis of Aphanomyces spp. identifies a new class of oomycete effector associated with host adaptation. *BMC Biol* 16, 43. doi: 10.1186/s12915-018-0508-5.

Giraldo, M. C., Dagdas, Y. F., Gupta, Y. K., Mentlak, T. A., Yi, M., Martinez-Rocha, A. L., et al. (2013). Two distinct secretion systems facilitate tissue invasion by the rice blast fungus Magnaporthe oryzae. *Nat Commun* 4, 1996. doi: 10.1038/ncomms2996.

Goto, C., Hashizume, S., Fukao, Y., Hara-Nishimura, I., and Tamura, K. (2019). Comprehensive nuclear proteome of *Arabidopsis* obtained by sequential extraction. *Nucleus* 10, 81–92. doi: 10.1080/19491034.2019.1603093.

Harris, J. M., Balint-Kurti, P., Bede, J. C., Day, B., Gold, S., Goss, E. M., et al. (2020). What are the Top 10 Unanswered Questions in Molecular Plant-Microbe Interactions? *MPMI* 33, 1354–1365. doi: 10.1094/MPMI-08-20-0229-CR.

Hartmann, F. E., Sánchez-Vallet, A., McDonald, B. A., and Croll, D. (2017). A fungal wheat pathogen evolved host specialization by extensive chromosomal rearrangements. *ISME J* 11, 1189–1204. doi: 10.1038/ismej.2016.196.

Howden, A. J. M., Stam, R., Martinez Heredia, V., Motion, G. B., Have, S., Hodge, K., et al. (2017). Quantitative analysis of the tomato nuclear proteome during *Phytophthora capsici* infection unveils regulators of immunity. *New Phytol* 215, 309–322. doi: 10.1111/nph.14540.

Joneson, S., Stajich, J. E., Shiu, S.-H., and Rosenblum, E. B. (2011). Genomic Transition to Pathogenicity in Chytrid Fungi. *PLoS Pathog* 7, e1002338. doi: 10.1371/journal.ppat.1002338.

Kim, K.-T., Jeon, J., Choi, J., Cheong, K., Song, H., Choi, G., et al. (2016). Kingdom-Wide Analysis of Fungal Small Secreted Proteins (SSPs) Reveals their Potential Role in Host Association. *Front. Plant Sci.* 7. doi: 10.3389/fpls.2016.00186.

Kiselev, A., San Clemente, H., Camborde, L., Dumas, B., and Gaulin, E. (2022). A Comprehensive Assessment of the Secretome Responsible for Host Adaptation of the Legume Root Pathogen Aphanomyces euteiches. *JoF* 8, 88. doi: 10.3390/jof8010088.

Kondorosi, E., Roudier, F., and Gendreau, E. (2000). Plant cell-size control: growing by ploidy? *Current Opinion in Plant Biology* 3, 488–492. doi: 10.1016/S1369-5266(00)00118-7.

Krupinska, K., Blanco, N. E., Oetke, S., and Zottini, M. (2020). Genome communication in plants mediated by organelle–n-ucleus-located proteins. *Phil. Trans. R. Soc. B* 375, 20190397. doi: 10.1098/rstb.2019.0397.

Kwon, S., Rupp, O., Brachmann, A., Blum, C. F., Kraege, A., Goesmann, A., et al. (2021). mRNA Inventory of Extracellular Vesicles from Ustilago maydis. *JoF* 7, 562. doi: 10.3390/jof7070562.

Langella, O., Valot, B., Balliau, T., Blein-Nicolas, M., Bonhomme, L., and Zivy, M. (2017). X!TandemPipeline: A Tool to Manage Sequence Redundancy for Protein Inference and Phosphosite Identification. *J. Proteome Res.* 16, 494–503. doi: 10.1021/acs.jproteome.6b00632.

Liu, L., Wang, Z., Li, J., Wang, Y., Yuan, J., Zhan, J., et al. (2021). *Verticillium dahliae* secreted protein Vd424Y is required for full virulence, targets the nucleus of plant cells, and induces cell death. *Mol Plant Pathol* 22, 1109–1120. doi: 10.1111/mpp.13100.

Liu, Y., Lan, X., Song, S., Yin, L., Dry, I. B., Qu, J., et al. (2018). In Planta Functional Analysis and Subcellular Localization of the Oomycete Pathogen Plasmopara viticola Candidate RXLR Effector Repertoire. *Front. Plant Sci.* 9, 286. doi: 10.3389/fpls.2018.00286.

Lo Presti, L., Lanver, D., Schweizer, G., Tanaka, S., Liang, L., Tollot, M., et al. (2015). Fungal Effectors and Plant Susceptibility. *Annu. Rev. Plant Biol.* 66, 513–545. doi: 10.1146/annurev-arplant-043014-114623.

Maunoury, N., Redondo-Nieto, M., Bourcy, M., Van de Velde, W., Alunni, B., Laporte, P., et al. (2010). Differentiation of Symbiotic Cells and Endosymbionts in Medicago truncatula Nodulation Are Coupled to Two Transcriptome-Switches. *PLoS ONE* 5, e9519. doi: 10.1371/journal.pone.0009519.

Narula, K., Datta, A., Chakraborty, N., and Chakraborty, S. (2013). Comparative analyses of nuclear proteome: extending its function. *Front. Plant Sci.* 4. doi: 10.3389/fpls.2013.00100.

Oerke, E.-C. (2006). Crop losses to pests. *J. Agric. Sci.* 144, 31–43. doi: 10.1017/S0021859605005708.

Pecrix, Y., Staton, S. E., Sallet, E., Lelandais-Brière, C., Moreau, S., Carrère, S., et al. (2018). Whole-genome landscape of Medicago truncatula symbiotic genes. *Nature Plants* 4, 1017–1025. doi: 10.1038/s41477-018-0286-7.

Petre, B., Contreras, M. P., Bozkurt, T. O., Schattat, M. H., Sklenar, J., Schornack, S., et al. (2021). Host-interactor screens of *Phytophthora infestans* RXLR proteins reveal vesicle trafficking as a major effector-targeted process. *The Plant Cell* 33, 1447–1471. doi: 10.1093/plcell/koab069.

Ramirez-Garcés, D., Camborde, L., Pel, M. J. C., Jauneau, A., Martinez, Y., Néant, I., et al. (2016). CRN13 candidate effectors from plant and animal eukaryotic pathogens are DNA-binding proteins which trigger host DNA damage response. *New Phytologist* 210, 602–617. doi: 10.1111/nph.13774.

Schornack, S., Damme, M. van, Bozkurt, T. O., Cano, L. M., Smoker, M., Thines, M., et al. (2010). Ancient class of translocated oomycete effectors targets the host nucleus. *PNAS* 107, 17421–17426. doi: 10.1073/pnas.1008491107.

Schwessinger, B., Bart, R., Krasileva, K. V., and Coaker, G. (2015). Focus issue on plant immunity: from model systems to crop species. *Front. Plant Sci.* 6. doi: 10.3389/fpls.2015.00195.

Shan, W., Cao, M., Leung, D., and Tyler, B. M. (2004). The *Avr1b* Locus of *Phytophthora sojae* Encodes an Elicitor and a Regulator Required for Avirulence on Soybean Plants Carrying Resistance Gene *Rps* 1b. *MPMI* 17, 394–403. doi: 10.1094/MPMI.2004.17.4.394.

Sonah, H., Deshmukh, R. K., and Bélanger, R. R. (2016). Computational Prediction of Effector Proteins in Fungi: Opportunities and Challenges. *Front. Plant Sci.* 7. doi: 10.3389/fpls.2016.00126.

Specht, H., Emmott, E., Petelski, A. A., Huffman, R. G., Perlman, D. H., Serra, M., et al. (2021). Single-cell proteomic and transcriptomic analysis of macrophage heterogeneity using SCoPE2. *Genome Biol* 22, 50. doi: 10.1186/s13059-021-02267-5.

Stam, R., Jupe, J., Howden, A. J. M., Morris, J. A., Boevink, P. C., Hedley, P. E., et al. (2013). Identification and Characterisation CRN Effectors in Phytophthora capsici Shows Modularity and Functional Diversity. *PLoS ONE* 8, e59517. doi: 10.1371/journal.pone.0059517.

Voß, S., Betz, R., Heidt, S., Corradi, N., and Requena, N. (2018). RiCRN1, a Crinkler Effector From the Arbuscular Mycorrhizal Fungus Rhizophagus irregularis, Functions in Arbuscule Development. *Front. Microbiol.* 9, 2068. doi: 10.3389/fmicb.2018.02068.

Wahyu Indra Duwi Fanata, Lee, S. Y., and Lee, K. O. (2013). The unfolded protein response in plants: A fundamental adaptive cellular response to internal and external stresses. *Journal of Proteomics* 93, 356–368. doi: 10.1016/j.jprot.2013.04.023.

Wilson, R. A., and McDowell, J. M. (2022). Recent advances in understanding of fungal and oomycete effectors. *Current Opinion in Plant Biology* 68, 102228. doi: 10.1016/j.pbi.2022.102228.

Xi, Y., Chochois, V., Kroj, T., and Cesari, S. (2021). A novel robust and high-throughput method to measure cell death in *Nicotiana benthamiana* leaves by fluorescence imaging. *Mol Plant Pathol* 22, 1688–1696. doi: 10.1111/mpp.13129.

Yan, X., Tang, B., Ryder, L. S., MacLean, D., Were, V. M., Eseola, A. B., et al. (2022). The transcriptional landscape of plant infection by the rice blast fungus *Magnaporthe oryzae* reveals distinct families of temporally co-regulated and structurally conserved effectors. Plant Biology doi: 10.1101/2022.07.18.500532.

Zhou, J., Qi, Y., Nie, J., Guo, L., Luo, M., McLellan, H., et al. (2022). A *Phytophthora* effector promotes homodimerization of host transcription factor StKNOX3 to enhance susceptibility. *Journal of Experimental Botany*, erac308. doi: 10.1093/jxb/erac308.

5.1 Additional results to the chapter V

Flow cytometry also allows to estimate the modification of plant cell cycle by measuring a C-value – the number of genome copies in the nucleus, where 2C value corresponds to a diploid cell. As could be seen from **additional figure 1**, when nuclei of healthy plants are analysed 3 major peaks could be identified, which represent different C-value of the cells. In healthy roots the major peak (60-70%) corresponds to 4C cells with two surrounding smaller peaks (10-20% each). 2C cells represent the cells in mitotic cycle, while 4C and 8C are differentiating cells with higher metabolic activity and often higher cell size, responsible for growth of the organ in size (Kondorosi et al., 2000).

The presence of *A. euteiches* reduces the share of 4C cells (from 70% to 50%) starting from seventh day of infection in our assay, and increases the number of 2C cells from 17% to 40% and 30% at 10dpi and 7dpi respectively). Later in infection *A. euteiches* also reduces the number of 8C cells at 10dpi.

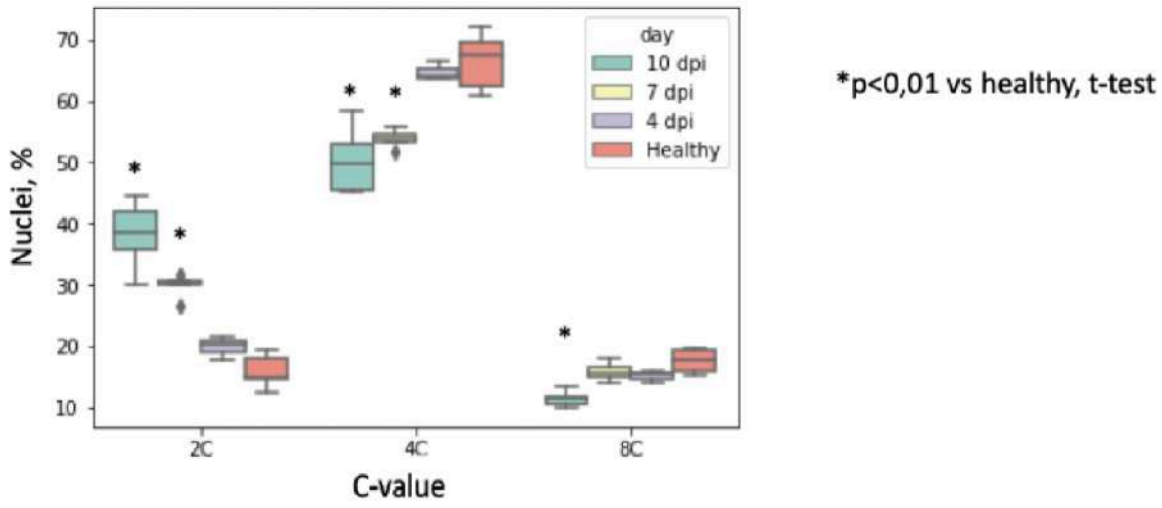

Additional figure 1. *A. euteiches* infection affects the host cell ploidy ratio in time-dependent manner

The sorting plots based on light scattering (nuclei shape) and fluorescence intensity (amount of DNA) allowed to identify clusters corresponding to host and pathogen nuclei. This information, in addition, allowed us to identify a shift of C-value in host tissue. It seems that infection *by A. euteiches* affects cell proliferation and division in the infected tissue, which is indicated as left-shift of a C-values, a measure of cell ploidy: increase of 2C cells and decrease

of 4C cells – the most metabolically active cells. This action of a pathogen is completely controversial to the action of symbiotic organisms, who induce a right-shift of the C-value in plant cells. During nodulation (Maunoury et al., 2010) or establishment of arbuscular mycorrhiza symbiosis (Carotenuto et al., 2019) the microorganisms induce the ccs52-dependent endoreplication, which leads to increase of cell size and metabolic activity of the cells, to serve the needs of hosting the symbiont intracellularly. Future analysis will aim to clarify these preliminary results.

6. General discussion

The global aim of my PhD thesis, was to develop original experimental approaches for identification of effector molecules from *A. euteiches* starting from prediction of the effectors using 'omics' data to functional characterization. This work was performed and coordinated according to a European project 'PROTECTA' funded through Marie Curie Fellowship aims to develop new and innovative ways to control oomycete diseases across the agriculture, environment, forestry and aquaculture sectors.

Plant and animal pathogens from *Aphanomyces* genus significantly affect the cultivation of its host and cause significant production losses, while the only limited disease control solutions are available against the pathogens. In **Chapter II** in collaboration with PhD students participating in the EU project I performed a review, which overlooks the different aspects of *Aphanomyces* biology with a focus on applied aspects of agri- and aquaculture. According to the goal of a 'PROTECTA' project we further performed multiomics analysis of *A. euteiches* – host interaction to perform high-throughput effector detection. In the study we combined genome analysis of *A. euteiches* with transcriptomics (**Chapter III**) and proteomics (**Chapter IV, V**) approach to detect effector repertoire implied in the infection process. Firstly, we obtained a high-quality genome assembly of a pea strain from *A. euteiches* (ATCC201684) and obtained Illumina assemblies from various strains that show different legume preference. A comparative genomics approach *A. euteiches* strains revealed the enrichment of several types of secreted proteins (e.g. proteases) in comparison to other oomycete pathogens. I performed a classification of the small secreted proteins (SSPs) and based on the distribution of various classes of SSPs between *A. euteiches* strains suggested that SSPs could play a key role for a host preference for various strains of the species. SSPs were previously identified as pathogenicity factors in fungi (Kim et al., 2016), while they also abundant in endophytic fungi and mycorrhiza (Daguerre et al., 2020). Within oomycetes several studies focused on Small Cysteine-rich Protein (SCP), which also contribute to the pathogenicity of *P. capsici* (Zhang et al., 2021). However, most of the *A. euteiches* SSPs are genus or species specific proteins (Gaulin et al., 2018) and have no homology with fungal SSPs or oomycete SCSPs. The catalogue of *A. euteiches* SSPs obtained in this study may help to unravel their unknown function. This is exemplified with AeSSP1256, a 'core SPP' from the G-rich class, which hijacks *Medicago truncatula* RNA-helicase from its nucleic target and promotes *A. euteiches* roots' infection (Camborde et al., 2022, **Annex I**)

The genome annotation of *A. euteiches* predicted 1515 secreted proteins, among them numerous as effectors during plant infection. Based on previous effector screening experiments the feasible amount of candidate genes reaches several dozens of genes (Robin et al., 2018). Thus, to restrict the set of effector candidates for functional studies we set up experimental system to reveal *A. euteiches* extracellular protein present during the infection process by proteomics. In addition, since *A. euteiches* is a species in which the genome modification / editing was not established, despite the report of successful CRISPR-Cas9 (Majeed et al., 2018) and RNAi silencing (Iberahim et al., 2020) of another species of the genus *A. invadans*, when required the corresponding effector was transiently expressed in *M. truncatuka* roots to evaluate its effect (Camborde et al., 2022, **Annex I**).

Two novel assays enabling proteomics detection of the effectors *in-vivo* were developed and validated during this PhD research. Both developed assays could be transferred into different plant – pathogen systems with minor modification, which makes those development useful for a whole research community working on plant-pathogen interaction. In **Chapter IV,** as a collaborative work, we focused on the identification of pathogen's secreted proteases present in the apoplasm of the infected plant. The study confirmed a genomics observation of a large secreted proteolytic repertoire of *A. euteiches* and led to identification of novel types of secreted modular proteases of *A. euteiches* which harbour an additional binding domain to the catalytic site. The **Chapter V** describes the work aiming at the identification of *A. euteiches* proteins able to target *M. truncatula* nucleus during the interaction, in order to identify for functional studies putative nuclear-targeting effector. Indeed numerous oomycete effectors have been reported to act within this compartment as previously exemplified in our research group with AeSS1256 (Camborde et al., 2022, **Annex I**) and AeCRN13 (Ramirez-Garcés et al., 2016, p.). As a collaborative work, we developed a FACS coupled with proteomics assay to detect *in-vivo* plant nuclear targeting proteins from *A. euteiches.* As a proof of concept, we identified two homologs of known nuclear effectors from other species as well as three SSP.

Overall, my PhD work gives new insights, presented here below, into oomycete genome organization and content and the effector repertoire deploys by these pathogens to facilitate infection. This work is also a continuation of a genomics study of *Aphanomyces spp.* performed in our research group (Gaulin et al., 2018; Gaulin et al., 2008b), altogether these studies broaden the understanding of plant-oomycete interaction mechanism as *Aphanomyces* genus is phylogenetically distant from other well-studied plant pathogenic oomycetes such as *Phytophthora spp., Peronospora spp, Pythium spp.*

6.1 Genomics studies in oomycetes

Genome analysis in oomycete began in 2009 from the publication of the *Phytophthora infestans* genome by Haas et al. Later it appeared that the 229 kb genome of *P. infestans* is a kind of a unique situation, while the most of the now sequenced genomes of oomycetes fit into a frame of 40-80 kb (McGowan and Fitzpatrick, 2020). The whole-genome studies allowed the understanding of the genome organisation of oomycetes. For many oomycetes Peronosporales and Pythiales orders the compartmentalization of the genome into gene-rich and gene-poor regions was demonstrated, suggesting that fast-evolving pathogenicity related genes are encoded in gene-poor region with larger proportion of repeats (Dong et al., 2015; Faure et al., 2020), which might play a role in effector evolution (Fouché et al., 2018). In contrast, genome of Saprolegniales oomycetes, such as *Saprolegnia parasitica* (Jiang et al., 2013b) and *A. euteiches* (Kiselev et al., 2022, **Chapter III**) didn't demonstrate as high compartimentalisation as other oomycetes. Interestingly, the long-read assembly of *A. euteiches* genome allowed sequencing of repeated regions in comparison to a previous genome version (E Gaulin et al., 2018), however, they were poorly assembled into long contigs and formed numerous short gene-poor contigs (**Chapter III, Fig. 1**).

Among the drivers for a rapid pathogen's evolution there are transposable elements (TE) and satellite DNA (satDNA). TE are able to translocate or replicate large genomic regions and facilitate the effector's set regulation as well as effectors transcription regulation (Wicker et al., 2007). SatDNA is usually represented by 100-500 bp tandemly repeated often found at centromeric, pericentromeric, and telomeric regions monomers, which are repeated in the genome hundreds or thousands of times (Garrido-Ramos, 2017). Knowing of the landscape of the repetitive sequences in the genome is crucial for a better understanding of their role in the pathogenicity evolution of oomycetes, many of which are able rapidly evolve into new races and overcome the resistant host genotypes (Hannat et al., 2021). In *P. parasitica* two families of satDNA were characterized upon the long-read genome assembly. *PpSat1* family is highly conserved among oomycetes and was found in *A. stellatus,* the potential role of *PpSat1* family could assigned to a centromeric satDNA, while the role of *PpSat2* is not known (Panabières et al., 2020). Our study demonstrated that both of the *P. parasitica* satDNA families are present in *A. euteiches* genome along with another 39 satDNA families. Three clusters of *A. euteiches* satDNA were represented as high-copy repeats with over 1000 occurrence in the genome. Therefore *A. euteiches* genome possesses the satDNA families previously identified in *P.*

parasitica together with unique families, while some of them appeared to highly copied in the genome.

Comparative genomics studies of oomycetes demonstrated that tandem gene duplication is one of the main drivers for effector set expansion in oomycetes (McGowan et al., 2019). In the evolution history of oomycetes the expansion of a kinome (set of kinases) happened upon the divergence of Saprolegniales order as well as the expansion of RxLR effectors happened upon the divergence of *Phytophthora* genus (Jiang et al., 2013b). Often effectors are physically present in the genome clusters, for example RxLR effectors in *Phytophthora* or *Peronospora* (Fletcher et al., 2022; Haas et al., 2009), in *A. euteiches* genome the clusters of small secreted proteins (SSP) were also identified (Gaulin et al., 2018). Interestingly, the localization in the same cluster doesn't mean the identical expression pattern of the effectors from the cluster. Studying the secretome of *A. euteiches* we observed the expansion of the secreted proteolytic enzymes (**Chapter III, Fig. 6**), which were previously thought to be an adaptation to an animal host in Saprolegniales order as much lower number of proteases are present in other phytopathogenic organisms. Closer look on the secreted proteases in *A. euteiches* genome (**Chapter IV, Fig. 1**) demonstrated that over 80% of the proteases are located are organized in cluster and are tandemly repeated within a cluster.

In the comparative genomics of *A. euteiches* strains we reported five categories of secreted proteins with a predictable PFAM domain to represent the core secretome of *A. euteiches*, those are adhesion, cysteine-rich, toxic, proteolytic and carbohydrate active (CAZy) proteins. Previously it was reported that the differences in CAZymes between *Aphanomyces* species is one of the key adaptation to plant or animal host (Gaulin et al., 2018). Variations in CAZyme repertoire within whole oomycete lineage is shown to be correlated with an oomycete lifestyle with a numerous gene losses in obligate biotrophs such as *Bremia lactucae* (McGowan and Fitzpatrick, 2020). The analysis of gene presence-absence in different strains of *A. euteiches* demonstrated that proteins with a predictable PFAM domain predominantly belong to core and accessory secretome, while the short proteins without a predictable domain are mainly present as singletons. This distribution suggests that small extracellular proteins might contribute to a local environment adaptation. Genome-wide association studies of fungal wheat pathogen *Zymoseptoria tritici* identified small cysteine-rich protein AvrStb6 as a rapidly evolving protein contributing to virulence or avirulence of the strain (Zhong et al., 2017).

6.2 Apoplastic effectors *in vivo* identification

In the genomics analysis of *A. euteiches* we have demonstrated the enrichment in secreted proteolytic enzymes. Secreted proteases are known to play a role in plant-pathogen interaction from both sides. P69B apoplastic cysteine protease from tomato is a key component of an apoplastic immune cascade (Paulus et al., 2020). On the pathogen's side the global proteomics analysis of plant-pathogen interaction revealed the presence of secreted proteases in the samples (Meijer et al., 2014; van der Hoorn et al., 2004). The global survey of *P. infestans* metalloproteases demonstrated their diversity in a genome and also showed that some of them could enhance or diminish the pathogenicity of *P. infestans* (Schoina et al., 2021).

To characterize *A. euteiches* secreted proteases were applied Activity Based Protein Profiling (ABPP) to identify secreted proteases in the apoplasm of infected tissue. This approach is widely used to monitor plant enzymatic activity in the apoplasm in different conditions (Kaschani et al., 2009; van der Hoorn, 2011; van der Hoorn et al., 2004). We exploited the similar approach to focus on survey of pathogen's proteases in the apoplasm of a natural host *A. euteiches – Pisum sativum.* Using two commercially available probes: FP and DCG-04 we targeted Serine and Cysteine proteases – two the most abundant classes of proteases in *A. euteiches.* Transcriptomics analysis revealed that 99 out of 115 Ser/Cys proteases have a transcript in any of the infection stages, while the ABPP proteomics analysis at 15 days post infection identified around 30% of the Ser/Cys proteases as proteins in the apoplasm. Among the identified proteins there were classical Serine proteases represented by trypsins, subtilisns and carboxypeptidases S10 and S28 and Papain-like cysteine proteases. In addition to classical protease we identified modular proteases, which consist of a proteolytic N-terminal domain and additional 'binding' domain attached through a linker, which predicted to be disordered (**Chapter IV, Fig. 6**). N-terminal part represented by domains with affinity to carbohydrates or lipids: CBD, PAN, CAP, ML. Papain-like + ML-domain proteases are present in several species of Stramenopiles lineages, while other combinations are specific to *A. euteiches.* The presence of a binding domain can direct the activity of the secreted proteases against specific targets. Further functional studies required to understand the targets of the identified modular proteases.

Secreted proteases can be active in remodeling of a host cell wall, as it was demonstrated for a Trypsin SNP1 trypsin from *Parastagonospora (Stagnosphora) nodorum*. (Carlile et al., 2000). It also cannot be excluded that extracellular proteases are aimed on a pathogen's cell wall remodeling or interaction with a host defense proteins or immune

proteolytic cascades, however, examples of these roles of extracellular proteases are missing. Taking in account the growing interest in studying proteolytic enzymes, we can expect further understanding of extracellular protease role in plant-oomycete interactions.

6.3 Nuclear effectors *in vivo* identification

Numerous fungal and oomycetes effectors are suspected to target host nuclei to modify its physiology. As example a high-throughput studies of RxLR and CRN effectors from oomycetes (Liu et al., 2018, Caillaud et al., 2012, Stam et al., 2013, Chen et al., 2020). showed that over 60% of the tested proteins were localized in nuclei. However, the studies were performed on overexpressed proteins tagged with a fluorescent tag. Similarly in our research group by using tagged-proteins we characterized the activity of AeCRN13 and AeSSP1256 within the plant nucleus (Camborde et al., 2022; Ramirez-Garcés et al., 2016). Up to now no *in vivo* proteomics studies were performed to demonstrate the presence of microbial eukaryotic proteins within the host nuclei during the infection and support genome prediction. Thus, to perform a global survey of the nuclear-targeting proteins from *A. euteiches* we developed a Fluorescence-assisted cell sorting (FACS) coupled with mass spec proteomics assay.

A quick and easy method for isolation of plant nuclei from non-infected leaves material was recently reported (Bourge et al., 2018), therefore we decided to test whether this method could be suitable for distinguishing of nuclei of two organisms in an infected root tissues. The distribution of the light intensity and light scattering from both species allowed to distinguish signals from different species and apply gating for collection of the nuclei from *M. truncatula* and *A. euteiches* into different wells. Whereas FACS output demonstrated clear peak separation of the species, the followed proteomics analysis showed that a large amount of proteins from host and pathogen were present in separately collected samples. Even if we cannot exclude transfer of proteins between the two types of nuclei or putative contaminations from cytosol, we can suggest to improve the separation to stricter gating, and to use smaller number of sorted nuclei for the proteomics analysis. This will decrease the concentration of proteins from 'contaminating' nuclei to an undetectable level. In addition, the use of microfluidic technology for isolation of nuclei could be used to perform a proteomics on a single cell level (Specht et al., 2021). In comparison to previous untargeted proteomics studies (Fabre et al., 2019) this method allows to target the particular cellular compartment and enrich the sample to increase the probability of effector detection.

Despite the lack of separation in the proteomics results we could quickly identify 25 potential effectors: among them Avr1b-like protein, nuclear localized GH11, GH18 and several SSPs. The Avr1b-like protein from *A. euteiches* has a very high similarity with the corresponding RxLR from *P. parasitica* at C-terminus of the protein while the N-terminus is highly distinct. The ortholog of the effector Vd424 from *V. dahliae* with a GH11 domain is unique to *A. euteiches* since no similar sequence have been detected in others oomycetes. SSPs identified in this work are also specific to *A. euteiches* and distinct from the previously characterized AeSSP1256. Using the developed assay, we identified the RxLR-like effector, which harbours the C-term domain of the Avr1b effector but lacks the RxLR motif itself and also identified atypical GH11 and GH18 putative nuclear effectors, which together with the previous evidence of Vd424 GH11 effector might postulate that glycoside hydrolases have the role within plant host nuclei during the infection process.

Perspectives of the PhD work

The assembly of a reference genome gives opportunities to study the effector repertoire of the species and performs comparative analysis with other species. In our work we assembled the high-quality genome of *A. euteiches* ATCC201684, however some parts of the genome remained unresolved and represented as short contigs (10-100 kb). Unfortunately, in our work we failed to produce genome optical mapping to compose a chromosome-level genome assembly. To further complete *A. euteiches* genome assembly, chromatin conformation capture sequencing could be used for production of telomere-to-telomere sequence, as was performed for arbuscular mycorrhizal fungus *Rhizophagus irregularis* (Yildirir et al., 2022). Whole chromosome genome assembly allows to trace the genomics rearrangement happened in species evolution (Fletcher et al., 2022), which is extremely interesting in case of *Aphanomyces* genus which demonstrates high diversity in hosts preferences (plants, animals) among the species.

Comparative analysis of five strains of *A. euteiches* with different host preferences highlighted the core and accessory secretome of the species, which can contribute to the host adaptation. The next level of understanding of a species evolution could be obtained through Genome Wide Associations study (GWAS) of pathogenicity and host preferences of various natural genotypes. Different research groups around the world have their collections of field-isolated *A. euteiches* genotypes tested for their pathogenicity against host (see the recent studies Quillévéré-Hamard et al., 2020; Sivachandra Kumar et al., 2021), therefore GWAS studies on these collections will shed a light on genomic regions responsible for determination of races

and pathotypes. To obtain enough genomics data for GWAS analysis the high-quality genome assembly of several distant strains must be obtained including one assembled in the present work, while for the most of the strains low-coverage sequences will be sufficient to map the polymorphisms (Chat et al., 2022). This work might have a distinct interest from both academic and industrial community since no molecular genomics studies were performed to unravel *A. euteiches* ability to overcome the resistance in cultivated crop genotypes. The emergence of new races causing a problem for agricultural sector, while the understanding of molecular bases of an adaptation and continuous surveillance of the genotypes in the soil could help in plant breeding and the risk assessments (Dussault-Benoit et al., 2020).

In this work, we aimed to develop two proteomics-based approaches for effector detection. *In-silico* prediction of the pathogenicity factors in the genome usually outputs several hundreds of potential effectors, therefore the robust method for detection of the effectors which are present as proteins during the infection is necessary for further shortlisting the candidates for functional studies, especially in the species without an established techniques of genome manipulation as *A. euteiches*. Finally, both approaches revealed few dozens of proteins, which is a reasonable quantity to process with functional characterization. Since unexpected extracellular proteins have been identified, I believe that the results present in the thesis will contribute to further identification of original molecular mechanism developed by *A. euteiches* to invade legume. For example, the identification of an additional 'binding' domain in *A. euteiches* modular extracellular proteases can help the identification of the target of the proteases.

The two developed assays with minor modifications could be applied to many filamentous pathogen – host pathosystems, since they do not include any species-specific steps neither in apoplastic fluid extraction nor the nuclei purification. To ensure the capturing of more complete snapshot of the secreted proteins various infection datapoints could be analysed (i.e early, later infection stages). In addition, both approaches allow the characterization of the plant proteins repertoire, the data could be analysed in comparison with experiments performed in *A. thaliana* and *N. benthamiana*, especially for extracellular proteolytic enzymes and protease-based immune cascade were numerous studies used these plants (Kaschani et al., 2009; Paulus et al., 2020). Despite we have identified interesting candidates, functional studies are required to unravel the complexity of the interaction with *M. truncatula.*

6.4 General Conclusion

This PhD work provided the novel long-read based assembly of a reference strain of *A. euteiches* ATCC201684 as well as Illumina-based assemblies of four other strains with various host preferences. The comparative analysis provided the insights into a core and specific secretome of *A. euteiches,* suggesting that a large set of Small Secreted Proteins could be a source for a host adaptation within a species. This research work set up two new proteomics technics to support effector repertoire prediction and to prioritize effector candidates for functional studies. With minors' modifications, the developed experimental systems could be applied to various plant-microbe pathosystems. Finally, the two proteomics approaches based either on apoplastic proteases or nuclear proteins characterization, revealed unexpected and original extracellular proteins form *A. euteiches* that probably have a key role for plant infection.

Both of the developed proteomics assays produced the dataset of the putative effectors, which included the typical effectors, e.g. Trypsins or Subtilisins of the apoplastic space and SSPs or RxLR-like proteins as nuclear proteins, which confirms the functionality of the assays and conformity with our previous knowledge on effectors spatial classification. In addition, the assays nominated atypical effector candidate such as 'modular' proteases active in the apoplasm and glycoside hydrolases as nuclear effectors. Therefore, it highlights the usefulness of direct proteomics-based approaches that they allow to select the effectors with limited or no use of the previous knowledge of which proteins are expected in the given compartment which allows the identification of atypical proteins which might contribute to plant-pathogen molecular cross-talk. Further functional assays are needed for the confirmation of the activity of atypical effectors.

Overall, this PhD work produced new knowledge on *A. euteiches* genome organisation and host adaptation. Together with the effectors candidates identified using multi-omics approaches this work will contribute to the functional characterization of new effector types of *A. euteiches* and will lead to the further understanding of oomycete pathogenicity.

7. References

Almagro Armenteros, Jose Juan, Salvatore, M., Emanuelsson, O., Winther, O., von Heijne, G., Elofsson, A., Nielsen, H., 2019. Detecting sequence signals in targeting peptides using deep learning. Life Sci. Alliance 2, e201900429. https://doi.org/10.26508/lsa.201900429

Almagro Armenteros, José Juan, Tsirigos, K.D., Sønderby, C.K., Petersen, T.N., Winther, O., Brunak, S., von Heijne, G., Nielsen, H., 2019. SignalP 5.0 improves signal peptide predictions using deep neural networks. Nature Biotechnology 37, 420–423. https://doi.org/10.1038/s41587-019-0036-z

Altschul, S.F., Gish, W., Miller, W., Myers, E.W., Lipman, D.J., 1990. Basic local alignment search tool. J. Mol. Biol. 215, 403–410. https://doi.org/10.1016/S0022-2836(05)80360-2

Anderson, R.G., Deb, D., Fedkenheuer, K., McDowell, J.M., 2015. Recent Progress in RXLR Effector Research. MPMI 28, 1063–1072. https://doi.org/10.1094/MPMI-01-15-0022-CR

Ashikari, M., Matsuoka, M., 2006. Identification, isolation and pyramiding of quantitative trait loci for rice breeding. Trends in Plant Science 11, 344–350. https://doi.org/10.1016/j.tplants.2006.05.008

Babadoost, M., Pavon, C., 2013. Survival of Oospores of *Phytophthora capsici* in Soil. Plant Disease 97, 1478–1483. https://doi.org/10.1094/PDIS-12-12-1123-RE

Badreddine, I., Lafitte, C., Heux, L., Skandalis, N., Spanou, Z., Martinez, Y., Esquerré-Tugayé, M.-T., Bulone, V., Dumas, B., Bottin, A., 2008. Cell Wall Chitosaccharides Are Essential Components and Exposed Patterns of the Phytopathogenic Oomycete *Aphanomyces euteiches*. Eukaryot Cell 7, 1980–1993. https://doi.org/10.1128/EC.00091-08

Balint-Kurti, P., 2019. The plant hypersensitive response: concepts, control and consequences. Molecular Plant Pathology mpp.12821. https://doi.org/10.1111/mpp.12821

Bari, R., Jones, J.D.G., 2009. Role of plant hormones in plant defence responses. Plant Mol Biol 69, 473–488. https://doi.org/10.1007/s11103-008-9435-0

Bazyli, C., Ewa, C.S., Adrianna, S.G., Bazyli, C., Ewa, C.S., Adrianna, S.G., 2015. Ecological diversity and economical importance of species from Aphanomyces genus. Afr. J. Agric. Res. 10, 4356–4363. https://doi.org/10.5897/AJAR2015.9736

Becking, T., Kiselev, A., Rossi, V., Street-Jones, D., Grandjean, F., Gaulin, E., 2021. Pathogenicity of animal and plant parasitic Aphanomyces spp and their economic impact on aquaculture and agriculture. Fungal Biology Reviews S1749461321000397. https://doi.org/10.1016/j.fbr.2021.08.001

Bi, G., Su, M., Li, N., Liang, Y., Dang, S., Xu, J., Hu, M., Wang, J., Zou, M., Deng, Y., Li, Q., Huang, S., Li, J., Chai, J., He, K., Chen, Y., Zhou, J.-M., 2021. The ZAR1 resistosome is a calcium-permeable channel triggering plant immune signaling. Cell 184, 3528-3541.e12. https://doi.org/10.1016/j.cell.2021.05.003

Białas, A., Zess, E.K., De la Concepcion, J.C., Franceschetti, M., Pennington, H.G., Yoshida, K., Upson, J.L., Chanclud, E., Wu, C.-H., Langner, T., Maqbool, A., Varden, F.A., Derevnina, L., Belhaj, K., Fujisaki, K., Saitoh, H., Terauchi, R., Banfield, M.J., Kamoun, S., 2018. Lessons in Effector and NLR Biology of Plant-Microbe Systems. MPMI 31, 34–45. https://doi.org/10.1094/MPMI-08-17-0196-FI

Bigeard, J., Colcombet, J., Hirt, H., 2015. Signaling Mechanisms in Pattern-Triggered Immunity (PTI). Molecular Plant 8, 521–539. https://doi.org/10.1016/j.molp.2014.12.022

Birch, P.R., Boevink, P.C., Gilroy, E.M., Hein, I., Pritchard, L., Whisson, S.C., 2008. Oomycete RXLR effectors: delivery, functional redundancy and durable disease resistance. Current Opinion in Plant Biology 11, 373–379. https://doi.org/10.1016/j.pbi.2008.04.005

Bogdan, J., Ag, P., 2019. Aphanomyces Root Rot in Pulse Crops 5.

Bonhomme, M., André, O., Badis, Y., Ronfort, J., Burgarella, C., Chantret, N., Prosperi, J.-M., Briskine, R., Mudge, J., Debéllé, F., Navier, H., Miteul, H., Hajri, A., Baranger, A., Tiffin, P., Dumas, B., Pilet-Nayel, M.-L., Young, N.D., Jacquet, C., 2014. High-density genome-wide association mapping implicates an F-box encoding gene in Medicago truncatula resistance to Aphanomyces euteiches. New Phytol 201, 1328–1342. https://doi.org/10.1111/nph.12611

Bonhomme, M., Jacquet, C., 2020. Genome-wide association mapping and population genomic features in *Medicago truncatula*, in: de Bruijn, F. (Ed.), The Model Legume Medicago Truncatula. Wiley, pp. 870–881. https://doi.org/10.1002/9781119409144.ch109

Bourge, M., Brown, S.C., Siljak-Yakovlev, S., 2018. Flow cytometry as tool in plant sciences, with emphasis on genome size and ploidy level assessment. GenApp 2, 1. https://doi.org/10.31383/ga.vol2iss2pp1-12

Brameier, M., Krings, A., MacCallum, R.M., 2007. NucPred Predicting nuclear localization of proteins. Bioinformatics 23, 1159–1160. https://doi.org/10.1093/bioinformatics/btm066

Brückner, A., Polge, C., Lentze, N., Auerbach, D., Schlattner, U., 2009. Yeast Two-Hybrid, a Powerful Tool for Systems Biology. IJMS 10, 2763–2788. https://doi.org/10.3390/ijms10062763

Camborde, L., Kiselev, A., Pel, M.J.C., Le Ru, A., Jauneau, A., Pouzet, C., Dumas, B., Gaulin, E., 2022. An oomycete effector targets a plant RNA helicase involved in root development and defense. New Phytologist nph.17918. https://doi.org/10.1111/nph.17918

Camborde, L., Raynaud, C., Dumas, B., Gaulin, E., 2019. DNA-Damaging Effectors: New Players in the Effector Arena. Trends in Plant Science 24, 1094–1101. https://doi.org/10.1016/j.tplants.2019.09.012

Caprioli, R., Mrugała, A., Di Domenico, M., Curini, V., Giansante, C., Cammà, C., Petrusek, A., 2018. Aphanomyces astaci genotypes involved in recent crayfish plague outbreaks in central Italy. Dis. Aquat. Org. 130, 209–219. https://doi.org/10.3354/dao03275

Carlile, A.J., Bindschedler, L.V., Bailey, A.M., Bowyer, P., Clarkson, J.M., Cooper, R.M., 2000. Characterization of SNP1, a Cell Wall-Degrading Trypsin, Produced During Infection by *Stagonospora nodorum*. MPMI 13, 538–550. https://doi.org/10.1094/MPMI.2000.13.5.538

Carrión, V.J., Perez-Jaramillo, J., Cordovez, V., Tracanna, V., Hollander, M. de, Ruiz-Buck, D., Mendes, L.W., Ijcken, W.F.J. van, Gomez-Exposito, R., Elsayed, S.S., Mohanraju, P., Arifah, A., Oost, J. van der, Paulson, J.N., Mendes, R., Wezel, G.P. van, Medema, M.H., Raaijmakers, J.M., 2019. Pathogen-induced activation of disease-suppressive functions in the endophytic root microbiome. Science 366, 606–612. https://doi.org/10.1126/science.aaw9285

Césari, S., Kanzaki, H., Fujiwara, T., Bernoux, M., Chalvon, V., Kawano, Y., Shimamoto, K., Dodds, P., Terauchi, R., Kroj, T., 2014. The NB - LRR proteins RGA 4 and RGA 5 interact functionally and physically to confer disease resistance. EMBO J 33, 1941–1959. https://doi.org/10.15252/embj.201487923

Chaparro-Garcia, A., Wilkinson, R.C., Gimenez-Ibanez, S., Findlay, K., Coffey, M.D., Zipfel, C., Rathjen, J.P., Kamoun, S., Schornack, S., 2011. The Receptor-Like Kinase

SERK3/BAK1 Is Required for Basal Resistance against the Late Blight Pathogen Phytophthora infestans in Nicotiana benthamiana. PLoS ONE 6, e16608. https://doi.org/10.1371/journal.pone.0016608

Chat, V., Ferguson, R., Morales, L., Kirchhoff, T., 2022. Ultra Low-Coverage Whole-Genome Sequencing as an Alternative to Genotyping Arrays in Genome-Wide Association Studies. Front. Genet. 12, 790445. https://doi.org/10.3389/fgene.2021.790445

Chen, J., Li, M., Liu, L., Chen, G., Fu, Z.Q., 2021. ZAR1 resistosome and helper NLRs: Bringing in calcium and inducing cell death. Molecular Plant 14, 1234–1236. https://doi.org/10.1016/j.molp.2021.06.026

Chen, S., Ma, T., Song, S., Li, X., Fu, P., Wu, W., Liu, J., Gao, Y., Ye, W., Dry, I.B., Lu, J., 2021. Arabidopsis downy mildew effector HaRxLL470 suppresses plant immunity by attenuating the DNA-binding activity of bZIP transcription factor HY5. New Phytol 230, 1562–1577. https://doi.org/10.1111/nph.17280

Chen, Xiaoyang, Duan, Y., Qiao, F., Liu, H., Huang, J., Luo, C., Chen, Xiaolin, Li, G., Xie, K., Hsiang, T., Zheng, L., 2022. A secreted fungal effector suppresses rice immunity through host histone hypoacetylation. New Phytologist 235, 1977–1994. https://doi.org/10.1111/nph.18265

Cheng, W., Lin, M., Chu, M., Xiang, G., Guo, J., Jiang, Y., Guan, D., He, S., 2022. RNAi-Based Gene Silencing of RXLR Effectors Protects Plants Against the Oomycete Pathogen *Phytophthora capsici*. MPMI 35, 440–449. https://doi.org/10.1094/MPMI-12-21-0295-R

Chepsergon, J., Motaung, T.E., Moleleki, L.N., 2021. "Core" RxLR effectors in phytopathogenic oomycetes: A promising way to breeding for durable resistance in plants? Virulence 12, 1921–1935. https://doi.org/10.1080/21505594.2021.1948277

Choi, J., Park, J., Kim, D., Jung, K., Kang, S., Lee, Y.-H., 2010. Fungal Secretome Database: Integrated platform for annotation of fungal secretomes. BMC Genomics 11, 105. https://doi.org/10.1186/1471-2164-11-105

Croll, D., McDonald, B.A., 2012. The Accessory Genome as a Cradle for Adaptive Evolution in Pathogens. PLoS Pathog 8, e1002608. https://doi.org/10.1371/journal.ppat.1002608

Daguerre, Y., Basso, V., Hartmann-Wittulski, S., Schellenberger, R., Meyer, L., Bailly, J., Kohler, A., Plett, J.M., Martin, F., Veneault-Fourrey, C., 2020. The mutualism effector MiSSP7 of Laccaria bicolor alters the interactions between the poplar JAZ6 protein and its associated proteins. Sci Rep 10, 20362. https://doi.org/10.1038/s41598-020-76832-6

Dahlin, P., Srivastava, V., Ekengren, S., McKee, L.S., Bulone, V., 2017. Comparative analysis of sterol acquisition in the oomycetes Saprolegnia parasitica and Phytophthora infestans. PLoS ONE 12, e0170873. https://doi.org/10.1371/journal.pone.0170873

Darino, M., Chia, K., Marques, J., Aleksza, D., Soto-Jiménez, L.M., Saado, I., Uhse, S., Borg, M., Betz, R., Bindics, J., Zienkiewicz, K., Feussner, I., Petit-Houdenot, Y., Djamei, A., 2021. *Ustilago maydis* effector Jsi1 interacts with Topless corepressor, hijacking plant jasmonate/ethylene signaling. New Phytol 229, 3393–3407. https://doi.org/10.1111/nph.17116

de Guillen, K., Ortiz-Vallejo, D., Gracy, J., Fournier, E., Kroj, T., Padilla, A., 2015. Structure Analysis Uncovers a Highly Diverse but Structurally Conserved Effector Family in Phytopathogenic Fungi. PLoS Pathog 11, e1005228. https://doi.org/10.1371/journal.ppat.1005228

de Jonge, R., Peter van Esse, H., Kombrink, A., Shinya, T., Desaki, Y., Bours, R., van der Krol, S., Shibuya, N., Joosten, M.H.A.J., Thomma, B.P.H.J., 2010. Conserved Fungal LysM Effector Ecp6 Prevents Chitin-Triggered Immunity in Plants. Science 329, 953–955. https://doi.org/10.1126/science.1190859

Derevnina, L., Dagdas, Y.F., Concepcion, J.C.D. la, Bialas, A., Kellner, R., Petre, B., Domazakis, E., Du, J., Wu, C.-H., Lin, X., Aguilera-Galvez, C., Cruz-Mireles, N., Vleeshouwers, V.G.A.A., Kamoun, S., 2016. Nine things to know about elicitins. New Phytologist 212, 888–895. https://doi.org/10.1111/nph.14137

Desgroux, A., L'Anthoëne, V., Roux-Duparque, M., Rivière, J.-P., Aubert, G., Tayeh, N., Moussart, A., Mangin, P., Vetel, P., Piriou, C., McGee, R.J., Coyne, C.J., Burstin, J., Baranger, A., Manzanares-Dauleux, M., Bourion, V., Pilet-Nayel, M.-L., 2016. Genome-wide association mapping of partial resistance to Aphanomyces euteiches in pea. BMC Genomics 17, 124. https://doi.org/10.1186/s12864-016-2429-4

Deutsch, C.A., Tewksbury, J.J., Tigchelaar, M., Battisti, D.S., Merrill, S.C., Huey, R.B., Naylor, R.L., 2018. Increase in crop losses to insect pests in a warming climate. Science 361, 916–919. https://doi.org/10.1126/science.aat3466

Diéguez-Uribeondo, J., García, M.A., Cerenius, L., Kozubíková, E., Ballesteros, I., Windels, C., Weiland, J., Kator, H., Söderhäll, K., Martín, M.P., 2009. Phylogenetic relationships among plant and animal parasites, and saprotrophs in Aphanomyces (Oomycetes). Fungal Genetics and Biology 46, 365–376. https://doi.org/10.1016/j.fgb.2009.02.004

Djamei, A., Schipper, K., Rabe, F., Ghosh, A., Vincon, V., Kahnt, J., Osorio, S., Tohge, T., Fernie, A.R., Feussner, I., Feussner, K., Meinicke, P., Stierhof, Y.-D., Schwarz, H., Macek, B., Mann, M., Kahmann, R., 2011. Metabolic priming by a secreted fungal effector. Nature 478, 395–398. https://doi.org/10.1038/nature10454

Djébali, N., Jauneau, A., Ameline-Torregrosa, C., Chardon, F., Jaulneau, V., Mathé, C., Bottin, A., Cazaux, M., Pilet-Nayel, M.-L., Baranger, A., Aouani, M.E., Esquerré-Tugayé, M.-T., Dumas, B., Huguet, T., Jacquet, C., 2009. Partial resistance of Medicago truncatula to Aphanomyces euteiches is associated with protection of the root stele and is controlled by a major QTL rich in proteasome-related genes. Mol. Plant Microbe Interact. 22, 1043–1055. https://doi.org/10.1094/MPMI-22-9-1043

Dodds, P.N., Rathjen, J.P., 2010. Plant immunity: towards an integrated view of plant–pathogen interactions. Nat Rev Genet 11, 539–548. https://doi.org/10.1038/nrg2812

Dong, S., Raffaele, S., Kamoun, S., 2015. The two-speed genomes of filamentous pathogens: waltz with plants. Curr. Opin. Genet. Dev. 35, 57–65. https://doi.org/10.1016/j.gde.2015.09.001

Dong, Y., Li, Y., Qi, Z., Zheng, X., Zhang, Z., 2016. Genome plasticity in filamentous plant pathogens contributes to the emergence of novel effectors and their cellular processes in the host. Curr Genet 62, 47–51. https://doi.org/10.1007/s00294-015-0509-7

Du, J., Verzaux, E., Chaparro-Garcia, A., Bijsterbosch, G., Keizer, L.C.P., Zhou, J., Liebrand, T.W.H., Xie, C., Govers, F., Robatzek, S., van der Vossen, E.A.G., Jacobsen, E., Visser, R.G.F., Kamoun, S., Vleeshouwers, V.G.A.A., 2015. Elicitin recognition confers enhanced resistance to Phytophthora infestans in potato. Nature Plants 1, 15034. https://doi.org/10.1038/nplants.2015.34

Dussault-Benoit, C., Arsenault-Labrecque, G., Sonah, H., Belzile, F., Bélanger, R.R., 2020. Discriminant haplotypes of avirulence genes of *Phytophthora sojae* lead to a molecular assay to predict phenotypes. Molecular Plant Pathology 21, 318–329. https://doi.org/10.1111/mpp.12898

Dussert, Y., Mazet, I.D., Couture, C., Gouzy, J., Piron, M.-C., Kuchly, C., Bouchez, O., Rispe, C., Mestre, P., Delmotte, F., 2019. A High-Quality Grapevine Downy Mildew Genome Assembly Reveals Rapidly Evolving and Lineage-Specific Putative Host Adaptation Genes. Genome Biology and Evolution 11, 954–969. https://doi.org/10.1093/gbe/evz048

Elad, Y., Williamson, B., Tudzynski, P., Delen, N., 2007. Botrytis spp. and Diseases They Cause in Agricultural Systems – An Introduction, in: Elad, Y., Williamson, B.,

Tudzynski, P., Delen, N. (Eds.), Botrytis: Biology, Pathology and Control. Springer Netherlands, Dordrecht, pp. 1–8. https://doi.org/10.1007/978-1-4020-2626-3_1

Erffelinck, M.-L., Ribeiro, B., Perassolo, M., Pauwels, L., Pollier, J., Storme, V., Goossens, A., 2018. A user-friendly platform for yeast two-hybrid library screening using next generation sequencing. PLoS ONE 13, e0201270. https://doi.org/10.1371/journal.pone.0201270

Fabre, F., Vignassa, M., Urbach, S., Langin, T., Bonhomme, L., 2019. Time-resolved dissection of the molecular crosstalk driving *Fusarium* head blight in wheat provides new insights into host susceptibility determinism. Plant Cell Environ 42, 2291–2308. https://doi.org/10.1111/pce.13549

Fabro, G., 2022. Oomycete intracellular effectors: specialised weapons targeting strategic plant processes. New Phytologist 233, 1074–1082. https://doi.org/10.1111/nph.17828

Fabro, G., Steinbrenner, J., Coates, M., Ishaque, N., Baxter, L., Studholme, D.J., Körner, E., Allen, R.L., Piquerez, S.J.M., Rougon-Cardoso, A., Greenshields, D., Lei, R., Badel, J.L., Caillaud, M.-C., Sohn, K.-H., Van den Ackerveken, G., Parker, J.E., Beynon, J., Jones, J.D.G., 2011. Multiple Candidate Effectors from the Oomycete Pathogen Hyaloperonospora arabidopsidis Suppress Host Plant Immunity. PLoS Pathog 7, e1002348. https://doi.org/10.1371/journal.ppat.1002348

Faure, C., Veyssière, M., Boëlle, B., Clemente, H.S., Bouchez, O., Lopez-Roques, C., Chaubet, A., Martinez, Y., Bezouška, K., Suchánek, M., Gaulin, E., Rey, T., Dumas, B., 2020. Long-Read Genome Sequence of the Sugar Beet Rhizosphere Mycoparasite Pythium oligandrum. G3: Genes, Genomes, Genetics 10, 431–436. https://doi.org/10.1534/g3.119.400746

Feldman, D., Yarden, O., Hadar, Y., 2020. Seeking the Roles for Fungal Small-Secreted Proteins in Affecting Saprophytic Lifestyles. Front. Microbiol. 11, 455. https://doi.org/10.3389/fmicb.2020.00455

Fernandez, M.R., Knox, R.E., 2012. Diseases of Durum Wheat, in: Durum Wheat. Elsevier, pp. 57–71. https://doi.org/10.1016/B978-1-891127-65-6.50009-X

Fesel, P.H., Zuccaro, A., 2016. β-glucan: Crucial component of the fungal cell wall and elusive MAMP in plants. Fungal Genetics and Biology 90, 53–60. https://doi.org/10.1016/j.fgb.2015.12.004

Ficke, A., Cowger, C., Bergstrom, G., Brodal, G., 2018. Understanding Yield Loss and Pathogen Biology to Improve Disease Management: Septoria Nodorum Blotch - A Case Study in Wheat. Plant Disease 102, 696–707. https://doi.org/10.1094/PDIS-09-17-1375-FE

Fletcher, K., Klosterman, S.J., Derevnina, L., Martin, F., Bertier, L.D., Koike, S., Reyes-Chin-Wo, S., Mou, B., Michelmore, R., 2018. Comparative genomics of downy mildews reveals potential adaptations to biotrophy. BMC Genomics 19, 851. https://doi.org/10.1186/s12864-018-5214-8

Fletcher, K., Martin, F., Isakeit, T., Cavanaugh, K., Magill, C., Michelmore, R., 2022. The genome of the oomycete *Peronosclerospora sorghi* , a cosmopolitan pathogen of maize and sorghum, is inflated with dispersed pseudogenes (preprint). Genomics. https://doi.org/10.1101/2022.07.13.499355

Fouché, S., Plissonneau, C., Croll, D., 2018. The birth and death of effectors in rapidly evolving filamentous pathogen genomes. Current Opinion in Microbiology 46, 34–42. https://doi.org/10.1016/j.mib.2018.01.020

Franceschetti, M., Maqbool, A., Jiménez-Dalmaroni, M.J., Pennington, H.G., Kamoun, S., Banfield, M.J., 2017. Effectors of Filamentous Plant Pathogens: Commonalities amid Diversity. Microbiol. Mol. Biol. Rev. 81. https://doi.org/10.1128/MMBR.00066-16

Free, R.B., Hazelwood, L.A., Sibley, D.R., 2009. Identifying Novel Protein-Protein Interactions Using Co-Immunoprecipitation and Mass Spectroscopy. Current Protocols in Neuroscience 46. https://doi.org/10.1002/0471142301.ns0528s46

French, E., Kim, B.-S., Iyer-Pascuzzi, A.S., 2016. Mechanisms of quantitative disease resistance in plants. Seminars in Cell & Developmental Biology 56, 201–208. https://doi.org/10.1016/j.semcdb.2016.05.015

Furzer, O.J., Cevik, V., Fairhead, S., Bailey, K., Redkar, A., Schudoma, C., MacLean, D., Holub, E.B., Jones, J.D.G., 2022. An Improved Assembly of the *Albugo candida* Ac2V Genome Reveals the Expansion of the "CCG" Class of Effectors. MPMI 35, 39–48. https://doi.org/10.1094/MPMI-04-21-0075-R

Gao, R., Ding, M., Jiang, S., Zhao, Z., Chenthamara, K., Shen, Q., Cai, F., Druzhinina, I.S., 2020. The Evolutionary and Functional Paradox of Cerato-platanins in Fungi. Appl Environ Microbiol 86, e00696-20. https://doi.org/10.1128/AEM.00696-20

García, N., González, M.A., González, C., Brito, N., 2017. Simultaneous Silencing of Xylanase Genes in Botrytis cinerea. Front. Plant Sci. 8, 2174. https://doi.org/10.3389/fpls.2017.02174

Garrido-Ramos, M., 2017. Satellite DNA: An Evolving Topic. Genes 8, 230. https://doi.org/10.3390/genes8090230

Gaspar, T., Franck, T., Bisbis, B., Kevers, C., Jouve, L., Hausman, J.F., Dommes, J., 2002. [No title found]. Plant Growth Regulation 37, 263–285. https://doi.org/10.1023/A:1020835304842

Gaulin, E., 2017. Effector-Mediated Communication of Filamentous Plant Pathogens With Their Hosts, in: Advances in Botanical Research. Elsevier, pp. 161–185. https://doi.org/10.1016/bs.abr.2016.09.003

Gaulin, E., Bottin, A., Jacquet, C., Dumas, B., 2008a. Chapter 18: Aphanomyces euteiches and legumes 23.

Gaulin, E., Dramé, N., Lafitte, C., Torto-Alalibo, T., Martinez, Y., Ameline-Torregrosa, C., Khatib, M., Mazarguil, H., Villalba-Mateos, F., Kamoun, S., Mazars, C., Dumas, B., Bottin, A., Esquerré-Tugayé, M.-T., Rickauer, M., 2006. Cellulose Binding Domains of a Phytophthora Cell Wall Protein Are Novel Pathogen-Associated Molecular Patterns. The Plant Cell 18, 1766–1777. https://doi.org/10.1105/tpc.105.038687

Gaulin, E., Jacquet, C., Bottin, A., Dumas, B., 2007a. Root rot disease of legumes caused by Aphanomyces euteiches. Mol Plant Pathol 8, 539–548. https://doi.org/10.1111/j.1364-3703.2007.00413.x

Gaulin, E., Jacquet, C., Bottin, A., Dumas, B., 2007b. Root rot disease of legumes caused by Aphanomyces euteiches. Mol Plant Pathol 8, 539–548. https://doi.org/10.1111/j.1364-3703.2007.00413.x

Gaulin, E., Jauneau, A., Villalba, F., Rickauer, M., Esquerré-Tugayé, M.-T., Bottin, A., 2002. The CBEL glycoprotein of *Phytophthora parasitica* var- *nicotianae* is involved in cell wall deposition and adhesion to cellulosic substrates. Journal of Cell Science 115, 4565–4575. https://doi.org/10.1242/jcs.00138

Gaulin, E., Madoui, M.-A., Bottin, A., Jacquet, C., Mathé, C., Couloux, A., Wincker, P., Dumas, B., 2008b. Transcriptome of Aphanomyces euteiches: New Oomycete Putative Pathogenicity Factors and Metabolic Pathways. PLOS ONE 3, e1723. https://doi.org/10.1371/journal.pone.0001723

Gaulin, Elodie, Pel, M.J.C., Camborde, L., San-Clemente, H., Courbier, S., Dupouy, M.A., Lengellé, J., Veyssiere, M., Le Ru, A., Grandjean, F., Cordaux, R., Moumen, B., Gilbert, C., Cano, L.M., Aury, J.M., Guy, J., Wincker, P., Bouchez, O., Klopp, C., Dumas, B., 2018. Genomics analysis of Aphanomyces spp. identifies a new class of

oomycete effector associated with host adaptation. BMC Biology 16. https://doi.org/10.1186/s12915-018-0508-5
Gaulin, E, Pel, M.J.C., Camborde, L., San-Clemente, H., Courbier, S., Dupouy, M.-A., Lengellé, J., Veyssiere, M., Le Ru, A., Grandjean, F., Cordaux, R., Moumen, B., Gilbert, C., Cano, L.M., Aury, J.-M., Guy, J., Wincker, P., Bouchez, O., Klopp, C., Dumas, B., 2018. Genomics analysis of Aphanomyces spp. identifies a new class of oomycete effector associated with host adaptation. BMC Biol 16, 43. https://doi.org/10.1186/s12915-018-0508-5
Gay, E.J., Soyer, J.L., Lapalu, N., Linglin, J., Fudal, I., Da Silva, C., Wincker, P., Aury, J.-M., Cruaud, C., Levrel, A., Lemoine, J., Delourme, R., Rouxel, T., Balesdent, M.-H., 2021. Large-scale transcriptomics to dissect 2 years of the life of a fungal phytopathogen interacting with its host plant. BMC Biol 19, 55. https://doi.org/10.1186/s12915-021-00989-3
Gideon Onyekachi, O., Ogbonnaya Boniface, O., Felix Gemlack, N., Nicholas, N., 2019. The Effect of Climate Change on Abiotic Plant Stress: A Review, in: Bosco de Oliveira, A. (Ed.), Abiotic and Biotic Stress in Plants. IntechOpen. https://doi.org/10.5772/intechopen.82681
Giraldo, M.C., Dagdas, Y.F., Gupta, Y.K., Mentlak, T.A., Yi, M., Martinez-Rocha, A.L., Saitoh, H., Terauchi, R., Talbot, N.J., Valent, B., 2013. Two distinct secretion systems facilitate tissue invasion by the rice blast fungus Magnaporthe oryzae. Nat Commun 4, 1996. https://doi.org/10.1038/ncomms2996
Gómez-Pérez, D., Kemen, E., 2021. Predicting Lifestyle from Positive Selection Data and Genome Properties in Oomycetes. Pathogens 10, 807. https://doi.org/10.3390/pathogens10070807
Gossen, B.D., Conner, R.L., Chang, K.-F., Pasche, J.S., McLaren, D.L., Henriquez, M.A., Chatterton, S., Hwang, S.-F., 2016. Identifying and Managing Root Rot of Pulses on the Northern Great Plains. Plant Dis. 100, 1965–1978. https://doi.org/10.1094/PDIS-02-16-0184-FE
Goyal, B.K., Kant, U., Verma, P.R., 1995. Growth of Albugo candida (race unidentified) on Brassica juncea callus cultures. Plant Soil 172, 331–337. https://doi.org/10.1007/BF00011336
Grattepanche, J., Walker, L.M., Ott, B.M., Paim Pinto, D.L., Delwiche, C.F., Lane, C.E., Katz, L.A., 2018. Microbial Diversity in the Eukaryotic SAR Clade: Illuminating the Darkness Between Morphology and Molecular Data. BioEssays 40, 1700198. https://doi.org/10.1002/bies.201700198
Grigoriev, I.V., Nikitin, R., Haridas, S., Kuo, A., Ohm, R., Otillar, R., Riley, R., Salamov, A., Zhao, X., Korzeniewski, F., Smirnova, T., Nordberg, H., Dubchak, I., Shabalov, I., 2014. MycoCosm portal: gearing up for 1000 fungal genomes. Nucl. Acids Res. 42, D699–D704. https://doi.org/10.1093/nar/gkt1183
Guo, L., Cesari, S., de Guillen, K., Chalvon, V., Mammri, L., Ma, M., Meusnier, I., Bonnot, F., Padilla, A., Peng, Y.-L., Liu, J., Kroj, T., 2018. Specific recognition of two MAX effectors by integrated HMA domains in plant immune receptors involves distinct binding surfaces. Proc. Natl. Acad. Sci. U.S.A. 115, 11637–11642. https://doi.org/10.1073/pnas.1810705115
Haas, B.J., Kamoun, S., Zody, M.C., Jiang, R.H., Handsaker, R.E., Cano, L.M., Grabherr, M., Kodira, C.D., Raffaele, S., Torto-Alalibo, T., 2009. Genome sequence and analysis of the Irish potato famine pathogen Phytophthora infestans. Nature 461, 393–398.
Hannat, S., Pontarotti, P., Colson, P., Kuhn, M.-L., Galiana, E., La Scola, B., Aherfi, S., Panabières, F., 2021. Diverse Trajectories Drive the Expression of a Giant Virus in the

Oomycete Plant Pathogen Phytophthora parasitica. Front. Microbiol. 12, 662762. https://doi.org/10.3389/fmicb.2021.662762
Hardham, A.R., 2007. Cell biology of plant–oomycete interactions. Cellular Microbiology 9, 31–39. https://doi.org/10.1111/j.1462-5822.2006.00833.x
Hartmann, F.E., Croll, D., 2017. Distinct Trajectories of Massive Recent Gene Gains and Losses in Populations of a Microbial Eukaryotic Pathogen. Molecular Biology and Evolution 34, 2808–2822. https://doi.org/10.1093/molbev/msx208
Hartmann, F.E., Sánchez-Vallet, A., McDonald, B.A., Croll, D., 2017. A fungal wheat pathogen evolved host specialization by extensive chromosomal rearrangements. ISME J 11, 1189–1204. https://doi.org/10.1038/ismej.2016.196
Hashemi, M., Tabet, D., Sandroni, M., Benavent-Celma, C., Seematti, J., Andersen, C.B., Grenville-Briggs, L.J., 2022. The hunt for sustainable biocontrol of oomycete plant pathogens, a case study of Phytophthora infestans. Fungal Biology Reviews 40, 53–69. https://doi.org/10.1016/j.fbr.2021.11.003
Hemetsberger, C., Herrberger, C., Zechmann, B., Hillmer, M., Doehlemann, G., 2012. The Ustilago maydis Effector Pep1 Suppresses Plant Immunity by Inhibition of Host Peroxidase Activity. PLoS Pathog 8, e1002684. https://doi.org/10.1371/journal.ppat.1002684
Horton, P., Park, K.-J., Obayashi, T., Nakai, K., 2005. PROTEIN SUBCELLULAR LOCALIZATION PREDICTION WITH WOLF PSORT, in: Proceedings of the 4th Asia-Pacific Bioinformatics Conference. Presented at the 4th Asia-Pacific Bioinformatics Conference, PUBLISHED BY IMPERIAL COLLEGE PRESS AND DISTRIBUTED BY WORLD SCIENTIFIC PUBLISHING CO., Taipei, Taiwan, pp. 39–48. https://doi.org/10.1142/9781860947292_0007
Iberahim, N.A., Sood, N., Pradhan, P.K., Boom, J., West, P., Trusch, F., 2020. The chaperone Lhs1 contributes to the virulence of the fish-pathogenic oomycete Aphanomyces invadans. Fungal Biol 124, 1024–1031.
Iberahim, N.A., Trusch, F., van West, P., 2018. Aphanomyces invadans, the causal agent of Epizootic Ulcerative Syndrome, is a global threat to wild and farmed fish. Fungal Biology Reviews 32, 118–130. https://doi.org/10.1016/j.fbr.2018.05.002
Iida, Y., van ‘t Hof, P., Beenen, H., Mesarich, C., Kubota, M., Stergiopoulos, I., Mehrabi, R., Notsu, A., Fujiwara, K., Bahkali, A., Abd-Elsalam, K., Collemare, J., de Wit, P.J.G.M., 2015. Novel Mutations Detected in Avirulence Genes Overcoming Tomato Cf Resistance Genes in Isolates of a Japanese Population of Cladosporium fulvum. PLoS ONE 10, e0123271. https://doi.org/10.1371/journal.pone.0123271
Iki, T., 2017. Messages on small RNA duplexes in plants. J. Plant Res. 130, 7–16. https://doi.org/10.1007/s10265-016-0876-2
Illergård, K., Ardell, D.H., Elofsson, A., 2009. Structure is three to ten times more conserved than sequence-A study of structural response in protein cores. Proteins 77, 499–508. https://doi.org/10.1002/prot.22458
Jacobs, K.A., Collins-Racie, L.A., Colbert, M., Duckett, M., Golden-Fleet, M., Kelleher, K., Kriz, R., LaVallie, E.R., Merberg, D., Spaulding, V., Stover, J., Williamson, M.J., McCoy, J.M., 1997. A genetic selection for isolating cDNAs encoding secreted proteins. Gene 198, 289–296. https://doi.org/10.1016/S0378-1119(97)00330-2
Jashni, M.K., Dols, I.H.M., Iida, Y., Boeren, S., Beenen, H.G., Mehrabi, R., Collemare, J., de Wit, P.J.G.M., 2015. Synergistic Action of a Metalloprotease and a Serine Protease from *Fusarium oxysporum* f. sp. *lycopersici* Cleaves Chitin-Binding Tomato Chitinases, Reduces Their Antifungal Activity, and Enhances Fungal Virulence. MPMI 28, 996–1008. https://doi.org/10.1094/MPMI-04-15-0074-R

Jiang, R.H.Y., de Bruijn, I., Haas, B.J., Belmonte, R., Löbach, L., Christie, J., van den Ackerveken, G., Bottin, A., Bulone, V., Díaz-Moreno, S.M., Dumas, B., Fan, L., Gaulin, E., Govers, F., Grenville-Briggs, L.J., Horner, N.R., Levin, J.Z., Mammella, M., Meijer, H.J.G., Morris, P., Nusbaum, C., Oome, S., Phillips, A.J., van Rooyen, D., Rzeszutek, E., Saraiva, M., Secombes, C.J., Seidl, M.F., Snel, B., Stassen, J.H.M., Sykes, S., Tripathy, S., van den Berg, H., Vega-Arreguin, J.C., Wawra, S., Young, S.K., Zeng, Q., Dieguez-Uribeondo, J., Russ, C., Tyler, B.M., van West, P., 2013a. Distinctive expansion of potential virulence genes in the genome of the oomycete fish pathogen Saprolegnia parasitica. PLoS Genet. 9, e1003272. https://doi.org/10.1371/journal.pgen.1003272

Jiang, R.H.Y., de Bruijn, I., Haas, B.J., Belmonte, R., Löbach, L., Christie, J., van den Ackerveken, G., Bottin, A., Bulone, V., Díaz-Moreno, S.M., Dumas, B., Fan, L., Gaulin, E., Govers, F., Grenville-Briggs, L.J., Horner, N.R., Levin, J.Z., Mammella, M., Meijer, H.J.G., Morris, P., Nusbaum, C., Oome, S., Phillips, A.J., van Rooyen, D., Rzeszutek, E., Saraiva, M., Secombes, C.J., Seidl, M.F., Snel, B., Stassen, J.H.M., Sykes, S., Tripathy, S., van den Berg, H., Vega-Arreguin, J.C., Wawra, S., Young, S.K., Zeng, Q., Dieguez-Uribeondo, J., Russ, C., Tyler, B.M., van West, P., 2013b. Distinctive Expansion of Potential Virulence Genes in the Genome of the Oomycete Fish Pathogen Saprolegnia parasitica. PLoS Genet 9, e1003272. https://doi.org/10.1371/journal.pgen.1003272

Jones, J.D.G., Dangl, J.L., 2006. The plant immune system. Nature 444, 323–329. https://doi.org/10.1038/nature05286

Jones, P., Binns, D., Chang, H.-Y., Fraser, M., Li, W., McAnulla, C., McWilliam, H., Maslen, J., Mitchell, A., Nuka, G., Pesseat, S., Quinn, A.F., Sangrador-Vegas, A., Scheremetjew, M., Yong, S.-Y., Lopez, R., Hunter, S., 2014. InterProScan 5: genome-scale protein function classification. Bioinformatics 30, 1236–1240. https://doi.org/10.1093/bioinformatics/btu031

Judelson, H.S., 2009. Sexual Reproduction in Oomycetes: Biology, Diversity, and Contributions to Fitness, in: Lamour, K., Kamoun, S. (Eds.), Oomycete Genetics and Genomics. John Wiley & Sons, Inc., Hoboken, NJ, USA, pp. 121–138. https://doi.org/10.1002/9780470475898.ch6

Judelson, H.S., Ah-Fong, A.M.V., 2019. Exchanges at the Plant-Oomycete Interface That Influence Disease. Plant Physiol. 179, 1198–1211. https://doi.org/10.1104/pp.18.00979

Jumper, J., Evans, R., Pritzel, A., Green, T., Figurnov, M., Ronneberger, O., Tunyasuvunakool, K., Bates, R., Žídek, A., Potapenko, A., Bridgland, A., Meyer, C., Kohl, S.A.A., Ballard, A.J., Cowie, A., Romera-Paredes, B., Nikolov, S., Jain, R., Adler, J., Back, T., Petersen, S., Reiman, D., Clancy, E., Zielinski, M., Steinegger, M., Pacholska, M., Berghammer, T., Bodenstein, S., Silver, D., Vinyals, O., Senior, A.W., Kavukcuoglu, K., Kohli, P., Hassabis, D., 2021. Highly accurate protein structure prediction with AlphaFold. Nature 596, 583–589. https://doi.org/10.1038/s41586-021-03819-2

Kamoun, Sophien, 2009. The Secretome of Plant-Associated Fungi and Oomycetes, in: Deising, H.B. (Ed.), The Mycota. Springer Berlin Heidelberg, Berlin, Heidelberg, pp. 173–180. https://doi.org/10.1007/978-3-540-87407-2_9

Kamoun, S., 2009. Plant Pathogens: Oomycetes (water mold), in: Encyclopedia of Microbiology. Elsevier, pp. 689–695. https://doi.org/10.1016/B978-012373944-5.00349-7

Kamoun, S., 2006. A Catalogue of the Effector Secretome of Plant Pathogenic Oomycetes. Annu. Rev. Phytopathol. 44, 41–60. https://doi.org/10.1146/annurev.phyto.44.070505.143436

Kamoun, S., Lindqvist, H., Govers, F., 1997. A Novel Class of Elicitin-like Genes from *Phytophthora infestans*. MPMI 10, 1028–1030. https://doi.org/10.1094/MPMI.1997.10.8.1028

Kamoun, S., van West, P., Vleeshouwers, V.G.A.A., de Groot, K.E., Govers, F., 1998. Resistance of *Nicotiana benthamiana* to *Phytophthora infestans* Is Mediated by the Recognition of the Elicitor Protein INF1. Plant Cell 10, 1413–1425. https://doi.org/10.1105/tpc.10.9.1413

Kaschani, F., Gu, C., Niessen, S., Hoover, H., Cravatt, B.F., van der Hoorn, Renier.A.L., 2009. Diversity of Serine Hydrolase Activities of Unchallenged and Botrytis-infected Arabidopsis thaliana. Molecular & Cellular Proteomics 8, 1082–1093. https://doi.org/10.1074/mcp.M800494-MCP200

Kettles, G.J., Bayon, C., Sparks, C.A., Canning, G., Kanyuka, K., Rudd, J.J., 2018. Characterization of an antimicrobial and phytotoxic ribonuclease secreted by the fungal wheat pathogen *Zymoseptoria tritici*. New Phytol 217, 320–331. https://doi.org/10.1111/nph.14786

Khan, M., Youn, J.-Y., Gingras, A.-C., Subramaniam, R., Desveaux, D., 2018. In planta proximity dependent biotin identification (BioID). Sci Rep 8, 9212. https://doi.org/10.1038/s41598-018-27500-3

Khan, S.U., Saeed, S., Khan, M.H.U., Fan, C., Ahmar, S., Arriagada, O., Shahzad, R., Branca, F., Mora-Poblete, F., 2021. Advances and Challenges for QTL Analysis and GWAS in the Plant-Breeding of High-Yielding: A Focus on Rapeseed. Biomolecules 11, 1516. https://doi.org/10.3390/biom11101516

Kim, K.-T., Jeon, J., Choi, J., Cheong, K., Song, H., Choi, G., Kang, S., Lee, Y.-H., 2016. Kingdom-Wide Analysis of Fungal Small Secreted Proteins (SSPs) Reveals their Potential Role in Host Association. Front. Plant Sci. 7. https://doi.org/10.3389/fpls.2016.00186

Kim, S., Kim, C.-Y., Park, S.-Y., Kim, K.-T., Jeon, Jongbum, Chung, H., Choi, G., Kwon, S., Choi, J., Jeon, Junhyun, Jeon, J.-S., Khang, C.H., Kang, S., Lee, Y.-H., 2020. Two nuclear effectors of the rice blast fungus modulate host immunity via transcriptional reprogramming. Nat Commun 11, 5845. https://doi.org/10.1038/s41467-020-19624-w

Kiselev, A., San Clemente, H., Camborde, L., Dumas, B., Gaulin, E., 2022. A Comprehensive Assessment of the Secretome Responsible for Host Adaptation of the Legume Root Pathogen Aphanomyces euteiches. JoF 8, 88. https://doi.org/10.3390/jof8010088

Klein, E., Ofek, M., Katan, J., Minz, D., Gamliel, A., 2012. Soil Suppressiveness to Fusarium Disease: Shifts in Root Microbiome Associated with Reduction of Pathogen Root Colonization. Phytopathology® 103, 23–33. https://doi.org/10.1094/PHYTO-12-11-0349

Klein, R.D., Gu, Q., Goddard, A., Rosenthal, A., 1996. Selection for genes encoding secreted proteins and receptors. Proceedings of the National Academy of Sciences 93, 7108–7113. https://doi.org/10.1073/pnas.93.14.7108

Kombrink, A., Thomma, B.P.H.J., 2013. LysM Effectors: Secreted Proteins Supporting Fungal Life. PLoS Pathog 9, e1003769. https://doi.org/10.1371/journal.ppat.1003769

Kong, L., Qiu, X., Kang, J., Wang, Yang, Chen, H., Huang, J., Qiu, M., Zhao, Y., Kong, G., Ma, Z., Wang, Yan, Ye, W., Dong, S., Ma, W., Wang, Yuanchao, 2017. A Phytophthora Effector Manipulates Host Histone Acetylation and Reprograms Defense Gene Expression to Promote Infection. Current Biology 27, 981–991. https://doi.org/10.1016/j.cub.2017.02.044

Kourelis, J., Sakai, T., Adachi, H., Kamoun, S., 2021. RefPlantNLR is a comprehensive collection of experimentally validated plant disease resistance proteins from the NLR family. PLoS Biol 19, e3001124. https://doi.org/10.1371/journal.pbio.3001124

Krogh, A., Larsson, B., von Heijne, G., Sonnhammer, E.L.L., 2001. Predicting transmembrane protein topology with a hidden markov model: application to complete genomes11Edited by F. Cohen. Journal of Molecular Biology 305, 567–580. https://doi.org/10.1006/jmbi.2000.4315

Lamour, K., Kamoun, S., 2009. Oomycete Genetics and Genomics: Diversity, Interactions and Research Tools. John Wiley & Sons.

Lang-Yona, N., Pickersgill, D.A., Maurus, I., Teschner, D., Wehking, J., Thines, E., Pöschl, U., Després, V.R., Fröhlich-Nowoisky, J., 2018. Species Richness, rRNA Gene Abundance, and Seasonal Dynamics of Airborne Plant-Pathogenic Oomycetes. Front. Microbiol. 9, 2673. https://doi.org/10.3389/fmicb.2018.02673

Lanver, D., Berndt, P., Tollot, M., Naik, V., Vranes, M., Warmann, T., Münch, K., Rössel, N., Kahmann, R., 2014. Plant Surface Cues Prime Ustilago maydis for Biotrophic Development. PLOS Pathogens 10, e1004272. https://doi.org/10.1371/journal.ppat.1004272

Lazar, N., Mesarich, C.H., Petit-Houdenot, Y., Talbi, N., Li de la Sierra-Gallay, I., Zélie, E., Blondeau, K., Gracy, J., Ollivier, B., Blaise, F., Rouxel, T., Balesdent, M.-H., Idnurm, A., van Tilbeurgh, H., Fudal, I., 2022. A new family of structurally conserved fungal effectors displays epistatic interactions with plant resistance proteins. PLOS Pathogens 18, e1010664. https://doi.org/10.1371/journal.ppat.1010664

Lee, Y., Cho, K.-S., Seo, J.-H., Sohn, K.H., Prokchorchik, M., 2020. Improved Genome Sequence and Gene Annotation Resource for the Potato Late Blight Pathogen Phytophthora infestans. MPMI 33, 1025–1028. https://doi.org/10.1094/MPMI-02-20-0023-A

Lei, X., Lan, X., Ye, W., Liu, Y., Song, S., Lu, J., 2019. *Plasmopara viticola* effector PvRXLR159 suppresses immune responses in *Nicotiana benthamiana*. Plant Signaling & Behavior 14, 1682220. https://doi.org/10.1080/15592324.2019.1682220

Li, B., Meng, X., Shan, L., He, P., 2016. Transcriptional Regulation of Pattern-Triggered Immunity in Plants. Cell Host & Microbe 19, 641–650. https://doi.org/10.1016/j.chom.2016.04.011

Li, Y., Han, Y., Qu, M., Chen, J., Chen, X., Geng, X., Wang, Z., Chen, S., 2020. Apoplastic Cell Death-Inducing Proteins of Filamentous Plant Pathogens: Roles in Plant-Pathogen Interactions. Front. Genet. 11, 661. https://doi.org/10.3389/fgene.2020.00661

Lievens, L., Pollier, J., Goossens, A., Beyaert, R., Staal, J., 2017. Abscisic Acid as Pathogen Effector and Immune Regulator. Front Plant Sci 8, 587. https://doi.org/10.3389/fpls.2017.00587

Liu, L., Wang, Z., Li, J., Wang, Y., Yuan, J., Zhan, J., Wang, P., Lin, Y., Li, F., Ge, X., 2021. *Verticillium dahliae* secreted protein Vd424Y is required for full virulence, targets the nucleus of plant cells, and induces cell death. Mol Plant Pathol 22, 1109–1120. https://doi.org/10.1111/mpp.13100

Lo Presti, L., Lanver, D., Schweizer, G., Tanaka, S., Liang, L., Tollot, M., Zuccaro, A., Reissmann, S., Kahmann, R., 2015. Fungal Effectors and Plant Susceptibility. Annu. Rev. Plant Biol. 66, 513–545. https://doi.org/10.1146/annurev-arplant-043014-114623

Lombard, V., Golaconda Ramulu, H., Drula, E., Coutinho, P.M., Henrissat, B., 2014. The carbohydrate-active enzymes database (CAZy) in 2013. Nucleic Acids Res 42, D490–D495. https://doi.org/10.1093/nar/gkt1178

Maccarrone, G., Bonfiglio, J.J., Silberstein, S., Turck, C.W., Martins-de-Souza, D., 2017. Characterization of a Protein Interactome by Co-Immunoprecipitation and Shotgun Mass Spectrometry, in: Guest, P.C. (Ed.), Multiplex Biomarker Techniques, Methods in Molecular Biology. Springer New York, New York, NY, pp. 223–234. https://doi.org/10.1007/978-1-4939-6730-8_19

Madoui, M.-A., Bertrand-Michel, J., Gaulin, E., Dumas, B., 2009. Sterol metabolism in the oomycete Aphanomyces euteiches, a legume root pathogen. New Phytol. 183, 291–300. https://doi.org/10.1111/j.1469-8137.2009.02895.x

Majeed, M., Soliman, H., Kumar, G., El-Matbouli, M., Saleh, M., 2018. Editing the genome of Aphanomyces invadans using CRISPR/Cas9. Parasites Vectors 11, 554. https://doi.org/10.1186/s13071-018-3134-8

Makkonen, J., Jussila, J., Kokko, H., 2012. The diversity of the pathogenic Oomycete (Aphanomyces astaci) chitinase genes within the genotypes indicate adaptation to its hosts. Fungal Genet. Biol. 49, 635–642. https://doi.org/10.1016/j.fgb.2012.05.014

Malvick, D.K., Grünwald, N.J., Dyer, A.T., 2009. Population structure, races, and host range of Aphanomyces euteiches from alfalfa production fields in the central USA. Eur J Plant Pathol 123, 171–182. https://doi.org/10.1007/s10658-008-9354-6

Mariotte, P., Mehrabi, Z., Bezemer, T.M., De Deyn, G.B., Kulmatiski, A., Drigo, B., Veen, G.F. (Ciska), van der Heijden, M.G.A., Kardol, P., 2018. Plant–Soil Feedback: Bridging Natural and Agricultural Sciences. Trends in Ecology & Evolution 33, 129–142. https://doi.org/10.1016/j.tree.2017.11.005

Marsian, J., Lomonossoff, G.P., 2016. Molecular pharming — VLPs made in plants. Current Opinion in Biotechnology 37, 201–206. https://doi.org/10.1016/j.copbio.2015.12.007

Mazau, D., Esquerré-Tugayé, M.T., 1986. Hydroxyproline-rich glycoprotein accumulation in the cell walls of plants infected by various pathogens. Physiological and Molecular Plant Pathology 29, 147–157. https://doi.org/10.1016/S0048-4059(86)80017-0

McGowan, J., Byrne, K.P., Fitzpatrick, D.A., 2019. Comparative Analysis of Oomycete Genome Evolution Using the Oomycete Gene Order Browser (OGOB). Genome Biology and Evolution 11, 189–206. https://doi.org/10.1093/gbe/evy267

McGowan, J., Fitzpatrick, D.A., 2020. Recent advances in oomycete genomics, in: Advances in Genetics. Elsevier, pp. 175–228. https://doi.org/10.1016/bs.adgen.2020.03.001

McGowan, J., Fitzpatrick, D.A., 2017. Genomic, Network, and Phylogenetic Analysis of the Oomycete Effector Arsenal. mSphere 2. https://doi.org/10.1128/mSphere.00408-17

Meijer, H.J.G., Mancuso, F.M., Espadas, G., Seidl, M.F., Chiva, C., Govers, F., Sabidó, E., 2014. Profiling the Secretome and Extracellular Proteome of the Potato Late Blight Pathogen Phytophthora infestans. Molecular & Cellular Proteomics 13, 2101–2113. https://doi.org/10.1074/mcp.M113.035873

Meng, X., Zhang, S., 2013. MAPK Cascades in Plant Disease Resistance Signaling. Annu. Rev. Phytopathol. 51, 245–266. https://doi.org/10.1146/annurev-phyto-082712-102314

Mikes, V., Milat, M.L., Ponchet, M., Panabières, F., Ricci, P., Blein, J.P., 1998. Elicitins, proteinaceous elicitors of plant defense, are a new class of sterol carrier proteins. Biochem. Biophys. Res. Commun. 245, 133–139. https://doi.org/10.1006/bbrc.1998.8341

Minardi, D., Studholme, D.J., van der Giezen, M., Pretto, T., Oidtmann, B., 2018. New genotyping method for the causative agent of crayfish plague (Aphanomyces astaci) based on whole genome data. J. Invertebr. Pathol. 156, 6–13. https://doi.org/10.1016/j.jip.2018.06.002

Misas-Villamil, J.C., Hoorn, R.A.L., Doehlemann, G., 2016. Papain-like cysteine proteases as hubs in plant immunity. New Phytol 212, 902–907. https://doi.org/10.1111/nph.14117

Mosquera, G., Giraldo, M.C., Khang, C.H., Coughlan, S., Valent, B., 2009. Interaction Transcriptome Analysis Identifies *Magnaporthe oryzae* BAS1-4 as Biotrophy-Associated Secreted Proteins in Rice Blast Disease. The Plant Cell 21, 1273–1290. https://doi.org/10.1105/tpc.107.055228

Mueller, A.N., Ziemann, S., Treitschke, S., Aßmann, D., Doehlemann, G., 2013. Compatibility in the Ustilago maydis–Maize Interaction Requires Inhibition of Host Cysteine Proteases by the Fungal Effector Pit2. PLoS Pathog 9, e1003177. https://doi.org/10.1371/journal.ppat.1003177

Muszewska, A., Stepniewska-Dziubinska, M.M., Steczkiewicz, K., Pawlowska, J., Dziedzic, A., Ginalski, K., 2017. Fungal lifestyle reflected in serine protease repertoire. Sci Rep 7, 9147. https://doi.org/10.1038/s41598-017-09644-w

Nelson, R., Wiesner-Hanks, T., Wisser, R., Balint-Kurti, P., 2018. Navigating complexity to breed disease-resistant crops. Nat Rev Genet 19, 21–33. https://doi.org/10.1038/nrg.2017.82

Ngou, B.P.M., Ahn, H.-K., Ding, P., Jones, J.D.G., 2021. Mutual potentiation of plant immunity by cell-surface and intracellular receptors. Nature. https://doi.org/10.1038/s41586-021-03315-7

Nguyen Ba, A.N., Pogoutse, A., Provart, N., Moses, A.M., 2009. NLStradamus: a simple Hidden Markov Model for nuclear localization signal prediction. BMC Bioinformatics 10, 202. https://doi.org/10.1186/1471-2105-10-202

O'Donnell, K., Ward, T.J., Robert, V.A.R.G., Crous, P.W., Geiser, D.M., Kang, S., 2015. DNA sequence-based identification of Fusarium: Current status and future directions. Phytoparasitica 43, 583–595. https://doi.org/10.1007/s12600-015-0484-z

Ottmann, C., Luberacki, B., Küfner, I., Koch, W., Brunner, F., Weyand, M., Mattinen, L., Pirhonen, M., Anderluh, G., Seitz, H.U., Nürnberger, T., Oecking, C., 2009. A common toxin fold mediates microbial attack and plant defense. Proc. Natl. Acad. Sci. U.S.A. 106, 10359–10364. https://doi.org/10.1073/pnas.0902362106

Panabières, F., Rancurel, C., da Rocha, M., Kuhn, M.-L., 2020. Characterization of Two Satellite DNA Families in the Genome of the Oomycete Plant Pathogen Phytophthora parasitica. Front. Genet. 11, 557. https://doi.org/10.3389/fgene.2020.00557

Panstruga, R., Kuhn, H., 2019. Mutual interplay between phytopathogenic powdery mildew fungi and other microorganisms. Molecular Plant Pathology 20, 463–470. https://doi.org/10.1111/mpp.12771

Paulus, J.K., Kourelis, J., Ramasubramanian, S., Homma, F., Godson, A., Hörger, A.C., Hong, T.N., Krahn, D., Ossorio Carballo, L., Wang, S., Win, J., Smoker, M., Kamoun, S., Dong, S., van der Hoorn, R.A.L., 2020. Extracellular proteolytic cascade in tomato activates immune protease Rcr3. Proc Natl Acad Sci USA 117, 17409–17417. https://doi.org/10.1073/pnas.1921101117

Pauly, M., Albersheim, P., Darvill, A., York, W.S., 1999. Molecular domains of the cellulose/xyloglucan network in the cell walls of higher plants. Plant J 20, 629–639. https://doi.org/10.1046/j.1365-313X.1999.00630.x

Pelgrom, A.J.E., Meisrimler, C.-N., Elberse, J., Koorman, T., Boxem, M., Van den Ackerveken, G., 2020. Host interactors of effector proteins of the lettuce downy mildew Bremia lactucae obtained by yeast two-hybrid screening. PLoS ONE 15, e0226540. https://doi.org/10.1371/journal.pone.0226540

Pendleton, A.L., Smith, K.E., Feau, N., Martin, F.M., Grigoriev, I.V., Hamelin, R., Nelson, C.D., Burleigh, J.G., Davis, J.M., 2014. Duplications and losses in gene families of rust pathogens highlight putative effectors. Front. Plant Sci. 5. https://doi.org/10.3389/fpls.2014.00299

Pennington, H.G., Jones, R., Kwon, S., Bonciani, G., Thieron, H., Chandler, T., Luong, P., Morgan, S.N., Przydacz, M., Bozkurt, T., Bowden, S., Craze, M., Wallington, E.J., Garnett, J., Kwaaitaal, M., Panstruga, R., Cota, E., Spanu, P.D., 2019. The fungal ribonuclease-like effector protein CSEP0064/BEC1054 represses plant immunity and

interferes with degradation of host ribosomal RNA. PLOS Pathogens 15, e1007620. https://doi.org/10.1371/journal.ppat.1007620
Petre, B., Saunders, D.G.O., Sklenar, J., Lorrain, C., Win, J., Duplessis, S., Kamoun, S., 2015. Candidate Effector Proteins of the Rust Pathogen *Melampsora larici-populina* Target Diverse Plant Cell Compartments. MPMI 28, 689–700. https://doi.org/10.1094/MPMI-01-15-0003-R
Pfender, W.F., Hagedorn, D.J., 1982. Aphanomyces euteiches f. sp. phaseoli, a causal agent of bean root and hypocotyl rot. Phytopathology (USA).
Pilet-Nayel, M.-L., Moury, B., Caffier, V., Montarry, J., Kerlan, M.-C., Fournet, S., Durel, C.-E., Delourme, R., 2017. Quantitative Resistance to Plant Pathogens in Pyramiding Strategies for Durable Crop Protection. Front. Plant Sci. 8. https://doi.org/10.3389/fpls.2017.01838
Plaumann, P.-L., Schmidpeter, J., Dahl, M., Taher, L., Koch, C., 2018. A Dispensable Chromosome Is Required for Virulence in the Hemibiotrophic Plant Pathogen Colletotrichum higginsianum. Front. Microbiol. 9, 1005. https://doi.org/10.3389/fmicb.2018.01005
Plissonneau, C., Benevenuto, J., Mohd-Assaad, N., Fouché, S., Hartmann, F.E., Croll, D., 2017. Using Population and Comparative Genomics to Understand the Genetic Basis of Effector-Driven Fungal Pathogen Evolution. Front. Plant Sci. 8. https://doi.org/10.3389/fpls.2017.00119
Polturak, G., Osbourn, A., 2021. The emerging role of biosynthetic gene clusters in plant defense and plant interactions. PLoS Pathog 17, e1009698. https://doi.org/10.1371/journal.ppat.1009698
Qiu, M., Li, Y., Ye, W., Zheng, X., Wang, Y., 2021. A CRISPR/Cas9-mediated in situ complementation method for *Phytophthora sojae* mutants. Mol. Plant Pathol. 22, 373–381. https://doi.org/10.1111/mpp.13028
Queiroz, C.B. de, Santana, M.F., 2020. Prediction of the secretomes of endophytic and nonendophytic fungi reveals similarities in host plant infection and colonization strategies. Mycologia 112, 491–503. https://doi.org/10.1080/00275514.2020.1716566
Quillévéré-Hamard, A., Le Roy, G., Lesné, A., Le May, C., Pilet-Nayel, M.-L., 2020. Aggressiveness of diverse French *Aphanomyces euteiches* isolates on pea Near-Isogenic-Lines differing in resistance QTL. Phytopathology® PHYTO-04-20-0147-R. https://doi.org/10.1094/PHYTO-04-20-0147-R
Quillévéré-Hamard, A., Le Roy, G., Moussart, A., Baranger, A., Andrivon, D., Pilet-Nayel, M.-L., Le May, C., 2018. Genetic and Pathogenicity Diversity of Aphanomyces euteiches Populations From Pea-Growing Regions in France. Front. Plant Sci. 9. https://doi.org/10.3389/fpls.2018.01673
Raffaele, S., Kamoun, S., 2012. Genome evolution in filamentous plant pathogens: why bigger can be better. Nat Rev Microbiol 10, 417–430. https://doi.org/10.1038/nrmicro2790
Rajput, N.A., Zhang, M., Ru, Y., Liu, T., Xu, J., Liu, L., Mafurah, J.J., Dou, D., 2014. Phytophthora sojae Effector PsCRN70 Suppresses Plant Defenses in Nicotiana benthamiana. PLoS ONE 9, e98114. https://doi.org/10.1371/journal.pone.0098114
Ramirez-Garcés, D., Camborde, L., Pel, M.J.C., Jauneau, A., Martinez, Y., Néant, I., Leclerc, C., Moreau, M., Dumas, B., Gaulin, E., 2016. CRN13 candidate effectors from plant and animal eukaryotic pathogens are DNA-binding proteins which trigger host DNA damage response. New Phytologist 210, 602–617. https://doi.org/10.1111/nph.13774
Rawlings, N.D., Waller, M., Barrett, A.J., Bateman, A., 2014. *MEROPS*: the database of proteolytic enzymes, their substrates and inhibitors. Nucl. Acids Res. 42, D503–D509. https://doi.org/10.1093/nar/gkt953

Ren, Y., Armstrong, M., Qi, Y., McLellan, H., Zhong, C., Du, B., Birch, P.R.J., Tian, Z., 2019. *Phytophthora infestans* RXLR Effectors Target Parallel Steps in an Immune Signal Transduction Pathway. Plant Physiol. 180, 2227–2239. https://doi.org/10.1104/pp.18.00625

Robin, G.P., Kleemann, J., Neumann, U., Cabre, L., Dallery, J.-F., Lapalu, N., O'Connell, R.J., 2018. Subcellular Localization Screening of Colletotrichum higginsianum Effector Candidates Identifies Fungal Proteins Targeted to Plant Peroxisomes, Golgi Bodies, and Microtubules. Front. Plant Sci. 9, 562. https://doi.org/10.3389/fpls.2018.00562

Rocafort, M., Fudal, I., Mesarich, C.H., 2020. Apoplastic effector proteins of plant-associated fungi and oomycetes. Current Opinion in Plant Biology 56, 9–19. https://doi.org/10.1016/j.pbi.2020.02.004

Roux, K.J., Kim, D.I., Raida, M., Burke, B., 2012. A promiscuous biotin ligase fusion protein identifies proximal and interacting proteins in mammalian cells. Journal of Cell Biology 196, 801–810. https://doi.org/10.1083/jcb.201112098

Saijo, Y., Loo, E.P., Yasuda, S., 2018. Pattern recognition receptors and signaling in plant-microbe interactions. Plant J 93, 592–613. https://doi.org/10.1111/tpj.13808

Sánchez-Vallet, A., Fouché, S., Fudal, I., Hartmann, F.E., Soyer, J.L., Tellier, A., Croll, D., 2018. The Genome Biology of Effector Gene Evolution in Filamentous Plant Pathogens. Annu. Rev. Phytopathol. 56, 21–40. https://doi.org/10.1146/annurev-phyto-080516-035303

Sarowar, M.N., van den Berg, A.H., McLaggan, D., Young, M.R., van West, P., 2013. Saprolegnia strains isolated from river insects and amphipods are broad spectrum pathogens. Fungal Biology 117, 752–763. https://doi.org/10.1016/j.funbio.2013.09.002

Sattelmacher, B., 2001. The apoplast and its significance for plant mineral nutrition. New Phytologist 149, 167–192. https://doi.org/10.1046/j.1469-8137.2001.00034.x

Savary, S., Willocquet, L., Pethybridge, S.J., Esker, P., McRoberts, N., Nelson, A., 2019. The global burden of pathogens and pests on major food crops. Nat Ecol Evol 3, 430–439. https://doi.org/10.1038/s41559-018-0793-y

Schoina, C., Rodenburg, S.Y.A., Meijer, H.J.G., Seidl, M.F., Lacambra, L.T., Bouwmeester, K., Govers, F., 2021. Mining oomycete proteomes for metalloproteases leads to identification of candidate virulence factors in *Phytophthora infestans*. Mol Plant Pathol 22, 551–563. https://doi.org/10.1111/mpp.13043

Schornack, S., Damme, M. van, Bozkurt, T.O., Cano, L.M., Smoker, M., Thines, M., Gaulin, E., Kamoun, S., Huitema, E., 2010. Ancient class of translocated oomycete effectors targets the host nucleus. PNAS 107, 17421–17426. https://doi.org/10.1073/pnas.1008491107

Schuster, M., Schweizer, G., Reissmann, S., Kahmann, R., 2016. Genome editing in Ustilago maydis using the CRISPR–Cas system. Fungal Genetics and Biology 89, 3–9. https://doi.org/10.1016/j.fgb.2015.09.001

Scott, W.W., 1961. A monograph of the genus Aphanomyces. Technical Bulletin. Virginia Agricultural Experiment Station 151.

Seidl, M.F., Van den Ackerveken, G., 2019. Activity and Phylogenetics of the Broadly Occurring Family of Microbial Nep1-Like Proteins. Annu. Rev. Phytopathol. 57, 367–386. https://doi.org/10.1146/annurev-phyto-082718-100054

Seong, K., Krasileva, K.V., 2021. Computational Structural Genomics Unravels Common Folds and Novel Families in the Secretome of Fungal Phytopathogen *Magnaporthe oryzae*. MPMI 34, 1267–1280. https://doi.org/10.1094/MPMI-03-21-0071-R

Serebriiskii, I., Estojak, J., Berman, M., Golemis, E.A., 2000. Approaches to Detecting False Positives in Yeast Two-Hybrid Systems. BioTechniques 28, 328–336. https://doi.org/10.2144/00282rr03

Shabab, M., Shindo, T., Gu, C., Kaschani, F., Pansuriya, T., Chintha, R., Harzen, A., Colby, T., Kamoun, S., van der Hoorn, R.A.L., 2008. Fungal Effector Protein AVR2 Targets Diversifying Defense-Related Cys Proteases of Tomato. The Plant Cell 20, 1169–1183. https://doi.org/10.1105/tpc.107.056325

Sivachandra Kumar, N.T., Caudillo-Ruiz, K.B., Chatterton, S., Banniza, S., 2021. Characterization of *Aphanomyces euteiches* Pathotypes Infecting Peas in Western Canada. Plant Disease 105, 4025–4030. https://doi.org/10.1094/PDIS-04-21-0874-RE

Snelders, N.C., Kettles, G.J., Rudd, J.J., Thomma, B.P.H.J., 2018a. Plant pathogen effector proteins as manipulators of host microbiomes?: Effectors manipulate microbiomes. Molecular Plant Pathology 19, 257–259. https://doi.org/10.1111/mpp.12628

Snelders, N.C., Kettles, G.J., Rudd, J.J., Thomma, B.P.H.J., 2018b. Plant pathogen effector proteins as manipulators of host microbiomes? Molecular Plant Pathology 19, 257–259. https://doi.org/10.1111/mpp.12628

Snelders, N.C., Rovenich, H., Petti, G.C., Rocafort, M., van den Berg, G.C.M., Vorholt, J.A., Mesters, J.R., Seidl, M.F., Nijland, R., Thomma, B.P.H.J., 2020. Microbiome manipulation by a soil-borne fungal plant pathogen using effector proteins. Nat. Plants. https://doi.org/10.1038/s41477-020-00799-5

Sonah, H., Deshmukh, R.K., Bélanger, R.R., 2016. Computational Prediction of Effector Proteins in Fungi: Opportunities and Challenges. Front. Plant Sci. 7. https://doi.org/10.3389/fpls.2016.00126

Spanu, P., Kämper, J., 2010. Genomics of biotrophy in fungi and oomycetes—emerging patterns. Current Opinion in Plant Biology 13, 409–414. https://doi.org/10.1016/j.pbi.2010.03.004

Sparkes, I.A., Runions, J., Kearns, A., Hawes, C., 2006. Rapid, transient expression of fluorescent fusion proteins in tobacco plants and generation of stably transformed plants. Nat Protoc 1, 2019–2025. https://doi.org/10.1038/nprot.2006.286

Specht, H., Emmott, E., Petelski, A.A., Huffman, R.G., Perlman, D.H., Serra, M., Kharchenko, P., Koller, A., Slavov, N., 2021. Single-cell proteomic and transcriptomic analysis of macrophage heterogeneity using SCoPE2. Genome Biol 22, 50. https://doi.org/10.1186/s13059-021-02267-5

Sperschneider, J., Dodds, P., 2021. EffectorP 3.0: prediction of apoplastic and cytoplasmic effectors in fungi and oomycetes. MPMI MPMI-08-21-0201-R. https://doi.org/10.1094/MPMI-08-21-0201-R

Sperschneider, J., Dodds, P.N., Gardiner, D.M., Singh, K.B., Taylor, J.M., 2018. Improved prediction of fungal effector proteins from secretomes with EffectorP 2.0: Prediction of fungal effectors with EffectorP 2.0. Molecular Plant Pathology 19, 2094–2110. https://doi.org/10.1111/mpp.12682

Spielmeyer, W., Mago, R., Wellings, C., Ayliffe, M., 2013. Lr67 and Lr34 rust resistance genes have much in common – they confer broad spectrum resistance to multiple pathogens in wheat. BMC Plant Biol 13, 96. https://doi.org/10.1186/1471-2229-13-96

Stam, R., Jupe, J., Howden, A.J.M., Morris, J.A., Boevink, P.C., Hedley, P.E., Huitema, E., 2013. Identification and Characterisation CRN Effectors in Phytophthora capsici Shows Modularity and Functional Diversity. PLoS ONE 8, e59517. https://doi.org/10.1371/journal.pone.0059517

Stam, R., Motion, G.B., Martinez-Heredia, V., Boevink, P.C., Huitema, E., 2021. A Conserved Oomycete CRN Effector Targets Tomato TCP14-2 to Enhance Virulence. MPMI 34, 309–318. https://doi.org/10.1094/MPMI-06-20-0172-R

Stephenson, S.-A., Hatfield, J., Rusu, A.G., Maclean, D.J., Manners, J.M., 2000. *CgDN3* : An Essential Pathogenicity Gene of *Colletotrichum gloeosporioides* Necessary to Avert a

Hypersensitive-Like Response in the Host *Stylosanthes guianensis*. MPMI 13, 929–941. https://doi.org/10.1094/MPMI.2000.13.9.929
Tabima, J.F., Grünwald, N.J., 2019. effectR: An Expandable R Package to Predict Candidate RxLR and CRN Effectors in Oomycetes Using Motif Searches. MPMI 32, 1067–1076. https://doi.org/10.1094/MPMI-10-18-0279-TA
Taguchi, K., Ogata, N., Kubo, T., Kawasaki, S., Mikami, T., 2009. Quantitative trait locus responsible for resistance to Aphanomyces root rot (black root) caused by Aphanomyces cochlioides Drechs. in sugar beet. Theor. Appl. Genet 118, 227–234.
Taguchi, Kazunori, Ogata, N., Kubo, T., Kawasaki, S., Mikami, T., 2009. Quantitative trait locus responsible for resistance to Aphanomyces root rot (black root) caused by Aphanomycescochlioides Drechs. in sugar beet. Theor Appl Genet 118, 227–234. https://doi.org/10.1007/s00122-008-0891-3
Tang, C., Xu, Q., Zhao, J., Yue, M., Wang, J., Wang, Xiaodong, Kang, Z., Wang, Xiaojie, 2022. A rust fungus effector directly binds plant pre-mRNA splice site to reprogram alternative splicing and suppress host immunity. Plant Biotechnology Journal 20, 1167–1181. https://doi.org/10.1111/pbi.13800
Tetorya, M., Rajam, M.V., 2021. RNAi-mediated silencing of PEX6 and GAS1 genes of Fusarium oxysporum f. sp. lycopersici confers resistance against Fusarium wilt in tomato. 3 Biotech 11, 443. https://doi.org/10.1007/s13205-021-02973-8
Thines, M., 2018. Oomycetes. Current Biology 28, R812–R813. https://doi.org/10.1016/j.cub.2018.05.062
Thines, M., Kamoun, S., 2010. Oomycete–plant coevolution: recent advances and future prospects. Current Opinion in Plant Biology 13, 427–433. https://doi.org/10.1016/j.pbi.2010.04.001
Tian, M., Benedetti, B., Kamoun, S., 2005. A Second Kazal-Like Protease Inhibitor from *Phytophthora infestans* Inhibits and Interacts with the Apoplastic Pathogenesis-Related Protease P69B of Tomato. Plant Physiology 138, 1785–1793. https://doi.org/10.1104/pp.105.061226
Tian, M., Huitema, E., da Cunha, L., Torto-Alalibo, T., Kamoun, S., 2004. A Kazal-like Extracellular Serine Protease Inhibitor from Phytophthora infestans Targets the Tomato Pathogenesis-related Protease P69B. Journal of Biological Chemistry 279, 26370–26377. https://doi.org/10.1074/jbc.M400941200
Tian, M., Win, J., Song, J., van der Hoorn, R., van der Knaap, E., Kamoun, S., 2007. A *Phytophthora infestans* Cystatin-Like Protein Targets a Novel Tomato Papain-Like Apoplastic Protease. Plant Physiology 143, 364–377. https://doi.org/10.1104/pp.106.090050
Torres, D.E., Oggenfuss, U., Croll, D., Seidl, M.F., 2020. Genome evolution in fungal plant pathogens: looking beyond the two-speed genome model. Fungal Biology Reviews 34, 136–143. https://doi.org/10.1016/j.fbr.2020.07.001
Tyler, B.M., 2006. Phytophthora Genome Sequences Uncover Evolutionary Origins and Mechanisms of Pathogenesis. Science 313, 1261–1266. https://doi.org/10.1126/science.1128796
Urban, M., Cuzick, A., Seager, J., Wood, V., Rutherford, K., Venkatesh, S.Y., De Silva, N., Martinez, M.C., Pedro, H., Yates, A.D., Hassani-Pak, K., Hammond-Kosack, K.E., 2019. PHI-base: the pathogen–host interactions database. Nucleic Acids Research gkz904. https://doi.org/10.1093/nar/gkz904
van der Burgh, A.M., Joosten, M.H.A.J., 2019. Plant Immunity: Thinking Outside and Inside the Box. Trends in Plant Science 24, 587–601. https://doi.org/10.1016/j.tplants.2019.04.009

van der Hoorn, R.A.L., 2011. Mining the active proteome of Arabidopsis thaliana. Front. Plant Sci. 2. https://doi.org/10.3389/fpls.2011.00089
van der Hoorn, R.A.L., Leeuwenburgh, M.A., Bogyo, M., Joosten, M.H.A.J., Peck, S.C., 2004. Activity Profiling of Papain-Like Cysteine Proteases in Plants. Plant Physiology 135, 1170–1178. https://doi.org/10.1104/pp.104.041467
van West, P., Morris, B.M., Reid, B., Appiah, A.A., Osborne, M.C., Campbell, T.A., Shepherd, S.J., Gow, N.A.R., 2002. Oomycete Plant Pathogens Use Electric Fields to Target Roots. MPMI 15, 790–798. https://doi.org/10.1094/MPMI.2002.15.8.790
Voß, S., Betz, R., Heidt, S., Corradi, N., Requena, N., 2018. RiCRN1, a Crinkler Effector From the Arbuscular Mycorrhizal Fungus Rhizophagus irregularis, Functions in Arbuscule Development. Front. Microbiol. 9, 2068. https://doi.org/10.3389/fmicb.2018.02068
Wang, D., Tian, L., Zhang, D., Song, J., Song, S., Yin, C., Zhou, L., Liu, Y., Wang, B., Kong, Z., Klosterman, S.J., Li, J., Wang, J., Li, T., Adamu, S., Subbarao, K.V., Chen, J., Dai, X., 2020. Functional analyses of small secreted cysteine-rich proteins identified candidate effectors in *Verticillium dahliae*. Molecular Plant Pathology 21, 667–685. https://doi.org/10.1111/mpp.12921
Wang, Jizong, Hu, M., Wang, Jia, Qi, J., Han, Z., Wang, G., Qi, Y., Wang, H.-W., Zhou, J.-M., Chai, J., 2019. Reconstitution and structure of a plant NLR resistosome conferring immunity. Science 364, eaav5870. https://doi.org/10.1126/science.aav5870
Wawra, S., Trusch, F., Matena, A., Apostolakis, K., Linne, U., Zhukov, I., Stanek, J., Koźmiński, W., Davidson, I., Secombes, C.J., Bayer, P., van West, P., 2017. The RxLR Motif of the Host Targeting Effector AVR3a of *Phytophthora infestans* Is Cleaved before Secretion. Plant Cell 29, 1184–1195. https://doi.org/10.1105/tpc.16.00552
Wei, M., Wang, A., Liu, Y., Ma, L., Niu, X., Zheng, A., 2020. Identification of the Novel Effector RsIA_NP8 in Rhizoctonia solani AG1 IA That Induces Cell Death and Triggers Defense Responses in Non-Host Plants. Front. Microbiol. 11, 1115. https://doi.org/10.3389/fmicb.2020.01115
Wicker, T., Sabot, F., Hua-Van, A., Bennetzen, J.L., Capy, P., Chalhoub, B., Flavell, A., Leroy, P., Morgante, M., Panaud, O., Paux, E., SanMiguel, P., Schulman, A.H., 2007. A unified classification system for eukaryotic transposable elements. Nat Rev Genet 8, 973–982. https://doi.org/10.1038/nrg2165
Williamson, B., Tudzynski, B., Tudzynski, P., Van Kan, J.A.L., 2007. Botrytis cinerea: the cause of grey mould disease. Mol Plant Pathol 8, 561–580. https://doi.org/10.1111/j.1364-3703.2007.00417.x
Wood, K.J., Nur, M., Gil, J., Fletcher, K., Lakeman, K., Gann, D., Gothberg, A., Khuu, T., Kopetzky, J., Naqvi, S., Pandya, A., Zhang, C., Maisonneuve, B., Pel, M., Michelmore, R., 2020. Effector prediction and characterization in the oomycete pathogen Bremia lactucae reveal host-recognized WY domain proteins that lack the canonical RXLR motif. PLoS Pathog 16, e1009012. https://doi.org/10.1371/journal.ppat.1009012
Wu, L., Chang, K.-F., Conner, R.L., Strelkov, S., Fredua-Agyeman, R., Hwang, S.-F., Feindel, D., 2018. Aphanomyces euteiches: A Threat to Canadian Field Pea Production. Engineering 4, 542–551. https://doi.org/10.1016/j.eng.2018.07.006
Xi, Y., Chochois, V., Kroj, T., Cesari, S., 2021. A novel robust and high-throughput method to measure cell death in *Nicotiana benthamiana* leaves by fluorescence imaging. Mol Plant Pathol 22, 1688–1696. https://doi.org/10.1111/mpp.13129
Ye, W., Wang, Yang, Wang, Yuanchao, 2015. Bioinformatics Analysis Reveals Abundant Short Alpha-Helices as a Common Structural Feature of Oomycete RxLR Effector Proteins. PLoS ONE 10, e0135240. https://doi.org/10.1371/journal.pone.0135240
Yildirir, G., Sperschneider, J., Malar C, M., Chen, E.C.H., Iwasaki, W., Cornell, C., Corradi, N., 2022. Long reads and Hi-C sequencing illuminate the two-compartment genome of

the model arbuscular mycorrhizal symbiont *Rhizophagus irregularis*. New Phytologist 233, 1097–1107. https://doi.org/10.1111/nph.17842

Yuan, M., Jiang, Z., Bi, G., Nomura, K., Liu, M., Wang, Y., Cai, B., Zhou, J.-M., He, S.Y., Xin, X.-F., 2021a. Pattern-recognition receptors are required for NLR-mediated plant immunity. Nature. https://doi.org/10.1038/s41586-021-03316-6

Yuan, M., Ngou, B.P.M., Ding, P., Xin, X.-F., 2021b. PTI-ETI crosstalk: an integrative view of plant immunity. Current Opinion in Plant Biology 62, 102030. https://doi.org/10.1016/j.pbi.2021.102030

Zhang, J., Zhou, J.-M., 2010. Plant Immunity Triggered by Microbial Molecular Signatures. Molecular Plant 3, 783–793. https://doi.org/10.1093/mp/ssq035

Zhang, Z.-H., Jin, J.-H., Sheng, G.-L., Xing, Y.-P., Liu, W., Zhou, X., Liu, Y.-Q., Chen, X.-R., 2021. A Small Cysteine-Rich Phytotoxic Protein of *Phytophthora capsici* Functions as Both Plant Defense Elicitor and Virulence Factor. MPMI 34, 891–903. https://doi.org/10.1094/MPMI-01-21-0025-R

Zhong, Z., Marcel, T.C., Hartmann, F.E., Ma, X., Plissonneau, C., Zala, M., Ducasse, A., Confais, J., Compain, J., Lapalu, N., Amselem, J., McDonald, B.A., Croll, D., Palma-Guerrero, J., 2017. A small secreted protein in *Zymoseptoria tritici* is responsible for avirulence on wheat cultivars carrying the *Stb6* resistance gene. New Phytol 214, 619–631. https://doi.org/10.1111/nph.14434

Zhou, J., Qi, Y., Nie, J., Guo, L., Luo, M., McLellan, H., Boevink, P.C., Birch, P.R.J., Tian, Z., 2022. A *Phytophthora* effector promotes homodimerization of host transcription factor StKNOX3 to enhance susceptibility. Journal of Experimental Botany erac308. https://doi.org/10.1093/jxb/erac308

Zuluaga, A.P., Vega-Arreguín, J.C., Fei, Z., Ponnala, L., Lee, S.J., Matas, A.J., Patev, S., Fry, W.E., Rose, J.K.C., 2016. Transcriptional dynamics of *Phytophthora infestans* during sequential stages of hemibiotrophic infection of tomato: Transcriptome of *P. infestans* in tomato. Molecular Plant Pathology 17, 29–41. https://doi.org/10.1111/mpp.12263

Annex I - An oomycete effector targets a plant RNA helicase involved in root development and defence (Camborde et al., 2022)

The work of functional characterization of the effectors is one of the major scientific activities of our research group. After the description of a unique set of Small Secreted Proteins (SSPs) in *A. euteiches* and identification of a AeSSP1256 gene, which promotes oomycete infection, the functional analysis led by Laurent Camborde began. In this annex chapter we present the study of mode of action of *A. euteiches* effector AeSSP1256, which is able to trigger nucleolar stress, when expressed in the host plant and hijacks host DEAD-box RNA Helicase MtRH10 from its binding to RNA. My role in this project consisted of material preparation and data analysis of RNASeq experiments and identification of the genes differentially regulated upon the expression of AeSSP1256 in the host roots.

Research

New Phytologist

An oomycete effector targets a plant RNA helicase involved in root development and defense

Laurent Camborde[1], Andrei Kiselev[1], Michiel J. C. Pel[1], Aurélie Le Ru[2], Alain Jauneau[2], Cécile Pouzet[2], Bernard Dumas[1] and Elodie Gaulin[1]

[1]Laboratoire de Recherche en Sciences Végétales (LRSV), Université de Toulouse, CNRS, UPS, Toulouse INP, Auzeville-Tolosane 31320, France; [2]Plateforme d'Imagerie FRAIB-TRI, Université de Toulouse, CNRS, Auzeville-Tolosane 31320, France

Author for correspondence:
Elodie Gaulin
Email: gaulin@lrsv.ups-tlse.fr

Received: *12 July 2021*
Accepted: *3 December 2021*

New Phytologist (2022) **233:** 2232–2248
doi: 10.1111/nph.17918

Key words: *Aphanomyces*, effectors, *Medicago*, MtRH10, nucleolar stress, oomycete, plant development, RNA-helicase.

Summary

- Oomycete plant pathogens secrete effector proteins to promote disease. The damaging soilborne legume pathogen *Aphanomyces euteiches* harbors a specific repertoire of Small Secreted Protein effectors (AeSSPs), but their biological functions remain unknown. Here we characterize AeSSP1256.
- The function of AeSSP1256 is investigated by physiological and molecular characterization of *Medicago truncatula* roots expressing the effector. A potential protein target of AeSSP1256 is identified by yeast-two hybrid, co-immunoprecipitation, and fluorescent resonance energy transfer–fluorescence lifetime imaging microscopy (FRET–FLIM) assays, as well as promoter studies and mutant characterization.
- AeSSP1256 impairs *M. truncatula* root development and promotes pathogen infection. The effector is localized to the nucleoli rim, triggers nucleoli enlargement and downregulates expression of *M. truncatula* ribosome-related genes. AeSSP1256 interacts with a functional nucleocytoplasmic plant RNA helicase (MtRH10). AeSSP1256 relocates MtRH10 to the perinucleolar space and hinders its binding to plant RNA. MtRH10 is associated with ribosome-related genes, root development and defense.
- This work reveals that an oomycete effector targets a plant RNA helicase, possibly to trigger nucleolar stress and thereby promote pathogen infection.

Introduction

Plant pathogens alter host cellular physiology to promote their own proliferation by producing effector proteins that interact with plant molecular targets. Previous studies have indicated large variations in the effector repertoire of plant pathogens, suggesting that a large number of molecular mechanisms are targeted by these effectors (He *et al.*, 2020).

Oomycetes constitute a large phylum and include important filamentous eukaryotic pathogens, many of which cause disease in plants or animals (van West & Beakes, 2014; Kamoun *et al.*, 2015). The presence of conserved motifs in some oomycete sequences has allowed the computational prediction of many candidate effectors in the oomycete genome (Haas *et al.*, 2009; McGowan & Fitzpatrick, 2017; Tabima & Grünwald, 2019). There is increasing evidence that the plant nucleus is an important compartment for effector function, mainly because of the large portfolio of putative nucleus-targeting effectors predicted in oomycete genomes (Schornack *et al.*, 2010; Stam *et al.*, 2013; Song *et al.*, 2015; Zhang *et al.*, 2015; Wang *et al.*, 2019). Accordingly, different mechanisms of action at the nuclear level have been reported, including alteration of gene transcription (Song *et al.*, 2015; Wirthmueller *et al.*, 2018; He *et al.*, 2019), mis-localization of transcription factors (McLellan *et al.*, 2013), suppression of RNA silencing by inhibition of siRNA accumulation (Xiong *et al.*, 2014; Qiao *et al.*, 2015), and plant DNA damage (Ramirez-Garcés *et al.*, 2016; Camborde *et al.*, 2019). However, only a small number of oomycete effectors have been assigned a specific function.

Aphanomyces euteiches, the causal agent of pea root rot disease, is a major pathogen that affects crop and forage legumes and naturally infects the model legume *Medicago truncatula* (Gaulin *et al.*, 2007). The severity of symptoms observed upon exposure of natural *M. truncatula* lines to the pathogen showed a continuous gradient, indicating that the interaction is quantitative, ranging from a relative resistance phenotype to a high susceptibility phenotype (Djébali *et al.*, 2009; Jacquet & Bonhomme, 2020). Among *M. truncatula*, the susceptible F83005.5 line developed symptoms within a few days and commonly died within 3 wk, whereas the A17-Jemalong partially resistant line displayed retarded growth and a delay in the appearance of symptoms (Djébali *et al.*, 2009; Jacquet & Bonhomme, 2020). Partial resistance to *A. euteiches* in *M. truncatula* and in pea has been shown to be controlled by numerous quantitative trait loci (QTLs) whose effects on the disease range from minor to major (Hamon *et al.*, 2013; Bonhomme *et al.*, 2014, 2019; Desgroux *et al.*,

2018). No fully resistant lines have been reported, and the observed partial resistance is commonly linked to the development of a large number of roots and lateral roots (Bonhomme *et al.*, 2014, 2019; Badis *et al.*, 2015; Desgroux *et al.*, 2018).

In our recent work, we have combined transcriptomics and genomics analyses to identify *A. euteiches* pathogenic determinants. We identified a new class of effectors of > 290 Small Secreted Proteins (AeSSPs) specifically found in *A. euteiches* (Gaulin *et al.*, 2018). These AeSSPs contain a predicted N-terminus signal peptide, are < 300 residues in length, and are devoid of any functional annotations. Many AeSSPs contain a predicted nuclear localization signal (NLS), suggesting that these are probably active within the host nucleus. Screening to identify plant nuclear-localized *A. euteiches* effectors that can promote *Phytophthora capsici* infection led to the identification of AeSSP1256. This effector, which is upregulated during early colonization of *M. truncatula* roots, presented a predicted signal peptide followed by a bipartite nuclear localization signal (NLS). The idea that AeSSP1256 targets the plant nucleus has been confirmed by its transient expression with or without its signal peptide, both in *Nicotiana benthamiana* leaves and A17 *M. truncatula* roots (Gaulin *et al.*, 2018).

In this study, to gain further insight into the role of AeSSP1256, we have investigated its activity in *M. truncatula*. We found that AeSSP1256 promotes pathogen infection of the A17 partially resistant line and restricts root development. Our microscopic studies and whole-transcriptome approaches in A17 *M. truncatula* roots expressing the effector showed that AeSSP1256 triggers nucleolar stress and downregulates host ribosome-related genes. Using yeast-two hybrid (Y2H), co-immunoprecipitation and FRET–FLIM assays, we identified that AeSSP1256 binds a nucleocytoplasmic DExD-box RNA-Helicase (RH) in *M. truncatula* (MtRH10). This interaction leads to the re-localization of MtRH10 to the perinucleolar space, and it is thus diverted away from its RNA target. Imaging studies using promoter:GUS and MtRH10:GFP constructs reveal the exact expression and localization of MtRH10 in the meristematic cells of the A17 root apex. Silencing of the corresponding gene delays root growth and affects expression of ribosome-related genes, while its overexpression counteracts this phenotype. In contrast to its overexpression, silencing of MtRH10 modifies the outcome of the infection, making the tolerant A17 roots susceptible to *A. euteiches* infection. This study demonstrates that soil-borne oomycete effectors possibly trigger nucleolar stress to promote infection by targeting host RHs, which contribute to root development and defense through the ribosome biogenesis pathway.

Materials and Methods

Plant material, microbial strains, and growth conditions

All experiments were carried out using the partially resistant line *M. truncatula* Jemalong-A17. Seeds were cultured *in vitro* and transformed as described by Boisson-Dernier *et al.* (2001); Djébali *et al.* (2009). *Aphanomyces euteiches* (ATCC 201684) zoospore inoculum was prepared as described by Badreddine *et al.* (2008). Root infection was performed using 10^3 zoospores as described by Ramirez-Garcés *et al.* (2016). *Nicotiana benthamiana* plants were grown under a 16 h : 8 h, 24°C : 20°C, light : dark photoperiod at 70% humidity. *Escherichia coli* (DH5α, DB3.1), *A. tumefaciens* (GV3101::pMP90) and *A. rhizogenes* (ARQUA-1) strains were grown on LB medium using the appropriate antibiotics.

Construction of plasmid vectors and *Agrobacterium*-mediated transformation

The green fluorescent protein (GFP) control plasmid (pK7WGF2), and the *35S:AeSSP1256:YFP, 35S:AeSSP1256:GFP, 35S:SP-AeSSP1256:GFP* (AeSSP1256 sequence with its own signal peptide) and minus or plus signal peptide *35S:AeSSP1256:GFP:KDEL* constructs are described in Gaulin *et al.* (2018). The primers used in this study are listed in Supporting Information Table S1. *Medicago truncatula* candidates sorted by Y2H assay (Table S2) were amplified using Pfx Accuprime polymerase (12344024; Thermo Fisher, Waltham, MA, USA) and introduced into the pENTR/D-TOPO vector by TOPO cloning (K240020; Thermo Fisher) and then transferred into the pK7WGF2, pK7FWG2 (http://gateway.psb.ugent.be/), pAM-PAT-35S::GTW:CFP and pAM-PAT-35S::CFP:GTW binary vectors. The cloning of the *MtRH10* gene (Legoo: MtrunA17_Chr5g0429221) into pK7WGF2 produced the *GFP:MtRH10* construct.

Using pENTR/D-TOPO:AeSSP1256, as described previously (Gaulin *et al.*, 2018), AeSSP1256 was transferred by LR recombination into pAM-PAT-35S::GTW:3HA to create an *AeSSP1256:HA* construct for co-immunoprecipitation and Western blot experiments, and into pUBC-RFP-DEST (Grefen *et al.*, 2010) to obtain the *AeSSP1256:RFP* construct for confocal analyses. For RNAi of MtRH10, a 328 nucleotide sequence in the 3′UTR was amplified by polymerase chain reaction (PCR; Table S1), introduced into the pENTR/D-TOPO vector and LR cloned into the pK7GWiWG2(II)-RedRoot binary vector to obtain the RNAi MtRH10 construct. This vector allows hairpin RNA expression and contains the red fluorescent marker DsRED under the constitutive *Arabidopsis* Ubiquitin10 promoter. For MtRH10 promoter expression analyses, a 1441 nucleotide region downstream of the start codon of the *MtRH10* gene was amplified by PCR (Table S1), fused to the *β-glucuronidase* gene (using the pICH75111 vector (Engler *et al.*, 2014)) and inserted into the pCambia2200:DsRED derivative plasmid (Fliegmann *et al.*, 2013) by Golden Gate cloning to generate the PromoterMtRH10:GUS vector.

Medicago truncatula composite plant hairy roots were generated as described elsewhere (Boisson-Dernier *et al.*, 2001) using the ARQUA-1 *Agrobacterium rhizogenes* strain. *Agrobacterium tumefaciens-transformed* strains were syringe-infiltrated into *N. benthamiana* as described by Gaulin *et al.* (2002).

RNA-Seq experiments

For *35S:GFP* and *35S:SP-AeSSP1256:GFP* RNA-Seq analysis, the total RNA of four biological replicates of transformed roots

were extracted. Before harvest, roots were checked for GFP-fluorescence by live macro-imaging (Axiozoom; Zeiss) and the GFP-positive roots were excised from the plants. Four replicates were prepared for each condition, with one replicate corresponding to the pool of transformed roots excised from 20–40 transgenic plants. Total RNA was extracted using the E.Z.N.A.® total RNA kit (Omega Bio-tek, Norcross, GA, USA) and purified using the Monarch® RNA Cleanup Kit (NEB, Ipswich, MA, USA). cDNA libraries were produced using the MultiScribe™ Reverse Transcriptase kit using a mix of random and poly-T primers under standard conditions for real-time polymerase chain reaction (RT-PCR). Library preparation was performed using the GeT-PlaGe genomic platform (https://get.genotoul.fr/en/) and sequenced using a HiSeq3000 sequencer (Illumina, San Diego, CA, USA). The raw data were trimmed with TrimGalore (v.0.6.5) (https://github.com/FelixKrueger/TrimGalore) with cutadapt and FastQC options, and mapped to *M. truncatula* cv Jemalong A17 reference genome v.5.0 (Pecrix *et al.*, 2018) using Hisat2 (v.2.1.0) (Kim *et al.*, 2019). Samtools (v.1.9) algorithms 'fixmate' and 'markdup' (Li *et al.*, 2009) were used to clean alignments from duplicated sequences. Reads were counted with HTseq (v.0.9.1) (Anders *et al.*, 2015) using the reference GFF file. The count files were normalized and differentially expressed genes (DEGs) were identified using the DESeq2 algorithm (Love *et al.*, 2014); false-positive hits were filtered using a high-throughput sequencing (HTS) filter (Rau *et al.*, 2013). The threshold of the adjusted *P*-values was set to 1×10^{-5} ($P_{adj} < 1 \times 10^{-5}$). Gene ontology (GO) enrichment of DEGs was performed using topGO (Alexa & Rahnenfuhrer, 2020) software. RNA-Seq experiments on susceptible F83005.5 (F83) plants infected by *A. euteiches* are described in Gaulin *et al.* (2018).

RNA extraction and quantitative qRT-PCR

Total RNA was extracted using the E.Z.N.A.® Plant RNA kit (Omega Bio-tek). For reverse transcription, 1 μg of total RNA was used, and reactions were performed with the High-Capacity cDNA Reverse Transcription Kit (Applied Biosystems, Foster City, CA, USA). Quantitative reverse transcription polymerase chain reaction was performed using SYBRGreen (Applied Biosystems) on a QuantStudio 6 (Applied Biosystems) device. The primers used are listed in Table S1.

To estimate the extent of infection by *A. euteiches*, the expression of the α-tubulin coding gene (*Ae_22AL7226* (Gaulin *et al.*, 2008)) was analyzed. The *Histone 3-like* and *EF1α* genes of *M. truncatula* (Rey *et al.*, 2013) were used to normalize *A. euteiches* RNA abundance during infection. For *Aphanomyces* quantification within *AeSSP1256*-expressing roots, five technical replicates and three biological replicates were performed for each time point. A technical replicate is a pool of three to five root systems from distinct composite plants' hairy roots from one *M. truncatula* transformation. Biological replicates correspond to infection assays performed on independent *M. truncatula* transformation assays. Thus, for each time point and construct, 45–75 transformed root systems were analyzed. For *MtRH10* gene quantification, four technical replicates and two biological replicates were performed for each time point (30–40 root systems analyzed per time point). For missense *MtRH10* experiments, cDNA from five samples was used, given that a sample was a pool of five plants (n = 25 plants for each construct). For *A. euteiches* quantification in infected roots transformed by GFP:MtRH10, RNAi MtRH10 constructs or in GFP control roots, three technical replicates and two biological replicates were performed each time (*c.* 50 root systems for GFP:MtRH10 or RNAi MtRH10, and 91 for GFP control plants). The relative expression of *Ae* α-tubulin and *MtRH10* helicase genes was calculated using the $2^{-\Delta\Delta C_t}$ method (Livak & Schmittgen, 2001). For reverse transcription polymerase chain reaction (qRT-PCR) validation of RNA-Seq experiments, cDNA were derived from five technical replicates, and two biological replicates. The relative expression levels of 17 ribosome-related genes (Table S3) were calculated using the $2^{-\Delta\Delta C_t}$ method.

Yeast two-hybrid assays

An ULTImate Y2H™ assay was carried out by Hybrigenics Services (https://www.hybrigenics-services.com) using the mature form of AeSSP1256 (20–208 aa) as bait against a library prepared from *M. truncatula* roots infected by *A. euteiches*. The library was prepared by Hybrigenics Services using a mixture of RNA isolated from uninfected *M. truncatula* F83005.5 (±12%), *M. truncatula* infected with *A. euteiches* ATCC201684 harvested 1 d post-infection (±46%), and *M. truncatula* infected with *A. euteiches* harvested 6 d post-infection (±42%). This library is now available to other customers at Hybrigenics Services. For each interaction identified during the screen performed by Hybrigenics (65 million interactions tested), a 'Predicted Biological Score (PBS)' was given, which indicates the reliability of the identified interaction. The PBSs range from 'A' (very high confidence of interaction) to 'F' (experimentally proven technical artifacts). In this study, we kept candidates with PBS values from 'A' to 'C' for validation.

Analysis of the amino acid sequence of *MtRH10*

MtRH10 (*MtrunA17_Chr5g042922I*) putative nuclear localization signal (NLS) motifs were predicted by cNLS Mapper with a cut-off score of 4.0 (Kosugi *et al.*, 2009). The putative nuclear export signal (NES) motifs were predicted using NES Finder v.0.2 (http://research.nki.nl/fornerodlab/NES-Finder.htm) and the NetNES 1.1 Server (la Cour *et al.*, 2004). Conserved motifs and domains of DExD-box R were found using the ScanProsite tool on the ExPASy website (https://prosite.expasy.org/scanprosite/).

For the phylogenetic tree, 29 sequences were selected based on BlastP results (cut off *e*-value < 10^{-30}) using *MtRH10* on the *Medicago truncatula* genome portal (Mt5.0 version, https://medicago.toulouse.inra.fr/). Three sequences with an alignment length < 30% (MtrunA17_Chr1g0155691; MtrunA17_Chr8g0349951; MtrunA17_Chr1g0155211) were removed from the dataset. The phylogenetic tree was constructed and visualized using the CLC Workbench (Qiagen), with ClustalW alignment and the neighbor-joining (NJ) method with default parameters and a bootstrap value of 1000.

Immunoblot analysis

For *N. benthamiana* protein analyses, at least three independent agroinfiltration assays were performed for each construct. Each assay represents the infiltration of three plants on two distinct leaves per plant. A technical replicate is a pool of the two leaves from the same plant (three technical replicates per assay). Each blot was performed with technical replicates from one assay, and blots were repeated using the replicates from the independent assays. For *M. truncatula* protein analyses, each blot was repeated using proteins extracted from the different biological replicates. Immunoblots were performed as described in Ramirez-Garcés *et al.* (2016) using 30 μg of total protein separated on 10% Stain-Free SDS-PAGE gels (1610173; Bio-Rad). For GFP detection, an anti-GFP from mouse IgG1κ (clones 7.1 and 13.1; 11814460 001, Roche) was used. A monoclonal anti-hemagglutinin (HA) antibody produced in mouse (H9658, Sigma-Aldrich) was used for HA detection. An anti-mouse secondary antibody coupled to horseradish peroxidase (BioRad; 170-6516) was used with an ECL Clarity Kit (BioRad; 170-5060) for visualization.

Co-immunoprecipitation assay

Co-immunoprecipitation was performed using *N. benthamiana* infiltrated leaves. Biological and technical replicates were harvested 24 h after treatment, and total proteins (50 μg) were incubated for 3 h at 4°C with 30 μl of GFP-Trap Agarose beads (gta-20; Chromotek, Planegg, Germany). After the washing steps, the GFP-beads were boiled in SDS loading buffer (Merck; S3401) and immunoblotting was performed.

Confocal microscopy

Scanning was performed on a TCS SP8 confocal microscope (Leica, Microsystems, UK). For GFP and GFP variant recombinant proteins, the excitation wavelength was 488 nm, with emission absorbance between 500 nm and 550 nm, whereas an excitation wavelength of 543 nm was used for RFP variant proteins, with emission absorbance between 560 nm and 600 nm. Images were acquired with a ×40 or ×20 water immersion lens and correspond to Z projections of the scanned tissues (*c.* 5 μm depth). All confocal images were analyzed and processed using the ImageJ software package (http://rsb.info.nih.gov/ij/).

Cytological observations of transformed roots

Roots of composite plants were prepared as described previously (Ramirez-Garcés *et al.*, 2016). For each construct, a total of nine roots from three independent transformation experiments were used. NDPview2 software was used to observe longitudinal root sections of GFP or missense MtRH10 plants and to measure the root apical meristem (RAM) was used for all other measurements. Average RAM cell sizes were estimated by measuring all the cells from the same layer from the quiescent center to the RAM boundary. Mean values were then calculated from > 200 cells. In the elongation zone (EDZ) of GFP, AeSSP1256: GFP or missense *MtRH10* roots, cell area and cell perimeter were measured in a rectangular measuring *c.* 300 × 600 μm (two selections per root). To obtain a normalized cell perimeter, each cell perimeter was proportionally recalculated for a 500 μm^2 area standard cell. To estimate cell shape differences, considering that cortical cells in the EDZ of GFP control roots are mostly rectangular, we measured the perimeter bounding rectangle (PBR), which represents the smallest rectangle enclosing the cell. We then calculated the perimeter : PBR ratio. Rectangular cells have a perimeter : PBR ratio close to 1.

Measurement of nucleolar surface

Ten roots from two independent *M. truncatula* transformations were fixed for 2 h under vacuum in fixation buffer 4% paraformaldehyde (15710; Electron Microscopy Sciences), 50 mM sodium cacodylate (12300; Electron Microscopy Sciences), 0.1% Triton X-100 (T8787; Merck) diluted in TBS 1× (ET220; Euromedex, Souffelweyersheim, France) and incubated overnight at 4°C. After washing in TBS 1×, roots were stained with 4′,6-diamidino-2-phenylindole (DAPI; D8417; Merck) for 30 min under vacuum before confocal imaging using the GFP channel (excitation 488 nm; emission 500–550 nm), DAPI channel (excitation 405 nm; emission 415–450 nm) or bright field (BF). The nucleolar surface was estimated using ImageJ software by combining measurements based on the three channels (GFP, DAPI, BF).

Fluorescent resonance energy transfer (FRET)/fluorescence lifetime imaging microscopy (FLIM) measurements

For protein–protein interactions, *N. benthamiana* agroinfiltrated leaves were analyzed as described previously (Tasset *et al.*, 2010). For protein–nucleic acid interactions, samples were prepared as described in (Camborde *et al.*, 2017; Escouboué *et al.*, 2019). Nucleic acid staining was performed by vacuum infiltrating a 5 μM Sytox Orange (S11368; Thermo Fisher) solution. Samples were observed on an inverted microscope (Eclipse TE2000E; Nikon, Tokyo, Japan). For RNase treatment, foliar discs were incubated for 15 min at room temperature with 0.5 mg ml^{-1} RNase A (R6513; Merck) before nucleic acid staining. Fluorescence lifetime measurements were performed in the time domain using a streak camera as described by Camborde *et al.* (2017). The fluorescence lifetime of the donor (GFP) was experimentally measured in the presence and absence of the acceptor (Sytox Orange). FRET efficiencies (E) were calculated by comparing the lifetime of the donor in the presence of the acceptor (τ_{DA}) to that in the absence of the acceptor (τ_D): $E = 1 - (\tau_{DA})/(\tau_D)$. Statistical comparisons between control (donor) and assay (donor + acceptor) lifetime values were made using Student's *t*-test. For each experiment, nine leaf discs collected from three agroinfiltrated leaves were used, and at least two independent infiltration assays were performed. A minimum of 30 nuclei were scanned to ensure the statistical significance of the data.

Results

AeSSP1256 impairs *Medicago truncatula* root development and promotes pathogen infection

To investigate the function of AeSSP1256 in the host plant, we expressed the *AeSSP1256* gene in *M. truncatula* A17-Jemalong roots (*35S:SP-AeSSP1256:GFP*). In these 'composite' plants generated using *Agrobacterium rhizogenes,* only the root system is transformed (Boisson-Dernier *et al.*, 2001). The presence of AeSSP1256 in the plant strongly affects root development, as shown in the photographs in Fig. 1(a). The total number of roots and primary root length per plant are significantly lower in AeSSP1256-expressing roots than in GFP control roots (Fig. 1b). The presence of the GFP-tagged AeSSP1256 protein (expected size 46.5 kDa) was confirmed by Western-blot analysis using anti-GFP antibodies on total proteins extracted from the transformed *Medicago truncatula* roots (Fig. 1c). A slight cleavage of the AeSSP1256-fusion protein was observed thanks to the presence of a GFP-band at *c.* 26 kDa. To check if the observed aberrant root development is due to the GFP-tag, we confirmed the phenotype on A17 roots expressing a HA-tagged version of AeSSP1256 (Fig. 1c,d).

To evaluate whether AeSSP1256 modifies the outcome of the infection, AeSSP1256:GFP-expressing roots were inoculated with *A. euteiches* zoospores. We observed browning of the roots, indicating root rot symptoms due to *A. euteiches*, from 7 to 21 d after inoculation of the pathogen in both the control GFP-roots and in AeSSP1256-expressing roots, but with greater severity in roots expressing the effector (Fig. 1e). We carried out RT-qPCR analyses at 7-, 14- and 21 d post-inoculation to monitor pathogen development and compared them with infected GFP-control roots. Our results showed that the presence of the effector rendered the partially resistant A17 *Medicago* roots more susceptible to the pathogen (1.5–5 times higher accumulation of the pathogen with time) (Fig. 1f). Thus, expression of AeSSP1256 alters root development and enhances host root infection.

AeSSP1256 localizes to the nucleolus rim and triggers nucleoli enlargement in *M. truncatula* root cells

The *Medicago* composite plant hairy roots were used to confirm the subcellular localization of the effector in the host. As depicted in Fig. 2(a), confocal analyses showed a fluorescent circle around the nucleolus for AeSSP1256 GFP-fusion protein in *Medicago* hairy roots cells. The nucleolus rim is not observed in GFP-transformed hairy roots (*35S:GFP*). We next found evidence that supports the subcellular localization of AeSSP1256 through confocal imaging of *N. benthamiana* leaves agroinfiltrated with *35S:SP-AeSSP1256:RFP* in combination with *35S:GFP:H2B* (Histone 2B). An RFP-fluorescence pattern at the nucleolus rim which surrounds the nucleolar GFP fluorescence pattern of GFP:H2B proteins was detected (Fig. S1), thus demonstrating the presence of AeSSP1256 at the nucleolus rim *in planta*.

We noticed that the peri-nucleolus localization of AeSSP1256 in *Medicago* roots seems to be correlated with enlarged nucleoli, as revealed in DAPI-stained samples (Fig. 2b). Measurements of nucleoli size from image analysis confirmed a variation from 4.5 μm^2 ($\pm$1.9) for control roots to 6.6 μm^2 ($\pm$3) for AeSSP1256:GFP-expressing roots (Fig. 2c). Changes in morphology and nucleolus size are linked to nucleolar activity (Ohbayashi & Sugiyama, 2018). Perturbation of the nucleolar structure ultimately impairs ribosome biogenesis and triggers so-called nucleolar/ribosomal stress (Ohbayashi & Sugiyama, 2018). Thus, the enlargement of *Medicago* nucleoli in the presence of AeSSP1256 suggests that the effector induces nucleolar stress by interfering with the ribosome biogenesis pathway.

To find out whether the effect of AeSSP1256 on *Medicago* roots is linked to the peri-nucleolar localization of the effector, a KDEL-endoplasmic reticulum (ER) retention signal was added to the *35S:SP-AeSSP1256:GFP* construct (Fig. S2a). The observed GFP fluorescence pattern in these transgenic roots is similar to that detected in roots transformed with the mCherry-ER marker (*ER-rb-CD3-960* construct) (Fig. S2a,b). As expected, this points to the retention of the effector in the endoplasmic reticulum. By contrast, a nuclear fluorescence pattern is detected when *Medicago* roots are transformed with a *35S:AeSSP1256:GFP:KDEL* construct (Fig. S2a,b). In each of these situations, the fluorescence pattern is distinctly different from that detected in GFP control roots. The presence of the different versions of the effector in transgenic roots was investigated using Western-blot analysis (Fig. S2c). As illustrated in Fig. S2(d) and quantified in Fig. S2(e), abnormal root development was observed only when the AeSSP1256 effector accumulated in the nuclei of *Medicago*. Taken together, our results demonstrate that the localization of the effector to the nucleolus rim is important for its biological activity.

AeSSP1256 affects the expression of genes related to ribosome biogenesis

We performed comparative whole-genome transcriptomic analysis using paired-end sequencing of four biological replicates of *35S:GFP* and *35S:SP-AeSSP1256:GFP* transformed roots. In all, we identified 4391 DEGs, 2129 of which were upregulated and 2262 of which were downregulated (adjusted *P*-value $< 1 \times 10^{-5}$; Table S3a). To identify the function of the DEGs, we performed gene set enrichment analysis using the TopGO software package for the three main GO categories (Fig. 3a; Table S3b): biological process, cellular component, and molecular function. The upregulated DEGs corresponded mainly to the 'photosynthesis' GO term. In the downregulated DEGs, we identified 'ribosome biogenesis', 'organonitrogen compound biosynthesis' and 'cellular amide metabolic processes' GO terms to be among the most represented, all of which were strikingly downregulated. We next selected 17 *M. truncatula* genes for qRT-PCR analysis to confirm the effect of AeSSP1256 on the ribosome biogenesis pathway of the host. First, we chose ten Arabidopsis genes that control plant development (i.e. mutants with shorter root phenotypes) (Table S3c) by Blast searches (> 80% identity) in the A17 line r5.0 genome portal (Pecrix *et al.*, 2018). We also selected seven genes coding for ribosomal

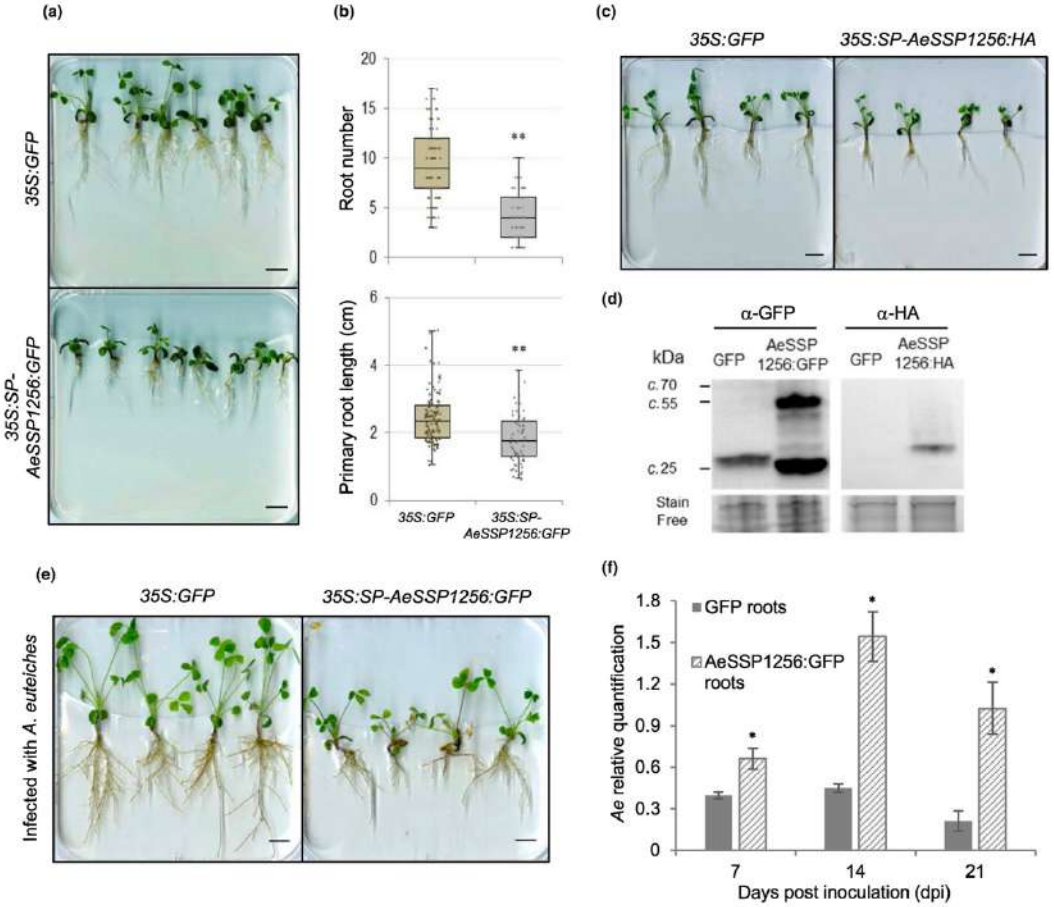

Fig. 1 AeSSP1256 perturbs *Medicago truncatula* root development and increases its susceptibility to *Aphanomyces euteiches*. Plants of the tolerant *M. truncatula* A17 line were transformed using *Agrobacterium rhizogenes* with *35S:GFP* or *35S:SP-AeSSP1256:GFP* constructs to generate composite plants in which only the root system was transformed. (a) Representative 35S:GFP and 35S:SP-AeSSP1256:GFP *M. truncatula* plants grown over 21 d. Note the reduced growth of the roots expressing AeSSP1256:GFP compared those expressing free green fluorescent protein (GFP). Bar, 1 cm. (b) Quantification of root number (upper panel) and primary root length (in cm; bottom panel) of transformed roots of control and 35S:SP-AeSSP1256:GFP plants at 21 d after transformation (DAT). Results were obtained from five independent experiments for a total of 126 GFP-transformed plants and 79 AeSSP1256:GFP-transformed plants. The boxes indicate the interquartile range (25th to the 75th percentile). The central line within the boxes represents the mean value. The whiskers indicate the minimum and maximum values. The jittered data points were superimposed onto the box plot to show the underlying distribution of the data. The asterisks indicate significant differences (Student's *t*-test; **, $P < 0.001$). (c) Representative *M. truncatula* roots transformed with the *35S:GFP* or *35S:SP-AeSSP1256:HA* constructs at 21 DAT. Note the reduction in the development of the root system. Bar, 1 cm. (d) Western-blot analysis using total proteins extracted from transformed *M. truncatula* roots at 21 DAT and anti-GFP or anti-HA antibodies. Protein loading was verified by stain-free imaging of polyacrylamide gel. The representative blot (from three independent analyses) shows a band at *c.* 28 kDa for the free GFP expressed from a pK7WGF2 vector in control roots. The GFP-tagged effector expressed from the pK7FWG2 vector is probably cleaved, with an expected band at *c.* 46.5 kDa and an additional band for the free GFP. (e) Representative root rot disease symptoms observed in 35S:GFP and 35S:SP-AeSSP1256:GFP *M. truncatula* plants at 14 d post-inoculation with *A. euteiches*. Transformed-roots (21 DAT) were inoculated with 10 µl of *A. euteiches* zoospores (10^5 spores ml^{-1}). Bar, 1 cm. (f) Relative quantification of the *A. euteiches* tubulin gene in transformed roots treated by the pathogen, as analyzed by quantitative polymerase chain reaction (qPCR). 35S:GFP- and 35S:SP-AeSSP1256:GFP-transformed roots were inoculated with 10 µl of *A. euteiches* zoospores (10^5 spores ml^{-1}). Data were collected from three to five different pools of roots for a total of 45 to 75 plants per time point at 7, 14 and 21 d post-infection. Bars represent the mean values (±SE). Asterisks indicate significant differences (Student's *t*-test; *, $P < 0.05$).

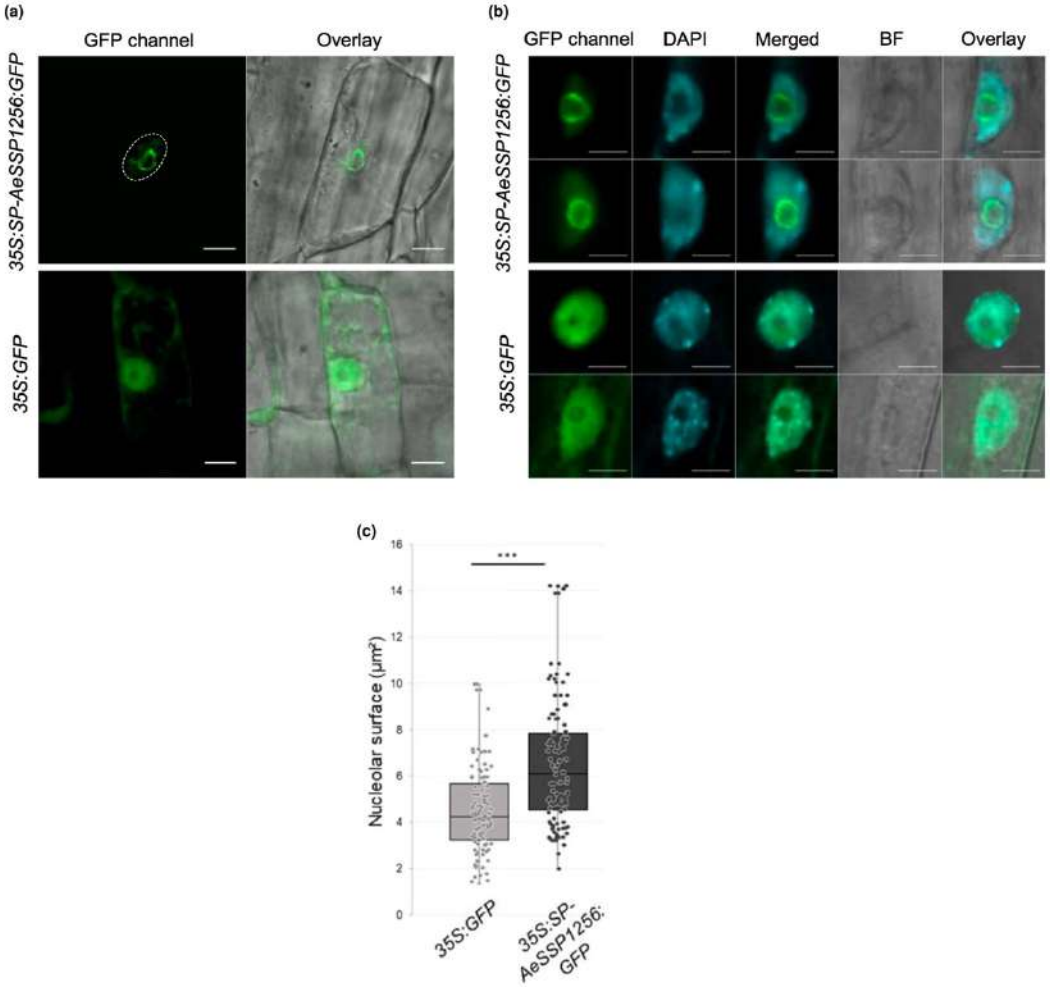

Fig. 2 AeSSP1256 localizes to the nucleolus rim and triggers nucleoli size enlargement in *Medicago truncatula* roots. Hairy root transformation of *M. truncatula* A17 line, using *Agrobacterium rhizogenes* to generate composite plants where only the root system was transformed. (a) Representative confocal analysis images of *M. truncatula* roots 21 d after *Agrobacterium* transformation (DAT) with *35S:GFP* or *35S:SP-AeSSP1256:GFP* constructs. Note that the free green fluorescent protein (GFP) shows a nucleocytoplasmic localisation, while AeSSP1256:GFP is localized as a ring around the nucleolus. Dashed lines indicate the nucleus. Bar, 5 µm. (b) Roots were fixed and nuclei were stained with 4′,6-diamidino-2-phenylindole (DAPI). Note the enlargement in the nucleoli surface where AeSSP1256:GFP proteins are present, as compared to cells expressing free GFP. BF, bright field. Bar, 5 µm. (c) Nucleoli surface measurements (in μm^2) for root cells expressing *35S:GFP* or *35S:SP-AeSSP1256:GFP* at 21 DAT. The boxes indicate interquartile range (25^{th} to the 75^{th} percentile). The central line within the boxes represents the mean value. The whiskers indicate the minimum and maximum values. The jittered data points were superimposed onto the box plot to show the underlying distribution of the data $n = 108$ nuclei for GFP, and 124 nuclei for AeSSP1256:GFP, using a total of 10 different roots for each construct. Independent experiments were conducted for a total of 126 GFP-transformed plants and 79 AeSSP1256:GFP-transformed plants. Asterisks indicate significant differences (Student's *t*-test; ***, $P = 1.51 \times 10^{-9}$).

proteins and related to 'ribosome biogenesis' in *M. truncatula* for expression analysis based on the KEGG pathway map (https://www.genome.jp/kegg-bin/show_pathway?ko03008) (Table S3c). As shown in Fig. 3(b), all of the seventeen selected genes from *M. truncatula* are downregulated in the presence of AeSSP1256. At this point, our results pointed to a perturbation of the ribosome biogenesis pathway of the host plant by the AeSSP1256 effector.

(a)

	Rank	GO ID	GO name	Total	Significant (%)	Expected	P-value
4391 DEGs							
Downregulated	1	GO:1901566	Organonitrogen compound biosynthetic process	1328	254 (19%)	101	< 1e−30
2262 total	2	GO:0006518	Peptide metabolic process	737	169 (23%)	56.05	< 1e−30
	3	GO:0043603	Cellular amide metabolic process	865	185 (21%)	65.78	< 1e−30
	4	GO:0042254	Ribosome biogenesis	573	144 (25%)	43.58	< 1e−30
	5	GO:0043604	Amide biosynthetic process	761	169 (22%)	57.87	< 1e−30
Upregulated	1	GO:0015979	Photosynthesis	186	51 (27%)	9.21	1.70E−24
2129 total	2	GO:0009765	Photosynthesis, light harvesting	24	15 (62%)	1.19	2.00E−14
	3	GO:0019684	Photosynthesis, light reaction	94	23 (24%)	4.65	1.20E−10
	4	GO:0007154	Cell communication	745	68 (9%)	36.87	6.90E−07
	5	GO:0007165	Signal transduction	610	58 (9%)	30.19	1.30E−06

(b)

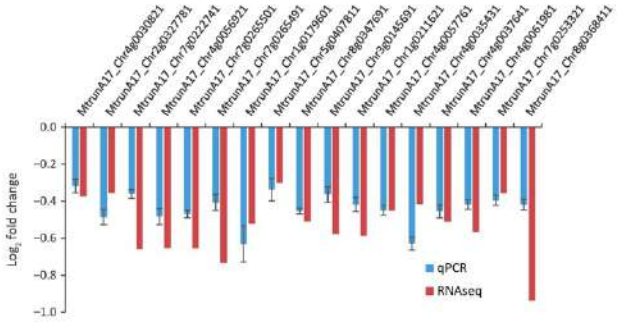

(c)

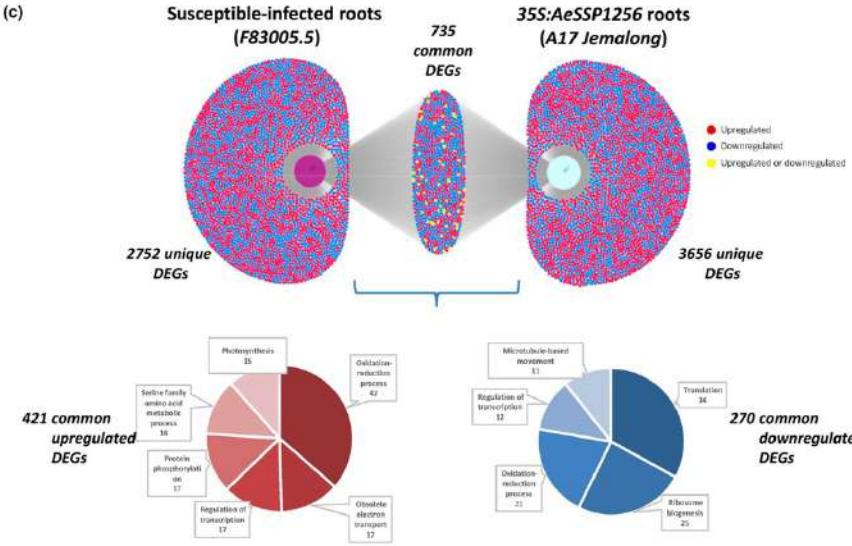

Fig. 3 Transcriptomic analyses reveal downregulation of genes related to ribosome biogenesis in both AeSSP1256-expressing roots and *Aphanomyces euteiches-infected* roots. (a) Top five enriched gene ontology (GO)-terms of downregulated and upregulated genes, obtained using classical gene set enrichment analysis (GSEA) with Fischer's exact test. Expected, enrichment threshold; Significant, number of differentially expressed genes (DEGs); Total, number of genes of the category in the genome. (b) Comparison of RNA-Seq ($n = 4$) and quantitative reverse transcription polymerase chain reaction (qRT-PCR) ($n = 5$, different samples of the RNA-Seq) analysis of selected ribosome biogenesis-related genes in AeSSP1256-expressing roots. Bars represent the mean values (±SE). (c) Upper panel: Venn diagram of DEGs for two RNA-Seq experiments (number of genes) in susceptible *Medicago truncatula* F83005.5 roots infected with *A. euteiches* at 9 dpi (data from Gaulin *et al.*, 2018) and the tolerant *M. truncatula* A17 line expressing the AeSSP1256:GFP effector (this study). Bottom panel: DEGs that are specific or common to the F83-infected line and the AeSSP1256-expressing roots (downregulated (blue) and upregulated (red)). Lower panel: Pie charts depicting the number of common DEGs associated with a GO term. Only GO terms associated with > 10 genes are represented. GO terms related to 'translation and ribosome-biogenesis' are the most represented in the downregulated category.

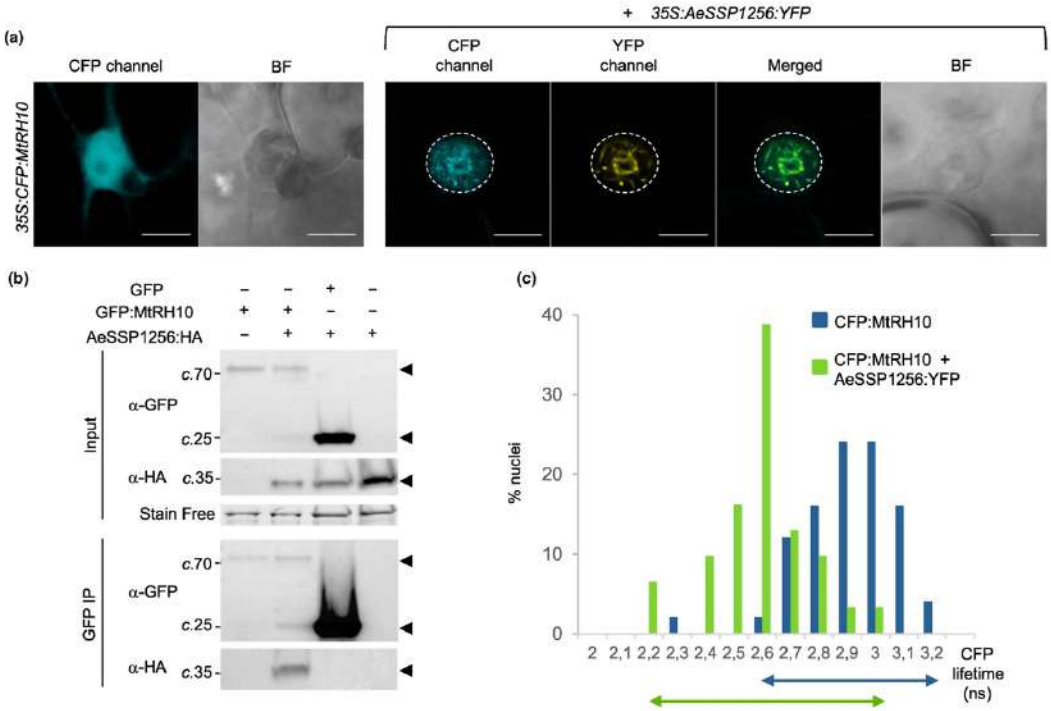

Fig. 4 AeSSP1256 associates with and relocalizes a nucleocytoplasmic host RNA helicase (MtRH10) to the nucleolus rim in *Nicotiana benthamiana* cells. Four-week-old *N. benthamiana* leaves were inoculated or co-inoculated with *Agrobacterium tumefaciens* harbouring the *35S:AeSSP1256:YFP* or *35S:CFP:MtRH10* constructs. For each construct, three independent replicates were performed; per repetition, two leaves from two distinct leaf stages and three independent plants were agroinfiltrated. (a) Representative fluorescence images obtained using confocal laser scanning microscopy 1 d after transient expression in leaves. Samples were randomly selected for fluorescence detection. MtRH10 shows a nucleocytoplasmic localization (left panel), while the presence of AeSSP1256 re-localizes MtRH10 to the peri-nucleolar space around the nucleolus (right panel) where the effector is localized. BF, bright field. The white dashed lines indicate the nuclear membrane. Bar, 10 μm. (b) Representative immunoprecipitation (IP) of protein extracts from agroinfiltrated leaves using GFP-Trap beads, confirming that AeSSP1256 associates with MtRH10. Expression of constructs in the leaves is indicated by 'plus' symbols (+). Protein size markers are indicated in kDa and protein loading is verified by stain-free imaging of polyacrylamide gel. Protein fusion bands are indicated by arrows. Upper panel: anti-GFP and anti-HA blots to confirm the presence of fusion proteins in the input fractions. Lower panel: anti-GFP and anti-HA blots on output fractions to reveal the presence of the corresponding protein. (c) Cyan fluorescent protein (CFP) lifetime distribution of the *35S:CFP:MtRH10* construct when expressed alone or in combination with the *35S:AeSSP1256:YFP* construct in transiently transformed *N. benthamiana* leaves. Histograms show the distribution of nuclei (%) according to classes of CFP:MtRH10 lifetime in the absence (blue bars) or presence (green bars) of AeSSP1256:YFP. The arrows represent the CFP lifetime distribution range. Statistical analyses are provided in Table 2. The significant decrease in fluorescence lifetime indicates a close association between AeSSP1256 and MtRH10.

We next investigated if the effector by itself mimics responses observed during pathogen infection of *M. truncatula*. This was done by mining the RNA-Seq experiment that we previously developed on the susceptible F83005.5 (F83) *M. truncatula* line (Gaulin *et al.*, 2018). As shown in the Venn diagram depicting both specific and common upregulated and downregulated genes in AeSSP1256:GFP-expressing roots and in susceptible F83-infected roots 9 d after infection, 735 are common DEGs (Fig. 3c; Table S3d). A number of the common upregulated DEGs are associated with 'oxido-reduction and photosynthesis' GO terms, while the downregulated DEGs are associated with 'ribosome biogenesis' and 'translation' GO terms. With regard to the total DEG analysis, these two categories mostly consist of downregulated genes, which occupy, respectively, 92% and 84% of the common DEGs (Fig. 3c; Table S3d,e). These results show that expression of AeSSP1256 within the host root cells mimics some of the effects induced by the pathogen when it infected the susceptible *Medicago* line.

AeSSP1256 associates with a nucleocytoplasmic host RNA helicase (MtRH10) and relocalizes it to the nucleolus rim

A yeast two hybrid (Y2H) library composed of cDNA from *M. truncatula* roots infected with *A. euteiches* was screened with the effector to identify AeSSP1256 protein targets. Through screening, we identified eight *M. truncatula* coding genes, seven

Table 1 Fluorescent resonance energy transfer–fluorescence lifetime imaging microscopy (FRET–FLIM) measurements of a *Medicago truncatula* cyan fluorescent protein (CFP)-tagged RNA helicase (MtRH10) in the presence or absence of the AeSSP1256:YFP effector, to detect protein–protein interactions.

Donor	Acceptor	τ^a	SEM[b]	n^c	E^d	P-value[e]
CFP:MtRH10	–	2.86	0.023	50	–	–
CFP:MtRH10	AeSSP1256:YFP	2.53	0.031	31	11.1	2.56×10^{-12}

[a]Mean lifetime in nanoseconds (ns).
[b]Standard error of the mean.
[c]Total number of measured nuclei.
[d]FRET efficiency in %: $E = 1 - (\tau DA/\tau D)$, where τDA is the lifetime of the donor in the presence of the acceptor, and τD is the lifetime of the donor in the absence of the acceptor.
[e]P-value (Student's t-test) for the difference between the donor lifetimes in the presence or absence of the acceptor.

Table 2 Fluorescent resonance energy transfer–fluorescence lifetime imaging microscopy (FRET–FLIM) measurements for GFP:MtRH10 with or without Sytox Orange, to detect protein–nucleic acid interactions.

Donor	Acceptor	τ^a	SEM[b]	n^c	E^d	P-value[e]
GFP:H2B	–	2.45	0.025	30	–	–
	Sytox	1.89	0.072	30	23	2.88×10^{-9}
GFP:H2B *(+RNase)*	–	2.36	0.032	32	–	–
	Sytox	1.92	0.056	31	19	1.12×10^{-9}
GFP	–	2.29	0.034	35	–	–
	Sytox	2.30	0.037	36	0	0.94
GFP:MtRH10	–	2.32	0.020	60	–	–
	Sytox	2.08	0.027	60	10.3	1.30×10^{-10}
GFP:MtRH10 *(+RNaSe)*	–	1.94	0.028	46	–	–
	Sytox	1.95	0.035	39	0	0.83

[a]Mean lifetime in nanoseconds (ns).
[b]Standard error of the mean.
[c]Total number of measured nuclei.
[d]FRET efficiency in %: $E = 1 - (\tau DA/\tau D)$, where τDA is the lifetime of the donor in the presence of the acceptor, and τD is the lifetime of the donor in the absence of the acceptor.
[e]P-value (Student's t-test) for the difference between the donor lifetimes in the presence or absence of the acceptor.

of which corresponded to putative nuclear proteins (Table S2). After testing six candidates for co-localization by transient expression in *N. benthamiana* (Fig. S3) we focused on a DExD-box ATP-dependent RH encoded by the *MtrunA17_Chr5g0429221* gene (Mt5.0 version). Indeed, co-expression in *Nicotiana* leaves of the nucleocytoplasmic GFP-RH with a CFP-tagged AeSSP1256 triggered a redistribution of the RH to the perinucleolar space (Fig. 4a). The redistribution of the RH to the nucleolus rim in *N. benthamiana* cells was also confirmed using a HA-tagged version of the effector and Western-blot analysis (Fig. S4a,b).

BLAST analysis revealed that the closest plant orthologs of the RH are AtRH10 in *Arabidopsis thaliana* (UniProtKb: Q8GY84) and OsRH10 in *Oryza sativa* (UniProtKb: A2XKG2) (% similarity 51.2% and 49.2% at the amino acid level), while there is no close ortholog in *N. benthamiana*. These two nucleolar RHs are involved in ribosome biogenesis (Matsumura *et al.*, 2016; Liu & Imai, 2018) and rRNA homeostasis, respectively (Wang *et al.*, 2016). Accordingly, the target *Medicago* protein of AeSSP1256 was named MtRH10. MtRH10 is related to the human nucleolar RH DDX47 (UniProtKb: Q9H0S4) (Sekiguchi *et al.*, 2006) and the yeast nuclear RH RRP3 (UniProtKb: P38712) (O'Day, 1996). MtRH10 harbors predicted putative NESs (positions 7–37; 87–103; 261–271), an NLS (position 384–416) and conserved functional domains, as inferred from its sequence alignment with DDX47, RRP3, AtRH10 and OsRH10 proteins (Fig. S5a).

Table 3 Fluorescent resonance energy transfer–fluorescence lifetime imaging microscopy (FRET–FLIM) measurements for GFP:MtRH10 with or without Sytox Orange, in the presence of AeSSP1256:HA, to detect protein–nucleic acid interactions.

Donor + AeSSP1256:HA	Acceptor	τ^a	SEM[b]	n^c	E^d	P-value[e]
GFP:MtRH10 (Relocalized)	–	2.30	0.023	60	–	–
GFP:MtRH10 (Relocalized)	Sytox	2.30	0.020	60	0	0.789

[a]Mean lifetime in nanoseconds (ns).
[b]Standard error of the mean.
[c]Total number of measured nuclei.
[d]FRET efficiency in %: $E = 1 - (\tau DA/\tau D)$, where τDA is the lifetime of the donor in the presence of the acceptor, and τD is the lifetime of the donor in the absence of the acceptor.
[e]P-value (Student's t-test) for the difference between the donor lifetimes in the presence or absence of acceptor.

BLASTP analysis of the *M. truncatula* proteome (https://medicago.toulouse.inra.fr/) revealed that MtRH10 has the highest identity at the amino acid level with MtrunA17_Chr6g0483491 and MtrunA17_Chr7g0236841 (> 62%) and *c.* 53% amino acid identity with MtrunA17_Chr1g0155201. The phylogenetic tree using full amino acid sequences from *M. truncatula* (cut off *e*-value $< 10^{-30}$) showed that the four sequences are classified within the same group, subdivided into two distinct classes and related to the RH10 family from different species (Fig. S5b). The other *M. truncatula* sequences are less similar and are related to other known DExD-box proteins such as AtRH36 from *Arabidopsis*.

Interaction between AeSSP1256 and MtRH10 was assessed using co-immunoprecipitation and FRET-FLIM experiments. Following immunoprecipitation with GFP beads at 24 dpi, we searched for the presence of the corresponding proteins by Western-blotting. The AeSSP1256:HA proteins were detected in the GFP:MtRH10 immunoprecipitated fraction but not with free GFP (Fig. 4b). We performed a FRET-FLIM analysis on *N. benthamiana* leaves to detect protein–protein interactions. At 24 hpi, we found that the fluorescence lifetime of CFP-MtRH10 was shifted to lower values in the presence of the effector (Fig. 4c). As listed in Table 1, the change in the mean CFP lifetime within the CFP:MtRH10-expressing nuclei from 2.86 ns (in the absence of the effector) to 2.53 ns (in the presence of the YFP-tagged effector) reveals association *in planta*. These data indicate

that the effector interacts with MtRH10 *in vivo* and causes its redistribution to the nucleoli rim.

MtRH10 binding to RNA is disrupted by AeSSP1256

To test whether MtRH10 is functionally active for RNA binding, we examined its interaction with nucleic acids by FRET-FLIM (Förster, 1948; Camborde *et al.*, 2017). The donors were GFP:MtRH10, GFP:H2B or GFP transiently expressed in *N. benthamiana* leaves. Agroinfiltrated samples were collected 1 d after treatment and labelled with Sytox Orange to convert nucleic acids to FRET acceptors. In the absence of Sytox Orange the mean lifetime of GFP:H2B was 2.45 ns, and it decreased to 1.89 ns in the presence of the dye, indicating the association of GFP:H2B with nucleic acids (Table 2). On the other hand, no significant difference in GFP lifetime was observed for free GFP samples (2.29 ns to 2.30 ns), in the absence or presence of Sytox Orange. Values for control samples are in accordance with our previous reports (Ramirez-Garcés *et al.*, 2016; Camborde *et al.*, 2017). We monitored the association of GFP:MtRH10 with nucleic acids by following the decrease in GFP lifetime in the presence of Sytox Orange. A significant decrease from 2.32 ns to 2.08 ns was observed, as noted in Table 2. Samples were further treated with RNase to check the specificity of the association of MtRH10 with nucleic acids. The results given in Table 2 show that RNase treatment of the GFP:H2B agroinfiltrated samples does not modify the significant decrease in GFP lifetime in the presence of Sytox Orange dye, indicating that GFP:H2B control proteins were associated with DNA. By contrast, there is no significant difference in GFP lifetime in the absence (1.94 ns ± 0.028) or presence of Sytox Orange (1.95 ns ± 0.035) in RNase-treated GFP:MtRH10 samples (Table 2). These results indicate that MtRH10 binds plant nuclear RNA.

To determine whether MtRH10 relocalization by AeSSP1256 to the nucleoli rim affects its binding capacity, we performed FRET-FLIM assays to evaluate nucleic acid interactions. A *35S:GFP:MtRH10* construct and a *35S:AeSSP1256:HA* construct were co-expressed in *N. benthamiana* leaves, and the recovery of GFP fluorescence lifetime was monitored 1 d after treatment. Measurements made in nuclei where both tagged-proteins were detected indicated that the GFP lifetime of GFP:MtRH10 remained unchanged, with or without the Sytox Orange acceptor (2.30 ns under both conditions) (Table 3). This assay shows the inability of MtRH10 to bind nucleic acids in the presence of the effector *in planta*.

MtRH10 is expressed in root meristematic tissue and is involved in the development of *M. truncatula* roots

To decipher the function of MtRH10, we first considered its expression by mining public transcriptomic databases PHYTOZOME (https://phytozome.jgi.doe.gov/pz/portal.html), MT EXPRESSV1 (https://lipm-browsers.toulouse.inra.fr/pub/expressionAtlas/app/) and MEDICAGOEFP BROWSER (http://bar.utoronto.ca/efpmedicago/cgi-bin/efpWeb.cgi). No significant variations were detected among the conditions tested in the databases, and no transcriptional changes were detected in our RNA-Seq data generated from *M. truncatula* roots infected by the pathogen, or in qRT-PCR using AeSSP1256-expressing roots (Fig. S6).

By using a MtRH10 promoter-driven GUS (β-glucuronidase) chimeric construct, we detected GUS activity mainly in meristematic cells at the root tip or in lateral emerging roots (Fig. 5a). We then overexpressed a GFP-tagged version of MtRH10 in *M. truncatula* roots. Confocal imaging confirmed the nucleocytoplasmic localization of MtRH10 when compared with GFP-control roots. We observed the accumulation of MtRH10 as brighter dots in the nucleolus of *M. truncatula* cells (Fig. 5b), probably corresponding to the fibrillar centers of nucleoli containing rDNA. No developmental defects were detected in roots

Fig. 5 MtRH10 is expressed in meristematic cells of *Medicago truncatula*, and its deregulation impacts root system architecture (RAS). (a) A 1.44 kb region of the MtRH10 promoter fused to a GUS-encoding gene was transformed into *M. truncatula* roots using *Agrobacterium rhizogenes*. Transformed roots (21 d old) were stained with X-Gluc for 2 h, after which blue colouring, corresponding to MtRH10 promoter expression, was observed. Photographs were taken of the root tip (top panel) and emerging lateral root (bottom panel). Arrows indicate the blue cells. Bar, 100 μm. (b) Representative fluorescence images taken using confocal laser scanning microscopy, of *M. truncatula* roots with a *35S:GFP* (top panel) or *35S:GFP:MtRH10* construct (bottom panel) 21 d after *A. rhizogenes*-mediated root transformation. Note the nucleocytoplasmic localization of GFP:MtRH10, with some brighter dots in the nucleolus (arrows). Lower panels represent the corresponding nucleus enlargements. n, nucleus. Bar, 10 μm. Left panel: 488 nm excitation wavelength; right panel: overlay (488 nm + bright field). (c) Representative photographic images of *M. truncatula* plants transformed at the root level with a *35S:GFP*, *35S:GFP:MtRH10* or *35S:RNAi MtRH10* construct at 21 d after transformation. No particular phenotype distinguished the control GFP roots from those that overexpress MtRH10. Developmental delay was observed in roots compromised for MtRH10 expression (missense MtRH10). Bar, 1 cm. (d) Quantification of root number (top panel) and primary root length (cm; bottom panel) of transformed control roots, *35S:MtRH10* and *35S:RNAi MtRH10* roots at 21 d after transformation. The boxes indicate the interquartile range (25th to the 75th percentile). The central line within the boxes represents the mean value. The whiskers indicate the minimum and maximum values. The jittered data points were superimposed onto the box plot to show the underlying distribution of the data. Results were obtained from three independent experiments for a total of 80 GFP-transformed plants, 55 *MtRH10*-transformed plants and 45 *RNAi:MtRH10*-transformed plants. The lowercase letters ('a' and 'b') indicate significant differences according to Student's *t*-test (where data belong to different classes if $P < 0.01$). (e) Representative longitudinal section of *M. truncatula* root tips transformed with a *35S:GFP* (left) or *35S:RNAi MtRH10* (right) construct. Root apical meristem (RAM) size is determined from the quiescent center (dot line) up to the elongation/differentiation zone (EDZ), defined by the first elongated cortex cell of the second cortical layer (arrowhead). Note the reduced RAM size and the modified shape of EDZ cells in roots in which MtRH10 expression is compromised. Bar, 100 μm. (f) Histograms of total RAM size and mean RAM cortical cell size of the corresponding transformed roots. Note that the RAM of roots in which MtRH10 expression is compromised are smaller than those of GFP control roots, but the average cell size of cortical cells in the RAM is not significantly different. Bars represent mean values and the error bars represent SD. Asterisks indicate a significant difference according to Student's *t*-test (***, $P < 0.0001$; ns, not significant).

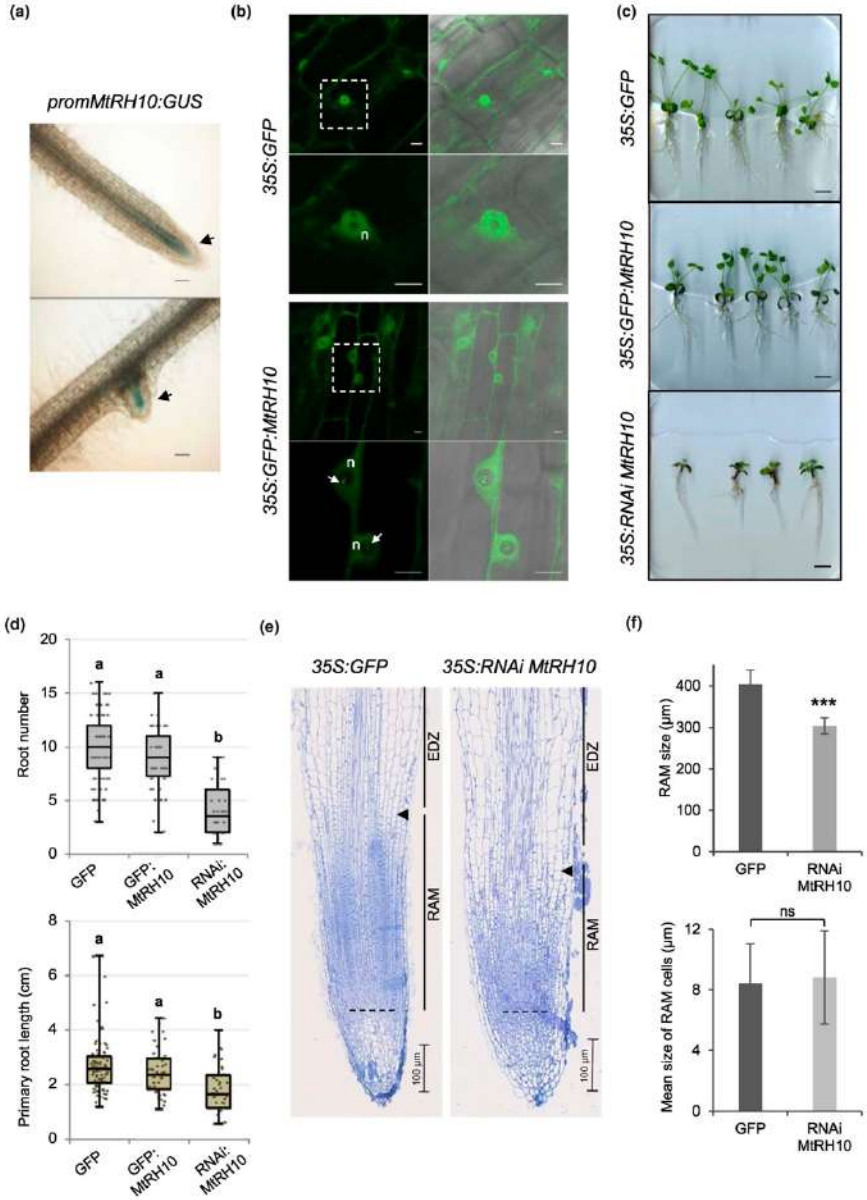

overexpressing MtRH10 (Fig. 5c,d). By contrast, in silenced MtRH10 roots, obtained with a specific 3′UTR region of the MtRH10 sequence (Fig. S7a), we detected a smaller number of roots and a reduced primary root length (Fig. 5c,d). Using qRT-PCR primers that amplified transcripts of MtrunA17_Chr1g0155201 and MtrunA17_Chr6g0483491 in combination with MtrunA17_Chr7g0236841, we confirmed the reduced expression of MtRH10 (by a factor of 3–5) in these transgenic

roots at 21 d post transformation (Fig. S7b), while the expression of MtRH10-related genes was maintained (Fig. S7c).

The reduced expression of MtRH10 triggers nucleoli enlargement in *M. truncatula* root cells, as depicted in Fig. S8(a) and quantified in Fig. S8(b). Longitudinal sections revealed a reduced RAM size in MtRH10 silenced cells, due to a decrease in cortical cell number rather than a smaller cell size (Fig. 5e,f). The cells in the EDZ of these transgenic roots lost their rectangular shape, and their sizes were decreased by a factor of two compared to control roots (Fig. S9). The same developmental defects were detected in roots expressing the AeSSP1256 effector (Fig. S9). The data show that in cell division zones, MtRH10 is associated with *M. truncatula* root development, and AeSSP1256 may affect its activity.

MtRH10 is associated with the ribosome biogenesis pathway and promotes *M. truncatula* tolerance to pathogen infection

To assess whether an impaired MtRH10 initiates nucleolar stress, as suggested by the presence of enlarged nucleoli in silenced MtRH10 roots, we performed qRT-PCR using the same set of primers to confirm this effect in AeSSP1256-expressing roots. As shown in Fig. 6(a), in silenced MtRH10 roots, all 17 ribosome-related genes were downregulated, indicating that MtRH10 is associated with the ribosome biogenesis pathway. Hence, we investigated whether MtRH10 contributes to *M. truncatula* root resistance to the soil-borne pathogen *A. euteiches*. MtRH10 overexpressing and MtRH10-silenced roots were inoculated with zoospores of *A. euteiches*. Western-blot analysis confirmed the presence of MtRH10 at all times of pathogen infection in MtRH10-overexpressing roots (Fig. S10). A reduced amount of mycelium was seen after 7, 14 and 21 d of infection in roots overexpressing MtRH10, compared to GFP-control roots, as shown by qPCR (Fig. 6b). By contrast, transgenic roots in which MtRH10 expression was compromised contained *c.* 5–10 times larger quantities of the pathogen at 7, 14 and 21 d post-infection (Fig. 6c). These assays show that MtRH10 is implicated in basal resistance to *A. euteiches* infection in *M. truncatula*.

Discussion

To modulate host cell processes and facilitate infection, filamentous plant pathogens secrete an array of effector proteins which target various plant components. Here we report that the small protein AeSSP1256 secreted by *A. euteiches* can potentially induce nucleolar stress to promote infection by targeting a host nucleocytoplasmic DExD-box RH (MtRH10) associated with ribosome biogenesis and root development.

Our experiments revealed that transient expression of AeSSP1256 in *M. truncatula* hairy roots triggers developmental defects and facilitates pathogen infection of the partially resistant A17-Jemalong line. This modification to the output of infection is highly relevant, since the quantitative resistance of *M. truncatula* to *A. euteiches* is correlated with root development, and this indicator is strongly correlated with other infection markers such as the death of the plant or the necrosis of cotyledons (Jacquet & Bonhomme, 2020). We have also demonstrated that the detrimental effect of the effector necessitated a localization to the nucleoli rim, showing that the plant nucleolus plays a key role in pathogen resistance.

The nucleolus is a membrane-free subnuclear compartment that is essential for the highly complex process of ribosome biogenesis. The sizes and morphologies of nucleoli are linked to nucleolar activity (Shaw & Brown, 2012). We observed that AeSSP1256 promotes nucleolar expansion of *M. truncatula* root cells. Similar enlargement of the nucleolus, together with excessive accumulation of pre-rRNA processing intermediate has been reported in several Arabidopsis ribosome-related mutants (Ohbayashi & Sugiyama, 2018). Moreover, defects in root development and retarded growth are typical characteristics of Arabidopsis ribosomal protein mutants (Wieckowski & Schiefelbein, 2012; Ohbayashi *et al.*, 2017). In animals, perturbation of any of the steps of ribosome biogenesis in the nucleolus can cause nucleolar stress that is associated with modification of the size and shape of the nucleolus. This in turn stimulates specific signaling pathways, leading, for example, to arrested cell growth (Pfister, 2019).

Considering the localization of AeSSP1256 to the nucleoli rim in combination with nucleoli hypertrophy, we hypothesize that AeSSP1256 most likely causes nucleolar stress by interfering with the host ribosome biogenesis pathway. RNA-Seq experiments showed that within A17-roots, AeSSP1256 downregulated numerous ribosome-related genes. This effect was also detected in susceptible F83005.5 *M. truncatula* lines infected by *A. euteiches*.

AeSSP1256 targets a nucleocytoplasmic DExD/H box RH in *M. truncatula* (MtRH10). The DExD/H box protein family includes the largest family of RHs (Fuller-Pace, 2006). These proteins participate in all RNA processes, including RNA export and translation, and splicing. However, the most common function of these proteins is in ribosome biogenesis, including the assembly process (Jarmoskaite & Russell, 2011). MtRH10 is related to the rice nucleolar RH OsRH10 (TOGR1), which is involved in rRNA homeostasis (Wang *et al.*, 2016), and the *Arabidopsis* nucleolar RH AtRH10, which is involved in ribosome biogenesis (Matsumura *et al.*, 2016; Liu & Imai, 2018). The human nucleolar RH DDX47 (Sekiguchi *et al.*, 2006) and yeast nuclear RH RRP3 (O'Day, 1996) orthologs are parts of a large ribonucleoprotein complex (SSU) that mediates 18S rRNA biogenesis in eukaryotes (Martin *et al.*, 2013; Vincent *et al.*, 2018). Like DDX47, MtRH10 possesses a bipartite nuclear transport domain that can function as an NLS, and two NESs. MtRH10 probably shuttles between the cytoplasm and the nucleus/nucleolus, as has been reported for many other RHs that are involved in rRNA biogenesis and splicing (Sekiguchi *et al.*, 2006; Wang *et al.*, 2009).

Plant genomes encode a large variety of DExD/H RH families, and several are associated with plant development, hormone signaling or responses to abiotic stresses (Liu & Imai, 2018). We show that MtRH10 expression is restricted to the root apical meristematic zone where cells divide. MtRH10 regulates primary

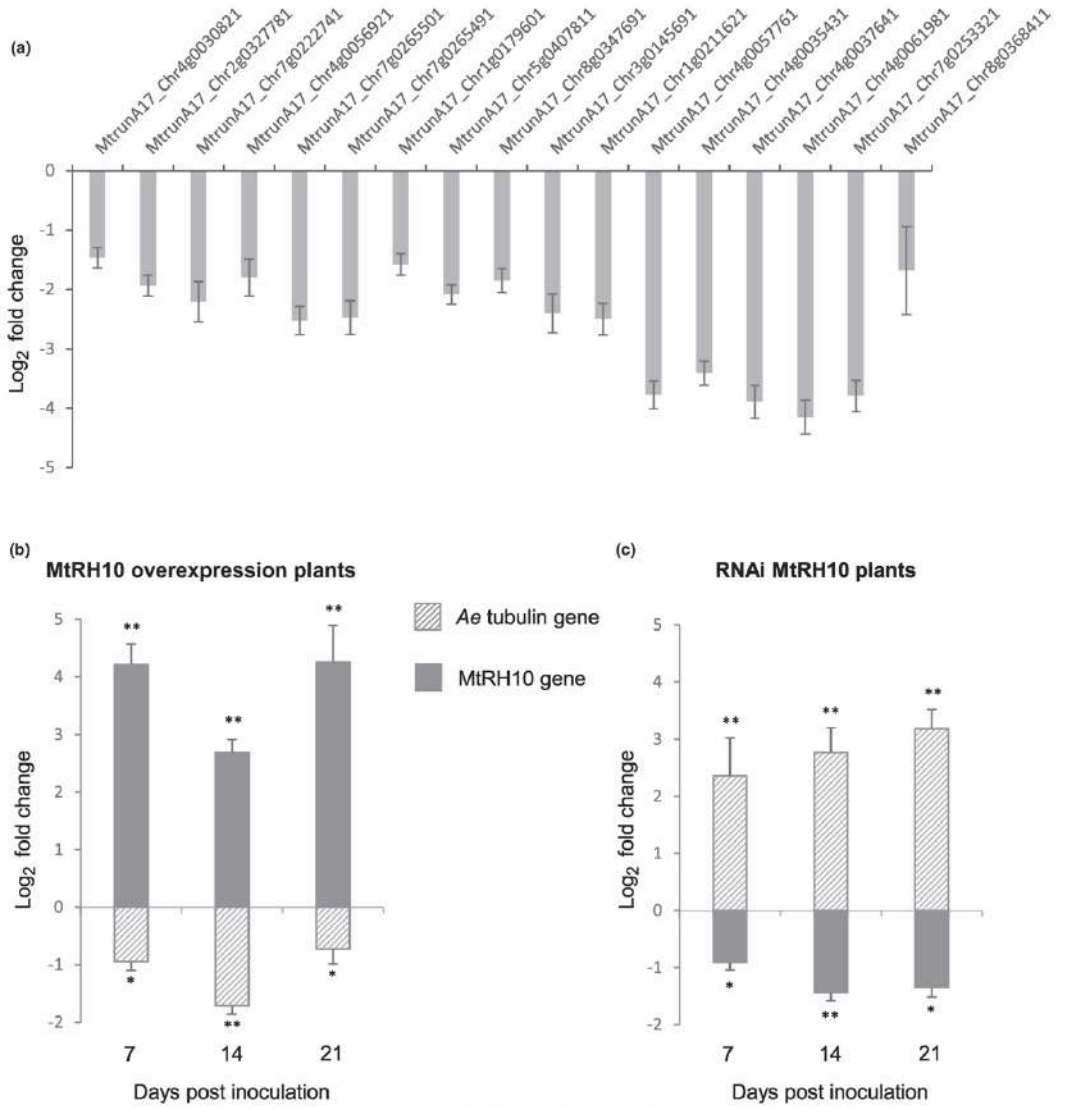

Fig. 6 MtRH10 is a DExD-box RNA helicase that is associated with the ribosome biogenesis pathway and is required for *Medicago truncatula* resistance to soil-borne pathogens. (a) Quantitative reverse transcription polymerase chain reaction (qRT-PCR) analyses for selected ribosome biogenesis-related genes in compromised MtRH10 (RNAi MtRH10) expressing roots compared to green fluorescent protein (GFP) control roots. Note that all these genes were also downregulated in AeSSP1256:GFP expressing roots as reported in Fig. 3(b). Bars and error bars represent, respectively, mean and SE values for two independent experiments. In total, $n = 30$ for GFP roots, and $n = 30$ for RNAi MtRH10 roots. Significant differences were observed for all genes (Student's t-test; $P < 0.05$). (b, c) Twenty-one days after root transformation by *Agrobacterium rhizogenes* with 35S:GFP, 35S:GFP:MtRH10 or 35S:RNAi:MtRH10 constructs, infection assays were performed using 1000 zoospores of *Aphanomyces euteiches* per plant. Expression analyses were conducted at 7, 14 and 21 d post-inoculation. Expression values (log_2 fold change) were estimated for *A. euteiches* tubulin or MtRH10 genes in *M. truncatula* infected plants at 7, 14 and 21 d post-inoculation in plants overexpressing GFP:MtRH10 (b), and in MtRH10-compromised (RNAi MtRH10) (c) plants, compared to GFP control roots. Note the enhanced susceptibility to *A. euteiches* infection in roots in which MtRH10 expression is compromised, as well as the reduced incidence of the pathogen in roots in which MtRH10 is overexpressed. Asterisks indicate significant differences according to Student's t-test (*, $P < 0.05$; **, $P < 0.01$). Bars and error bars represent, respectively, mean and SE values for three independent experiments. In total, $n = 91$ for GFP roots, $n = 50$ for GFP:MtRH10 roots and $n = 50$ for RNAi MtRH10 roots.

and lateral root development, similar to its orthologs AtRH10 and OsRH10 (Matsumura *et al.*, 2016; Wang *et al.*, 2016). In view of the reduced expression of ribosome-related genes in silenced MtRH10 roots, and enlarged nucleoli, we propose that MtRH10 may be part of the nucleolar stress response in *M. truncatula*.

There have been few reports on how DExD/H RHs are involved in plant responses to pathogens. One example is that of OsBIRH1, which enhances disease resistance against *Alternaria brassicicola* and *Pseudomonas syringae* by activating defense-related genes (Li *et al.*, 2008). Another report concerns the PSR1 effector of *Phytophthora sojae*, which targets a putative plant nuclear DExD/H RH and promotes pathogen infection by suppressing small RNA biogenesis of the plant (Qiao *et al.*, 2015). Here we have shown the involvement of MtRH10 in *M. truncatula* resistance to *A. euteiches*.

This work has revealed that microbial effectors possibly promote infection by triggering plant nucleolar stress, but the precise mechanisms linking the MtRH10-mediated signaling pathway and *M. truncatula* susceptibility require further clarification. How plant cells sense perturbations of the ribosome biogenesis pathway and nucleolar problems also remains unclear (Sáez-Vásquez & Delseny, 2019). However, it seems that AeSSP1256 may act as a stimulus of nucleolar disorder. It is worth bearing in mind that MtRH10 may have functions other than the modulation of nucleolar stress, as exemplified by its ortholog TOGR1 in rice (OsRH10), which mediates adaptation of the primary metabolism required for plant growth at high temperatures by acting as an RNA chaperone (Wang *et al.*, 2016). In addition, the phenotypes of MtRH10-silenced mutant plants and AeSSP1256-expressing plants are very similar to those of auxin-related mutants (Ohbayashi *et al.*, 2017), suggesting that MtRH10 could be directly linked to auxin-regulated morphogenesis in *M. truncatula* roots. Further clarification of which ribosome-related genes, hormones and metabolites cause aberrant root phenotypes would improve our understanding of how defects in the MtRH10-mediated signaling pathway promote *A. euteiches* infection.

In conclusion, we found that soil-borne oomycetes promote disease via small secreted effectors which inhibit plant nuclear DExD/H RHs associated with the ribosome biogenesis pathway and resistance to pathogens. This work provides new insights into plant–root oomycete interactions and also highlights the need for the fine-tuning of plant ribosome biogenesis pathways to successfully combat pathogen infection.

Acknowledgements

The authors would like to thank the GeT-PlaGe genomic platform (https://get.genotoul.fr/en/; Toulouse, France) for RNA-Seq studies, H. San-Clemente and M. Aguilar for help with statistical analysis (LRSV, France), and S. Courbier and A. Camon for their assistance in cloning steps. Editorial assistance from R. Bacsa is acknowledged. The authors would like to thank the reviewers for their insightful suggestions which helped to improve the manuscript. This work was supported by the French Laboratory of Excellence project 'TULIP' (ANR-10-LABX-41; ANR-11-IDEX-0002-02) and by the H2020 European Union's Horizon Research and Innovation program under grant agreement no. 766048 (MSCA-ITN-2017 PROTECTA). The authors declare that they have no conflicts of interest.

Author contributions

LC designed and performed the molecular experiments on AeSSP1256 and contributed to the writing of the manuscript; AK prepared and analyzed the RNA-Seq experiments and contributed to the writing of the manuscript; AJ and LC performed the FRET/FLIM analyses; CP and LC carried out the confocal studies; ALR performed the cross-sectional and longitudinal studies and analyzed the root architecture of the samples; MJCP prepared and analyzed the yeast two-hybrid assay and performed candidate cloning; BD analyzed the data and contributed to the writing of the manuscript; EG conceived, designed, and analyzed the experiments, managed the collaborative work, and contributed to the writing of the manuscript. All authors read and approved the final draft of the manuscript.

ORCID

Laurent Camborde https://orcid.org/0000-0003-3044-7500
Bernard Dumas https://orcid.org/0000-0002-4138-3533
Elodie Gaulin https://orcid.org/0000-0003-0572-8749
Andrei Kiselev https://orcid.org/0000-0003-0737-4921
Aurélie Le Ru https://orcid.org/0000-0002-0236-791X
Michiel J. C. Pel https://orcid.org/0000-0003-1615-5018
Cécile Pouzet https://orcid.org/0000-0002-2464-1940

Data availability

Data that support the findings of this study are openly available in the Gene Expression Omnibus (GEO) (reference number GEO:GSE109500) and the Sequence Read Archive (SRA) (reference number PRJNA631662), and these and all other data are available from the corresponding author (gaulin@lrsv.ups-tlse.fr) upon reasonable request.

References

Alexa A, Rahnenfuhrer J. 2020. *topGO: enrichment analysis for gene ontology.* R package v.2.40.0 [WWW document] URL https://bioconductor.org

Anders S, Pyl PT, Huber W. 2015. HTSeq–a Python framework to work with high-throughput sequencing data. *Bioinformatics* **31**: 166–169.

Badis Y, Bonhomme M, Lafitte C, Huguet S, Balzergue S, Dumas B, Jacquet C. 2015. Transcriptome analysis highlights preformed defences and signalling pathways controlled by the *prAe1* quantitative trait locus (QTL), conferring partial resistance to *Aphanomyces euteiches* in *Medicago truncatula*. *Molecular Plant Pathology* **16**: 973–986.

Badreddine I, Lafitte C, Heux L, Skandalis N, Spanou Z, Martinez Y, Esquerré-Tugayé MT, Bulone V, Dumas B, Bottin A. 2008. Cell wall chitosaccharides are essential components and exposed patterns of the phytopathogenic oomycete *Aphanomyces euteiches*. *Eukaryotic Cell* **7**: 1980–1993.

Boisson-Dernier A, Chabaud M, Garcia F, Bécard G, Rosenberg C, Barker DG. 2001. *Agrobacterium rhizogenes-transformed* roots of *Medicago truncatula* for the

study of nitrogen-fixing and endomycorrhizal symbiotic associations. *Molecular Plant–Microbe Interactions* **14**: 695–700.

Bonhomme M, André O, Badis Y, Ronfort J, Burgarella C, Chantret N, Prosperi J-M, Briskine R, Mudge J, Debéllé F *et al.* 2014. High-density genome-wide association mapping implicates an F-box encoding gene in *Medicago truncatula* resistance to *Aphanomyces euteiches*. *New Phytologist* **201**: 1328–1342.

Bonhomme M, Fariello MI, Navier H, Hajri A, Badis Y, Miteul H, Samac DA, Dumas B, Baranger A, Jacquet C *et al.* 2019. A local score approach improves GWAS resolution and detects minor QTL: application to *Medicago truncatula* quantitative disease resistance to multiple *Aphanomyces euteiches* isolates. *Heredity* **123**: 4.

Camborde L, Jauneau A, Brière C, Deslandes L, Dumas B, Gaulin E. 2017. Detection of nucleic acid–protein interactions in plant leaves using fluorescence lifetime imaging microscopy. *Nature Protocols* **12**: 1933–1950.

Camborde L, Raynaud C, Dumas B, Gaulin E. 2019. DNA-damaging effectors: new players in the effector arena. *Trends in Plant Science* **24**: 1094–1101.

la Cour T, Kiemer L, Mølgaard A, Gupta R, Skriver K, Brunak S. 2004. Analysis and prediction of leucine-rich nuclear export signals. *Protein Engineering, Design and Selection* **17**: 527–536.

Desgroux A, Baudais VN, Aubert V, Le Roy G, de Larambergue H, Miteul H, Aubert G, Boutet G, Duc G, Baranger A *et al.* 2018. Comparative genome-wide-association mapping identifies common loci controlling root system architecture and resistance to *Aphanomyces euteiches* in Pea. *Frontiers in Plant Science* **8**: 2195.

Djébali N, Jauneau A, Carine AT, Chardon F, Jaulneau V, Mathé C, Bottin A, Cazaux M, Pilet-Nayel ML, Baranger A *et al.* 2009. Partial resistance of *Medicago truncatula* to *Aphanomyces euteiches* is associated with protection of the root stele and is controlled by a major QTL rich in proteasome-related genes. *Molecular Plant–Microbe Interactions* **22**: 1043–1055.

Engler C, Youles M, Gruetzner R, Ehnert TM, Werner S, Jones JDG, Patron NJ, Marillonnet S. 2014. A Golden Gate modular cloning toolbox for plants. *ACS Synthetic Biology* **3**: 839–843.

Escouboué M, Camborde L, Jauneau A, Gaulin E, Deslandes L. 2019. Preparation of plant material for analysis of protein–nucleic acid interactions by FRET-FLIM. In: Gassmann W, ed. *Plant innate immunity. Methods in molecular biology, vol. 1991*. New York, NY, USA: Humana, 69–77.

Fliegmann J, Canova S, Lachaud C, Uhlenbroich S, Gasciolli V, Pichereaux C, Rossignol M, Rosenberg C, Cumener M, Pitorre D *et al.* 2013. Lipo-chitooligosaccharidic symbiotic signals are recognized by LysM receptor-like kinase LYR3 in the legume *Medicago truncatula*. *ACS Chemical Biology* **8**: 1900–1906.

Förster T. 1948. Intermolecular energy migration and fluorescence. *Annals of Physics* **437**: 55–75.

Fuller-Pace FV. 2006. DExD/H box RNA helicases: multifunctional proteins with important roles in transcriptional regulation. *Nucleic Acids Research* **34**: 4206–4215.

Gaulin E, Jacquet C, Bottin A, Dumas B. 2007. Root rot disease of legumes caused by *Aphanomyces euteiches*. *Molecular Plant Pathology* **8**: 539–548.

Gaulin E, Jauneau A, Villalba F, Rickauer M, Esquerré-Tugayé M-T, Bottin A. 2002. The CBEL glycoprotein of *Phytophthora parasitica* var-*nicotianae* is involved in cell wall deposition and adhesion to cellulosic substrates. *Journal of Cell Science* **115**: 4565–4575.

Gaulin E, Madoui M-A, Bottin A, Jacquet C, Mathé C, Couloux A, Wincker P, Dumas B. 2008. Transcriptome of *Aphanomyces euteiches*: new oomycete putative pathogenicity factors and metabolic pathways. *PLoS ONE* **3**: e1723.

Gaulin E, Pel MJC, Camborde L, San-Clemente H, Courbier S, Dupouy M-A, Lengellé J, Veyssiere M, Le Ru A, Grandjean F *et al.* 2018. Genomics analysis of *Aphanomyces* spp. identifies a new class of oomycete effector associated with host adaptation. *BMC Biology* **16**: 43.

Grefen C, Donald N, Hashimoto K, Kudla J, Schumacher K, Blatt MR. 2010. A ubiquitin-10 promoter-based vector set for fluorescent protein tagging facilitates temporal stability and native protein distribution in transient and stable expression studies. *The Plant Journal* **64**: 355–365.

Haas BJ, Kamoun S, Zody MC, Jiang RHY, Handsaker RE, Cano LM, Grabherr M, Kodira CD, Raffaele S, Torto-Alalibo T *et al.* 2009. Genome sequence and analysis of the Irish potato famine pathogen *Phytophthora infestans*. *Nature* **461**: 393–398.

Hamon C, Coyne CJ, McGee RJ, Lesné A, Esnault R, Mangin P, Hervé M, Le Goff I, Deniot G, Roux-Duparque M *et al.* 2013. QTL meta-analysis provides a comprehensive view of loci controlling partial resistance to *Aphanomyces euteiches* in four sources of resistance in pea. *BMC Plant Biology* **13**: 45.

He Q, McLellan H, Hughes RK, Boevink PC, Armstrong M, Lu Y, Banfield MJ, Tian Z, Birch PRJ. 2019. *Phytophthora infestans* effector SFI3 targets potato UBK to suppress early immune transcriptional responses. *New Phytologist* **222**: 438–454.

He Q, McLellan H, Boevink PC, Birch PRJ. 2020. All roads lead to susceptibility: the many modes of action of fungal and oomycete intracellular effectors. *Plant Communications* **1**: 4.

Jacquet C, Bonhomme M. 2020. Deciphering resistance mechanisms to the root rot disease of legumes caused by *Aphanomyces euteiches* with *Medicago truncatula* genetic and genomic resources. In: de Bruijin F, ed. *The model legume* Medicago truncatula. Hoboken, NJ, USA: John Wiley & Sons, 307–316.

Jarmoskaite I, Russell R. 2011. DEAD-box proteins as RNA helicases and chaperones. *Wiley Interdisciplinary Reviews: RNA* **2**: 135–152.

Kamoun S, Furzer O, Jones JDG, Judelson HS, Ali GS, Dalio RJD, Roy SG, Schena L, Zambounis A, Panabières F *et al.* 2015. The top 10 oomycete pathogens in molecular plant pathology. *Molecular Plant Pathology* **16**: 413–434.

Kim D, Paggi JM, Park C, Bennett C, Salzberg SL. 2019. Graph-based genome alignment and genotyping with HISAT2 and HISAT-genotype. *Nature Biotechnology* **37**: 907–915.

Kosugi S, Hasebe M, Tomita M, Yanagawa H. 2009. Systematic identification of cell cycle-dependent yeast nucleocytoplasmic shuttling proteins by prediction of composite motifs. *Proceedings of the National Academy of Sciences, USA* **106**: 10171–10176.

Li D, Liu H, Zhang H, Wang X, Song F. 2008. OsBIRH1, a DEAD-box RNA helicase with functions in modulating defence responses against pathogen infection and oxidative stress. *Journal of Experimental Botany* **59**: 2133–2146.

Li H, Handsaker B, Wysoker A, Fennell T, Ruan J, Homer N, Marth G, Abecasis G, Durbin R. 2009. The sequence alignment/map format and SAMtools. *Bioinformatics* **25**: 2078–2079.

Liu Y, Imai R. 2018. Function of plant DExD/H-Box RNA helicases associated with ribosomal RNA biogenesis. *Frontiers in Plant Science* **9**: 125.

Livak KJ, Schmittgen TD. 2001. Analysis of relative gene expression data using real-time quantitative PCR and the $2^{-\Delta\Delta CT}$ method. *Methods* **25**: 402–408.

Love MI, Huber W, Anders S. 2014. Moderated estimation of fold change and dispersion for RNA-seq data with DESeq2. *Genome Biology* **15**: 550.

Martin R, Straub AU, Doebele C, Bohnsack MT. 2013. DExD/H-box RNA helicases in ribosome biogenesis. *RNA Biology* **10**: 4–18.

Matsumura Y, Ohbayashi I, Takahashi H, Kojima S, Ishibashi N, Keta S, Nakagawa A, Hayashi R, Saeź-Váquez J, Echeverria M *et al.* 2016. A genetic link between epigenetic repressor AS1-AS2 and a putative small subunit processome in leaf polarity establishment of *Arabidopsis*. *Biology Open* **5**: 942–954.

McGowan J, Fitzpatrick DA. 2017. Genomic, network, and phylogenetic analysis of the oomycete effector arsenal. *mSphere* **2**: 6.

McLellan H, Boevink PC, Armstrong MR, Pritchard L, Gomez S, Morales J, Whisson SC, Beynon JL, Birch PRJ. 2013. An RxLR effector from *Phytophthora infestans* prevents re-localisation of two plant NAC transcription factors from the endoplasmic reticulum to the nucleus. *PLoS Pathogens* **9**: e1003670.

O'Day C. 1996. 18S rRNA processing requires the RNA helicase-like protein Rrp3. *Nucleic Acids Research* **24**: 3201–3207.

Ohbayashi I, Lin CY, Shinohara N, Matsumura Y, Machida Y, Horiguchi G, Tsukaya H, Sugiyama M. 2017. Evidence for a role of ANAC082 as a ribosomal stress response mediator leading to growth defects and developmental alterations in *Arabidopsis*. *Plant Cell* **29**: 2644–2660.

Ohbayashi I, Sugiyama M. 2018. Plant nucleolar stress response, a new face in the NAC-dependent cellular stress responses. *Frontiers in Plant Science* **8**: 2247.

Pecrix Y, Staton SE, Sallet E, Lelandais-Brière C, Moreau S, Carrère S, Blein T, Jardinaud M-F, Latrasse D, Zouine M *et al.* 2018. Whole-genome landscape of *Medicago truncatula* symbiotic genes. *Nature Plants* 4: 1017–1025.

Pfister AS. 2019. Emerging role of the nucleolar stress response in autophagy. *Frontiers in Cellular Neuroscience* 13: 156.

Qiao Y, Shi J, Zhai Y, Hou Y, Ma W. 2015. *Phytophthora* effector targets a novel component of small RNA pathway in plants to promote infection. *Proceedings of the National Academy of Sciences, USA* 112: 5850–5855.

Ramirez-Garcés D, Camborde L, Pel MJC, Jauneau A, Martinez Y, Néant I, Leclerc C, Moreau M, Dumas B, Gaulin E. 2016. CRN13 candidate effectors from plant and animal eukaryotic pathogens are DNA-binding proteins which trigger host DNA damage response. *New Phytologist* 210: 602–617.

Rau A, Gallopin M, Celeux G, Jaffrézic F. 2013. Data-based filtering for replicated high-throughput transcriptome sequencing experiments. *Bioinformatics* 29: 2146–2152.

Rey T, Nars A, Bonhomme M, Bottin A, Huguet S, Balzergue S, Jardinaud M-F, Bono J-J, Cullimore J, Dumas B *et al.* 2013. NFP, a LysM protein controlling Nod factor perception, also intervenes in *Medicago truncatula* resistance to pathogens. *New Phytologist* 198: 875–886.

Sáez-Vásquez J, Delseny M. 2019. Ribosome biogenesis in plants: from functional 45S ribosomal DNA organization to ribosome assembly factors. *Plant Cell* 31: 1945–1967.

Schornack S, van Damme M, Bozkurt TO, Cano LM, Smoker M, Thines M, Gaulin E, Kamoun S, Huitema E. 2010. Ancient class of translocated oomycete effectors targets the host nucleus. *Proceedings of the National Academy of Sciences, USA* 107: 17421–17426.

Sekiguchi T, Hayano T, Yanagida M, Takahashi N, Nishimoto T. 2006. NOP132 is required for proper nucleolus localization of DEAD-box RNA helicase DDX47. *Nucleic Acids Research* 34: 4593–4608.

Shaw P, Brown J. 2012. Nucleoli: composition, function, and dynamics. *Plant Physiology* 158: 44–51.

Song T, Ma Z, Shen D, Li Q, Li W, Su L, Ye T, Zhang M, Wang Y, Dou D. 2015. An oomycete CRN effector reprograms expression of plant *HSP* genes by targeting their promoters. *PLoS Pathogens* 11: 1–30.

Stam R, Jupe J, Howden AJM, Morris JA, Boevink PC, Hedley PE, Huitema E. 2013. Identification and characterisation CRN effectors in *Phytophthora capsici* shows modularity and functional diversity. *PLoS ONE* 8: e59517.

Tabima JF, Grünwald NJ. 2019. *EFFECTR*: an expandable R package to predict candidate RxLR and CRN effectors in oomycetes using motif searches. *Molecular Plant–Microbe Interactions* 32: 1067–1076.

Tasset C, Bernoux M, Jauneau A, Pouzet C, Brière C, Kieffer-Jacquinod S, Rivas S, Marco Y, Deslandes L. 2010. Autoacetylation of the *Ralstonia solanacearum* effector PopP2 targets a lysine residue essential for RRS1-R-mediated immunity in *Arabidopsis*. *PLoS Pathogens* 6: e1001202.

Vincent NG, Michael Charette J, Baserga SJ. 2018. The SSU processome interactome in *Saccharomyces cerevisiae* reveals novel protein subcomplexes. *Wiley Interdisciplinary Reviews: RNA* 24: 77–89.

Wang D, Qin B, Li X, Tang D, Zhang Y, Cheng Z, Xue Y. 2016. Nucleolar DEAD-Box RNA Helicase TOGR1 regulates thermotolerant growth as a pre-rRNA chaperone in rice. *PLoS Genetics* 12: e1005844.

Wang H, Gao X, Huang Y, Yang J, Liu ZR. 2009. P68 RNA helicase is a nucleocytoplasmic shuttling protein. *Cell Research* 19: 1388–1400.

Wang S, McLellan H, Bukharova T, He Q, Murphy F, Shi J, Sun S, Van Weymers P, Ren Y, Thilliez G *et al.* 2019. *Phytophthora infestans* RXLR effectors act in concert at diverse subcellular locations to enhance host colonization. *Journal of Experimental Botany* 70: 343–356.

van West P, Beakes GW. 2014. Animal pathogenic oomycetes. *Fungal Biology* 118: 525–526.

Wieckowski Y, Schiefelbein J. 2012. Nuclear ribosome biogenesis mediated by the DIM1A rRNA dimethylase is required for organized root growth and epidermal patterning in *Arabidopsis*. *Plant Cell* 24: 2839–2856.

Wirthmueller L, Asai S, Rallapalli G, Sklenar J, Fabro G, Kim DS, Lintermann R, Jaspers P, Wrzaczek M, Kangasjärvi J *et al.* 2018. *Arabidopsis* downy mildew effector HaRxL106 suppresses plant immunity by binding to RADICAL-INDUCED CELL DEATH1. *New Phytologist* 220: 232–248.

Xiong Q, Ye W, Choi D, Wong J, Qiao Y, Tao K, Wang Y, Ma W. 2014. *Phytophthora* suppressor of RNA silencing 2 is a conserved RxLR effector that promotes infection in soybean and *Arabidopsis thaliana*. *Molecular Plant–Microbe Interactions* 27: 1379–1389.

Zhang M, Li Q, Liu T, Liu L, Shen D, Zhu Y, Liu P, Zhou J-M, Dou D. 2015. Two cytoplasmic effectors of *Phytophthora sojae* regulate plant cell death via interactions with plant catalases. *Plant Physiology* 167: 164–175.

Supporting Information

Additional Supporting Information may be found online in the Supporting Information section at the end of the article.

Fig. S1 AeSSP1256 preferentially accumulates at the nucleolus rim in *Nicotiana benthamiana* cells.

Fig. S2 Nuclear localization of AeSSP1256 is required for its biological activity in *Medicago truncatula* roots.

Fig. S3 Subcellular localization of AeSSP1256 and its putative host targets in *N. benthamiana* leaves.

Fig. S4 AeSSP1256 drives the relocalization of a nucleocytoplasmic host RNA helicase (MtRH10) around the nucleolus in *N. benthamiana* cells.

Fig. S5 Sequence analyses of the MtRH10 DExD-box RNA helicase.

Fig. S6 AeSSP1256 proteins do not alter MtRH10 expression levels in *M. truncatula* roots.

Fig. S7 Expression of MtRH10 is reduced in *M. truncatula*-silenced roots.

Fig. S8 MtRH10-silenced roots displayed enlarged nucleoli.

Fig. S9 *Medicago truncatula* root cell morphology is affected in roots in which MtRH10 expression is compromised or in which the AeSSP1256 effector is expressed.

Fig. S10 Western blot for MtRH10-overexpression roots infected by *Aphanomyces euteiches*.

Table S1 List of primers used in this study.

Table S2 List of putative AeSSP1256 interactors after yeast two-hybrid screening of *M. truncatula* roots infected by the pathogen.

Table S3 RNA-Seq data for *M. truncatula* roots (A17) expressing either the GFP construct or the AeSSP1256:GFP construct.

Please note: Wiley Blackwell are not responsible for the content or functionality of any Supporting Information supplied by the authors. Any queries (other than missing material) should be directed to the *New Phytologist* Central Office.